STUDIES OF LIQUID PHASE MIXING AND BED EXPANSION OF GAS PRODUCING ANAEROBIC FLUIDIZED BED BIOREACTOR

ABDURRAHMAN GARBA YAMMAMA

A Dissertation submitted in partial fulfillment of the requirements for the degree of Doctor of Philosophy

Chemical and Process Engineering Department
University of Strathclyde, Glasgow

1992

To my wife Rabia and daughters
Halimatu, Aishatu and Maryamu.

ABSTRACT

Liquid phase mixing and holdup are two important parameters required for the modelling and consequent evaluation of the performance of anaerobic fluidized bed bioreactors. Few papers have appeared in recent times, attempting to characterize liquid phase mixing and holdup in simulated biological reactors. But, the peculiar nature of biological systems as regards *in situ* gas production, which is difficult to simulate, mean that results from simulated studies need to be verified against active biological system. One of the problems hindering this verification is finding suitable tracer for use, in determining the axial liquid dispersion coefficient, with microbial system.

In this work, the effects of superficial liquid and gas velocities in the ranges 0.0084 to 0.0351 cm/s and 0.054 to 0.335 cm/s respectively, on axial liquid dispersion coefficient (D_2) and liquid holdup (e_L), were studied in an anaerobic column bioreactor, of 3.81 cm internal diameter, containing flocculent strains of *Saccharomyces cerevisiae*. The strains used are Y6 and NCYC 1026. The gas velocities were calculated from the ethanol concentrations and were varied by varying the glucose feed rate. Since D and e_L were determined from the liquid residence time distribution, a search for a tracer suitable, for use with the yeast, was conducted. In addition the performance of the bioreactor was studied under the same liquid and gas flow conditions.

Five tracers, methyl violet, methyl green, aniline blue, fluorescein and dextran blue, were tested at three stages. In the first stage, shake flask fermentations were performed. Methyl violet was found to affect yeast metabolism by hindering it while methyl green promoted yeast metabolism. These tracers were also partly lost due to adsorption on cells surfaces. Fluorescein, aniline blue

and dextran blue had no significant effect on the yeast metabolism, but the optical density of fluorescein was affected by pH changes. This necessitated the recalibration of fluorescein solutions, taking into consideration the effect of pH.

In the second stage, anaerobic batch fermentations were performed in a one liter LH batch fermenter. All the tracers used, aniline blue, fluorescein and dextran blue, did not affect the bioconversion. But, aniline blue was completely lost after eight hours of fermentation. On the other hand, the concentrations of fluorescein and dextran blue remained unchanged for the entire fermentation period.

In the third stage, fluorescein and dextran blue were tested in column anaerobic bioreactor containing flocculent yeast, strain Y6. Both fluorescein and dextran blue were, in turn, injected into the column and the response determined at a point downstream. The results indicated that fluorescein was absorbed by the yeast floes and the response curves had very long tails; only about 9.7% of the tracer injected was recovered. On the other hand, dextran blue was not absorbed and its recovery was over 70%. Therefore, dextran blue was chosen for use as tracer, for the purpose of determining the liquid residence time, in the bioreactor.

Study of the performance of the bioreactor were performed with inlet glucose concentrations of 30, 50 and 70 g/1 and liquid flow rates of 5.75, 12, 18 and 24 ml/min respectively. The results have indicated that the reactor was similar to tower fermenters reported in the literature. Biomass concentrations of about 48 and 63 g/1 were obtained for strains NCYC 1026 and Y6 respectively. The fluidized bed height ranged from 49 to 129 cm throughout the course of the experiments. Ethanol productivity, based on liquid volume, was in the range 28.76 to 138.37 g/(l.hr). Ethanol concentrations in the

range 9.2 to 31.6 g/1 were obtained. Glucose consumption was over 80% for all conditions except at inlet glucose concentration of 70 g/1 and liquid flow rate of 24 ml/min, where it was 76%. Ethanol yield was over 67% in all cases, except at inlet glucose concentration of 70 g/1 and liquid flow rate of 24 ml/min, where it was 48%.

Axial liquid dispersion coefficient and liquid holdup were evaluated from the liquid residence time distribution. Attempt to determine the liquid holdup by draining the liquid content of the bed, failed because gas production continued even when liquid flow was stopped and the yeast bed blocked the base of the tower, preventing the liquid from draining. Measurement of liquid holdup using the pressure drop method also failed, because yeast escaped into the manometer tubes and gas production interfered with manometer readings. Nonetherless, estimate of the bed voidage was made using the height difference between the fluidized bed and the bed under no flow condition. Consequently, the gas holdup and the solid hold up were obtained by difference.

Results from the dispersion study, indicated that the axial dispersion coefficient was correlated by the following relationship:

$$D_z = 7.047 li_g^{0197} u_L^{0-347}$$

with a goodness of fit of 52.9%, and D_z was given in cm /s. Significance testing has shown that the gas superficial velocity has little effect on the axial liquid dispersion coefficient and as such, for these type of system, the dispersion coefficient can be evaluated from the liquid velocity alone. Furthermore, axial variation in the dispersion coefficient was negligible, due to the weak effect of gas velocity on D_z. Values of the dispersion coefficient obtained were in the range 0.47x10 to 8.3x10"* nr/s and are lower than values reported for non-active

fluidized beds.

Results for the liquid holdup indicated that this parameter was increased linearly by increased liquid velocity and decreased linearly by increased gas velocity. The liquid holdup was correlated to liquid and gas velocities by the realtionship:

$$C_L = 0.124 - 0.067u_g + 3.85u_L$$

with a goodness of fit of 75.1%. Significance test also indicated that the influence of gas velocity on liquid holdup, was marginal and therefore, the liquid holdup can be obtained from the liquid velocity alone. The correlation of Richardson and Zaki (1954) was also noted to fit the data and values of the exponent n were found to depend on inlet glucose concentration and strain type. The values obtained were in the range 0.227 to 0.528 for strain NCYC 1026 and 0.997 for strain Y6 respectively. Axial variation in liquid holdup was not pronounced due to the weak effect of gas velocity on this parameter. Liquid holdup values were in the range 0.111 to 0.243 and are generally low, below the value of 0.4 regarded as the voidage at minimum fluidization condition.

The contribution of the gas holdup to the bed voidage was found to be significant; a maximum of 59.8% was obtained while the minimum was 0.58%. Therefore, this contribution depended on the process condition.

It should be noted that in this system, due to the flocculant nature of the yeast, proper fluidization of the yeast bed was not achieved inspite of using higher inlet glucose concentration of 100 g/1. However when a 3 Molar solution of sodium chloride was added into the growth medium, fluidization was achieved, but there was total inactivation of the bed.

ACKNOWLEDGEMENT

I wish to express gratitude to my supervisor Dr. V.F.Larsen for his guidance, advices and constant encouragement.

My gratitude to the Head of Chemical and Process Engineering Department, Professor C.D.Grant, for the provision of facilities.

I also wish to acknowledge the financial support of the Commonwealth Scholarship Commission in the United Kingdom.

My gratitude to the technicians of the Biotechnology Unit, Mr. S.Adams and Mr. I.Airdrie, for their assistance.

My thanks also to Mr. K.Campbell and his staff for the construction and assembly of the equipment.

I would like to thank my colleagues, whose friendship I enjoyed during the entire period of this work.

Finally I wish to thank, my wife Rabia for her moral support and understanding, my parents, relatives and many other friends who helped me in different ways towards successful completion of this thesis.

TABLE OF CONTENTS

Title		Page
Abstract		i
Acknowledgement		v
Table of contents		vi
List of tables		xii
List of figures		xiv
Abbreviations and notations		xix
CHAPTER ONE: INTRODUCTION		
1.1	GENERAL	1
1.2	IMMOBILIZATION OF MICROBIAL CELLS	3
1.2.1	Attachment of cells	4
1.2.1.1	*Cells aggregation*	5
1.2.1.2	*Attachment to surfaces*	6
1.2.2	Entrapment of cells	6
1.2.2.1	*Encapsulation*	7
1.2.2.2	*Membranes*	7
1.2.2.3	*Porous materials*	8
1.3	BIOLOGICAL REACTORS	8
1.3.1	Continuously stirred tank fermenter	9
1.3.2	Packed bed fermenter	10
1.3.3	Hollow fibre fermenter	11
1.3.4	Fluidized bed fermenter	12
1.3.5	Other fermenter types	15
1.3.6	Choice of reactor type	16
1.4	OPERATIONS OF FLUIDIZED BED FERMENTER	18
1.4.1	FBAF with *in situ* gas production	19
1.5	OBJECTIVES	22
CHAPTER TWO: ETHANOL FORMATION AND PRODUCTION		
2.1	INTRODUCTION	24
2.2	ETHANOL FORMATION	25
2.2.1	Effect of glucose concentration	27
2.2.2	Ethanol inhibition	30

2.2.3 Combined glucose and ethanol inhibition 33
2.2.4 Effects of pH 35
2.2.5 Temperature effects 37
2.2.6 Effects of feed components 39
2.2.7 Mass transfer effects 40
2.3 ETHANOL PRODUCTION 45
2.3.1 Batch fermentation 45
2.3.2 Continuously stirred tank fermentation 46
2.3.3 Hollow fibre fermentation 47
2.3.4 Packed bed fermentation 48
2.3.5 Tower fermentation 50

CHAPTER THREE: LIQUID MIXING AND HYDRODYNAMICS IN THREE PHASE FLUIDIZED BEDS
3.1 INTRODUCTION 55
3.2 PRINCIPLES OF FLUIDIZATION 55
3.3 LIQUID MIXING 60
3.3.1 Mechanisms of liquid mixing in fluidized beds 60
3.3.2 Types of liquid mixing 62
3.3.2.1 *Micromixing* 62
3.3.2.2 *Macromixing* 63
3.3.3 Tracer requirements 65
3.4 AXIAL LIQUID DISPERSION COEFFICIENT 68
3.4.1 Effect of gas velocity 68
3.4.2 Effects of liquid velocity 72
3.4.3 Effect of particle properties 76
3.4.3.1 *Particle size* 76
3.4.3.2 *Particle density* 80
3.4.4 Effect of liquid properties 81
3.4.4.1 *Liquid viscosity* 81
3.4.4.2 *Surface tension* 83
3.4.5 Effect of column diameter 84

3.4.6	Correlations for axial liquid dispersion coefficient	86
3.4.6.1	*Correlations for three phase systems*	87
3.4.6.2	*Correlations for two phase systems*	94
3.5	BED EXPANSION CHARACTERISTICS	98
3.5.1	Bed behaviour	99
3.5.1.1	*Bed contraction*	102
3.5.1.2	*Expansion of bioactive bed*	103
3.5.2	Correlations for bed voidage and phase holdups	104
3.5.2.1	*Two phase fluidized beds*	104
3.5.2.2	*Three phase system*	108
3.5.2.3	*Biological system*	111
CHAPTER FOUR: MATERIALS AND METHODS		
4.1	MATERIALS	114
4.1.1	Chemicals	114
4.1.2	Organisms	114
4.1.3	Media	115
4.1.4	Tracer material	115
4.2	EQUIPMENT	115
4.2.1	Fluidized bed fermenter	116
4.2.1.1	*Temperature control*	120
4.2.1.2	*Aeration*	120
4.2.2	LH batch fermenter	120
4.2.3	Chemap fermenter	122
4.2.3.1	*Temperature control*	122
4.2.3.2	*Aeration*	122
4.2.4	Equipment used in sample analysis	122
4.3	EXPERIMENTAL METHODS	124
4.3.1	Preparation of media	124
4.3.2	Media and equipment sterilization	124
4.3.3	Preparation of subculture	125
4.3.4	Preparation of inoculum	125
4.3.5	Selection of yeast strain	126
4.3.6	Operation of continuous reactor	127

4.3.6.1 *Start-up of column* 127
4.3.6.2 *Medium addition during continuous fermentation* 127
4.3.6.3 *Reactor sampling* 128
4.3.7 Axial dispersion experiments 128
4.3.7.1 *Selection of tracer material* 129
4.3.7.2 *Tracer injection into column* 131
4.3.7.3 *Tracer sampling from column* 132
4.4 ANALYTICAL METHODS 132
4.4.1 pH 132
4.4.2 Biomass 133
4.4.3 Glucose analysis 133
4.4.4 Ethanol analysis 135
4.4.5 Measurement of bed height 135
4.4.6 Measurement of particle size 135
4.4.7 Measurement of tracer concentration 136
4.4.8 Determination of carbon dioxide flow rate 138
4.5 DATA ANALYSIS 138
4.5.1 Calculation of axial liquid dispersion coefficient 138
4.5.1.1 *Pulse method* 139
4.5.1.2 *Step change method* 141
4.5.2 Calculation of liquid holdup 141
4.5.3 Calculation of gas flow rate 142
4.5.4 Regression analysis 142

CHAPTER FIVE: RESULTS AND DISCUSSIONS

5.1 INTRODUCTION 143
5.2 TRACER SELECTION 143
5.2.1 Determination of λ_{max} 144
5.2.2 Calibrations for tracer concentration 144
5.2.3 Effects of tracer materials on yeast metabolism in shake flasks 146
5.2.4 Tracer recovery in shake flasks 149
5.2.4.1 *pH effects* 150

5.2.4.2 *Conclusion* 153
5.2.5 Effects of tracer materials on yeast metabolism during anaerobic batch fermentation 154
5.2.6 Tracer choice in continuous column operation 158
5.3 PERFORMANCE OF BIOREACTOR 166
5.3.1 Trends and general observations 167
5.3.1.1 *Trends in pH* 168
5.3.1.2 *Glucose concentration* 169
5.3.1.3 *Ethanol concentration* 170
5.3.1.4 *Ethanol yield* 172
5.3.1.5 *Gas production* 173
5.3.1.6 *Ethanol productivity* 175
5.3.1.7 *Biomass concentration* 178
5.3.1.8 *Conclusion* 182
5.3.2 Effects of inlet glucose concentration 182
5.3.3 Effects of liquid flow rate 187
5.3.4 Reliability of concentration measurements 191
5.3.5 Conclusion 191
5.4 AXIAL LIQUID DISPERSION COEFFICIENT 193
5.4.1 Maganitude of D_z values obtained 194
5.4.2 Effects of gas superficial velocity on D_z 196
5.4.3 Effects of superficial liquid velocity on D_z 201
5.4.4 Axial variation in D_z 206
5.4.5 Correlations for axial liquid dispersion coefficient 207
5.4.6 Conclusion 209
5.5 BED EXPANSION CHARACTERISTICS 210
5.5.1 Liquid holdup 213
5.5.1.1 *Effects of gas velocity on liquid holdup* 214

5.5.1.2 *Effects of Liquid velocity on liquid holdup* 218
5.5.1.3 *Axial variation in liquid holdup* 221
5.5.1.4 *Correlations for liquid holdup* 222
5.5.2 Estimation of bed voidage 227
5.5.3 Estimations of gas and solid holdups 229
5.5.4 Conclusion 230

CHAPTER SIX: OVERALL DISCUSSION 232
CHAPTER SEVEN: CONCLUSIONS 237
CHAPTER EIGHT: RECOMMENDATIONS 239
REFERENCES 241
APPENDICES 262

LIST OF TABLES

Table	Title	Page
1.1	Some applications of fluidized bed fermenters in wastewater treatment	13
1.2	Some applications of fluidized bed fermenters in bioproduction	14
1.3	Characteristics of continuous fermenters	16
1.4	Capabilities of bioreactors in anaerobic wastewater treatment	17
1.5	Capabilities of bioreactors in ethanol production	17
2.1	Effects of inlet sugar concentration on the specific rates of growth and ethanol production	29
2.2	Effects of pH on ethanol production rate and cell concentration	36
2.3	Inhibition of feed components	40
2.4	Effects of inlet glucose concentration on productivity of packed bed fermenter	49
3.1	Tracers used in RTD studies of liquid phase in active bioreasctors	66
3.2	Influence of gas velocity on D_z	72
3.3	Influence of particle size on D_z	77
3.4	Influence of particle density on D_z	81
3.5	Comparison of published correlations for simulated biological system	92
3.6	Prediction of D_z for same operating conditions in tower fermenter	93
3.7	Density changes due to biomass growth	104
4.1	Tracer materials selected	129
5.1	λ_{max} for the tracer materials	144
5.2	Regression analysis for calibration curves	145
5.3	pH effect on fluorescein OD_{490}	151
5.4	Reproducibility of optical density for fluorescein	152
5.5	pH effect on OD_{625} reading for dextran blue	153

5.6 Tracer performance in column bioreactor 161
5.7 Fluidized bed height 167
5.8 Liquid holdup 167
5.9 Glucose concentration at top of bed 170
5.10 Ethanol concentration at top of bed 171
5.11 Ethanol yield at top of bed 173
5.12 The difference in gas flow rates between the bottom and top of yeast bed 174
5.13 Ethanol productivity (Empty column) 176
5.14 Comparison of the productivity of bioreactors 177
5.15 Ethanol productivity (Liquid volume) 177
5.16 Comparison of fermentation parameters for strain Y6 178
5.17 Biomass concentration above bed 182
5.18 Axial liquid dispersion coefficient 195
5.19 Comparison of D_z values 195
5.20 Changes in D_z with gas velocity 199
5.21 Gas flow regimes 200
5.22 The effect of axial variation in gas velocity on D_z 206
5.23 Effect of bed breakage on measured liquid holdup and D_z 211
5.24 Values of liquid holdup obtained 213
5.25 Axial variation in liquid holdup 221
5.26 Values of n and settling velocity 225
5.27 Estimate of bed voidage 228
5.28 Estimates of gas and liquid holdups 230

LIST OF FIGURES

Figure	Title	Page
1	Types of continuous bioreactors	10
2.1	Aerobic and anaerobic catabolism of *S. cerevisiae*	26
2.2	Glucose inhibition effect	28
2.3	Ethanol inhibition effect	32
2.4	Effects of pH on ethanol production rate for free and immobilized cells	37
2.5	Effects of temperature on ethanol production rate for free and immobilized cells	38
2.6	Productivity of tower fermenter	52
2.7	pH profile in tower fermenter	53
3.1	Fluidization process	56
3.2	Characteristics of 2-phase systems	57
3.3	Characteristics of 3-phase systems	58
3.4	Effect of gas velocity on dispersion coefficient	70
3.5	Effect of gas velocity on dispersion coefficient in fluidized bed bioreactor for bottom and top of bed	71
3.6	Effect of liquid velocity on dispersion coefficient	74
3.7	Effect of particle size on dispersion coefficient for two phase fluidized bed	78
3.8	Effect of liquid viscosity on dispersion coefficient	82
3.9	Effect of surface tension on dispersion coefficient	84
3.10	Influence of column diameter on dispersion coefficient	86
3.11	Effect of gas and liquid velocities on liquid holdup	100
3.12	Velocity-voidage relationship for biological system	112

4.1 Details of fluidized bed fermenter 116
4.2 Schematic diagram of fluidized bed fermenter 117
4.3 Experimental set-up 118
4.4 LH batch fermenter 121
4.5 Chemap batch fermenter 123
5.1 Glucose consumption in shake flasks 147
5.2 Ethanol production in shake flasks 147
5.3 Biomass production in shake flasks 148
5.4 Ethanol yield in shake flasks 148
5.5 Biomass yield in shake flasks 149
5.6 Recovery of tracers in shake flasks 150
5.7 Calibration for fluorescein concentration 152
5.8 Ethanol production in anaerobic batch fermentation 155
5.9 Glucose concentration in anaerobic batch fermentation 155
5.10 Biomass production in anaerobic batch fermentation 156
5.11 Recovery of dextran blue during anaerobic batch fermentation 157
5.12 Recovery of aniline blue and fluorescein 157
5.13 E curve for 0.2 ml of 25 g/l fluorescein at liquid superficial velocity of 0.0351 cm/s 159
5.14 E curve for 1.5 ml of 25 g/l fluorescein at liquid superficial velocity of 0.0084 cm/s 160
5.15 E curve for 4 ml of 10 g/l dextran blue at liquid superficial velocity of 0.0351 cm/s 160
5.16 E curve for 2 ml of 22.2 g/l dextran blue at liquid superficial velocity of 0.0351 cm/s 162
5.17 E curve for 2 ml of 22.2 g/l dextran blue at liquid superficial velocity of 0.0263 cm/s 163
5.18 E curve for 2 ml of 22.2 g/l dextran blue at liquid superficial velocity of 0.0175 cm/s 163
5.19 F curve for 0.25 g/l fluorescein at liquid superficial velocity of 0.0084 cm/s 164

5.20 F curve for 0.005 g/l fluorescein at liquid superficial velocity of 0.0351 cm/s 165
5.21 pH profile along column height 168
5.22 Profile of glucose concentration along column height 169
5.23 Profile of ethanol concentration along column height 171
5.24 Profile of ethanol yield along column height 172
5.25 Gas production along column height 174
5.26 Ethanol productivity along column height 175
5.27 Bed of strain Y6 180
5.28 Bed of strain NCYC 1026 181
5.29 Effect of inlet glucose concentration on glucose concentration above bed 183
5.30 Effect of inlet glucose concentration on ethanol concentration 184
5.31 Effect of inlet glucose concentration on ethanol yield 185
5.32 Influence of inlet glucose concentration on ethanol productivity 186
5.33 Influence of inlet glucose concentration on gas velocity 186
5.34 Effect of liquid flow rate on gas velocity 187
5.35 Effect of liquid flow rate on ethanol concentration 188
5.36 Effect of liquid flow rate on ethanol yield 189
5.37 Effect of liquid flow rate on ethanol productivity 190
5.38 Effect of liquid flow rate on glucose concentration above bed 190
5.39 Influence of glucose consumption rate on gas velocity 194
5.40 Effect of gas velocity on axial liquid dispersion coefficient at liquid velocity of 0.0084 cm/s 197

5.41 Effect of gas velocity on D_z at liquid velocity of 0.0175 cm/s 198
5.42 Effect of gas velocity on D_z at liquid velocity of 0.0263 cm/s 198
5.43 Effect of gas velocity on D_z at liquid velocity of 0.0351 cm/s 199
5.44 Overall effects of gas velocity on D_z at all liquid velocities 201
5.45 Influence of liquid velocity on D_z at inlet glucose concentration of 30 g/l 202
4.46 Influence of liquid velocity on D_z at inlet glucose concentration of 50 g/l 203
5.47 Effect of liquid velocity on D_z at inlet glucose concentration of 70 g/l 203
5.48 Overall effect of liquid velocity on D_z at all liquid velocities 204
5.49 Bed breakage during fermentation 212
5.50 Effect of gas velocity on liquid holdup at liquid velocity of 0.0084 cm/s 215
5.51 Effect of gas velocity on liquid holdup at liquid velocity of 0.0175 cm/s 215
5.52 Effect of gas velocity on liquid holdup at liquid velocity of 0.0263 cm/s 216
5.53 Effect of gas velocity on liquid holdup at liquid velocity of 0.0351 cm/s 216
5.54 Overall effect of gas velocity on liquid holdup at all liquid velocities 217
5.55 Influence of liquid velocity on liquid holdup at inlet glucose concentration of 30 g/l 218
5.56 Influence of liquid velocity on liquid holdup at inlet glucose concentration of 50 g/l 219
5.57 Influence of liquid velocity on liquid holdup at inlet glucose concentration of 70 g/l 220
5.58 Overall influence of liquid velocity on liquid holdup at all inlet glucose concentrations 220

5.59 Liquid velocity and holdup relationship at inlet glucose concentration of 30 g/l 223
5.60 Liquid velocity and holdup relationship at inlet glucose concentration of 50 g/l 223
5.61 Liquid velocity and holdup relationship at inlet glucose concentration of 70 g/l 224
5.62 Liquid velocity and holdup relationship at inlet glucose concentration of 50 g/l for strain Y6 224

ABBREVIATIONS AND NOTATIONS

Abbreviations

cm Centimeter

cP Centipoise

g Gramme

HRT Hydraulic retention time

SRT Solids residence time

Notations

A Cross sectional area of column (m^2)

A_{es} Projected area of standard EtOH (m^2)

A_{eu} Projected area of unknown sample (m^2)

A_{mr} Projected area of MeOH reference (m^2)

A_p Surface area of particle (m^2)

Ar Archimedes number

Bo' Bond number

Bo_R Bodestein number based on hydraulic radius

C Tracer response to pulse injection

C_{ab} Concentration of aniline blue (g/l)

C_b Concentration of biomass (g/l)

C_D Drag coefficient defined

C_{db} Concentration of dextran blue (g/l)

C_e Ethanol concentration (g/l)

C_{ee} Concentration of ethanol at exit (g/l)

C_{em} Maximum concentration of ethanol (g/l)

C_{es} Concentration of standard EtOH (g/l)

C_f Concentration of ethanol in feed (g/l)

C_{fc} Concentration of feed component (mol/l)

C_{fl} Concentration of fluorescein (g/l)

C_{mg} Concentration of methyl green (g/l)

C_{mv} Concentration of methyl violet (g/l)

C_s Substrate concentration (g/l)

C'_s Substrate concentration at bioparticle surface (g/l)

C_{si} Inlet glucose concentration (g/l)

C_{tr} Tracer concentration (g/l)

C_{mt} Minimum tracer concentration (g/l)

$c_{tr,t}$ Tracer concentration at time t (g/l)

$c_{tr,\infty}$ Tracer concentration at infinite time (g/l)

D_c Column diameter (m)

D_e Diffusion coefficient (m^2/s)

D_i Dilution factor

d_i Diameter of particle i (m)

d_p Particle diameter (m)

d_{sph} Diameter of sphere (m)

D_z Axial liquid dispersion coefficient (m^2/s)

D_{zc} Axial liquid dispersion coefficient for empty column (m^2/s)

E_i Energy dissipation per unit mass of liquid in equation 3.17b (m^2/s^3)

E_z Energy dissipation per unit mass of liquid in equation 3.8b (m^2/s^3)

F Tracer response to step input

F_d Apparent drag force on particle (N)

f_g Gas flow rate (ml/min)

F_c Effective gravitational force (N)

f_{gz} Gas flow rate at axial position z (ml/min)

f_L Liquid flow rate (ml/min)

$Fr_{p,g}$ Froude number for gas

$Fr_{p,L}$ Froude number for liquid

g Gravitational acceleration (m^2/s)

G Mass flow rate per unit cross-sectional area of column ($Kg/m^2.s$)

Ga Galileo number

G_u Glucose consumed (%)

H_b Fluidized bed height (m)

HMU Height of liquid phase axial mixing unit (m)

H_0 Unfluidized bed height (m)

K'_p Product saturation constant for product formation (g/l)

K'_s Substrate saturation constant for product formation (g/l)

k_1 First order rate constant in eqn. 2.18 ($m^3Kg^{-1}s^{-1}$)

k_2 Kinetic constant defined in equation 2.21c (m^{-1})

K_2 Kinetic constant (l/g)

K_3 Kinetic constant (l/g)

K_4 Kinetic constant (l/g)

k_L Mass transfer coefficient (m/s)

k_o Zero order rate constant in eqn. 2.16c (s^{-1})

K_p Product saturation constant for biomass growth (g/l)

K_s Substrate saturation constant for biomass growth (g/l)

L Length of test section (m)

L_b Thickness of biomass particle or film (m)

L_c Characteristic length of particle (V_p/A_p)

L_p Length of extruded particle (m)

m Hydraulic radius of column (m)

M_d Mean deviation (%)

ΔP Total pressure drop across bed (N/m^2)

P Ethanol productivity based on liquid volume (g/l.hr)

P'' Rate of ethanol production (g/hr)

P' Ethanol productivity based on empty column (g/l.hr)

P_{atm} Atmospheric pressure (N/m^2)

Pe Peclet number defined as ($u_L L/D_z$)

Pe' Peclet number defined as ($v_L L/D_z$)

Pe'_c Peclet number defined as ($v_L D_c/D_z$)

Pe_c Peclet number defined as ($u_L D_c/D_z$)

Pe'_p Peclet number defined as ($v_L d_p/D_z$)

Pe(BC) Peclet number for bubble column ($u_g D_c/D_z$)

$Pe_{p,t}$ Peclet number defined as ($u_t d_p/D_z$)

r Radial position in the column (m)

R Correlation coefficient

R^2 Goodness of fit

$(Re_p)_{mf}$ Particle Reynolds number at minimum fluidization condition

Re Reynolds number defined as ($\rho_L D_c u_L/\eta$)

Re'_p Reynolds number defined as ($\rho_L d_p v_L/\eta$)

Re_p Reynolds number defined as ($\rho_L d_p u_L/\eta$)

$Re_{p,g}$	Reynolds number defined as $(\rho_L u_g d_p/\eta)$
$Re_{p,t}$	Reynolds' number defined as $(\rho_L d_p u_t/\eta)$
r_m	Radius of support particle (m)
R_s	Reaction rate (g/l.s)
Sc	Schmidt number
Sh	Sherwood number
t	Time (s)
T	Temperature ($^{\circ}C$)
t_f	Fermentation time (min)
$t_{g,avg}$	Average gas residence time (min)
$t_{L,avg}$	Average liquid residence time (min)
u_b	Rising velocity of bubble (m/s)
u_c	Liquid circulation velocity defined by equation 3.6b (m/s)
u_{gL}	Slip velocity (m/s)
u_L	Superficial liquid velocity (cm/s)
u_R	Velocity ratio defined as (v_L/u_t)
u_t	Particle terminal velocity (m/s)
V_b	Volume of fluidized bed (m^3)
V_f	Volume of culture filtered (m^3)
V_{inj}	Volume of tracer injected (m^3)
v_L	Interstitial liquid velocity (u_L/ε_L) (cm/s)
V_p	Particle volume (m^3)
We	Weber number
W_f	Weight of filter paper (g)
W_{fd}	Weight of filter paper plus deposit (g)
W_s	Total weight of solids (g)
W_{tr}	Weight of tracer injected into column (g)
Y_{bs}	Biomass yield
Y_{ps}	Product yield
z	Axial position in the bioreactor (cm)

Greek Letters

β	Production rate per unit volume of biomass (g/l.s)
α	Diffusivity ratio
ε_L	Liquid holdup
ε_g	Gas holdup
ε_s	Solid holdup
ε	Bed voidage
ε_0	Bed porosity at zero gas and liquid velocities
ζ	Particle effectiveness factor
ζ_0	Particle effectiveness factor for zero order reaction rate
ζ_1	Particle effectiveness factor for first order reaction rate
ζ'	Particle effectiveness factor defined by eqn. 2.19
η	Liquid viscosity (cP)
η_w	Water viscosity (cP)
Θ	Dimensionless residence time
Θ_{avg}	Average dimensionless residence time
λ_{max}	Wavelength of maximum light absorption (nm)
μ	Specific growth rate (hr^{-1})
μ_{max}	Maximum specific growth rate (hr^{-1})
μ_s	Specific rate of substrate assimilation (hr^{-1})
ν	Specific rate of ethanol production (hr^{-1})
ν_0	Specific rate of ethanol production at zero ethanol concentration (hr^{-1})
ν_{max}	Maximum specific rate of ethanol production (hr^{-1})
ρ_p	Particle density (Kg/m^3)
ρ_b	Dry density of bioparticle (Kg/m^3)
ρ_s	Solid density (Kg/m^3)
σ	Variance of tracer curve (s^2)
σ_θ	Dimensionless variance
τ	Residence time (s)
τ_s	System residence time (s)
τ_e	Residence time based on empty column (s)
τ_c	Residence time calculated from RTD data (s)

τ_d	Diffusion time of tracer into biomass (s)
υ	Generalized viscosity constant
Φ_R	Dimensionless parameter defined by equation 2.21c
Φ_{om}	Modified zero order Thiele modulus
Φ_o	Thiele modulus for zero order reaction
Φ_{1m}	Modified first order Thiele modulus
Φ_1	Thiele modulus for first order reaction
ψ	Surface tension (dyne/cm)
ψ_p	Particle sphericity
ω	Degree of substrate inhibition for ethanol
ξ	Danckwerts degree of segregation

CHAPTER ONE

GENERAL INTRODUCTION

1.1 GENERAL

In biotechnology, microorganisms are used as catalysts in two major areas of application; in the stabilization or treatment of domestic and industrial wastewaters and in bioproduction of useful materials such as enzymes, antibiotics, fuel, alcoholic beverages and vinegar and numerous other organic compounds.

The basic principle, in most of these applications, is the same. The microorganisms are supplied with adequate growth nutrients. The limiting substrate is usually the carbon source. Environmental conditions such as temperature and pH, are controlled at optimum values conducive for the healthy growth of the microorganisms. Oxygen may be supplied in form of air or pure oxygen. There are, however, some microorganisms which require an absence of oxygen. These types are called anaerobic so as to distinguish them from those needing oxygen or aerobic types. In wastewater stabilization, the main cause of pollution, the carbon source, serves as the substrate.

At favourable environmental conditions, the microorganisms consume the substrate and their population increases while byproducts of metabolism, which may be useful materials, are produced. The nature of the products formed and the rate at which the production or waste stabilization proceeds, are dependent on the type of the microorganisms, the food source and the prevailing enviromental conditions in which the organisms live.

Bioconversions proceed via a multiple of complex biochemical reactions taking place within the microbial cells. In some cases the substrate or the byproduct, formed, could inhibit some of these reactions causing low rate of microbial activity and this may affect the overall rate of the bioconversion. Transportation of substrate in and products out of the microbial cells can also, significantly, affect the performance of the microorganisms. It is thus essential to ensure that

transport phenomena are not rate limiting or that their effects must be considered in determining the overall rate of product formation or wastewater stabilization.

In suitable environment, the rate of growth of the microorganisms depends on the nature of the organisms and substrate, concentration of the microorganisms and the kinetics of the bioreaction; whether it is product or substrate inhibited. The specific growth rate of the microorganisms (μ) is defined as shown in equation 1.1.

$$\frac{dC_b}{dt} = \mu C_b \qquad 1.1)$$

The specific growth rate is not a constant; it is dependent on substrate concentration. The most commonly used equation, giving the relationship between specific growth rate and the limiting substrate concentration, is the Monod's equation (Eqn. 1.2).

$$\mu = \mu_{max} \frac{C_s}{K_s + C_s} \qquad 1.2)$$

Substituting this value of μ into equation 1.1, gives

$$\frac{1}{C_b}\frac{dC_b}{dt} = \mu_{max} \frac{C_s}{K_s + C_s} \qquad 1.3)$$

The left hand side of equation 1.3 is the specific growth rate of the microorganisms and its inverse gives the solids or cells retention time (SRT). Thus, the minimum solids retention time is closely related to the maximum growth rate of the organisms. An efficient microbial process must have solid retention time (SRT) that is ten times the minimum SRT (Jewel, 1985).

The rate of growth of microorganisms is related to the rate of substrate utilization via the yield factor (Y_{bs}) and is given by equation 1.4.

$$-\frac{dC_s}{dt} = \frac{1}{Y_{bs}}\frac{dC_b}{dt} \qquad 1.4)$$

Therefore, if the endogenous respiration of the cells is neglected and neither the product nor the substrate are inhibiting, the rate of substrate utilization is given by equation 1.5 (Bailey and Ollis, 1977; Jewel, 1985).

$$-\frac{dC_s}{dt} = \frac{\mu_{max}}{Y_{bs}}\frac{C_s\, C_b}{K_s + C_s} \qquad 1.5)$$

It is evident, from equations 1.3 and 1.5, that high concentration of microorganisms coupled with high SRT are essential if efficient microbial process, as seen by high rate of substrate utilization and high rate of bioconversion, is required. A means to achieving high SRT and high biomass concentration, in biological systems, is the immobilization of the microbial cells. Immobilization was reported to cause tremendous increases in biomass concentration and solids retention time (Kosaric and Blaszczyk, 1990).

1.2 IMMOBILIZATION OF MICROBIAL CELLS

Microorganisms are said to be immobilized if they are physically confined to particular regions in space and used repeatedly without losing their microbial activity or characteristics (Klein and Wagner, 1983). Godia, Casas and Sola (1987b) have outlined the advantages of immobilization as follows:-

i) Population of microbial cells is substantially increased and this results in increased rate of substrate utilization and productivity.

ii) Risk of contamination is minimized because of the high density of immobilized cells in the reactor.

iii) Accidental changes in the feed composition or other operating conditions can be contained easily. This is

because fermentation activity can be restored quickly once the problem is solved.

iv) Immobilized systems are very suitable for use in continuous operations and hence, effective system control can be applied.

Cell immobilization can, however, have negative effects on the behaviour of cells. The extent of any effect depends on the type of microorganism, carrier, immobilization technique and the biochemical reaction of interest. Common effects encountered include poisoning of cells, high diffusional resistance of carrier material, and partitioning effects (Klein and Wagner, 1983; Kennedy and Cabral, 1983; Fan, 1989). In spite of these, immobilized microbial systems have been used in the production of enzymes, fuel ethanol, vinegar, beverages and a number of organic acids and substances and for the treatment of municipal and many industrial effluents (Linko and Linko, 1983; Jewel, 1985; Fan, 1989).

There are, broadly, two methods of cell immobilization; attachment and entrapment (Scott, 1987). The later refer to cases where organisms are caught in the interstices of fibrous or porous materials or are restrained within by a solid or porous matrix such as stabilized gel or membrane. Attachment refers to methods in which the organisms are made to adhere to surfaces or other organisms by self adhesion or chemical bonding. There are also many sub-categories within each of these types of immobilization. These are reviewed elsewhere (Klein and Wagner, 1983; Kennedy and Cabral, 1983; Scott, 1987; Godia, *et al.*, 1987b; Fan, 1989) and, as such, only brief discussion is presented here.

1.2.1 Attachment of cells

Many types of cells have the ability to aggregate with other organisms or to adhere to inert solid surfaces. Immobilization of microorganisms to solid surfaces is an

ancient practice for the manufacture of vinegar and in trickling filters, used for the treatment of potable water (Karkare, Dean. Jr. and Venkatasubramanian, 1985). The mechanism involved in the immobilization is not fully understood (Atkinson and Fowler, 1974). It is however believed that some types of organisms secrete macro molecules such as polymucosaccharides that act as a 'glue' which binds cells, together, or to the solids' surfaces (Scott, 1987; Kosaric and Blaszczyk, 1990). The two most important methods of cell attachment are aggregation and attachment to surfaces.

1.2.1.1 *Cell aggregation*

Some organisms tend to form aggregates or floc particles. This occur with various yeast strains including *Saccharomyces cerevisiae* and some bacteria; for example certain strains of *Zymomonas mobilis* (Prince and Barford, 1982c). The size of flocs depend on the type of microorganisms and on other factors such as cell age, ionic strength, pH, and medium composition (Scott, 1987). Greenshields and Smith (1971) have observed that the yeast *S. cerevisiae* has strains of differing flocculation capacity; the physically limited and the fermentation limited. With the former, increase of liquid flow rate, above a certain value, can cause the complete washout of the yeast flocs. With the later type, the flocs do not get washed out even at considerably high liquid flow rates, but the fermentation becomes less efficient. Self flocculating microorganisms have been used for the manufacture of ethanol (Ault, Hampton, Newton and Roberts, 1969; Prince and Barford, 1982a).

Microbial aggregation can be induced under some enviromental conditions and can also be enhanced by the addition of polyelectrolytes (Aiba and Nagatani, 1971; Kosaric and Blaszczyk, 1990).

1.2.1.2 *Attachment to surfaces*

Many types of microorganisms have a tendency to adhere to solid surfaces. This sometimes causes problems as in the case of marine fouling or tooth plaque, but it also has bioprocessing applications. A thin microbial layer or biofilm, of thickness about 50 to 200 μm, is made to grow on the surfaces of stones and sand, coal, or resin particles of sizes 0.2 to 0.8 cm (Heijnen, Mulder, Enger and Hoeks, 1989). There is, usually, an optimum biofilm thickness above which penetration of nutrients into the microbial film is hindered. This means that there is no supply of essential nutrients to the cells at points deep inside the biofilm. Decay of these cells could lead to the loss of the entire biofilm (Atkinson and Fowler, 1974).

Factors affecting the formation of biofilm on inert surfaces are still being studied (Gorris, van Deursen, van der Drift and Vogels, 1989), however, addition of synthetic polymer was found to enhance retention of biomass on solid surfaces (Stronach, Diaz-Baez, Rudd and Lester, 1987).

Microbial cells have been attached to surfaces of granular activated carbon, coal and sand particles and used for the treatment of biodegradable and non-biodegradable wastewaters (Pfeffer and Suidan, 1989), whey (Boening and Larsen, 1982), and synthetic waste waters (Chen, Li, and Shieh, 1985a; Gommers, Bijleveld and Kuenen, 1988a).

1.2.2 Entrapment of cells

These techniques of immobilization do not depend on cell properties. The cells are held within the interstices of porous materials such as sponge or fibrous substances, or physically restrained by membrane or encapsulating gel matrices.

1.2.2.1 *Encapsulation*

Physical entrapment of organisms inside a polymeric matrix is a widely used technique for cell immobilization. The biocatalysts are mostly used in form of beads and are formed by first adding the cell suspension to an aqueous solution of the gelling material. The resultant mixture is then formed into droplets either by forcing it dropwise through a nozzle or orifice or by dispersing it into a non interacting liquid medium (Klein, Vorlop, Eng, Kluge and Washausen, 1979; Scott, 1987). Natural gels such as alginate and K-carrageenan are mostly used (Godia, Casas and Sola, 1987a). However, other synthetic materials such as polyacrylamide are also used (Morikawa, Karube and Suzuki, 1980). Alginate beads have been used for the manufacture of ethanol (Williams and Munnecke, 1981; Lee, Ahn and Ryu, 1983).

The choice of carrier depends on the process requirements, but materials which are cheap, have high porosity and mechanical strength and do not have any harmful effects on the microorganisms, are preparable (Nagashima, Azuma, Noguchi, Inuzuka and Samejima, 1984).

1.2.2.2 *Membranes*

Semipermeable membrane materials are used to isolate cells from the bulk liquid. The membrane allows the molecular transport of soluble matter to and from the immobilized cells while confining and protecting the organisms. This method of immobilization has been used for the manufacture of ethanol (Mehaia and Cheryan, 1984) and for the hydrolysis of protein (Deeslie and Cheryan, 1981).

Substrate and product diffusion, membrane plugging, and low operational stability are the main problems associated with this immobilization technique (Godia *et al.*, 1987b). It is also necessary to control microbial growth in order to prevent excessive build-up of biomass since this could cause high pressure that may rupture the

membrane.

1.2.2.3 *Porous materials*

Mats of fibres such as cotton, nylon mesh or cloth, metallic mesh and various types of foams or sponge have voids that allow organisms to penetrate and grow into large colonies. This immobilization method was used for conversion of xylose to ethanol (MacDonald, 1991) and for the manufacture of vinegar (Ationu, 1986).

1.3 BIOLOGICAL REACTORS

Numerous types of biological reactors or fermenters are used in processing of biochemicals. There are, however, two types of operational modes; batch and continuous. The batch mode is the traditional means of carrying out bioconversions. A batch fermenter is a large vessel into which the organisms, substrate and nutrients are placed together. Stirring may be provided while the temperature and pH are, usually, controlled until virtually all the substrate is utilised. The product and the organisms are then removed and separated.

The major problem with batch fermenters is that they cannot easily be integrated into continuous operation systems (Margaritis and Merchant, 1987). They are also not suitable for processes exhibiting substrate inhibited kinetics because of the high starting concentration of substrate. Furthermore, biomass build-up in the batch fermenter is limited. When immobilized cells are used, a separation process is required to recover the cell preparation, to permit its re-use. During the operation of this recovery process, appreciable loss of biomass may occur, as well as, loss of activity. So, for industrial processes, the use of immobilized cells in a batch operation will be limited to the production of rather small amounts of fine chemicals (Kennedy and Cabral, 1983).

Other forms of batch fermenter are the batch recirculation and fed batch bioreactors. The former may be packed or fluidized bed with complete recycle of the effluent. It is useful in cases where a single pass gives inadequate conversion and it has the advantage that mass transfer effects can be reduced due to the high operational fluid velocities (Kennedy and Cabral, 1983). In the fed batch fermenter, the substrate is fed continuously and no outlet is provided. The advantage of this system over the conventional batch fermenter, is that the substrate inhibition effect could be reduced, because of the high biomass concentration and low substrate feed rate. However its major drawback is the accumulation of product in the fermenter, and this could interfere with the viability of the organisms, expecially for processes exhibiting product inhibition.

There are many types of continuous fermenters in use for biochemical reactions. Four of these are most widely used and are disscussed in the proceeding sections.

1.3.1 Continuously Stirred Tank Fermenter (CSTF)

The CSTF is a stirred tank, containing the organisms, into which the substrate and nutrients are continuously fed (Fig. 1a). The product and biomass are also, continuously, removed in the effluent. The rate of biomass removal, in the effluent, is balanced by the rate of biomass production in the bioreactor. Because of this biomass wastage, it is difficult to obtain high biomass concentration in the CSTF. Productivity of the CSTF is, therefore, limited as a result of relatively low biomass concentration. Even where the organisms are immobilized in alginate beads, significant leakage and attrition of active cells has been observed (Lee *et al.*, 1983). Constant stirring may also cause destruction of viable cells and carrier, due to the shearing effect.

The CSTF is suitable for processes with substrate

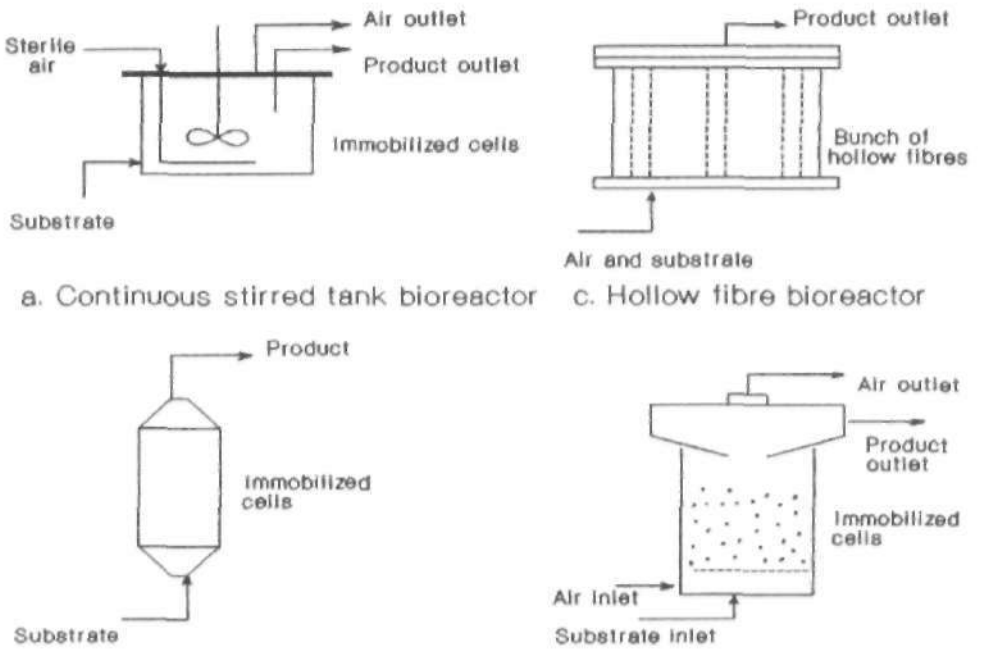


Fig. 1: Types of continuous bioreactors

(Venkatasubramanian, Karkare and Vieth, 1983)

inhibited kinetics because the substrate concentration anywhere within the bioreactor is the same as the substrate concentration in the effluent. On the other hand, high product concentration in the reactor make CSTF unsuitable for processes having product inhibited kinetics.

1.3.2 Packed Bed Fermenter (PBF)

This is the commonest bioreactor used with immobilized cell systems. When the biocatalyst is in the form of beads, chips, disks, foam, fibre, pellets or sponge, it can be packed easily into a column (Fig. 1b). Usually liquid, containing the substrate, is passed into the column from the bottom, though, it can also be passed from the top as in trickle filters. If the velocity profile across the packed bed is flat, then the reactor is said to operate as a plug flow. But, deviations from this

idealized condition do occur (Anselme and Tedder, 1987; Swaine and Daugulis, 1989).

Packed bed fermenters have the advantage of simplicity in operation and are particularly suitable for processes with product inhibited kinetics, because high product concentration occurs at the reactor exit only. On the other hand, PBF is not suitable for processes inhibited by substrate due to high concentration of substrate at the entrance to the reactor.

For aerobic systems or where gas is produced, poor gas-liquid contact may cause inefficient bioconversion. Furthermore, packed bed fermenters have the disadvantage of relatively poor mass transfer rates, channelling (which inactivates portions of the bed) and compaction under downward flow conditions (Karkare *et al.*, 1985). Moreover, plugging of packed beds also does occur due to biomass growth or presence of inert solids in the feed. This could result in high pressure drop across the bed and high gas hold up (Anselme and Tedder, 1987).

However, in spite of the above shortcommings, packed bed fermenters have been used, in the laboratory, for the manufacture of ethanol, using yeast immobilized in calcium alginate (Williams and Munnecke, 1981), carrageenan (Godia *et al.*, 1987a) and on brick particles (Anselme and Tedder, 1987). They were also used for pilot scale manufacture of ethanol (Nagashima *et al.*, 1984). Packed bed fermenters, often referred to anaerobic filters, have been used for anaerobic treatment of wastewaters (Sahm, 1984; Kosaric and Blaszcyk, 1990).

1.3.3 Hollow Fiber Fermenter (HFF)

As the name suggests, this fermenter is made-up of layers of hollow fibers that separate the biocatalysts from the substrate (Fig. 1c). The biocatalyst is immobilized either on the shell or tube side of the hollow fiber. This type of fermenter was used by Mehaia and

Cheryan (1984), for the production of ethanol using *S. cerevisiae*. They obtained ethanol productivity of 10 g/(l.hr), which was about five times that of a batch fermenter. Their observations indicated that the fibre barrier causes very low mass transfer rates. Also cells far from the fibre become non-viable due to lack of nutrients. Removal of these cells form the reactor was necessary, otherwise the high cell density could cause pumping problems that may lead to rupture of the sensitive fibre.

The hollow fiber fermenter is not suitable for processes with substrate inhibited kinetics, because due to poor liquid mixing, the cells at the entrance to the reactor experiance high substrate concentrations. But it is suitable for processes exhibiting product inhibition, because high product concentration occurs only at the exit of the reactor.

1.3.4 Fluidized Bed Fermenter (FBF)

The FBF is in between the CSTF and the packed bed fermenter. The substrate is passed through the bottom of the reactor (Fig. 1d) at a velocity sufficient enough to expand the bed of particles, of immobilized microorganisms, beyond the point at which the frictional drag, exerted on the particles by the flowing liquid, is balanced by the down-ward force, exerted by gravity. Usually, the organisms are either self flocculating or immobilized on fine inert particles such as sand, coal, charcoal and beads made from natural or artificial materials (Setiadi, 1989). The support particles are usually of size 0.2-0.8 mm in diameter, creating a surface area in the order of 2000 m^2/m^3 of bed; and fluidization allows the entire surface of each particle to be colonized by the organisms, resulting in a biomass concentration near 40 g/l (Heijnen *et al.*, 1989). This high biomass concentration allows the reactor size and processing times

to be markedly reduced (Switzenbaum, 1985).

Fluidized beds containing flocculant yeast have been used in the production of beer and fuel ethanol (Ault *et al.*, 1969; Prince and Barford, 1982a). FBF have also been used for the treatment of domestic wastewater and many types of industrial effluents (Sahm, 1984), and for the manufacture of antibiotics, enzymes, and vinegar (Fan, 1989). Examples of these applications are listed in Tables 1.1 and 1.2 for wastewter treatment and bioproduction, respectively.

Table 1.1 Some applications of fluidized bed fermenters in wastewter treatment

Type of wastewater	Reference
Sulphide and acetate waste	Gommers *et al.*, 1988a&b
Nitrate waste	Narji, Khilar, and Mahajan, 1984
Phenolic waste	Pfeffer and Suidan, 1989
Dairy waste	Bull, Sterritt and Lester, 1982
Whey treatment	Boening and Larsen, 1982
Synthetic meat waste	Stronach *et al.*, 1987
Industrial waste	Bull, Sterritt and Lester, 1984
Sewage and Municipal waste	Yoda, Hattori and Miyaji, 1985; Stronach, Rudd and Lester, 1986a&b; Goris *et al.*, 1989
Synthetic waste	Chen *et al.*, 1985a

Sahm (1984) has outlined some of the advantages of fluidized bed biorectors as follows:-

i) Maximum contact between liquid and immobilised microorganisms is provided. This enhances the mass transport rates, in and out of cells.

Table 1.2 Some applications of fluidized bed fermenters in bioproduction

Product	Reference
Ethanol	Ault *et al.*, 1969; Greenshields and Smith, 1971; Scott, 1983; Bland, Chen, Jewel, Bellanny, and Zall, 1982; Prince and Barford, 1982b; Jones, Korus, Admassu and Heimsch, 1984; Nagashima *et al.*, 1984; Karkare *et al.*, 1985; Davison, 1988
Fructose	Ching, Ho, and Rathor, 1984
Hydrolysis of maltodextrins	Hamdane, Wilhem and Riba, 1988
Glycerol	Vijaikishore and Karanth, 1986
Isopropanol	Schoutens, Guilt, Zielemen, Luyben, and Kossen, 1986
Bacitracin	Morikawa *et al.*, 1980
Patulin	Berk, Behie, Jones, Lesser, and Gaucherl, 1984

ii) Problems of channelling, plugging and gas hold-up are avoided because the bed can expand to accomodate the gas bubbles or growing biomass (Andrews and Przezdziecki, 1986).

iii) Ability to control and optimize the size of the immobilized organisms.

iv) The support medium enables the FBF to retain high biomass concentrations and thereby operate at significantly reduced hydraulic retention time.

v) In wastewater treatment, large changes in organic loading rates and temperature can be tolerated without significantly damaging the treatment efficiency; and both high and low strength wastewaters originating from diverse sources can be treated successfully.

vi) There is relatively better fluid mixing in FBF

compared to PBF and because of this mixing, processes with both substrate and product inhibition, can fairly be handled in FBF (Venkatasubramanian, Karkare and Vieth, 1983; Fan, 1989).

However, operation of a fluidized bed bioreactor could be curtailed by shearing effects, on immobilized cells, due to liquid and gas flows. Therefore, both gas and liquid flows have to be properly controlled (Fan, 1989). Moreover, there is also inevitably some liquid back mixing which reduces the overall efficiency of the reactor (Ching *et al.*, 1984).

1.3.5 Other Fermenter types

Other types of bioreactors, used particularly in wastewater treatment, are the contact reactor (CR) and the upflow anaerobic sludge blanket (UASB). The contact reactor is essentially a CSTF with biomass recycle; the effluent from the CSTF is passed into a clarifier where the biomass is settled and returned into the CSTF. Because the biomass is retained and recycled, the performance of this system could be better than that of the CSTF. However, a major difficulty encountered with this reactor is in the biomass separation process, where gas bubbles tend to adhere to the biomass flocs and hinder proper settling (Sahm, 1984).

The UASB is very much similar to the fluidized bed bioreactor. The liquid is passed, from the bottom, through a bed of flocculated biomass. The performance of UASB depends on the flocculating characteristics of the biomass (Sahm, 1984).

Various combinations or variations of these bioreactors can be used in order to achieve the desired objective (Venkatasubramanian *et al.*, 1983).

1.3.6 Choice of reactor type

The choice of the reactor type is very much influenced by the operational requirements. Type of organisms, method of immobilization, nature of the support material and the chemical and the physical properties of the substrate and the products also influence the choice of reactor type (Venkatasubramanian *et al.*, 1983). A summary of some of the characteristics of these bioreactors is presented in Table 1.3.

Table 1.3 *Characteristics of continuous* fermenters

Character	CSTF	HFF	PBF	FBF
Operation	Easy	Easy	Easy	Difficult
Catalyst: Attrition Replacement	 High Easy	 Low Easy	 Low Difficult	 Low Easy
Cell removal	Easy	Easy	Difficult	Easy
Pressure drop	Low	Low	High	Low
Mixing	Good	Fair	Poor	Good
Viable cells	Uniform	Uneven	Uneven	Uniform
Oxygen transfer	Good	Fair	Poor	Good
Scale-up	Easy	Difficult	Easy	Difficult
Cost	Low	Low	Low	High
Control	Easy	Difficult	Difficult	Easy
Suitability for: Product inhibited Kinetics Substrate inhibited kinetics	 Poor Good	 Good Poor	 Good Poor	 Fair Fair

(CSTF = Continously stirred tank fermenter; PBF = Packed bed fermenter; HFF = Hollow fibre fermenter; FBF = Fluidized bed fermenter)

(Fan, 1989)

A comparism of their capabilities, in anaerobic treatment of wastewater and ethanol production, are shown in Tables 1.4 and 1.5 respectively.

Table 1.4 Capabilities of bioreactors in anaerobic wastewater treatment

Reactor type	HRT, t_h (days)	SRT, t_s (days)	Loading rate, L_r (kg COD $m^{-3}d^{-1}$)
CSTF	10-60	10-60	0.25-3
CR	12-15	20	0.25-4
UASB	0.5-7	20	10-30
PBF	0.5-12	20	1-40
FBF	0.2-5	30	1-100

(CR = Contact reactor; UASB = Upflow anaerobic sludge blanket; HRT = Hydraulic retention time; SRT = Solids retention time)

(Kosaric and Blaszczyk, 1990)

Table 1.5 Capabilities of bioreactors in ethanol production

Reactor	Inlet sugar, C_{si} (g/l)	Glucose used, G_u (g/l)	Ethanol concn., C_e (g/l)	Productivity P g/(l.hr)
CSTF	300	-	130	4.8
HFF	89	27	12	26
PBF	127	100	59.7	8.9
FBF	100	94	47	21.2

(Godia, Casas and Sola, 1987b)

It is evident, from these tables, that the fluidized bed bioreactor has some unique advantages over the rest. It enjoys good mixing of phases, low catalyst attrition, uniform distribution of viable cells, high solids retention time (SRT) and high through-put at relatively short hydraulic retention time (HRT). Ethanol productivity and sugar utilization in the FBF are also high compared to other fermenter types.

1.4 OPERATION OF FLUIDIZED BED FERMENTER

A FBF can be operated either as a two phase (S-L) or as a three phase (S-L-G) system. In both cases, the immobilized cells form the solid phase and the growth medium is the liquid phase. The gas phase, in the three phase system, may be oxygen or air if an aerobic condition is required. It will be another gas if an anaerobic condition is needed.

An example of the fluidized bed anaerobic fermenter (FBAF) is the tower fermenter used in the production of beer and fuel ethanol from glucose, using flocculating strains of the yeast *S. cerevisiae* or the bacterium *Z. mobilis* (Greenshields and Smith, 1971; Prince and Barford, 1982b).

Much work on FBAF is, at present, mainly in laboratory and pilot scales. FBAF has successfully been employed, in the laboratory, for the treatment of municipal and industrial wastewaters, and for the manufacture of ethanol as earlier presented in Tables 1.1 and 1.2. Pilot scale testings have shown that the reactors are very effective for the treatment of various wastewaters including those from the dairy, chemical, food processing, and soft drink industries; where more than 80% COD removal at organic loading rates of 16 $kgm^{-3}day^{-1}$ COD or higher, has been achieved (Sahm, 1984).

Three full scale fluidized bed anaerobic fermenters have been constructed, for wastewater treatment, by three

companies; Ecolotrol HY-FLO, Dorr-Oliver and Gist-Brocades (Heijnen *et al.*, 1989). Also, industrial scale reactors have been in use in the U.K., for the manufacture of beverages and vinegar, since 1971 (Greenshields and Smith, 1971).

Many applications of fluidized bed anaerobic fermenters produce gas *in situ* as a by-product of the biochemical reactions. This gas constitutes the gas phase in an otherwise, two phase, S-L system.

1.4.1 FBAF with *in situ* gas production

In conventional fluidized bed anaerobic bioreactors, the particles are supported by the combined flow of liquid and gas, both of which are introduced at the bottom of the reactor. In FBAF with *in situ* gas production, no gas is passed into the reactor; it is produced *in situ* as a result of the biochemical reactions. Because of the low liquid flow experienced in this type of reactors, the generated gas bubbles were thought to support the bioparticles (Gommers *et al.*, 1986; Fan, 1989). Examples of such applications include the treatment of sewage and industrial effluents where carbon dioxide, methane, nitrogen, and hydrogen sulphide gases could be produced. Also in beer and fuel ethanol manufacture, large amounts of carbon dioxide are produced.

Despite the numerous advantages of FBAF and its potential for use for many biochemical processes, it is not in much commercial use when compared to batch fermenters or CSTF (Fan, 1989). The main reason for this is that fluidized beds have traditionally been associated with problems of cumbersome and difficult operation; a tendency exacerbated by the difficulty of modelling the behaviour of fluidized bed reactors and, consequently, the inability to predict accurately the performance of the scaled-up version of the reactor (Vekatasubramanian *et al.*, 1983). But, in spite of these complications, many

researchers have directed efforts at modeling the FBF (Ching *et al.*, 1984; Hamdane *et al.*, 1988; Davison, 1988; Setiadi, 1989; Lin, 1991; Setiadi and Larsen, 1991). The model they generally used is that of a plug flow with superimposed dispersion, which accounts for the deviation from ideal plug flow behaviour. It consists of three terms; dispersion, convection and reaction. In this model the substrate concentration, at any point along the column length, is given by equation 1.6, for steady state situation.

$$D_z \frac{d^2 C_s}{dz^2} - \frac{u_L}{\varepsilon_L} \frac{dC_s}{dz} + R_s = 0 \qquad 1.6)$$

The basic assumptions, in using this model, are that the axial liquid dispersion coefficient (D_z) and phase holdups are uniform throughout the column and the radial dispersion is negligible. The assumption of negligible radial dispersion holds well particularly for beds of small diameter particles because, for these systems, the D_z was found to be twenty to thirty times higher than the radial dispersion coefficient (El-Temtamy, El-Sharnoubi and El-Halwagi, 1979b).

On the other hand, assumptions regarding the uniformity of axial liquid dispersion coefficient and phase holdups may not hold, particularly in fluidized bed anaerobic bioreactors with *in situ* gas production. This is because D_z and the holdups may be dependent on gas velocity which increases with increasing bed height.

The dispersion model, shown in equation 1.6, is a single parameter model in which deviation from ideal plug flow is represented by the axial liquid dispersion coefficient, D_z. This deviation occurs as a result of backmixing of the liquid phase caused by the rising gas bubbles, liquid turbulence and the motion of the suspended particles (El-Temtamy, El-Sharnoubi and El-Halwagi,

1979a). Thus, the dispersion coefficient, is a measure of the extent of liquid mixing, in fluidized bed bioreactors. It is evident, from equation 1.6, that liquid mixing, represented by D_L, is an important phemonenon in the modelling and subsequent scale-up of FBF. It has been noted that liquid mixing in fluidized bed bioreactors has significant influence on physical processes such as interphase, intercellular or interparticle mass and heat transfer (Kikuchi, Konno, Kakutani, Sugawara and Ohashi, 1984). Liquid mixing also affects the residence time of fluid elements that enter the reactor which, in turn, determines the reactor height required to achieve a given substrate conversion level (Setiadi and Larsen, 1991).

A further look at equation 1.6 indicates that the liquid holdup (ε_L) is another important parameter, for modelling of fluidized bed bioreactors. This parameter also affects the residence time of fluid elements entering the system and, as such, it also determines the conversion level achievable.

There exists much information concerning the estimation of the dispersion coefficient and liquid holdup in fluidized bed reactors. But, much of this information relates to the applications of fluidized bed reactors in chemical processes, whereas different particles and process conditions are used in bioprocesses. Typical bioparticles have density very close to that of the liquid medium and, because of the low density of the particles, the operating gas and liquid velocities are very small. In FBAF with *in situ* gas production, the velocity of gas is in the order of 0.05 to 0.20 cms^{-1} (Gommers, Christoffels, Kuenen and Luyben, 1986).

It is, perhaps, the realization of these basic differences between chemical and biological processes that induced some researchers (Kikuchi *et al.*, 1984; Gommers *et al.*, 1986; Setiadi 1989) to study axial liquid dispersion in fluidized bed reactors, at conditions similar to those

obtained in fluidized bed bioreactors. Unfortunately, these studies were carried out with abiotic systems in which gas was supplied externally and, as such, the correlations arrived at cannot, with certainty, be said to be applicable to biological systems. Moreover, according to Gommers *et al.* (1986), results obtained with external gas supply set the upper limit for modelling of reactors with *in situ* gas production. But, results obtained from experiments with two phase, liquid-solid systems may not be of use either, because as Brohan and McLoughlin (1984a) observed, the liquid velocity at which complete liquid mixing occured in tower fermenter was about eighteen times higher in abiotic systems compared to bioactive ones.

Measurements of axial liquid dispersion coefficients in fluidized bed anaerobic bioreactors were made by a few researchers (Brohan and McLoughlin, 1984a; Admassu, Korus and Heimsch, 1985; Davison, 1988). These measurements were independently made at selected liquid velocities and the attempt, to correlate the measured dispersion coefficients to particle properties and liquid velocity, was not made.

1.5 OBJECTIVES

The primary objectives of this project are the study of liquid mixing and bed expansion behaviour in fluidized bed anaerobic bioreactors with *in situ* gas production; in particular, the effects of gas and liquid velocities on the axial liquid dispersion coefficient, and liquid phase holdup. An active column bioreactor, containing flocculating yeast strains of *S. cerevisiae* was used. The reactor was operated anaerobically with glucose as the sole and limiting substrate while ethanol and carbon dioxide gas were produced *in situ* as a by-products.

The liquid axial dispersion coefficient and liquid holdup were determined using the residence time distribution (RTD) technique. A dye was used as the tracer material and, for this reason, preliminary experiments

were performed in order to find out the most suitable tracer material for RTD determination. The performance of the bioreactor was also studied so as to enable comparison with other bioreactors and the quantification of the *in situ* gas production.

CHAPTER TWO

ETHANOL FORMATION AND PRODUCTION

2.1 INTRODUCTION

Manufacture of ethanol is probably one of the best known industrial bioprocesses. Ethanol is the principal constituent in beer (Smith and Greenshields, 1973). Concentrated ethanol can be used as substitute for motor vehicle fuel and as a raw material for the manufacture of numerous organic compounds (Kosaric, Duvnjak and Stewart, 1981).

Though industrial ethanol is currently mainly produced by hydration of ethylene, there is now a general drive towards the use of renewable resources processed biochemically (Keim and Venkatasubramanian, 1989). Moreover, all beverage ethanol is produced by biological processes (Gong, Chen, Flickinger and Tsao, 1981). The production of ethanol using renewable resources such as biomass and industrial wastes, has found favour in many countries; for example the United States of America and Brazil have established such fermentation plants. In these countries, the potentials of ethanol for use as a substitute for motor vehicle fuel, are being investigated and developed through Government funded projects (Keim and Venkatasubramanian, 1989).

Many different microorganisms can be used for the production of ethanol, but the yeast *Sacharomyces cerevisiae* is predominantly used (Kosaric *et al.*, 1981) and can utilise, as substrate, a variety of raw materials. However, sugars and starches are most widely used. Materials containing cellulose may also be used to produce ethanol after some pretreatment (Chang, Chou and Tsao, 1981). Whey and some industrial wastewaters have also been used for ethanol production (Boontanjai, 1983).

In this section, the kinetics of ethanol formation using *S. cerevisiea* and glucose substrate, is discussed. Factors affecting the kinetics of ethanol formation will be highlighted. Other factors affecting the production of ethanol, particularly in tower fermenters, will also be

reviewed.

2.2 ETHANOL FORMATION

At suitable environmental conditions and in the absence of molecular oxygen, the yeast *S. cerevisiae* metabolizes glucose ($C_6H_{12}O_6$) and produce ethanol (C_2H_5OH) and carbon dioxide (CO_2) as primary metabolites (Maiorella, Wilke and Blanch, 1981). For every mole of glucose consumed, two moles each of ethanol and carbon dioxide is produced. In addition energy is released some of which are required for biosynthesis. This reaction, in its simplest form, is shown in equation 2.1 (Lievense and Lim, 1982).

$$C_6H_{12}O_6 \rightarrow 2C_2H_5OH + 2CO_2 + Energy \qquad 2.1)$$

The stoichiometry of equation 2.1 indicates that, on a weight basis, every gramme of glucose can, theoretically, yield 0.51 g of ethanol. In practice, though, actual ethanol yields are about 90 % of the theoretical value because a portion of the glucose is being used for synthesis of new cells (Maiorella, *et al.*, 1981).

Under aerobic conditions and at high glucose concentration, glucose is predominantly fermented in accordance with equation 2.1. Under these conditions, the maximum specific growth rate of the yeast (μ_{max}) is 0.4 - 0.45 hr^{-1} and the biomass yield (Y_{bs}) is about 0.15 g dry biomass per g glucose consumed (Coppella and Dhurjati, 1989). But, at low glucose concentration (50 - 130 mg/l), glucose is oxidised to CO_2 and new cells (Eqn. 2.2), with μ_{max} of 0.25 - 0.30 hr^{-1} and Y_{bs} of 0.5 g dry biomass per g glucose consumed and very little or no ethanol formed (Coppella and Dhurjati, 1989).

$$C_6H_{12}O_6 + 6O_2 \rightarrow 6H_2O + 6CO_2 + Energy \qquad 2.2)$$

When the glucose becomes exhausted, yeast then oxidises ethanol to produce more cell mass and CO_2 according to

equation 2.3 (Lievense and Lim, 1982).

$$C_2H_5OH + 3O_2 \rightarrow 2H_2O + 2CO_2 + Energy \qquad 2.3)$$

A μ_{max} of 0.14 - 0.20 hr^{-1} and Y_{bs} of 0.6 - 0.7 g dry biomass per g ethanol consumed were obtained (Coppella and Dhurjati, 1989).

The entire set of enzymatic reactions for ethanol formation are very complex, but a simplified chart, indicating some of the path ways, is shown in figure 2.1.

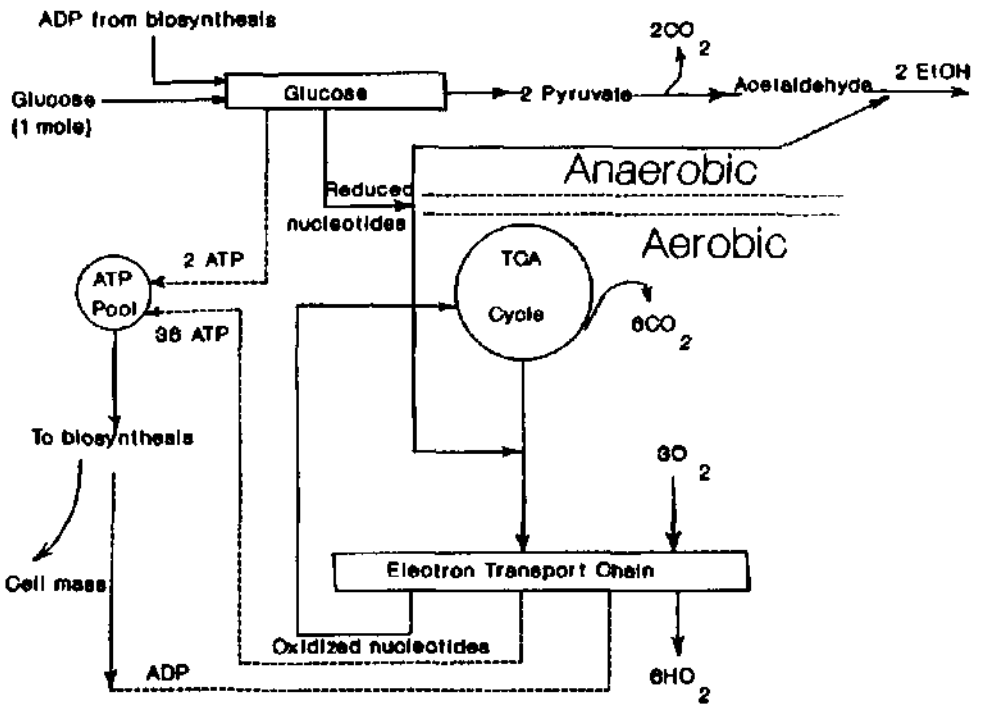


Fig. 2.1: Aerobic and anaerobic catabolism of *S. cerevisiae*
(Maiorella *et al.*, 1981)

The overall rate of ethanol formation depends, primarily, on the nature and concentration of the microorganism used and on the type of raw material utilized. Enviromental factors that include temperature, medium pH, substrate and product concentrations, and concentrations of medium additives, can have significant

effects on the growth rate of the microorganisms and subsequently on the kinetics of ethanol formation (Jones, Pamment and Greenfield, 1981). Process conditions such as the dilution rate or residence time and internal and external mass transfer rates could also have considerable effects on the overall rate of ethanol production (Greenshields and Smith, 1971).

2.2.1 Effects of glucose concentration

Maiorella *et al.* (1981) stated that at glucose concentrations, less than 10 mg/l, ethanol production proceeds at a rate that varies linearly with the glucose concentration or first order reaction rate. But, at high glucose concentration (above 150 g/l), glucose inhibits ethanol production, while at intermediate glucose concentrations, the rate of ethanol production is given roughly by a Monod type relationship;

$$v = v_{max}\frac{C_s}{K_s' + C_s} \qquad 2.4)$$

However, under anaerobic conditions, the specific rate of ethanol production is essentially at its maximum value, independent of glucose concentration, for glucose concentrations above 3.5 g/l and less than 150 g/l, because the saturation constant K_s' has a low value in the order of 0.35 g/l (Maiorella *et al.*, 1981). The low value of the saturation constant also indicates that ethanol production proceeds at zero order rate at intermediate glucose concentrations.

The effect of glucose on ethanol formation was also reported by Lee *et al.* (1983). They used a packed bed fermenter containing cells of *S. cerevisiae* immobilized in calcium alginate beads. Their results shown in figure 2.2 indicated an optimum specific rate of glucose assimilation at an inlet glucose concentration of 80 g/l.

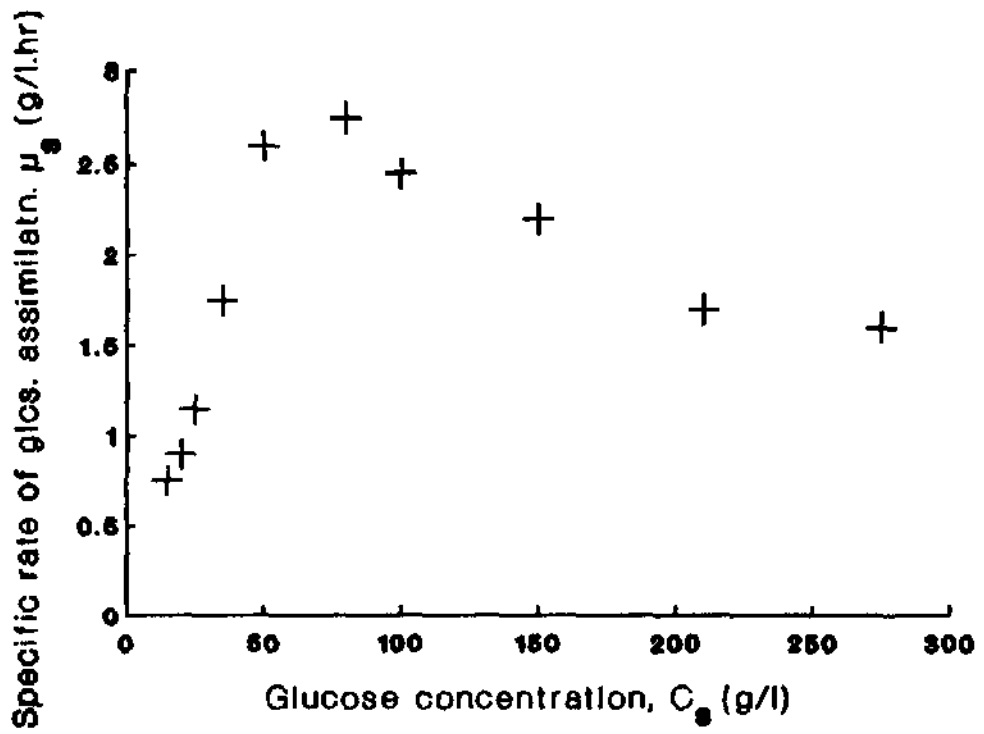


Fig. 2.2: Glucose inhibition effect
(Ahn, Lee and Ryu, 1983)

Subsequent increases in inlet glucose concentration caused decreases in the specific rate of glucose assimilation. The existence of an optimum specific rate of glucose assimilation confirmed substrate inhibition of the yeast metabolism.

The results of Ghose and Tyagi (1979b) have not shown an optimum glucose consumption rate, within inlet glucose concentration range of 71 g/l to 357 g/l, but a steady decrease of specific growth rate and specific rate of ethanol production as shown in Table 2.1. This was probably because the fermentation was started at a high glucose concentration, near that at which the optimum was observed by Lee *et al.* (1983).

The gradual decrease in the specific rate of ethanol production due to increased concentration of glucose was in accordance with the observation of Lee *et al.* (1983).

cellodextrines like cellotriose, cellotetrose, etc.) that may not have undergone fermentation was probably responsible for the high inhibitory effect of sugars in bagasse hydrolysate.

2.2.2 Ethanol inhibition

Ethanol, which is the main product in alcohol fermentation, is itself toxic to yeast. Several researchers have studied the effect of ethanol concentration on the kinetics of ethanol formation by *S. cerevisiae*.

Aiba, Shoda and Nagatani, (1968) have studied the effects of ethanol inhibition in chemostat and batch fermenters, in situations where glucose was not limiting. They found that the inhibition effect of ethanol was given by equation 2.6, irrespective of the mode of operation.

$$v = v_o \, e^{-K_2 C_e} \frac{C_s}{K_s' + C_s} \qquad 2.6)$$

However, they found values of v_0 to be 3.4 hr^{-1} and 1.1 hr^{-1} and the kinetic parameter, K_2, to be 0.029 1/g and 0.015 1/g for the continuous and batch fermentations respectively, thus, showing different kinetic behaviour in batch and continuous fermentations. The saturation constant, K_s' of 0.44 g/l was also obtained. Complete inhibition of yeast growth occured at ethanol concentrations of 65 g/l for the batch experiment and 90 g/l for the continuous process, but ethanol production appeared not to be completely inhibited.

Bazua and Wilke (1977) also studied ethanol inhibition effects on a glucose fermentation in a CSTF, using glucose concentration of 50 g/l and a constant pH of 4.0. Their data did not fit equation 2.6, but a linear type equation (Eqn. 2.7) with a standard deviation of 0.0172.

$$\nu_{max} = \nu_o - \frac{K_3 C_e}{K_4 - C_{em}} \qquad 2.7)$$

The kinetic parameters K_3 and K_4 were found to have values of 0.506 hr^{-1} and 119.25 g/l respectively. The ν_o was 1.802 and K_s' was 0.329 g/l. Their results indicated that cell growth was completely inhibited at ethanol concentrations of 93.1 g/l, confirming the findings of Aiba *et al.* (1968). However, their data also indicated that ethanol production was stopped at ethanol concentration of 93.84 g/l.

Ghose and Tyagi (1979b), have reported that their data did not fit the equation of Aiba *et al.* (1968) or that of Bazua and Wilke (1977), but an equation of the form:

$$\nu = \nu_o(1 - C_e/C_{em}) \qquad 2.8)$$

Furthermore, ethanol production was completely inhibited at ethanol concentration of 114 g/l. But, yeast growth was completely inhibited at an ethanol concentration of 87 g/l, which was in reasonable agreement with the result of Aiba *et al.* (1968) and Bazua and Wilke (1977). They also found the value of ν_o to be 1.4 hr^{-1}. A similar result was obtained by Lee *et al.* (1983), but they observed (Fig. 2.3) complete inhibition of the specific rate of glucose assimilation at a higher ethanol concentration of 140 g/l when a growth medium containing 50 g/l glucose was used. This slightly higher ethanol concentration at which ethanol production stops may be due to an increased mass transfer resistance and poor liquid/solid contact in the pached bed used by Lee *et al.* (1983).

A different approach was used by Hoppe and Hansford (1982) in their study of the effects of ethanol concentration on the growth of *S. cerevisiae*, in a CSTF. They observed the effects of ethanol, produced by the

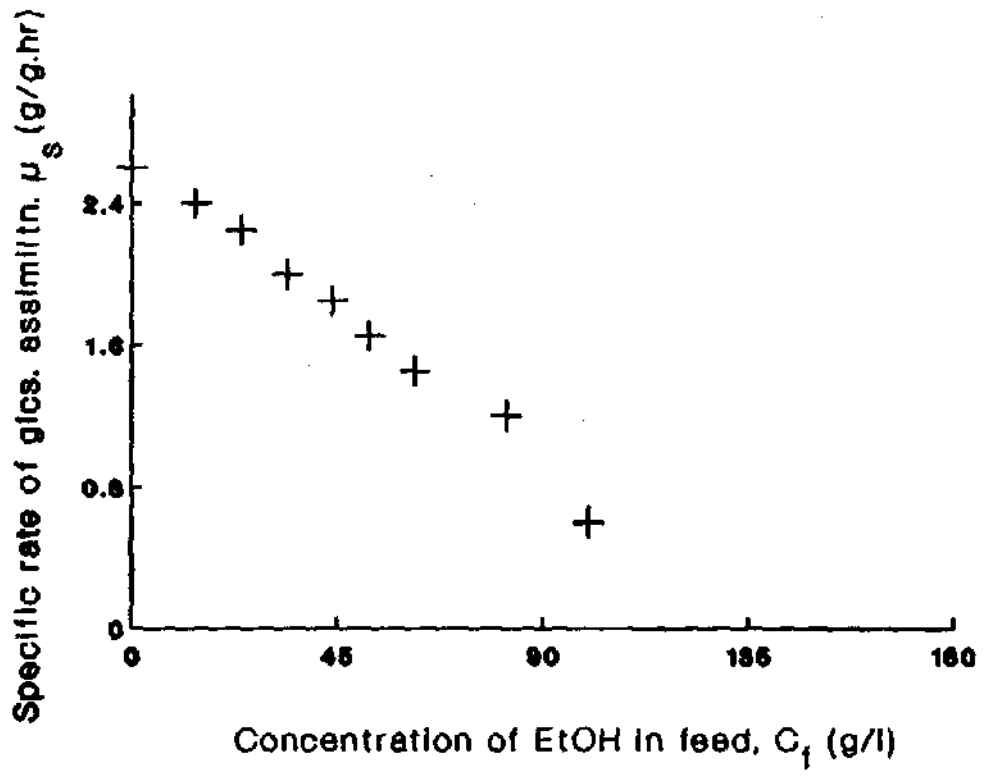


Fig. 2.3 Ethanol inhibition effect
(Lee, Ahn and Ryu, 1983)

yeast itself, at glucose concentrations of 20, 100 and 200 g/l, temperature of 30 °C and pH of 4.0. Their results further confirmed the inhibition of yeast growth by ethanol, but their data did not fit any of the equations discussed above. The data was correlated by equation 2.9.

$$\mu = \mu_{max} \frac{C_s}{K_s + C_s} \frac{K_p}{K_p + C_e} \qquad 2.9)$$

Values of K_s, the ethanol saturation constant K_p, and the maximum specific growth rate μ_{max}, were found to be 3.3 g/l, 5.2 g/l and 0.64 hr^{-1} respectively. Their results showed that, at a glucose concentration of 20 g/l, yeast growth was completely inhibited at ethanol concentration of 10 g/l, whereas complete inhibition of yeast growth occured

at ethanol concentration of 50 g/l for glucose concentrations of 100 g/l and 200 g/l. These results indicate that complete inhibition of yeast growth occurs at a relatively low ethanol concentrations. They argued that ethanol added extracellularly is not as strongly inhibitory as that produced intracellularly by the yeast itself.

Differences between the reported observations and kinetic parameters obtained, may be attributed to the use of different yeast strains and fermentation conditions. The *mode of operation, initial glucose concentration* and the type of fermenter used, may have significant effects on the resulting values of the kinetic parameters obtained. It is worth noting that all the above studies have concluded that ethanol inhibition of glucose fermentation is non-competitive.

Prolonged, continuous, exposure of yeast to high concentrations of ethanol results in loss of viability of cells and consequently, the rate of ethanol formation (Jones *et al.*, 1981). However, adaptation of yeast cells to 7 % ethanol was found to lower the specific rate of cell death, at various ethanol concentrations, by a factor of 40 fold compared to non-adapted culture (Jones and Greenfield, 1984). Hoppe and Hansford (1984) have reported that the use of oxygen at a concentration of 0.5% of saturation was found to enhance the utilisation of sugar by increasing the ethanol tolerance of yeast, without any significant decrease in the ethanol yield per unit sugar consumed. Moreever, the ethanol inhibition constant K_p in equation 2.9 was found to increase from 5.2 g/l to 14.0 g/l.

0052

2.2.3 Combined glucose and ethanol inhibition

Fermentation runs at high glucose concentrations could be inhibited by both glucose and ethanol. Ghose and Tyagi (1979b) combined equations 2.5 and 2.8 to describe

UNIVERSITY

the combined effects of inhibition exerted by glucose and ethanol, by equation 2.10.

$$v = v_o(1 - C_e/C_{em}) \frac{C_s}{K_s' + C_s + C_s^2/K_s'\omega} \qquad 2.10)$$

This contradicted the results of Godia *et al.* (1987a) who found that their batch data was not correlated by equation 2.10, but by equation 2.11, with a relative error of 5 % for initial glucose concentrations of 75, 100, 150 and 185 g/l.

$$v = v_{max} \frac{C_s}{K_s'+C_s} \frac{K_p'}{K_p'+C_e} \qquad 2.11)$$

They obtained mean values of v_{max} = 1.8 hr^{-1}, K_p' = 7.2 g/l and K_s' = 1.9 g/l. Different results were reported by Anselme and Tedder (1987), who found that the use of the simple Monod type equation (Eqn. 2.4) fitted their data best, suggesting that there was no ethanol inhibition in their experiment with 100 g/l glucose and ethanol concentration of 8%. A similar value of v_{max} = 1.44 hr^{-1} was reported by Admassu, Korus and Heimsch (1985) at initial glucose concentration of 60 g/l. But, their data were correlated by the equation of Aiba *et al.* (1968) which, for large sugar concentration, was reduced to:

$$v = v_{max} e^{-K_2 C_e} \qquad 2.12)$$

They obtained K_2 = 0.0944 l/g which was about three times the value reported by Aiba *et al.* (1968). They also observed that with an initial glucose concentration of 200 g/l, ethanol formation was completely inhibited at an ethanol concentration of 115 g/l, confirming the results of Ghose and Tyagi (1979b).

Jones, *et al.* (1984) have also observed that

production of ethanol stops at an ethanol concentration of 115 g/l. But they reported different values of v_{max} of 0.7 hr^{-1} for batch fermentation, at an initial glucose concentration of 100 g/l, and 0.21 hr^{-1} for tower fermentation, at initial glucose concentrations of 130 and 180 g/l. Moreover, data from their fermentation runs, were correlated by equation 2.13 which was different from those described above.

$$v = v_{max}(1 - C_e/C_{em}) \frac{C_s}{K_s' + C_s} \qquad 2.13)$$

The saturation constant for the batch fermentation was found to be K_s' = 0.9 g/l, but values of 25 g/l and 60 g/l were obtained, in the tower fermentation, for initial glucose concentrations of 130 g/l and 180 g/l respectively. These high values of the saturation constant may be due to increased resistance to mass transfer in the tower; as the cells were reportedly densely packed and liquid appeared to move through channels opened by the released carbon dioxide. The low value of v_{max} in the tower may also be due to decreased cell viability, as approximately 40 % of the cells' viability in the tower was reported to have been lost, probably as a result of poor mixing in the tower.

2.2.4 Effects of pH

Parsons, McDuffie and Din (1984) have performed fermentations in a chemostat at dilution rates of 0.04 to 0.05 per hour. They observed that changing the pH of the feed from 6.6 to 6.0 produced pronounced differences at similar dilution rates. Their data, shown in Table 2.2, indicate that at a feed pH of 6.6, there results lower cell concentration, lower ethanol production rate and higher output pH when compared to the feed pH of 6.0.

Table 2.2 Effects of pH on ethanol production rate and cell concentration

pH	Biomass concentration C_b (g/l)	EtOH productivity P' (g/l.hr)	Output pH
6.6	2.4-2.6	1.0-1.5	5.0-5.5
6.0	5.0-8.0	2.0-2.4	2.8-3.2

(Parsons, McDuffie and Din, 1984)

Similarly, Williams and Munnecke (1981) have also reported pH effects on ethanol production in shake flasks, at 30 ^{0}C, with both free cell culture and cells immobilized in calcium alginate. They used pH ranging from 2.0 to 10.0. Their results are presented in figure 2.4 and showed that the free cell system has an optimal ethanol production rate at a pH of 4.5 whereas the immobilized system has optimal ethanol production rate at a pH ranging between 3.0 to 7.5. The absolute limits of a pH for growth for most strains of *S. cerevisiae* have been reported to be 2.4 to 8.6, with an optimum growth at a pH of 4.5 (Jones *et al.*, 1981) but, Coppella and Dhurjati (1989) did not observe any changes in yeast growth rate, in aerobic conditions, in the pH range of 4.5 to 7.0.

A large number of laboratory fermentation studies, for example Aiba *et al.* (1968); Bazua and Wilke (1977); Ghose and Tyagi (1979b); Hoppe and Hansford (1982), were conducted at controlled pH in the range 4.0 to 5.0, showing that most fermentation studies were carried out near optimum pH.

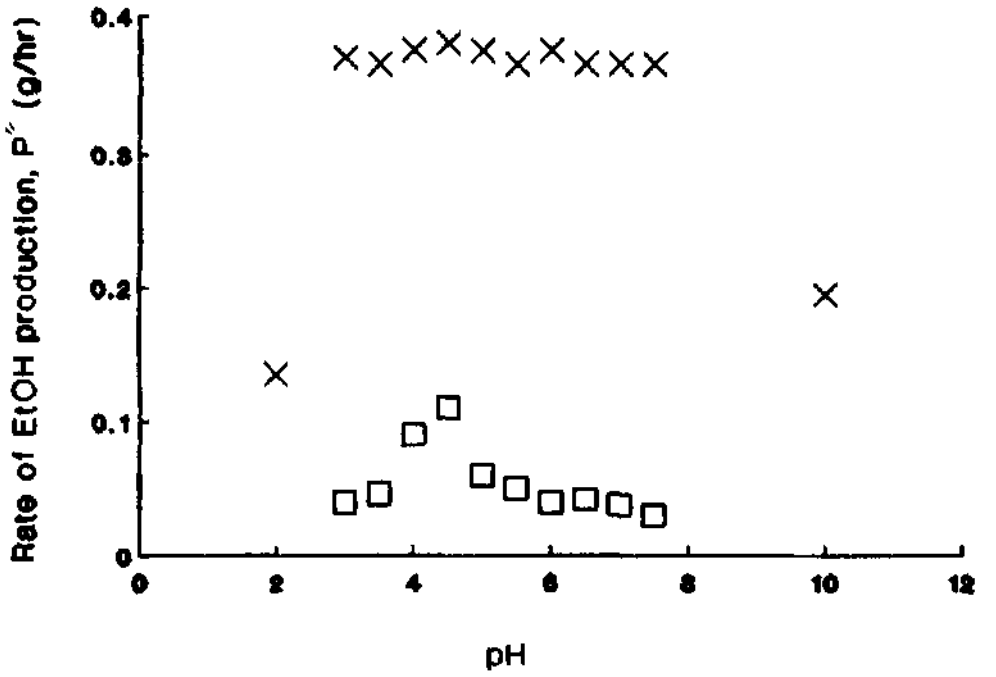


Fig. 2.4 Effect of pH on ethanol production rate for free (-□-) and immobilized cells (-x-) (Williams and Munnecke, 1981)

2.2.5 Temperature effects

The effects of temperature on ethanol production by *S. cerevisiae* was studied by Williams and Munnecke, (1981) for both free cell culture and cells immobilized in calcium alginate. They observed (Fig. 2.5) that for, free cells, ethanol production and yeast growth rates increased as the temperature was increased gradually from 25 ^{0}C to 42 ^{0}C. Beyond 42 ^{0}C the yeast stopped growing, but ethanol production continued. For immobilized cells, there was a sharp increase in ethanol production rate with increasing temperature up to 30 ^{0}C, after which, the production rate decreased as the temperature increased.

According to Jones *et al.* (1981) the optimum and maximum tolerable temperatures, for yeast fermentations, are strongly strain dependent; mesophilic strains of *Saccharomyces* have maximum process temperatures in the

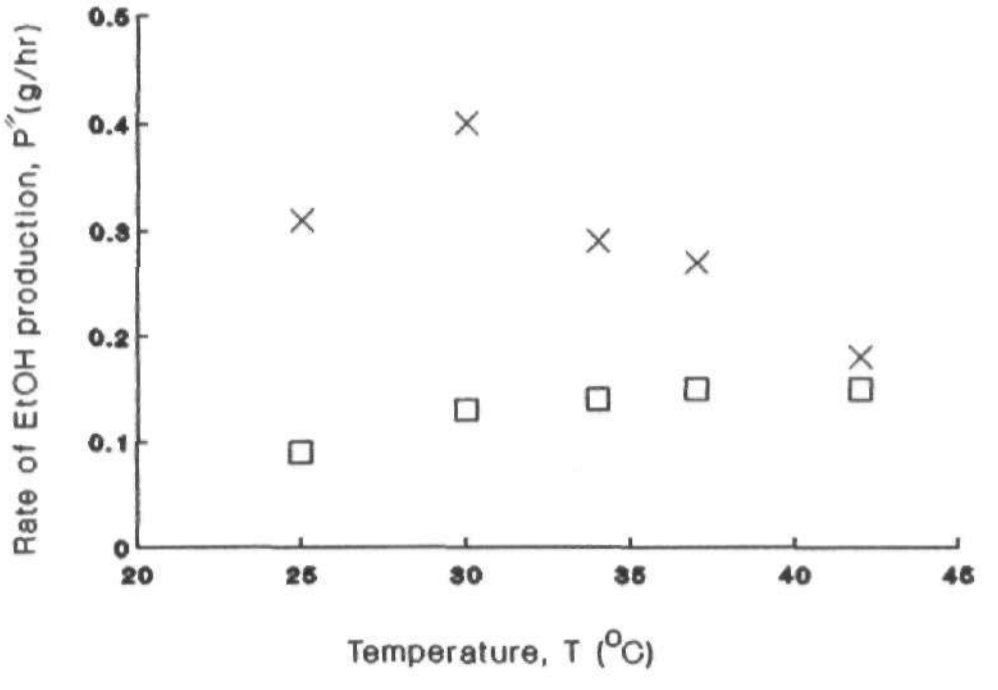


Fig. 2.5 Effects of temperature on ethanol production for free (-□-) and immobilized cells (-x-) (Williams and Munnecke, 1981)

absence of ethanol in the range 35 to 40 °C, but this is reduced by about 1 °C for every percent increase in ethanol concentration. This suggested that ethanol concentration lowers the optimum temperature for ethanol fermentation. Similar observations were recorded by Williams and Munnecke (1981). They noticed that as the temperature was increased, there was a decrease in cell growth and ethanol production rates, when the cells were subjected to increasing ethanol concentrations. This indicated that temperature and extracellular ethanol concentration are directly related with regard to inhibition of ethanol production.

The choice of operating temperature is influenced by physiological factors and the physical problem of evaporative ethanol loss and foaming at elevated temperatures (Jones *et al.*, 1981). However, a large number

of laboratory fermentation experiments, for example: Prince and Barford (1982a); Hoppe and Hansford (1982); Anselme and Tedder (1987); Ruggeri, Specchia, Sassi and Gianetto (1988), were carried out at controlled, constant, temperature of 30 ^{0}C, indicating that temperature variation is not usually allowed in laboratory fermentation experiments.

2.2.6 Effects of feed components

Components of feed or growth medium can exert a considerable inhibitory effect on yeast metabolism in ethanol fermentation. These components are either added into the growth medium as essential nutrients for yeast metabolism, or are naturally present in the feed medium. Wall and Hill (1992) have noted that yeast extract added to growth medium has considerable effects on yeast metabolism. They observed maximum yeast growth at a yeast extract concentration of 10% of the feed glucose concentration. Similarly, Maiorella, Blanch and Wilke (1984) have shown that calcium chloride and ammonium sulphate were the most inhibitory salts, while potassium chloride was the least inhibitory. Their data, presented in Table 2.3, indicate that the concentration levels at which 20% and 80% reductions in cell productivity are experienced in continuous fermentation, are different for all the salts they used.

Feed components' effects on yeast metabolism have also been reported by Jones, *et al.* (1981). However, the concentration at which a feed component becomes harmful, depends on the type of feed medium. For example, copper at a concentration of 1 mg/l is completely inhibitory to yeast in sucrose medium, whereas a concentration of 30 mg/l could be tolerated by yeast, without any deleterious effects, if the feed is a malt wort medium.

Table 2.3: Inhibition of feed components

Component	Concentration of feed component C_{fc}, (mol/L)	
	20% inhibition	80% inhibition
Sodium chloride	0.24	0.45
Potassium chloride	0.60	1.74
Potassium hydrogen phosphate	0.66	0.73
Calcium chloride	0.08	0.23
Magnesium chloride	0.58	0.92
Magnesium sulphate	0.63	0.97
Ammonium chloride	0.12	0.46
Ammonium sulphate	0.11	0.24
Xylose	0.58	0.92

(Maiorella, Blanch and Wilke, 1984)

2.2.7 Mass transfer effects

Before bioreaction takes place, both substrate and nutrients in the liquid phase, must be transported through the bulk liquid to the surface of the biocatalyst, across the biomass-liquid interface and to reaction sites within the biocatalyst.

Transfer of substrate through the bulk fluid to the cells surfaces is termed external transport, as distinct from internal transport which is the transportation of mass to the reaction sites within the biomass or through pores, if the biomass is supported on a porous medium or is in form of flocs. Usually, however, resistance to transport through the bulk liquid is negligible because the substrate concentrations within the bulk liquid and

the biocatalyst surface are uniform. Shieh and Keenan (1986) have used equation 2.14 to estimate the rate of external mass transfer.

$$k_L = \frac{0.81}{\varepsilon} \frac{D_e^{0.67} u_L^{0.5} \rho_L^{0.25}}{\eta^{0.25} d_p^{0.5}} \qquad 2.14)$$

They showed that a typical value of k_L for a denitrification process in a fluidized bed, is of the order of 0.01 cms^{-1}, and the error in neglecting the external mass transfer effect ranged from 2.6% to 7.1% for bulk liquid nitrate concentrations of 6 to 43 mg/l at a superficial liquid velocity of 1.07 cm/sec and biomass thickness of 2.07 mm.

A similar conclusion was reached by Smith and Greenshields (1973) for glucose fermentation, in a tower fermenter, using flocs. But, they used a slightly different relationship given by equation 2.15.

$$\frac{k_L \rho_L}{G} (N_{SC})^{2/3} . \varepsilon = 1.09 \left(\frac{d_p G}{\eta}\right)^{-2/3} \qquad 2.15)$$

They further showed that for flocs of diameter 0.1 cm to 0.4 cm, resistance to external mass transfer is negligible at superficial liquid velocities of 0.00694 cms^{-1} and 0.0625 cms^{-1}.

Resistance to substrate transport across the biomass-fluid interface or film diffusion, as it is commomnly called, may be appreciable if there is significant difference in substrate concentrations between the biomass surface and the bulk liquid, as is often the case if there is poor mixing. Similarly, resistance to pore diffusion may be significant if the substrate has large molecular size and the pore is narrow.

In bioreaction systems where resistance to mass transport is significant, the corresponding effect on the

reaction rate is described by the use of an effectiveness factor, which is defined as the ratio of reaction rate with transport resistance to reaction rate without transport resistance or intrinsic reaction rate. Thus,

$$\zeta = \frac{\textit{Reaction rate with transport resistance}}{\textit{Intrinsic reaction rate}}$$

Assuming a spherical support medium with uniform biofilm thickness, negligible external mass transfer resistance, a single limiting substrate and steady state, Shieh and Keenan (1986), have developed mathematical equations describing effectiveness factors for zero order (Eqn. 2.16) and first order (Eqn. 2.17) intrinsic kinetics, for systems in which the internal mass transfer is governed by Fick's law.

$$\zeta_o = 1.2712\ \phi_{cm}^{-1} = \frac{3.814\sqrt{B\ C_s}}{(1 - A)} \qquad 2.16)$$

where, $B = \dfrac{D_e}{\rho_b\ k_o\ r_p^2}$ and $A = \left(\dfrac{r_m}{r_p}\right)^3$

The modified zero order Thiele modulus $\phi_{cm} = r_{sp}\sqrt{\dfrac{\rho_b k_o}{D_e C_s}}$, and

the specific biofilm thickness is defined as:

$$r_{sp} = \frac{\textit{Biofilm volume}}{\textit{Biofilm exterior surface area}} = \frac{(r_p^3 - r_m^3)}{3r_p^2}$$. For

$\Phi_{cm} \leq 1.27$, the whole biofilm is active and the intrinsic zero order kinetics is observed (i.e $\zeta_o = 1$). For $\Phi_{cm} \geq 1.27$, the inner portion of the biofilm is inactive and the observed reaction rate is proportional to the square root

of the bulk substrate concentration.

For intrinsic first order reactions, the authors expressed the effectiveness factor as:

$$\zeta_1 = \frac{Coth(3\,\phi_{1m})}{\phi_{1m}} - \frac{1}{3\phi_{1m}^2} \qquad 2.17)$$

where the first order modified Thiele modulus is given by,

$$\phi_{1m} = \frac{r_{sp}}{r_p}\,\phi_1 \;;\; with\ \phi_1 = \sqrt{\frac{\rho_p k_1 r_p^2}{D_e}} \qquad 2.18)$$

It can be seen, from equations 2.17 and 2.18, that the first order effectiveness factor is a function of the bioparticle size only and is independent of the substrate concentration. The authors noted that the value of the modified first order Thiele modulus for which the effectiveness factor is unity, is 0.11 and this marked the transition from observable intrinsic kinetics to a regime in which the internal mass transfer is significant. A further look at these equations reveals that high effectiveness factors are obtained for flocs. Greenshields and Smith (1971) have used these equations to show that for ethanol production in a tower fermenter, pore diffusion may affect the overall rate of glucose conversion, but if flocs have sizes in the order of 0.1 cm in diameter, pore diffusion may have a negligible effect on the overall rate of glucose conversion.

Andrews (1986), has also agreed that flocs provide high effectiveness factors. He defined the effectiveness factor as a ratio of the actual substrate uptake rate to uptake rate if the whole particle were biomass, and showed that

$$\zeta' = \frac{E_o\,E_\infty}{E_o + E_\infty} \qquad 2.19)$$

where, $E_o = \frac{3Sh}{2\alpha(\theta+\beta)^2}$ and

$$E_\eta = \frac{3}{\theta+\beta}\left[\frac{\beta\tanh(\theta+1)}{\tanh(\theta+\beta)} - \frac{1}{\theta+\beta}\right]$$

Both β and Θ are dimensionless, representing the radius of the support particle and the thickness of the biofilm respectively, while α is the ratio of substrate diffusivities in the biomass and water. The Sherwood number is given by $Sh = \frac{2(r_m + L_b)k_L\alpha}{D_e}$. Also, for Monod type intrinsic kinetics,

$$\beta = r_m\left(\frac{\mu_{max}}{D_e Y_{bs} K_s}\right)^{0.5} \quad \text{and} \quad \theta = L_b\left(\frac{\mu_{max}}{D_e Y_{bs} K_s}\right)^{0.5}$$

For negligible external mass transfer resistance, higher effectiveness factors are obtained for flocs ($\beta = 0$), and they decrease with increasing particle size or biofilm thickness.

A different relationship was used by Atkinson and Daoud (1976). They showed that for biochemical reactions with diffusional limitations, the effectiveness factor, defined as the ratio of the observed substrate uptake rate to the intrinsic uptake rate, is given by:

$$\zeta = 1 - \frac{G\phi_R}{\tanh(\phi_R)} + G \; ; \; for \; \phi_R \le 1 \qquad 2.20)$$

and $$\zeta = \frac{1}{\phi_R} - G\left[\frac{1}{\tanh(\phi_R)} - 1\right] \; ; \; for \; \phi_R \ge 1 \qquad 2.21a)$$

where $$G = \frac{\tanh(k_2 L_c)}{k_2 L_c} \qquad 2.21b)$$

For flocs, $L_c = V_p/A_p$ and for Monod type intrinsic kinetics

$$\phi_R = \frac{k_2 L_c}{(1+2K_s C_s^*)^{0.5}} \quad \text{and} \quad k_2 = \sqrt{\frac{\mu_{max}\rho_b}{Y_{bs}K_s D_e}} \qquad 2.21c)$$

Further look at these equations reveals that diffusion limitations may occur for large floc sizes.

2.3 ETHANOL PRODUCTION

Most of the bioreactors discussed in chapter one have been used or proposed for use in the production of ethanol. However, ethanol productivity depends on the type of the reactor, nature of microorganisms, type of raw materials and operating conditions used. In this section, ethanol production using *S. cerevisiae*, in batch and continuous bioreactors, is discussed.

2.3.1 Batch fermentation

Batch fermentation is the most common process for industrial production of portable ethanol. It is a simple sytem with production times of 36 to 72 hours. Mehaia and Cheryan (1984) have reported a productivity of 2.1 g/(l.hr) at 100% glucose utilization, using a yeast concentration of 2.6 g/l and 100 g/l glucose. This result was in agreement with the report of Godia *et al.* (1987b) who mentioned that the productivity of batch fermenters is between 1.8 to 2.5 g/(l.hr). The results were, however, contradicted by Ghose and Tyagi (1979a) who have shown that a 97 g/l ethanol concentration was obtained in a period of 5 to 6 hours using an initial glucose concentration of 220 g/l. This level of ethanol production corresponds to a fermenter productivity of about 16.2

g/(l.hr) at 86% glucose utilization. The high initial yeast concentration of 23.6 g/l, high glucose concentration and low glucose utilization may be responsible for this high productivity.

Batch fermentation is associated with frequent shutdown and startup of the fermenter, which has to be cleaned before the start of any batch; this makes the fermenter inefficient. Moreover, the time required for the yeast to acclimatize adds to the low efficiency of this system. All these combine to cause low productivity in batch fermentation (Margaritis and Merchant, 1987).

2.3.2 Continuously stirred tank fermentation

A continuously stirred tank fermenter (CSTF) was used by Ghose and Tyagi (1979a) with feed containing 160 g/l glucose. The optimum dilution rate for a maximum productivity of ethanol of 4.1 g/(l.hr) was found to be 0.13 hr^{-1}, with a yield of 95% of theoretical. Similar productivity values, in the range from 6 to 8 g/(l.hr), were reported by Godia *et al.* (1987b). The productivity of CSTF is, therefore, about 2 to 4 times the average productivity obtained from batch fermentation. However, because the reactor and effluent ethanol concentrations, in this system, are the same, CSTF has limitations arising from ethanol inhibition.

The use of cascade CSTF connected in series, was found to reduce the effects of ethanol inhibition (Wall and Hill, 1992). In this arrangement, only the last reactor has an ethanol concentration level that is inhibitory. Combination of CSTF in series allows the use of higher throughput rates and a higher glucose conversion is achieved compared to single CSTF (Wall and Hill, 1992). Ghose and Tyagi (1979b) have shown that a two stage CSTF of equal volume has productivity which is 2.3 times that of a single CSTF. Nonetheless, the productivity in these systems, is limited because it is determined by the growth

charateristics of the yeast strain used. When the system is operating at steady state, the dilution rate equals the specific growth rate of the organims. Thus, the dilution rate could only be increased to the value of the maximum growth rate, beyond which, wash out occurs and viable cells are lost.

Separating the cells and recycling them back into the reactor is one method of circumventing this problem. When the cells were recycled, maximum ethanol productivity of 18.3 g/(l.hr) at a dilution rate of 0.3 hr^{-1} was obtained, representing about 4.5 times the productivity in CSTF without cell recycle (Ghose and Tyagi, 1979a). Furthermore, sparging air at a low flow rate of 0.125 volume per volume per minute (vvm) was found to further increase the productivity to 32 g/(l.hr), equivalent to 7.5 times that of single CSTF without recycle (Ghose and Tyagi, 1979a). The substantial increase in cell concentration to 32 g/l, in the recycle CSTF, compared to 5.5 g/l, in the non-recycle CSTF, may be responsible for the large increase in reactor productivity. However, the increase in operating costs and higher risk of contamination, inherent in cells recycling and aeration systems, could offset the increased productivities *obtained (Maiorella et al.*, 1981).

The use of a gas stirred immobilized-cell CSTF was reported to overcome the problem of cells recycle, but breakage of immobilizing alginate beads was observed at higher dilution rates (Lee *et al.*, 1983). Stability tests have shown that the viability of the yeast in the CSTF remained above 94% for a continuous 10-day steady state experiment and ethanol yield was constant at 0.495, representing 98% of the theoretical yield (Ghose and Tyagi, 1979a).

2.3.3 Hollow fiber fermentation

Mehaia and Cheryan (1984) have produced ethanol using

a hollow fiber fermenter and *S. cerevisiae* packed into the shell side of the reactor. Using an inlet glucose concentration of 100 g/l, they obtained an optimum ethanol productivity of 40 g/(l.hr), based on the total reactor volume, at a dilution rate of 3 hr^{-1}. The corresponding glucose utilization was 30%. Reducing dilution rate to 0.25 hr^{-1} resulted in an increase in glucose utilization to 85% and reduced ethanol productivity of 10 g/(l.hr). Similarly, a productivity of 26 g/(l.hr), at 27% glucose utilization was obtained by Inloes, Tylor, Cohen, Michaels and Robertson (1983).

In a long term stability test, Mehaia and Cheryan (1984) noticed that ethanol productivity and glucose utilization were constant at 17 g/(l.hr) and 66% respectively, for about 93 hrs of fermentation, and the yeast concentration increased from an initial 100 g/l to 260 g/l within the same period.

Though hollow fiber fermenter may be stable during operation, the build-up of yeast and high carbon dioxide production may limit productivity, as excessive pressure drop, that could cause membrane rupture, results (Margaritis and Merchant, 1987).

2.3.4 Packed bed fermention

Several researchers (Williams and Munnecke, 1981; Lee, *et al.*, 1983; Godia, *et al.*, 1987a; Anselme and Tedder, 1987) have studied ethanol production in packed bed fermenters. Williams and Munnecke (1981) have used yeast immobilized in alginate beads and reported ethanol productivities of 8.96 g/(l.hr) at a dilution rate of 0.5 hr^{-1} to a maximum of 53.8 g/(l.hr) at a dilution rate of 4.6 hr^{-1}, using initial glucose concentration of 127 g/l.

Similar results were reported by Lee, *et al.* (1983), who obtained maximum ethanol productivity of 49.6 g/(l.hr) at glucose concentration of 100 g/l and mean residence time of 0.6 hr. But, Godia, *et al.* (1987a) used

carrageenan beads for yeast immobilization and reported a lower productivity of 23.45 g/(l.hr), at feed glucose concentration of 71 g/l and residence time of 0.5 hr. These results suggest that the productivity depends on the initial glucose concentration. However, the results of Godia, *et al.* (1987a), summarized in Table 2.4, indicated only slight effect of initial glucose concentration, in the range 71 g/l to 185 g/l.

Table 2.4 Effects of inlet glucose concentration on productivity of packed bed fermenter

Inlet glucose, C_{si} (g/l)	Liquid flow, f_l (ml/min)	Glucose used, G_u (%)	Exit EtOH, C_{ee} (g/l)	EtOH Productivity P' (g/l.hr)
71	110	100	31.32	17.02
95	110	97.1	40.53	22.02
150	112	69	40.96	22.63
185	110	52.5	40.18	21.83

(Godia, Casas and Sola, 1987a)

In a separate experiment, Anselme and Tedder (1987) have used low density brick particles for yeast immobilization and a constant residence time of 4.75 hrs. They obtained ethanol productivities, based on total reactor volume, of 7.25 g/(l.hr) to 10.19 g/(l.hr).

It is clear that packed bed fermenters have superior performance compared to CSTF. The higher ethanol productivities obtained in these fermenters may be due to increased yeast concentration arising from the immobilization. Since the capacity to increase yeast concentration depends on the immobilization technique employed, the productivities of packed bed fermenters may

depend on the nature of immobilization material or immobilization method used.

Stability tests have shown that the packed bed fermentation process is very stable. In 20 days of continuous operation, about 70 g/l of ethanol, representing a yield of 92% of theoretical, and ethanol productivity of 37.8 g/(l.hr) was achieved (Lee *et al.*, 1983). Furthermore, this process produced a very high ethanol concentration, which may be an advantage in the downstream processing. An ethanol concentration of 98 g/l at a mean residence time of 3.8 hr, using a feed glucose concentration of 250 g/l with corresponding conversion of 77% of the theoretical, was reported by Godia *et al.* (1987a).

However, packed bed fermenters may have serious limitations due to high mass transfer resistance, poor gas disengagement, poor mixing of phases and poor liquid-solid contact. These may be responsible for an observed low glucose conversion, in the order of 32.9% of the theoretical at dilution rate of 6.67 hr^{-1} (Williams and Munnecke, 1981).

2.3.5 Tower fermentation

In tower fermentation systems, the yeast is either self flocculating or immobilized in a porous gel matrix. Pioneering work on tower fermentation was carried out by Ault *et al.* (1969) who showed that the beer produced in aerobic tower fermentation is, in all respects, similar to that produced by the conventional batch process. Tower fermentation systems have also been used for the production of fuel ethanol (Prince and Barford, 1982a&b; Nagashima *et al.*, 1984). Prince and Barford (1982a) have observed that the carbon dioxide produced, during ethanol formation, rises through the bed of yeast flocs and in so doing, carries along light flocs; this phenomenon makes the entire bed resemble a fluidized bed system. The bed

expands to accomodate increased liquid flow and carbon dioxide gas generated. Productivity of tower fermentation depends on the flocculation characteristics of the yeast strain employed (Greenshields and Smith, 1971). Highly flocculent strains can tolerate high liquid flow rate with consequent increase in productivity. On the other hand, attrition of viable cells may occur with poorly flocculating strains, at high liquid flow rates and this limits the productivity.

A productivity of 23.6 g/(l.hr), based on liquid volume, and an ethanol concentration of 58 g/l at a conversion of 95% was achieved in a residence time of 3.8 hrs, with 125 g/l inlet glucose concentration, by Prince and Barford (1982b). However, this productivity was increased to 44.8 and 51.9 g/(l.hr) at reduced conversion of 90% and 80% respectively. In another experiment, 180 g/l glucose was consumed with 100% conversion in 11.4 hrs, giving reactor productivity, based on total reactor volume, of 6.0 g/(l.hr) (Prince and Barford, 1982a). But, relaxing the conversion level to 95% reduced the fermentation time to 5.5 hrs and increased the the productivity to 12.2 g/(l.hr).

Similarly, Admassu *et al.* (1985) have also observed changes in productivity with bed height, which is an indication of the fermentation time, using 215 g/l glucose. They obtained productivities of 80 g/(l.hr) and 23 g/(l.hr), based on liquid volume, at bed heights of 10 cm and 70 cm respectively, as is shown in fiqure 2.6. Productivity, based on liquid volume, was also observed to decrease from 70 g/(l.hr) to 20 g/(l.hr) within a fermentation time of 2 hrs (Jones *et al.*, 1984).

The high productivities obtained in tower fermentations may be due to high yeast concentrations associated with immobilized systems. Yeast concentration in the order of 60 g/l to 90 g/l have been reported (Netto, Destruhaut and Goma, 1985; Prince and Barford,

1982a). Smith and Greenshields (1973) have mentioned that yeast concentration of 250 g/l could be obtained in tower fermenters.

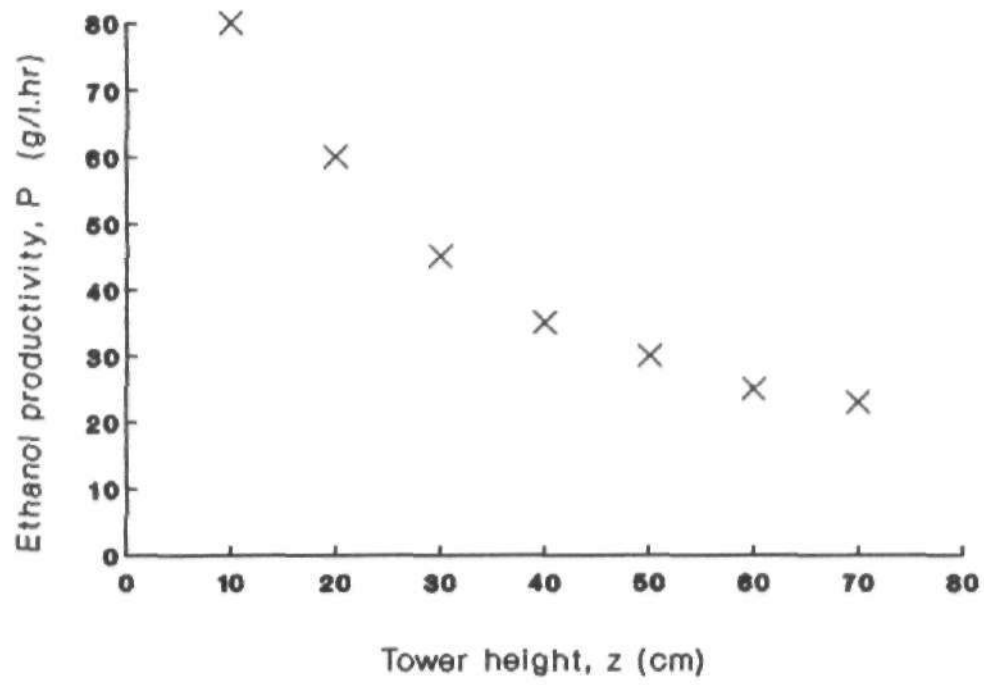


Fig. 2.6 Productivity of tower fermenter
(Admassu, Korus and Heimsch, 1985)

Ethanol yield in tower fermentaion systems was reported to be about 91% to 98% of the theoretical (Jones *et al.*, 1984; Prince and Barford, 1982a), while pH was noticed to drop from a value of about 5.42 at the bottom of the tower, to 4.5 at the exit as shown in figure 2.7 (Jones *et al.*, 1984). This gredient in pH may indicate that gredients in glucose and ethanol concentrations also exist in the tower.

Stability tests have indicated the stable nature of tower fermentation processes. Nagashima *et al.* (1984) have observed that ethanol concentration was constantly within the range of 69 g/l to 111 g/l during six months continuous operation and the corresponding average reactor productivity, based on total reactor volume, was 11.7

g/(l.hr) with an ethanol yield of about 95% of theoretical. A similar conclusion was reached by Prince and Barford (1982a); they operated their tower fermenter for 14 weeks without evidence of deterioration in performance or change in yeast flocculation characteristics. However, Netto, Destruhaut and Goma (1985) have noted that the stability of the system is limited to a fermentation rate of 40 g/(l.hr) because a higher fermentation rate was found to cause deflocculation and loss of viable cells.

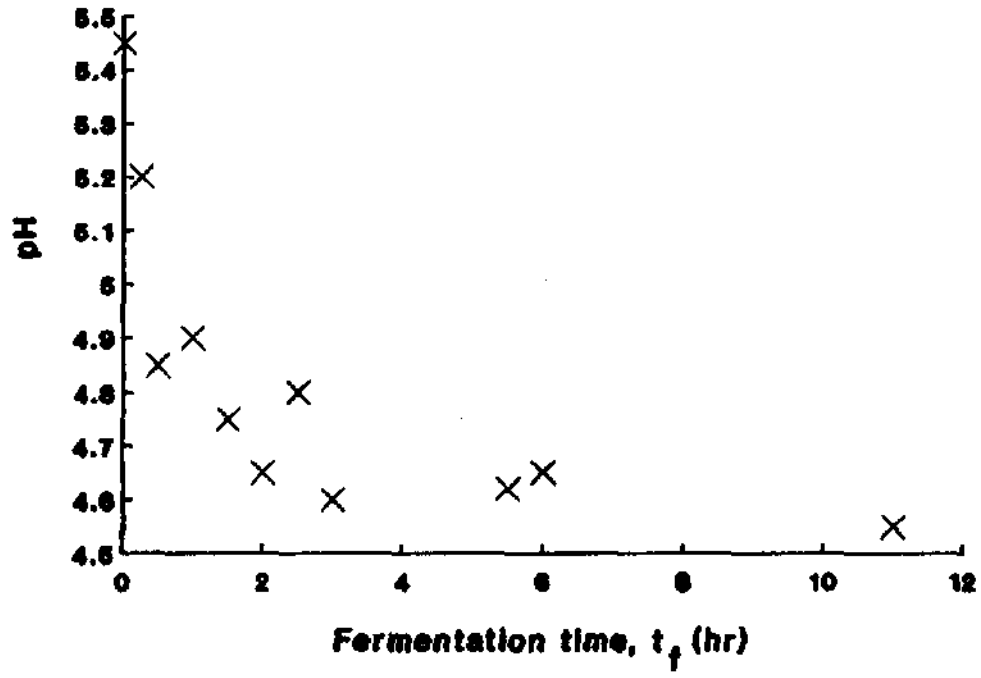


Fig. 2.7 pH profile in tower fermenter
(Jones, Korus, Admassu and Heimsch, 1984)

Ethanol production in tower fermenters has many advantages. Added complexities in form of cell separation and recycling equipment, which are often associated with a high risk of contamination, are not needed (Prince and Barford 1892a). Similarly, bacterial contamination could easily be arrested by either dropping the pH to 3.5 and increasing liquid flow rate, to wash off the contaminating

bacteria, or flushing the tower, at high liquid flow rate, with 9% saline solution (Prince and Barford, 1982a; Nagashima *et al.*, 1984; Jones *et al.*, 1984). Furthermore, better gas disengagement, fluid mixing and liquid/solid contact, are advantages of the tower fermentation systems over the packed bed fermentations. In addition, the use of flocs is associated with lower mass transfer resistance (Andrews and Przezdziecki, 1986).

There is, however, the tendency that flocs at the base of the tower could grow very large due to the presence of high sugar concentration and rich growth medium. This could eventually plug-up the base of the tower causing channelling, poor mixing and finally inefficient production.

3.1 INTRODUCTION

The performance of fluidized bed bioreactors depends not only on the kinetics of the biochemical reaction concerned, but also on physical processes such as interphase and interparticular or intercellular mass and heat transfer, which are inturn also dependent on the mixing characteristics of the various phases involved (Swaine and Daugulis, 1988). Therefore, an understanding of liquid phase mixing, in three phase fluidized beds, is essential for proper design of this reactor (Wen and Fan, 1973; Smith, James and Fidgett, 1978). Moreover, mixing and bed expansion characteristics determine the residence time of fluid elements, in fluidized bed bioreactors, which in turn determine the bioconversion level achievable in these reactors. Setiadi and Larsen (1991) have shown that the height required to achieve a given conversion of glucose to ethanol, in a tower fermenter, increases markedly with increase in axial liquid mixing within the bioreactor.

In this section both mixing and bed expansion characteristics are discussed. In particular, the effects of process conditions, liquid and particle properties on liquid axial dispersion coefficient, bed voidage and liquid holdup, are reviewed. However, a background on the basic aspects of fluidization is first presented before discussing the mixing and hydrodynamic phenomena.

3.2 PRINCIPLES OF FLUIDIZATION

Fluidization is observed when a bed of solid particles come in contact with a vertical upward flow of fluid in an intermediate range of velocities. At low fluid velocities, the bed is in a fixed state and particles are supported by the porous bottom of the column while at high fluid velocities, the particles are conveyed out of the column. However, at intermediate velocities, each particle becomes individually suspended in the fluid, while the

whole bed remain motionless relative to the column walls; the bed is said to be fluidized (Coderc, 1985).

Figure 3.1 shows the basic features of fluidization process.

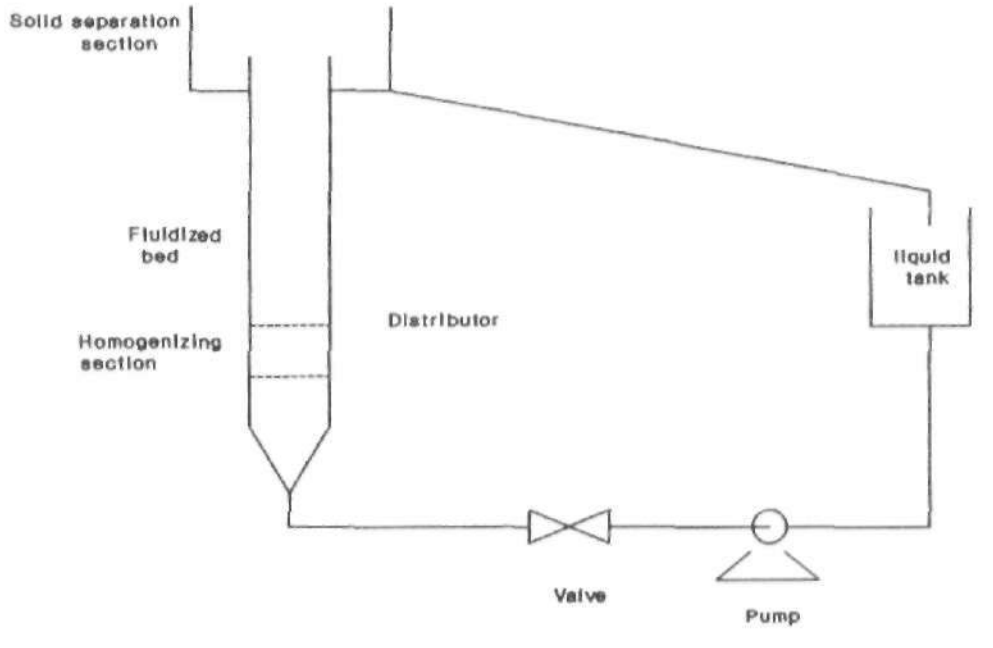


Fig. 3.1: Fluidization process
(Couderc, 1985)

Part of the effluent is often recycled in order to have sufficient fluid flow to suspend the solid particles. A homogenizing section is also provided at the column inlet and it helps to produce an uniform fluid velocity distribution thoughout the entire cross section of the column. Above the bed of particles, is a solids free zone where solids disengagement, from fluid, takes place.

Figure 3.2 shows the characteristics of an ideal two phase S-L, fluidized bed. For solid particles of uniform shapes and sizes, an initial increase of liquid velocity causes steady increase in pressure drop across the bed while the bed height remains virtually unchanged. At a certain liquid velocity, the bed height begins to change while the pressure drop across the bed stabilizes and

becomes constant.

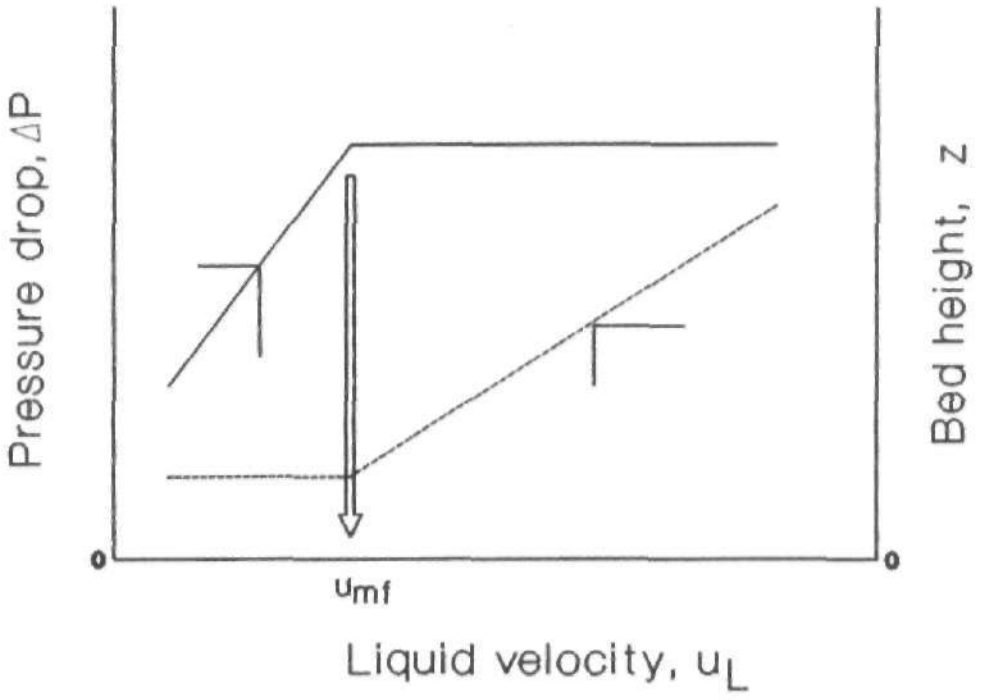


Fig. 3.2: Characteristics of 2-phase systems
(Couderc, 1985)

The velocity at which this change begins, is referred to as the minimum fluidization velocity, u_{mf}. Further increase in liquid velocity, causes the bed to expand while the pressure drop remains constant until finally, the particles are conveyed out of the reactor.

A three phase (S-L-G) fluidized bed show similar characteristics when the liquid velocity is changed at constant gas flow. However, there appears to be a gradual increase in pressure drop across the bed as the liquid velocity increases, even when the bed is fully fluidized, as shown in fiqure 3.3 (Fan, 1989). For beds of fine particles transition from the fixed state to the fluidized state is often not sharp, but show a kind of a transition zone, while beds of large particles tend to show a distinct change from fixed to fluidized states.

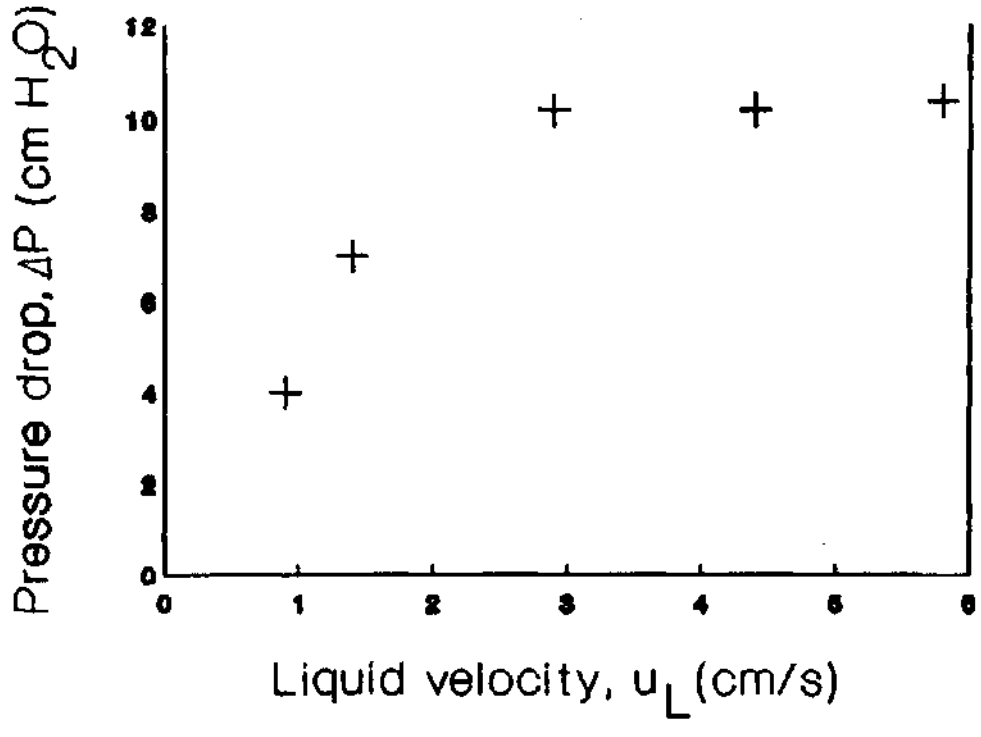


Fig. 3.3: Characteristics of 3-phase system
(Fan, 1989)

A three phase fluidized bed in which the gas phase is produced *in situ* could be expected to have characteristics in between two extremes; one being the two phase (S-L) system in cases where the gas production is very small, thus having an insignificant effect on the characteristics of the reactor. An example of this, is the denitrification of dilute waste where small nitrogen bubbles, produced *in situ*, were found to have negligible effects on the hydrodynamics of the reactor (Schoutens *et al.*, 1986). The other is one in which the rate of gas generation is considerably higher and, therefore, has significant effects on the reactor hydrodynamics. This would be similar to the conventional three phase system; an example is the ethanol fermentation where carbon dioxide generation causes flow pattern similar to those of three phase fluidized beds (Prince and Barford, 1982a). The

transition between fixed and fluidised states, in these bioreactors, was observed to pass through a long intermediate zone (Smith and Greenshields, 1973), and it was suggested that because of very low liquid velocities, encountered in these bioreactors, the bioparticles are fluidized by the gas phase (Gommers *et al.*, 1986).

In three phase fluidized beds, the gas phase from bubbles that rise through the bed at velocities much higher than that of the liquid phase. These bubbles may coalesce and increase in size as they rise up. The size of the gas bubbles depends on the design of the gas distributor and the gas and liquid flow rates (El-Temtamy *et al.*, 1979b). Three flow regimes, depending on the size of the bubbles formed, could be identified. At increasing gas flow, the bubbles are at first small and appear homogeneously dispersed in the reactor, then they begin to coalesce and increase in size until, finally, their sizes become about equal to the diameter of the column. These three transitional stages are referred to as the dispersed, coalescence and slug regimes respectively (Fan 1989). The specific operating conditions for the transition between these three regimes depend chiefly upon the physical properties of gas and liquid, the particle size and the liquid and gas flow rates, since these are the factors that principally determine the onset of coalescence (Darton and Harrison, 1975). However, the slug flow regime occurs when the ratio of superficial liquid velocity to superficial gas velocity equals 0.4 (Darton and Harrison, 1975).

For bioreactors with *in situ* gas production, there is an absence of gas distibutor, the gas comes out of solution as microscopic bubbles and these coalesce and increase in size as they rise through the bed. In this case, all the three flow regimes may be present, in the reactor, at the same time. Thus, the bioreactor is divided into three distinct flow regimes, with dispersed,

coalesced, and slug regimes being at the bottom, middle region and top of the bed respectively. The existence of these three flow regimes, in fluidized bed bioreactors with *in situ* gas production, was reported by Davison (1988). The boundries of these flow regimes will be expected to depend on the prevailing liquid flow rate, rate of gas generation and the bioparticle size. Other factors such as biomass sloughing caused by rising gas bubbles (Chen *et al.*, 1985b) and floc breakup and agglomeration (Smith *et al.*, 1978), which are often observed in these bioreactors, would further complicate the transition between the three flow regimes.

3.3 LIQUID MIXING

In fluidized beds, liquid mixing takes place as a result of interactions between solids and fluid phases. The degree to which this mixing takes place could depend on a the number of factors including the nature of the interaction between the various phases, the liquid and solid properties and the process conditions upon which the fluidization takes place. In this section, the mechanisms responsible for the liquid mixing, the different categories of liquid mixing, often encountered, and the determination of the axial liquid dispersion coefficient, will be discussed.

3.3.1 Mechanisms of liquid mixing in fluidized beds

Liquid mixing may be caused by the presence of bubbles and particles, motion of bubbles and particles, and the radial velocity profile (El-Temtamy *et al.*, 1979a).

The particles obstruct the liquid flow, causing the splitting up of the liquid streamlines. It is, therefore, not surprizing that the presence of solids, in fluidized beds, was found to increase the axial liquid mixing (Michelsen and Ostergaard, 1970; El-Temtamy *et al.*,

1979a). Mixing in the liquid phase may be induced by the continuous splitting and recombination of the liquid streams around the particles. Furthermore, particles suspended in the liquid are in constant oscillatory movement caused by liquid flow. The amplitude of this oscillation, in the vertical direction, increases with increasing liquid velocity. This particle motion could be one of the phenomena reponsible for fluid mixing in two and three phase fluidized beds. Therefore, increasing the size or the concentration of the particles, will be expected to cause increase in the effective magnitude of the resulting turbulence and thereby intensify the axial liquid mixing (El-Temtamy *et al.*, 1979a).

In three phase beds, rising gas bubbles push through bed of solid particles, causing some to be transported up through the bed. The amount of solid particles moved, in this manner, increase with increase in both the number and sizes of gas bubbles. Axial liquid mixing may be caused by the continuous movements of these particles (Muroyama and Fan, 1985).

Moreover, rising bubbles are trailed by a turbulent wake consisting of a particle free liquid, or liquid wake, immediately below the bubble and a lower region of particles and liquid apparently moving with the bubble (Darton and Harrison, 1975). These wakes move at velocities greater than the average insterstitial liquid velocity and are recurrently formed and shed during their upward movements. The resultant effects are the increase in liquid axial mixing and the reduction of the average liquid velocity through the bed, which may subsequently cause the decrease of the entire bed height and lead to bed contraction. The phenomenon of bed contraction, when gas is injected into liquid fluidized beds containing small particles was reported by Michelsen and Ostergaard (1970). The extent of liquid mixing which is caused by the movements of liquid and solid wakes, depends on the bubble

size and the difference between bubbles and liquid velocities, or the slip velocity (El-Temtamy *et al.*, 1979a).

3.3.2 Types of liquid mixing

There are basically two types of mixing processes; micromixing and macromixing. These are discussed in this section.

3.3.2.1 *Micromixing*

Micromixing describes the mixing of fluid elements of different ages, at molecular level, in a reactor (Swaine and Daugulis, 1988). Situations in which entering fluid elements come into intimate contact with other fluid elements of all ages, is refered to as maximum mixedness, and prevails in an ideal continuously stirred tank reactor. On the other hand, complete segregation occurs if fluid elements of different ages do not intermix in the reactor, but only come together when withdrawn in the effluent stream. This situation prevails in an ideal plug flow reactor. Column or tubular reactors tend to exhibit the plug flow ideal, in theory, but in practice deviation from this ideal occurs.

A quantitative assesment of micromixing is made by measuring the Danckwert's degree of segregation (Danckwerts, 1981), defined as:

$$\xi = \frac{(\overline{\tau - t})^2}{\theta^2} \qquad 3.1)$$

Where $(\overline{\tau - t})^2$ is the mean square deviation of the ages of all points in the system from the mean age. The quantity θ^2 is defined as: $\theta^2 = \int_0^\infty (\tau - t)^2 F(t)\, d(t)$ and F(t) is the age

distribution function that can be evaluated from the residence time distribution (RTD) of the fluid elements. For complete segregation, $\xi = 1$ and for maximum mixedness, $\xi = 0$.

The effect of micromixing on reaction rates has been summarized by Coulson and Richardson (1979). For reactions with order less than 1, the reaction rate is highest with maximum mixedness, while it is highest with complete segregation for reactions with order higher than 1. Micromixing does not affect the rate of first order reactions. For second order irreversible reactions the difference in reaction rate, between maximum mixedness and complete segregation, is about 10% (Bailey and Ollis, 1977). Therefore for reactions with orders, in the range of 0.5 to 2, the effect of micromixing on reaction rates, can be ignored (Nauman, 1981).

However, micromixing may be important in fermentation systems using immobilized microorganisms, since transport of nutrients and substrate into the immobilized microorganisms could be rate limiting (Tsai, Erickson and Fan, 1982). But its effects on reaction rate, can in all practical cases, be included in the mass transfer considerations (van Deemter, 1985).

3.3.3.2 *Macromixing*

Macromixing examines the retention time of fluid elements entering a reactor (Swaine and Daugulis, 1989). There are also two extremes of macromixing; the continuously stirred tank reactor exhibits complete macromixing, as all fluid elements of all ages are instantaneously mixed in the reactor, while the plug flow reactor shows zero macromixing because fluid elements of different ages do not mix in the reactor (Levenspiel, 1972). Though tubular reactors are better operated with plug flow characteristics, the fluidized bed bioreactors are, in practice, far from being ideal due to the

interactions and movements of the various phases. Consequently, there is always some backmixing in the continuous phase (Swain and Daugulis, 1989).

A number of flow models could be used to model non ideal flow in fluidized bed bioreactors, but the dispersed plug flow model is mostly used. In this model, macromixing is quantified by the dispersion coefficient. A two-dimensional unsteady state dispersion model is given in equation 3.2 (Fan, 1989).

$$\frac{\partial C_g}{\partial t} = D_z \frac{\partial^2 C_g}{\partial z^2} + \frac{D_r}{r} \frac{\partial}{\partial r}\left(r \frac{\partial C_g}{\partial r}\right) - \frac{u_L}{e_L} \frac{\partial C_g}{\partial z} + R_S \qquad 3.2)$$

The parameter D_r is the radial dispersion coefficient. It is often neglected because it is small in comparison to the axial or longitudinal dispersion coefficient (D_z). El-Temtamy *et al.* (1979b) have shown that for beds of 0.45 and 0.96 mm glass beads, the axial dispersion coefficient is roughly 20 to 30 times the radial dispersion coefficient, while in beds of 3 mm glass beads the axial dispersion coefficient is 2 to 10 times higher. Moreover the radial dispersion coefficient may be of importance only in large diameter columns. For a steady state process, and negligible radial dispersion, equation 3.2 is reduced to equation 1.6 (Section 1.4.1).

To evaluate the axial dispersion coefficient, the residence time distribution (RTD) technique is most widely used. This technique requires the injection of a tracer material into the reactor and then monitoring of the response at a point downsteam of the injection point. The mixing coefficient is then calculated using the first and second moments of the response curve (Levenspiel, 1972; Nauman, 1981). Though the RTD method has been widely used in chemical reactors, it has not been used, with the same regularity, in bioreactors. This is probably because of the complex nature of these reactors and the difficulty of

selecting a suitable tracer material (Swaine and Daugulis, 1989). The presence of microorganisms in bioreactors make tracer selection difficult because poisoning of these microorganisms or degradation of the tracer, by the microorganisms, can alter the entire results and the consequent conclusions, on bioreactor performance, drawn therefrom.

3.3.3 Tracer requirements

The major requirements for a tracer material for use in RTD study, in bioreactors, have been outlined by Falch and Gaden. Jr. (1970) and Swaine and Daugulis (1989), as follows:

1. The tracer should have no effect on surface tension or growth rate of the microorganisms, and it should not be metabolizable by the organisms.
2. Changes in the pH and redox potential in the reaction system should have no effects on the tracer material.
3. The tracer must be soluble and should not be absorbable or adsorbable on to the microorganisms or reactor equipment.
4. Its method of detection must not be interfered with by any component in the reaction mixture and the tracer must be detectable even at extremely low concentrations.
5. The tracer must be cheap and easy to dispose of.

These stringent requirements constrained many researchers (Gommers *et al.*, 1986; Setiadi, 1989; Garcia, Martin, Ruiz and Perez, 1989; MacDonald, 1991) forcing them to carry out RTD determinations on abiotic systems and use the results obtained to model the performance of active bioreactors. Nonetheless, some other researchers have performed RTD studies in active bioreactors, using different types of tracer materials as summarized in Table 3.1.

Toxicity of the tracer material to the microbial

functions or metabolization of the tracer are serious constraints. Very often, materials which are known not to be harmful to the microorganisms and which are not motabolizable, are used. This is the case of D-xylose and lactose in the case of *S. cerevisiae*. The toxicities of Rodamine WT and Dextran blue have not been reported. But, Brilliant blue was found to have slight repressive effect on *Eschericia coli* (Falch and Gaden. Jr., 1970).

Diffusion of tracer in and out of the biomass, causes a long tail in the RTD and this can invalidate the use of a dispersed plug flow model (Levenspiel, 1972).

Table 3.1 Tracers used in RTD studies of the liquid phase in active bioreactors

Tracer	Organism	Reference
Brilliant blue	*E. coli*	Falch and Gaden. Jr. (1970)
D-xylose	*S. cerevisiae*	Admassu *et al.* (1985)
Ethanol	*S. cerevisiae*	Anselme and Tedder (1987)
Lactose	*S. cerevisiae*	Godia *et. al.* (1987a)
Flourescein	*S. cerevisiae* and *S. carlbergensis*	Brohan and Mcloughlin (1984a)
Dextran blue	Mixed	Jimnez *et al.* (1988)
Rhodamine WT	Mixed	Stevens *et al.* (1986)
2,3,butanediol and 2-ethoxyethanol	*Z. mobilis* and *S. cerevisiae*	Swaine and Daugulis (1989)

Stevens, Berthouex and Chapman (1986) have studied this diffusion phenomenon. They defined the diffusion time of

tracer into biomass as:

$$\tau_d = \frac{L_b^2}{D_e} \qquad 3.3)$$

D_e is the diffusivity of the tracer material in the biomass, which could be approximated to the diffusivity of the tracer in water. They urgued that for systems with residence time τ_s, the ratio $\tau_d/\tau_s \geq 100$ signifies negligible tracer diffusion into the biomass. When the ratio is less than 0.1, then diffusion into the biomass is so rapid that its concentration in the biomass is always equal to that in the bulk solution. In this case, the porous biomass behaves as though it is part of the bulk solution and the tracer residence time will be increased in propotion to the biomass volume. At intermediate values of the ratio; between 0.1 and 100, the tracer concentration in the biomass lags that in the bulk solution and the RTD will have a long tail. The solution to this long tail is to incorporate a diffusion term in the dispersion model. Also, the use of a tracer of large molecular weight would increase D_e and consequently lower τ_d. This may have the effect of significantly decreasing the tracer diffusion. Jimnez, Noyola, Capdeville, Roustan and Faup (1988) have shown that this is indeed the case with respect to Dextran blue which indicated negligible diffusion in submerged biofilter; its high molecular weight of 2,000,000, was thought to be responsible for that observation.

Adsorption of tracer material on the biomass and subsequent desorption may also be responsible for long tail in RTD determination. Rodrigues, Zuping and Loureiro (1991) have developed a model in which the effect of tracer adsorption has been considered. They added a linear adsorption term to the dispersed plug flow model.

It must be remembered that different microorganisms

have different capabilities and responses to the same type of tracer material. For example, while *S. cerevisiae* cannot metabolize D-xylose, *Pachysolen tannophilus* converts D-xyloxe to ethanol (MacDonald, 1991). Therefore, the suitability of any tracer material must be tested against the microorganisms to be used prio to RTD studies, for evaluation of the dispersion coefficient. Moreover, the bioreactor must be tested regularly against contamination by microorganisms capable of metabolizing the tracer.

3.4 AXIAL LIQUID DISPERSION COEFFICIENT

It was argued earlier in section 1.4.1 that the use of plug flow model in designing and predicting the performance of fluidized bed bioreactors, is not adequate. Consequently, the dispersion term was included, in the ideal plug flow equation. The cause of axial liquid mixing in fluidized bed bioreactors is similar to that in other fluidized bed reactors. Numerous researchers have studied axial liquid mixing in fluidized bed reactors and have determined the values of axial liquid dispersion coefficients for varieties of operating conditions. Many have also proposed correlations for calculating this parameter from known process parameters and liquid and solid properties. These correlations are reviewed in this section. In addition, the effects of particle and liquid properties and process parameters, on the axial liquid dispersion coefficient, are discussed.

3.4.1 Effect of gas velocity

An increase in gas velocity, at constant liquid flow, will be expected to cause an increase in the size of gas bubbles, slip velocity and bed voidage. These changes would lead to changes in flow regimes as discussed earlier (Sections 3.2 and 3.3.1). The magnitude of axial liquid mixing has been shown to depend on the prevailing flow

regime (Michelsen and Ostergaard, 1970; El-Temtamy *et al.*, 1979a; Fan, 1989). Small dispersed bubbles will result in little axial liquid dispersion compared to large coalesced bubbles or slugs. Therefore, an increase in gas velocity will produce an increase in axial liquid dispersion coefficient (D_z) at all liquid velocities (Kim and Kim, 1983).

Vail, Manakov and Manshilin (1968) observed an increase in D_z with increasing superficial gas velocity in the range 1.5 to 9.9 cm/s, at liquid velocities of 1.74 and 3.07 cm/sec, in a bed containing particles of an average size of 0.87 mm in diameter.

Similarly, Michelsen and Ostergaard (1970) have reported increases in D_z with increases in gas velocity in the range 0 to 27 cm/s, at liquid velocities of 10 to 26 cm/s, but the extent of the increase was found to be dependent on the particle size. Beds of 1mm particles showed a higher increase in D_z whereas beds of 6 mm particles showed no effect of gas velocity on D_z. This observation was, however, refuted by Kim, Baker and Bergougnou (1972) and Kim and Kim (1983) who reported increases in D_z with increasing gas velocity even for a bed of 6 mm particles. The differences in these observations may be due to different liquid velocities used in the studies; Kim *et al.* (1972) and Kim and Kim (1983) have used lower liquid velocities in the range 1.4 to 10.21 cm/s, whereas Michelsen and Ostergaard (1970) used higher liquid velocities of 10 to 26 cm/s, and this could account for the observed increase in D_z, with increasing gas velocity, for the case of 6 mm particles. Furthermore, Kim *et al.* (1972) and Kim and Kim (1983) experimented with a two dimensional column, which was not common. Thus, the difference may also be due to the geometry of their column.

El-Temtamy *et al.* (1979a) have also observed increases in D_z with increasing gas velocity and have

agreed that the particle size affects the rate at which D_z increases. They did not detect axial liquid mixing in a bed of 3 mm particles even at a gas velocity of 5 cm/sec, due perhaps to their method of tracer injection. They used the steady state injection method which does not take into consideration other causes of axial dispersion beside physical liquid backflow (Mecklenburgh and Hartland, 1975). A typical effect of gas velocity is shown in fiqure 3.4 and it can be seen that an increase in D_z, with increasing gas velocity, occured at all liquid velocities.

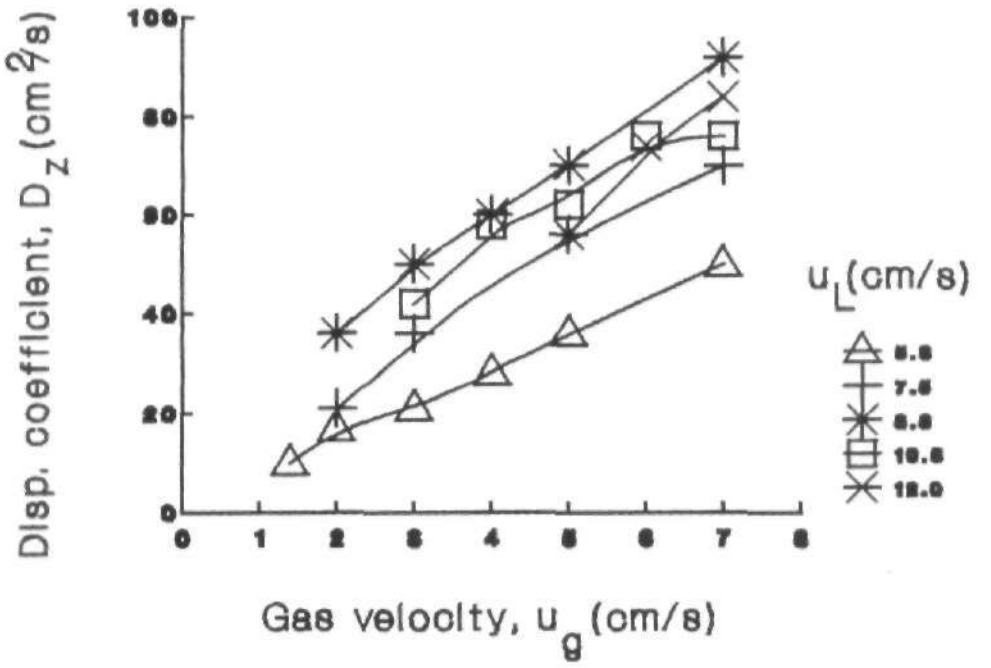


Fig. 3.4: Effect of gas velocity on dispersion coefficient (El-Temtamy *et al.*, 1979a)

Studies on the effect of gas velocity, in active fluidized bed bioreactors, are few. Using particles containing yeast immobilized in calcium alginate, Davison (1988) found that increases in gas velocity, at constant liquid flow, caused decrease in particle Peclet number ($Pe_p = u_L d_p / D_z$), which was an indication of an increase in axial liquid dispersion coefficient (Fig. 3.5). Similarly,

Brohan and MacLoughlin (1984a) and Smith and Greenshields (1973) indicated that carbon dioxide production in tower fermenters could cause significant increases in axial liquid mixing.

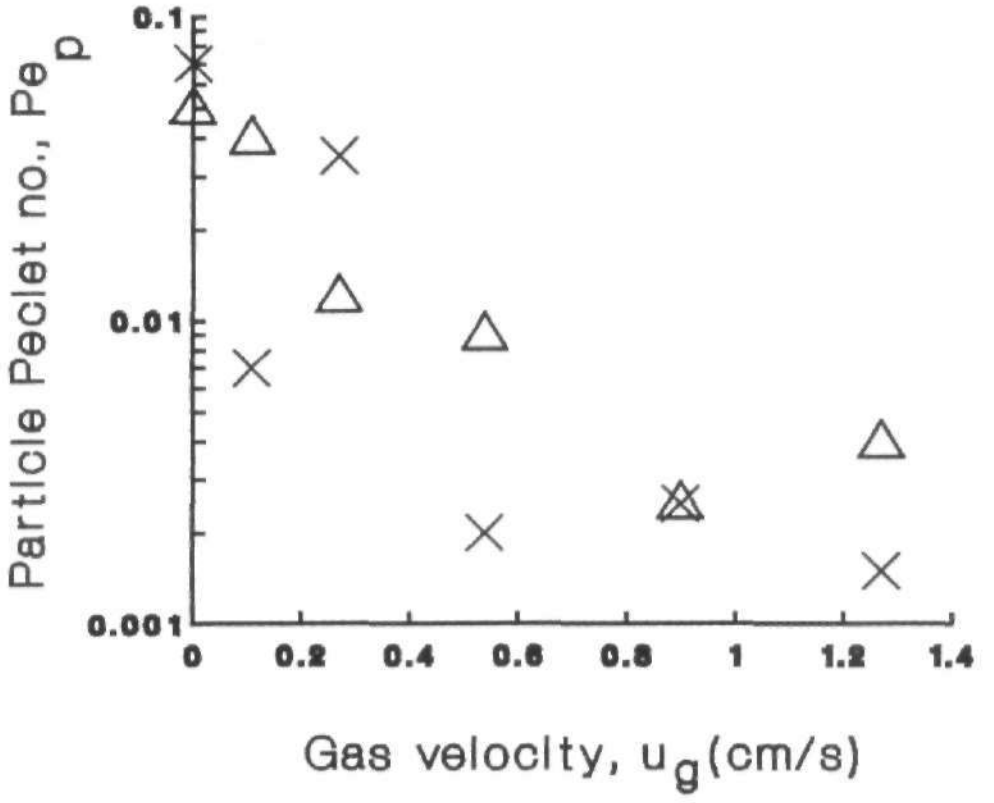


Fig. 3.5: Effect of gas velocity on dispersion coefficient in fluidized bed bioreactor for bottom (-X-) and top (-Δ-) of bed
(Davison, 1988)

Furthermore, using process conditions and particles similar to those obtained in bioreactors, Gommers *et al.* (1986) showed that gas velocities, in the range 0.05 to 0.2 cm/s, have a strong influence on the mixing characteristics of fluidized bed reactors. Their results are reproduced in Table 3.2 and it indicates that a low gas velocity of 0.083 cm/s could increase the axial liquid dispersion coefficient from 0.7 to 10.1 cm^2/sec in a 4 cm

ID column or from 0.9 to 34 cm^2/sec, in an 8 cm ID column.

Table 3.2: Influence of gas velocity on D_z

Column diam., D_c (cm)	Liquid vel., u_L (cm/s)	Gas vel., u_g (cm/s)	Disp. coefficient, $D_z \times 10^4$ (m^2/sec)	
			Without gas	With gas
2	1.3	0.111	1.0-2.0	1.0-2.0
4	1.2	0.083	0.7-1.5	2.9-10.1
8	1.0	0.083	0.9-1.9	8.0-34.0
12	1.0	0.114	2.1-4.9	55

(Gommers *et al.*, 1986)

This strong influence, of a small gas velocity in a simulated biological system, was confirmed by Setiadi (1989) who found that a change in gas velocity from 0.0085 to 0.085 cm/s, caused D_z to double from 27.6 to 52.5 cm^2/s, for 1.15 mm alginate beads.

In summary, therefore, it can be concluded that increasing gas velocity has the effect of increasing the axial liquid dispersion coefficient. This increase is due to the rising motion of gas bubbles and their wakes which were shown to be some of the main causes of axial liquid mixing. The extent of increase in D_z, due to increase in gas velocity, may depend on the particle size and the prevailing flow regime.

3.4.2 Effects of liquid velocity

Increases in liquid velocity will result in decreases of bubble sizes at low gas flow rate, higher bed voidage and increased particle oscillation (Kim and Kim, 1983).

While decreases in bubble sizes and increases in bed voidage have decreasing effects on the axial liquid dispersion coefficient, the increase in particle oscillation enhances it (El-Temtamy *et al.*, 1979a). Michelsen and Ostergaard (1970) and El-Temtamy *et al.* (1979a) have agreed that the effect of liquid velocity on the axial liquid dispersion, depends on the gas flow regime and the particle size used.

El-Temtamy *et al.* (1979a) observed that, at constant gas flow, with increase in liquid velocity, the axial liquid dispersion coefficient increased and approached an asymptotic value in a bed of 0.96 mm particles. It increased and passed through a maximum in beds of 2 mm particles.

A similar observation was made by Kim and Kim (1983) who showed that axial liquid dispersion coefficient increased with increasing liquid velocity up to 6 cm/s, in beds containing 1.7 mm glass beads, as shown in figure 3.6. But, the rate of increase in D_z became marginal at liquid velocities higher than 6 cm/s, probably due to lower particle concentration at these velocities, as that could cause a decrease in D_z. They also observed the same trend in a bed of 3.0 mm particles at a gas velocity less than 6.0 cm/sec, but in this bed, D_z continued to increase with increases in liquid velocity when gas velocity was more than 6.0 cm/s.

The difference in these observations, at gas velocities higher than 6 cm/s, was probably the effect of particle size as will be discussed in section 3.4.3.1. Moreover, at a low gas rate, the effect of liquid velocity was found to depend on the bed voidage; D_z increased with increased liquid velocity till the bed voidage reached 0.62-0.65, after which further increases in liquid velocity caused a decrease in D_z. But, at high gas velocities, the value of D_z did not show a maximum, but continued to increase with increasing liquid velocity.

This may be due to changes in the flow regime, from the dispersed to the coalescence regime, which occurs at high gas velocities; an increase in liquid velocity does not, therefore, reduce the bubble size any further. Thus, the observed increase in axial liquid dispersion coefficient could be because of the increase in gas flow rather than the increase in liquid velocity.

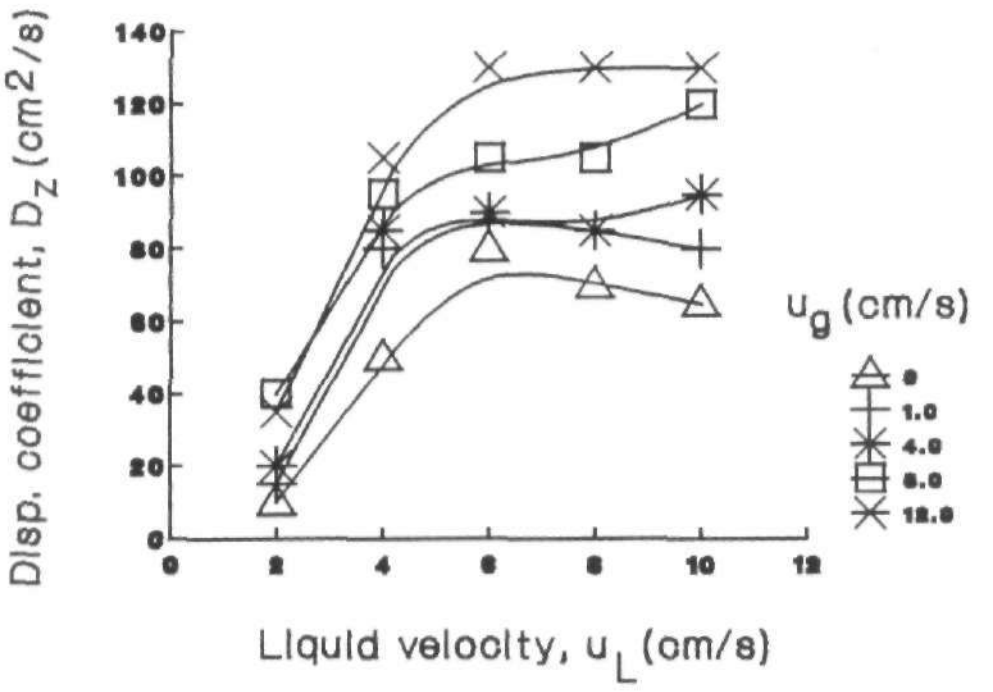


Fig. 3.6: Effect of liquid velocity on dispersion coefficient
(Kim and Kim, 1983)

Using small sand particles of 0.152 mm in diameter, Setiadi (1989) has shown that, at a gas velocity of 0.0085 cm/s, the axial liquid dispersion coefficient increased with increases in liquid superficial velocity, due perhaps to increased particle oscillation. But, at gas velocities higher than 0.0085 cm/s, more complex behaviour of the bed was observed; the axial liquid dispersion coefficient increased with increases in liquid flow rate, to a bed

voidage of 0.65, and then decreased with further increases in liquid velocity. This observation was in agreement with that of Kim and Kim (1983) and might be due to lower particle concentration which was noticed to cause a decrease in D_z. But, there appeared to be a remarkably large difference between gas velocities of 0.0085 and 6.0 cm/s at which Setiadi (1989) and Kim and Kim (1983) respectively, observed changes in flow regime. The cause for this difference is not known.

However, not everyone agreed with these observations. Ostergaard (1978) has pointed out that liquid velocity has no significant influence on D_z for 1 mm glass beads, while El-Temtamy *et al.* (1979a) have reported decreases in D_z with increases in liquid velocity for bed of 0.45 mm particles.

The effect of liquid velocity on the axial liquid dispersion coefficient in two phase (S-L) fluidized beds was studied by Chung and Wen (1968). They showed that the axial liquid dispersion coefficient increased with increases in liquid velocity, which is in line with the observations in three phase fluidized beds discussed above. This report was in agreement with the results of Wen and Fan (1973) and Setiadi (1989). Kikuchi *et al.* (1984) have also observed increases in D_z with increases in liquid velocity. They found that the axial liquid dispersion coefficient was subject to a peculiar influence of bed voidage; it reached a maximum value at a bed voidage between 0.7 and 0.8. This observation was in agreement with the results of Cairns and Prausnitz (1960) and Mehta and Shemilt (1976), who independently showed that the axial liquid dispersion coefficient was strongly influenced by the bed voidage.

The effect of liquid velocity on D_z in anaerobic fluidized beds, with *in situ* gas production, has not been studied. But in a simulated biological system, Gommers *et al.* (1986) have not observed any substantial effect of

liquid velocity, in the range 0.5-2.0 cm/s, on axial liquid dispersion coefficient (D_z).

3.4.3 Effect of particle properties

There are two particle properties that may be expected to have effects on axial liquid dispersion coefficients; density and size. The nature of the effects of these parameters, on the axial liquid dispersion coefficient, are discussed in this section.

3.4.3.1 *Particle size*

The effect of particle size on D_z was studied by Michelsen and Ostergaard (1970) with 0.25, 1.00, 3.00 and 6.00 mm glass beads. They observed that the bed of 6 mm particles gave a very low degree of mixing, lower than that observed in a solids free system, while the bed of 1 mm particles was characterised by high degree of mixing, comparable to that of the solids free system both in trend and intensity. The bed of 0.25 mm particles showed a high degree of liquid circulation which made dispersion models inapplicable. But the bed of 3 mm particles exhibited rather complex behaviour. These observations could be due to the fact that large particles cause bubble break-up resulting in smaller bubbles while smaller particles cause the bubbles to coalesce (Epstein, 1981). The uniform bubble size distribution and small average bubble size observed, in a bed of 6 mm particles, proves this.

Kim *et al.* (1972) have also observed two distinct flow regimes depending on the particle sizes. Their results indicated that bubble coalescence occurred when particles were less than a critical size of 2.5 mm, while bubble disintegration occured when the particles are larger than this critical value. This may explain why Michelsen and Ostergaard (1970) observed a higher degree of mixing in beds of 1 mm particles than those of 6 mm, as bubble coalescence may have occured with the smaller

particles leading to higher axial liquid mixing.

Kim and Kim (1983) have agreed that D_L is a decreasing function of the particle diameter. A higher degree of axial liquid dispersion for smaller particles was also reported by Saberian-Broudjenni, Wild and Kim (1989). Their results, summarized in Table 3.3, indicated that increasing particle size has the effect of decreasing D_L, which confirmed the observations in earlier reports. It also confirmed that the degree of change in D_L, due to changes in particle size, is dependent on the prevailing gas velocity.

Table 3.3: Influence of particle size on D_L

Particle diameter, d_p (mm)	Dispersion coefficient, D_L (m^2/sec)	
	u_g = 5.5 cm/sec	u_g = 13.5 cm/sec
1.4	0.009	0.018
3.2	0.006	0.009

(Saberian-Broudjenni, Wild and Kim, 1989)

In another experiment, performed at a low gas velocity similar to that obtainable in fluidized beds with *in situ* gas production, Setiadi (1989) had observed that particle size, in the range 0.389 to 0.78 mm had no effect on axial liquid dispersion coefficient at low gas velocity of 0.0085 cm/sec. But at higher gas velocities the D_L, in a bed of 0.389 mm particles, was found to be higher than that of 0.78 mm particles, indicating that intensity of liquid mixing was higher with smaller particles, and thus, further confirming the earlier reported observations.

There were, however, a few dissenting views. El-Temtamy *et al.* (1979a) have reported that the D_L did not

vary with particle size. Similarly, Nguyen-Tien, Patwari, Schumpe and Deckwer (1984) have reported that small particles of size less than 0.3 mm do not significantly influence liquid phase dispersion.

The effect of particle diameter, in two phase (S-L) fluidized beds, was also investigated. Chung and Wen (1968) have realised the effect of particle properties and, therefore, expressed those effects through the use of the minimum fluidization velocity and the bed voidage. Krishnaswamy and Shemilt (1973) have, similarly, noted the effect of particle size on D_L; they observed that the Bodenstein number Bo_m ($4mu_L/D_L$) for 0.33 mm sand particles was consistently lower than that for 0.5 mm glass particles (Fig. 3.7).

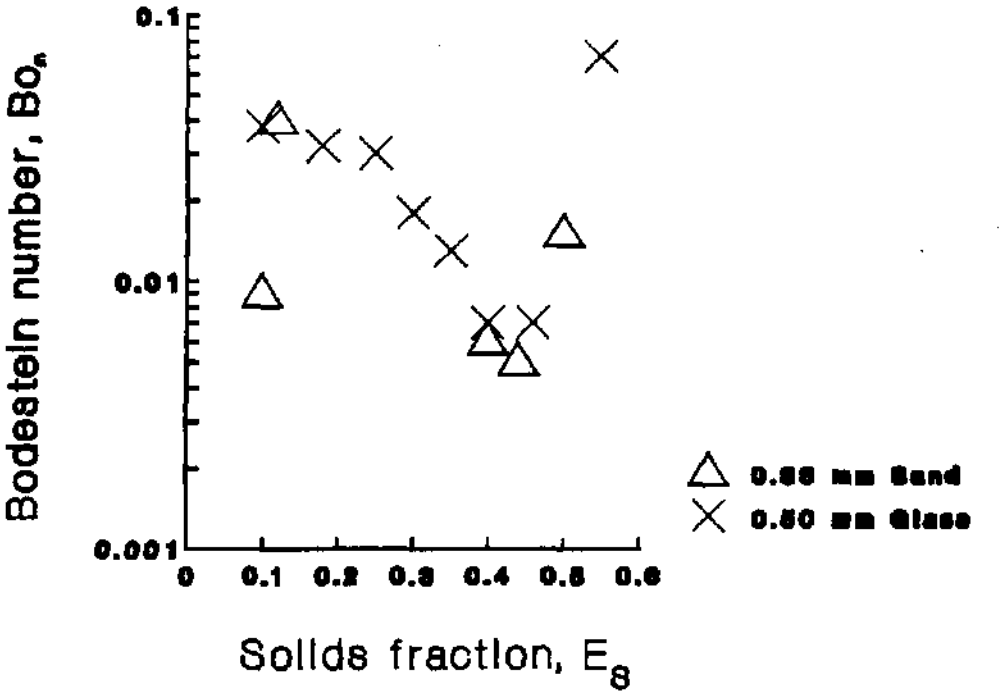


Fig. 3.7: Effect of particle size on dispersion coefficient for two phase fluidized bed (Krishnaswamy and Shemilt, 1973)

This indicated that the axial liquid dispersion

coefficient was higher with smaller size particles. The higher dispersion coefficient for smaller particles of the same density and at the same bed voidage may be due to more rapid particle circulation and possibly greater freedom of movement for smaller particles.

However, Kikuchi *et al.* (1984) observed differently. Their results showed that the axial liquid dispersion coefficient for 0.239 mm glass beads was lower than that for 0.440 mm glass beads, at the same voidage, indicating that D_z was an increasing function of the particle size. The same observation was made by Setiadi (1989) with respect to coal particles. The D_z for 0.55 mm coal was found to be consistently lower than that for 1.09 mm coal. The same trend was also observed for bone charcoal particles. However, for sand particles, the D_z was about 117% higher for 0.152 mm particles compared to 0.462 mm particles. Therefore the nature of effect, of particle size on D_z, was contradictory. Furthermore, Wen and Fan (1973) have indicated that physical properties of solids have no significant effect on the axial liquid dispersion coefficient.

In biologically active fluidized beds, changes in particle size may occur due to biomass growth or sloughing. An increase in particle size, in the order of 2.7 times, was reported by Lee *et al.* (1983). This increase may cause changes of flow regime and may affect the axial liquid dispersion coefficient. There is no report on the effect of size of bioparticles on D_z, though, Setiadi (1989) had shown that for two phase (S-L) system, an increase in bioparticle size had insignificant effect on D_z; a 50% increase in particle size, due to biomass growth, changed D_z by only 6%. However, for three phase systems, it will be expected that both biomass growth and biomass sloughing will add to the complexity of the relationship between particle size and D_z.

It can be concluded that, though particle size has

been demonstrated to have influence on the axial liquid dispersion coefficient, the nature of the effect will depend on the prevailing process conditions.

3.4.3.2 *Particle density*

The density of particles could affect the axial liquid dispersion coefficient because higher liquid and gas velocities will be required to fluidize, to the same bed voidage, a bed of heavy particles compared to light ones. Most studies on the axial liquid dispersion coefficient of three phase (S-L-G) system related to particles with densities in the range 2.3 - 2.9 g/cm^3, though, Kato, Morooka, Koyama, Kago and Yang (1985) have used particles of lower density (1.2 g/cm^3). But, they have not considered the effect of particle density on D_z.

However, in two phase (S-L) system, Cairns and Praunsnitz (1960) have noticed a higher value of D_z in a bed of 2.96 mm lead spheres compared to bed of 3.2 mm glass beads, at the same bed voidage. They concluded that the particle density has a positive effect on D_z. Krishnaswamy and Shemilt (1973) have also noted positive effect of particle density on D_z. Their results, presented in Table 3.4, showed that D_z for 0.5 mm steel spheres was about twice that of 0.5 mm glass beads, at the same bed voidage. They, however, noted that the high D_z obtained for steel, as compared to glass, related to the high velocity required for equivalent expansion of the denser particles.

Using a simulated biological bed, Setiadi (1989) has shown that the effect of particle density, in the range 1.2-1.05 g/cm^3, depended on the gas velocity. At a gas velocity of 0.0085 cm/s, the D_z of sand particles with density of 2.65 g/cm^3 was lower than that of coal particles, density of 1.31 g/cm^3, by 39% at the same gas and liquid velocities. However, the difference reduced to 17%, at a gas velocity of 0.042 cm/s, while, at gas velocity of 0.085 cm/s, the effect of particle density, on

D_z was not observed; D_z appeared to be a function of liquid velocity only. Any influence of particle density on D_z for the two phase system, was not observed.

Table 3.4: Influence of particle density on D_z

Particle	Particle density, ρ_p (g/cm^3)	Dispersion coefficient, D_z (cm^2/s)	Bed voidage, ε (-)
0.7 mm Resin	1.28	1.41	0.85
0.5 mm Glass	2.50	35.22	0.89
0.5 mm Steel	7.02	57.52	0.70

(Krishnaswamy and Shemilt, 1973)

3.4.4 Effect of liquid properties

The liquid properties of viscosity and surface tension may affect D_z, as liquid mixing in 3-phase fluidization, has been shown to be primarily caused by the rising motion of gas bubbles. The liquid viscosity and surface tension might have an effect on the bubble rising velocity, which in turn would influence D_z (Kim and Kim, 1983).

3.4.4.1 *Liquid viscosity*

Liquid viscosity will be expected to affect the bubble size and bubble rising velocity. Since these two parameters have been shown to influence the axial liquid dispersion coefficient, changes in liquid viscosity will therefore be expected to have some influence on D_z. Studies on the effect of liquid viscosity on axial liquid dispersion coefficient are few.

Kim and Kim (1983) studied the effects of liquid viscosity, in the range 1-27 cP, on the D_z. They noted that the nature of viscosity effect on D_z depends on the gas

velocity. Their result, presented in figure 3.8, showed that D_z increased with viscosity in two phase (S-L) beds and three phase beds of 6 mm, 3 mm and 1.7 mm particles, at low gas velocities less than 4 cm/s. In contrast, D_z decreased with increases in viscosity in beds of 1.7 and 3.0 mm particles at high gas flow rates. They further noted that the effect of liquid viscosity on D_z was very small; a twenty-seven fold increase in viscosity increased D_z by only 20%.

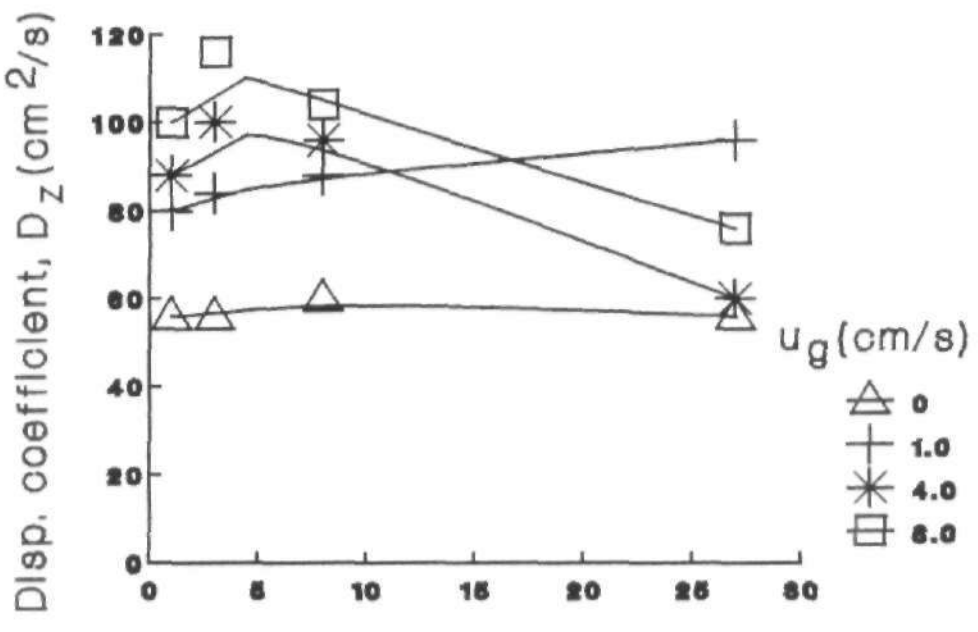


Fig. 3.8: Effect of liquid viscosity on dispersion coefficient

(Kim and Kim, 1983)

This was due to the liquid viscosity having little effect either on bubble size or rising velocity, the two parameters that were shown to cause axial liquid mixing.

For two phase (S-L) systems, Mehta and Shemilt (1976), using 0.5 mm glass beads and a viscosity range of 0.56 to 7.74 cP, have shown that the nature of the

viscosity effect on D_z depends on the bed voidages; at bed voidages greater than 0.85, there was a major dependence of D_z on viscosity. At this condition, there was a linear logarithmic relationship with a negative slope of about 1. While, at voidage lower than 0.8, there was no evidence of any relationship between axial liquid dispersion coefficient and viscosity. This observation contradicted that of Kim and Kim (1983), for the two-phase systems. The contradiction could be due to the differences in particle sizes employed for the two studies; Mehta and Shemilt (1976) used 0.5 mm glass beads whereas Kim and Kim (1983) used particles of 1.7 mm, 3 mm and 6 mm diameter, which are three to twelve times bigger. Chung and Wen (1968) also realized the effect of viscosity on D_z. In their correlation, D_z varied with viscosity to a power of 0.48.

The effects of liquid viscosity on D_z for anaerobic systems with *in situ* gas production, have not been studied. But, Setiadi (1989) showed that, for a simulated biological system, D_z varied with viscosity to the power of 0.509, for three phase, and -1.57, for two phase, systems respectively. These results indicated that the presence of gas caused the reversal of the effect of viscosity on D_z. It can be concluded that, though liquid viscosity may have some effect on D_z, the nature and intensity of this effect could depend on gas flow rate and the bed voidage.

3.4.4.2 *Surface tension*

Increased liquid surface tension reduces the bubble size and rising velocity and hinders bubble coalescence (Gorowara and Fan, 1990). But, Kim, Baker and Bergougnou (1977) have shown that surface tension has small positive effects on bubble size and rise velocity. Therefore, surface tension can be expected to have some influence on axial liquid dispersion coefficient, because both bubble size and rise velocity have been shown to affect the axial liquid dispersion coefficient.

There has only been one report on the effect of surface tension on D_z. Kim and Kim (1983) have reported that the effect of surface tension, on D_z, in the range 38.5-76 dynes/cm was very small, as shown in figure 3.9. This was expected, because surface tension had limited influence on bubble size and rize velocity.

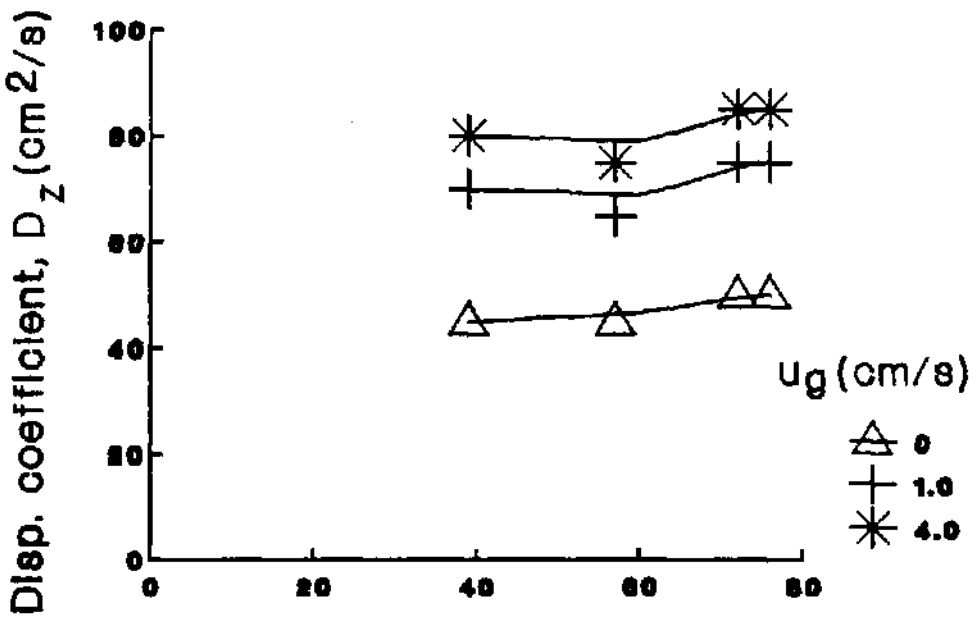


Fig. 3.9: Effect of surface tension on dispersion coefficient

(Kim and Kim, 1983)

There was no reported effect of surface tension on D_z for two phase (S-L) systems. But, since surface tension mainly affects the bubble characteristics, it can be expected to have no significant influence on D_z, in two phase systems.

3.4.5 Effect of column diameter

An increase in column size will be expected to cause

an increase in radial velocity profile and a consequent increase in axial liquid dispersion coefficient. Ostergaard (1978) has noted that the D_z values he obtained in a 22.86 cm ID column, for 1 mm and 6 mm particles, were respectively 50% and 100% higher than those reported by Michelsen and Ostergaard (1970), for the same particles, in a 15.24 ID column. This observation suggested that the column diameter has a positive effect on D_z. Muroyama *et al.* (1978) also noted this positive effect. They found that D_z varied with column diameter to the power of 1.58 for the coalesced bubble regime and 1.5 for the dispersed bubble regime. This result was in agreement with the findings of El-Temtamy *et al.* (1979a) and Kim and Kim (1983). They reported D_z varying with column diameter to the power of 1.6 and 1.66 respectively, though they did not observe any difference between coalesced and dispersed bubble regimes.

For two phase (S-L) systems, Cairns and Prausnitz (1960) have observed a very large D_z increase with decreasing ratio of particle diameter to column diameter (d_p/D_c), indicating a positive effect of column diameter. Similarly, Krishnaswammy and Shemilt (1972) have also acknowledged the positive effect of column diameter on axial liquid dispersion coefficient and have, accordingly, introduced this effect in their correlation for D_z, through the use of an open tube dispersion coefficient.

Gommers *et al.* (1986) have shown that, for particles and conditions similar to those of biological systems, column diameter had a positive effect on D_z. However, the effect was more pronounced when gas was flowing, as presented in figure 3.10. Similarly, Setiadi (1989) has acknowledged the positive effect of column diameter on D_z, and has consequently, raised the column diameter to the power of 1.58 and 0.75 in his proposed correlations for D_z, for three and two phase systems respectively. This indicated that the effect of column diameter is more

pronounced in three phase systems as compared to the two phase beds.

There was unanimous agreement that the column diameter has a positive influence on the axial liquid dispersion coefficients in both the three phase and the two phase systems. However, the extent of this effect could depend on the flow regime or the flow rate of the gas phase.

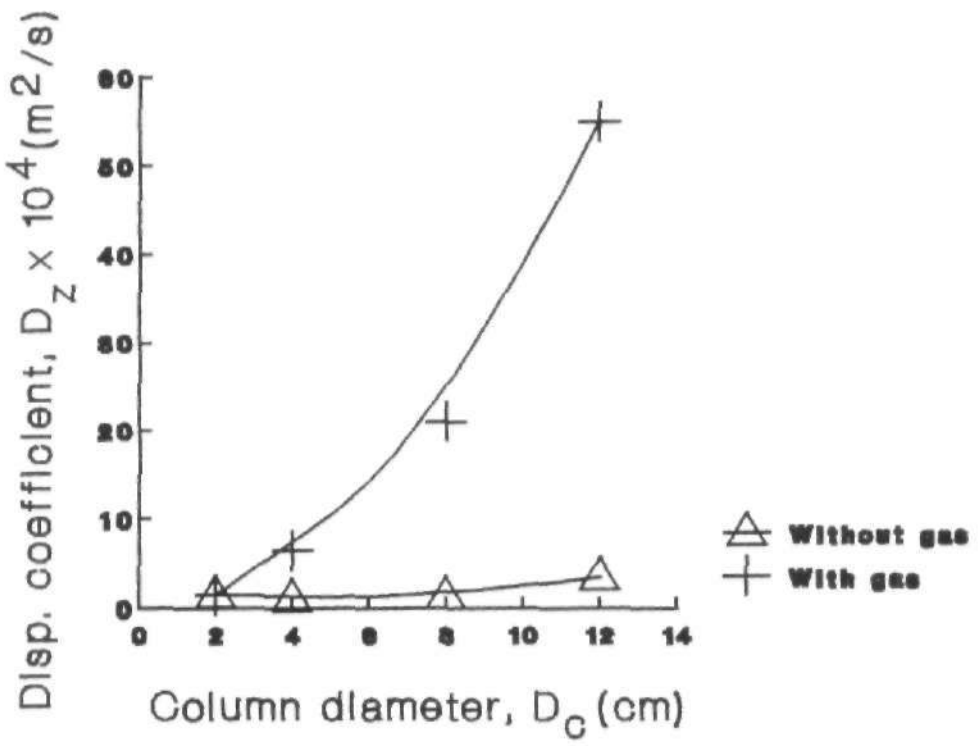


Fig. 3.10: Influence of column diameter on dispersion coefficient
(Gommers *et al*, 1986)

3.4.6 Correlations for axial liquid dispersion coefficient

Many studies on axial liquid dispersion coefficient have correlated this important parameter with others that were known to affect it, including gas and liquid velocities as well as the particle and liquid properties and column diameter. All aimed at the prediction of D_z from

other known or easily measured parameters. A number of these correlations were reviewed by Muroyama and Fan (1985) and more recently by Fan (1989) and Setiadi (1989). Therefore, only a brief discussion of these correlations is presented here. Moreover, correlations, for three and two phase systems, are separately presented and discussed.

3.4.6.1 *Correlations for three phase systems*

Using trial and error least squares analysis, Kim *et al.* (1972) have correlated the height of mixing unit (HMU = 2H/Pe) to the liquid and gas phase Reynolds and Froude numbers and the ratios of the solids and fluid densities. Their correlation, given by equation 3.2, was valid for:

$$1.4 < u_L < 10.2 \text{ cm/s}$$

$$u_g < 26.03 \text{ cm/s}$$

$$2.6 \text{ mm} < d_p < 6.0 \text{ mm}.$$

$$\frac{HMU}{H_o} - \left(\frac{HMU}{H_o}\right)_{u_g=0} = 0.068\left(\frac{Fr_{L,p}\rho_s}{\rho_L}\right)^{0.128}\left(\frac{Fr_{g,p}\rho_s}{\rho_L}\right)^{0.168}\left(\frac{Re_{L,p}}{Re_{g,p}}\right)^{0.128} \qquad 3.2)$$

The Reynolds and Froude numbers were based on the particle diameter. The equation fitted their data with a standard error of estimate of 0.018. However, their experiment was conducted in a two dimensional fluidized bed which is not common. Furthermore, the gas velocity, at which this equation is applicable, is very high and outside the range usually obtained in bioreactors with in *situ gas* production.

A different approach was employed by Muroyama *et al.* (1978) who used a cylindrical column of 12 cm ID and obtained empirical relationships, for both the coalesced bubble and the dispersed bubble regimes, as given by equations 3.3 and 3.4 respectively.

$$\acute{P}e_c = \frac{V_L D_c}{D_z} = 1.07 u_L^{0.738} u_g^{-0.167} D_c^{-0.583} \qquad 3.3)$$

$$\acute{P}e_c = \frac{v_L D_c}{D_z} = 26\sqrt{\frac{d_p}{D_c}} \qquad 3.4)$$

D_z has the dimension of cm^2/s and the equations are valid for $0.02 < d_p/D_c < 0.12$. The problem of equation 3.3 is that at zero gas velocity, the dispersion coefficient is indeterminate. Moreover, for the dispersed bubble regime, there was no influence of gas velocity on D_z. This was contradicted especially for simulated biological systems where a gas velocity as low as 0.05 cm/s was found to have a tremendous influence on D_z (Gommers *et al.*, 1986; Setiadi, 1989). The difficulty in determining the flow regime is however the greatest problem in using the correlations of Muroyama *et al.* (1978).

Unable to predict their data from the above correlations, El-Temtamy *et al.* (1979a) have used least squares fits to derive another empirical relationship, given by equation 3.5.

$$\acute{P}e_p = \frac{v_L d_p}{D_z} = 0.0012 Re_p^{1.156} D_c^{-1.156} \qquad 3.5)$$

D_z was given in cm^2/s. The equation was used to predict 209 data points, including the data of Michelsen and Ostergaard (1970), with high average deviation of 75% and low correlation coefficient of 0.8. But, its major set back is that it did not take into account the effect of gas velocity, which was known to have strong influence on D_z even at very low values.

Using a completely different approach, Joshi (1980) has proposed a theoretical relationship (Eqn. 3.6) which was derived from energy balances.

$$D_z = 0.29\,(u_L + u_c)\,D_c \qquad 3.6a)$$

Where, the liquid circulation velocity u_c, was given by

$$u_c = 1.31\left[gD_c\left(u_g+u_L-\frac{\rho_L u_L}{\varepsilon_s\rho_s+\varepsilon_L\rho_L}-\varepsilon_s\left(\frac{\rho_s}{\varepsilon_s\rho_s+\varepsilon_L\rho_L}-1\right)u_t-\varepsilon_g u_b\right)\right]^{\frac{1}{3}}$$

3.6b)

This equation was fitted to 200 data points, from the results of Michelsen and Ostergaard (1970), Ostergaard (1978) and Vail *et al.* (1968), with a standard deviation of 16%. The value of D_z was given in m^2/s and the equation was applicable for a d_p range of 0.149 to 6.0 mm and D_c of 0.066 to 0.214 m. Though, this equation fitted some reported data successfully, its major set back is that special parameters including liquid and solid holdups and the rising bubble velocity are required before D_z is evaluated. Moreover deriving these special parameters from other relationships will further add to the error in D_z.

Kim and Kim (1983) have found that their data was not predicted by the above correlations. They, therefore, derived another empirical relationship that covered a wide range of operating and fixed parameters and was not restricted by the flow regimes. They, however, did not take the effects of viscosity and surface tension into consideration. Their correlation is given by equation 3.7.

$$Pe_p = \frac{d_p u_L}{D_z} = 20.19\left(\frac{d_p}{D_c}\right)^{1.66}\left(\frac{u_L}{u_L+u_g}\right)^{1.03} \qquad 3.7)$$

This equation is valid for $0.143 < u_L/(u_L+u_g) < 0.962$ and $0.0022 < d_p/D_c < 0.08$, while D_z was given in cm^2/sec.

Nguyen-Tien, Patwari, Schumpe and Deckwer (1984) have shown that the equation of Kim and Kim (1983) fitted their data, with 45% mean deviation, for particles greater than 3 mm in diameter, but for particles 0.3, 0.5 and 1 mm in diameter, a good prediction, with minimum deviation of 30%, was obtained when the coefficient was changed from 20.19 to 61.

Similarly, Saberian-Broudjenni *et al.* (1989) have

reported that the equation of Kim and Kim (1983) predicted their data well, but only after the coefficient was also changed from 20.19 to 6.6. These authors further derived another empirical relationship (Eqn. 3.8) which took into consideration other parameters that were known to affect D_z. But, they acknowledged that equation 3.7, with the changed coefficient, predicted their data better than their own correlation.

$$Pe_p = \frac{v_L d_p}{D_z} = 1.24x10^{-5} d_p^{2.5} E_3^{-1.15} \qquad 3.8a)$$

Where E_3 is the energy dissipation and was given by:

$$E_3 = \frac{[(u_L+u_g)(\varepsilon_g\rho_g+\varepsilon_L\rho_L+\varepsilon_s\rho_s) - u_L\rho_L]\, g}{\varepsilon_L\rho_L} \qquad 3.8b)$$

Moreover, to evaluate D_z from equation 3.8, both liquid and solid or gas hold ups must be known. Measurements of these parameters are difficult and estimation from established correlations will add to the error in D_z. Furthermore, the equation did not consider the column diameter which is known to affect D_z, significantly.

Another different correlation was derived by Kato *et al.* (1985) by adapting the equation for liquid dispersion in bubble columns (BC). They proposed three empirical correlations, for axial liquid dispersion coefficient in three-phase fluidized beds (TPFB), depending on the gas velocity. For low gas velocity, u_g < 9 cm/sec,

$$Pe_c(TPFB) = \frac{u_g D_c}{D_z} = (1+\frac{u_t}{u_L})^{0.4Bo'^{0.225}} Pe_c(BC) \qquad 3.9)$$

Where, Bond number $Bo' = \frac{\rho_L d_p^2 g}{\psi}$

At u_g > 25 cm/sec, the gas Peclet number in both the bubble

column and three phase fluidized bed are the same. Thus,

$$Pe_c(TPFB) = \frac{u_g D_c}{D_z} = Pe_c(BC) \qquad 3.10)$$

However, at gas velocities in the range 9 to 25 cm/s, the Pe_g in three phase fluidized bed was given by the equation:

$$\frac{u_g D_c}{D_z} = Pe_1 \left(\frac{u_g}{9}\right)^{2.31 \log_{10}(Pe_2/Pe_1)} \qquad 3.11a)$$

Where, $Pe_1 = Pe_c$ (TPFB) at $u_g = 9$ cm/sec, $Pe_2 = Pe_c$ (TPFB) at $u_g = 25$ cm/s and

$$Pe_c(BC) = \frac{u_g D_c}{D_z} = \left(\frac{\eta}{\eta_w}\right)^{0.07} \frac{13 Fr_{g,c}}{(1+6.5 Fr_{g,c}^{0.8})} \qquad 3.11b)$$

These equations predicted D_z values which differ by only 30% in comparison to the experimental data. The equations were also used to predict the data of Michelsen and Ostergaard (1970) and Muroyama *et al.* (1978) with an error of 50%. Furthermore, the equations do indicate that, at high gas velocities, the axial liquid dispersion coefficient was independent of liquid velocity. This was, however, yet to be verified.

Simulated biological systems: Using a simulated biological system, Setiadi (1989) has found that the existing correlations predicted his data with mean deviation in the range 157% to 1742% as shown in Table 3.5. This lack of fit, induced the author to derive another relationship using the dimensional analysis technique.

The relationship obtained is given by equation 3.12 and is valid for:

$$0.15 < d_p < 3 \text{ mm}$$
$$1.05 < \rho_p < 2.65 \text{ g/cm}^3$$
$$8.5\text{x}10^{-3} < u_g < 0.2 \text{ cm/s}$$

$$D_z = 25.7 d_p^{0.198} \eta^{0.509} u_L^{-0.285} u_g^{0.779} D_c^{1.58} \qquad 3.12)$$

The equation was found to fit the 191 data points, from different authors, with mean deviation of 56%. In addition, it also predicted the data of Gommers *et al.* (1986) better than the other correlations. But, its applicability to active biological fluidized bed, with *in situ* gas production, is yet to be tested.

Table 3.5 Comparison of published correlations for simulated biological system

Correlation	Mean deviation, M_d (%)
Muroyama *et al.* (1978)	157
El-Temtamy *et al.* (1979a)	1742
Kim and Kim (1983)	135
Kato *et al.* (1985)	567
(Setiadi, 1989)	

It can, thus, be seen that various relationships, giving the value of axial liquid dispersion coefficient in terms of other parameters, that affect it, have been proposed. Each of these correlations was derived for some specific conditions and, therefore, has limitations. Furthermore, only the correlation of Setiadi (1989) was derived for biological systems and it was shown to be applicable at small gas velocities and to low density particles. However, the correlation is yet to be verified against a biologically active fluidized bed.

Application to active biological systems: Davison (1988) has found that the correlations of Muroyama *et al.* (1978) and Kim and Kim (1983) are not suitable for both

active and non active biological fluidized beds; the experimental D_z values were found to be lower than the values predicted by these correlations. This observation may be due to the fact that the correlations were derived for systems with high densities and Reynold numbers in the range 10 to 500 or more, whereas, bioparticles have densities in the range 1.05 to 1.15 g/cm^3 and Reynolds numbers less than 1 (Davison, 1988).

Setiadi and Larsen (1991) have also tested some of these correlations against the same operating conditions of tower fermenter. Their results is presented in Table 3.6 and showed significant variations in the values of D_z obtained. They were of the opinion that care must be taken when using published correlations rather than experimental data for the evaluation of D_z.

Table 3.6 Prediction of D_z for same operating conditions in tower fermenter

Correlation	Dispersion coefficient, $D_z \times 10^4$ (m^2/sec)
Muroyama *et al.* (1978)	0.94
El-Temtamy *et al.* (1979a)	0.20
Kim and Kim (1983)	0.19
Kato *et al.* (1985)	3.5

(Setiadi and Larsen, 1991)

In the light of this discussion, there is therefore, the need to further test the existing correlations against biologically active systems and, if necessary, develop new relationships to relate D_z to other parameters.

3.4.6.2 *Correlations for two phase systems*

Correlations for axial liquid dispersion coefficient in two phase (S-L) systems have also been proposed. Chung and Wen (1968) have developed an empirical correlation of the form:

$$\frac{\varepsilon Pe_p}{\chi} = 0.20 + 0.011 Re_p^{0.48} \qquad 3.13a)$$

Where, $\chi = \frac{(Re_p)_{mf}}{Re_p}$ for fluidized bed and 1 for fixed bed,

$$(Re_p)_{mf} = \sqrt{((33.7)^2 + 0.0408Ga)} - 33.7 \qquad 3.13b)$$

and Galileo number $Ga = \frac{[d_p^3 \rho_L (\rho_s - \rho_L) g]}{\eta^2}$ 3.13c)

This equation was used to fit 482 data points, with a standard deviation of 46%. The applicable ranges of this correlation were summarized by Wen and Fan (1973) as:

$10^{-3} < Re_p < 10^3$

$0.4 < \varepsilon < 0.8$

$1.52 < \rho_p < 11.3$ g/cm^3

$0.012 < d_p < 1.43$ cm

$1 < \rho_L < 1.02$ g/cm^3

$5 < D_c < 10.2$ cm

They also showed that the relationship is applicable for both Newtonian and non-Newtonian fluids. Furthermore, it predicted their data with a standard deviation of 18%. However, its major setback is that both $(Re_p)_{mf}$ and the bed voidage are required to evaluate the D_z. These parameters are difficult to measure and if obtained from existing correlations, the error in estimating D_z will be larger. Krishnaswamy, Ganapathy and Shemilt (1978) have shown that the above equation for $(Re_p)_{mf}$ is subject to an average

deviation of 25% and when used, will certainly increase the error in D_z estimates.

A simpler correlation was proposed by Krishnaswamy and Shemilt (1972). They accounted for the effects of particle density and shape, on D_z, by using the particle terminal velocity (u_t). Their correlation was of the form:

$$\frac{D_z}{D_{zo}} = 0.7\left(\frac{u_L}{u_t}\right)^{1.69} \qquad 3.14)$$

Where D_{zo} is the axial liquid dispersion coefficient for the empty column in units of cm^2/s. Equation 3.14 fitted 210 data points, with standard deviation of 17%. It is applicable to particles with diameters of 0.31 to 6.4 mm and densities of 1.28 to 11.3 g/cm^3. Though this equation is simple to use, it is very sensitive to changes in particle terminal velocity as noticed by Wen and Fan (1974); an error of 10% in estimating the terminal velocity, will possibly cause a 19.5% deviation from the true value of D_z.

The practical difficulty of the above two correlations is that special parameters such as u_t, (Re_p), D_{zo}, and ε_L, are required to evaluate the axial liquid dispersion coefficient. The correlations derived by Kim *et al.* (1972) and Krishnaswamy *et al.* (1978) have avoided some of these special parameters. The former gave a relationship for the height of mixing unit against the particle and fluid properties and operating conditions. This relationship has the form:

$$\left(\frac{HMU}{H_o}\right)_{u_g=0} = 5.05\left(Fr_{L,p}\frac{\rho_s}{\rho_L}\right)^{0.843}\left(Re_{L,p}\right)^{-0.450} \qquad 3.15)$$

and has the same conditions of applicability as equation 3.2. This relationship fitted their data with a standard error of estimate of 0.037, but it was not tested against other literature data.

The correlation of Krishnaswamy *et al.* (1978) is simpler and has the form:

$$(1 - (\frac{2D_z}{u_L H_b})^{0.5})\varepsilon^{0.25} = 0.74 \qquad 3.16)$$

The equation was fitted to 314 data points, with a standard deviation of 8%. It is applicable for particles of 0.5 to 14.3 mm in diameter and density of 1.28 to 11.3 g/cm^3. Though simple, the equation did not consider other parameters such as particle density and size and column diameter that were known to influence D_z. Furthermore, the bed voidage is required and it has to either be measured or obtained from existing correlations. This will, undoubtedly, increase the error in the D_z estimate.

It is obvious that all the above correlations are applicable for large or heavy particles. Kikuchi *et al.* (1984) have reported that the use of the above correlations, for particles with sizes in the range 0.444 to 1.88 mm and densities of 1.05 to 2.5 g/cm^3, resulted in predicted D_z values with standard deviations of 160% to 2900%, due perhaps, to the low Reynolds numbers of these particles. They, therefore, proposed another correlation (Eqn. 3.17a) which is applicable to the low Reynolds number region, in the range $0.15 < Re_p < 100$.

$$\frac{D_z \rho_L}{\eta} = 500 E_2^{0.43} Exp(-20.5(0.75-\varepsilon)^2) \qquad 3.17a)$$

The equation is also applicable for $0.41 < \varepsilon < 0.93$, and $8 \times 10^{-5} < E_1 < 0.44$. The energy dissipation per unit mass of liquid was given by $E_2 = \frac{(\rho_s-\rho_L)(1-\varepsilon)u_L g}{\rho_L \varepsilon}$ 3.17b)

and D_z was given in m^2/sec. The correlation was found to fit their experimental data and literature data, which had

Reynolds numbers less than 100, with a standard deviation of 38%.

It is not difficult to notice that this relationship also suffers from shortcommings of the earlier ones, because the bed voidage is needed to evaluate D_z. This was probably the reason why Setiadi (1989) went further to derive another correlation that will be applicable to low density small particles, which are typical of bioparticles, using easy to measure parameters. His correlation is of the form:

$$D_z = 5.49 \times 10^{-7} D_c^{0.751} d_p^{-0.144} \eta^{-0.157} u_L^{0.854} \qquad 3.18)$$

This equation fitted 194 data points with a correlation coefficient of 88.2% It was also used to predict large quantities of literature data, with a mean deviation of 20%. Moreover, it is applicable over a wide range of conditions:

$0.15 < d_p < 3$ mm

$1.8 < D_c < 100$ cm

$0.06 < Re_p < 35$

$0.6 < Ga < 7665$

$1.05 < \rho_p < 2.97$ g/cm^3

$0.6 < \eta < 2.5$ cP

Application to active biological systems: For biological systems, with their characteristic low liquid velocity, the use of equation 3.18 will result in very low values of D_z. Setiadi and Larsen (1991) have, conclusively, shown that the D_z values calculated using the correlation of Kikuchi *et al.* (1984), which was derived for a two phase system, was below the level at which it influenced the predicted concentration profile in a tower fermenter. Therefore, there was no gain in using the dispersed plug flow model over that of ideal plug flow. Though this statement needs to be further verified, it indicates that correlations derived for two phase systems may not be

applicable for D_z prediction in biological fluidized beds with *in situ gas production*.

3.5 BED EXPANSION CHARACTERISTICS

As mentioned earlier, a proper understanding of the expansion characteristics of fluidized beds, is central to efficient design and evaluation of the performance of these reactors. In addition, it was shown that the bed voidage determines the residence time of liquid elements in fluidized bed reactors and hence, the achievable reactant conversion level.

In a three phase fluidized bed, each of the phases occupies a portion of the bed; the volume fraction that a particular phase occupies is referred to as the holdup of that phase. Thus, liquid holdup is the volume fraction that the liquid phase occupies and is required for the evaluation of the exit substrate concentration in the dispersed plug flow model (Eqns. 1.6 and 3.2). Bed voidage or porosity is used to describe the space not occupied by the solids and for three phase systems, is the sum of the liquid and gas holdups. By definition, all the phase holdups add-up to one as given in equation 3.19a. However, for a two phase (S-L) fluidized bed, $\varepsilon_g = 0$.

$$\varepsilon_s + \varepsilon_L + \varepsilon_g = 1 \qquad 3.19a)$$

In addition, the total pressure gradient at any bed level is simply the bed weight per unit volume at that level (Epstein, 1981), thus;

$$\frac{-dP}{dz} = (\rho_s \varepsilon_s + \rho_L \varepsilon_L + \rho_g \varepsilon_g) g \qquad 3.19b)$$

If any one of the holdups is known, the others can be obtained by solving, simulteneously, equations 3.19a and 3.19b. The solid holdup can be obtained, easily, from the weight and density of the particles used, as follows:

$$\varepsilon_s = \frac{W_s}{\rho_s A H_b} \qquad 3.19c)$$

Similarly, both the gas, and liquid holdups can be obtained from the residence time distribution of each phase as given in equations 3.20 and 3.21 respectively (Michelsen and Ostergaard, 1970).

$$\varepsilon_g = \frac{t_{g,avg} f_g}{A H_b} \qquad 3.20)$$

$$\varepsilon_L = \frac{t_{L,avg} f_L}{A H_b} \qquad 3.21)$$

Since the phase holdups are defined as the volumetric fractions of the fluidized bed, they depend on the height of the fluidized bed and are, therefore, affected by the process conditions and solid and liquid properties. Moreover, the process conditions and the physical properties of liquid and particles determine the behaviour of the bed. Evaluation of phase holdups or bed voidage cannot, always, be done by experimentation; consequently, many correlations were developed in order to evaluate these parameters using known process conditions and easily measured liquid and particle properties.

The nature of the effects of process conditions and solid and liquid properties, on the behaviour of fluidized beds, are briefly discussed in this section. In addition, the various correlations, for the prediction of bed voidage, liquid, gas and solid holdups, have been highlighted.

3.5.1 Bed behaviour

Changes in liquid and particle properties and operating conditions will be expected to change the

behaviour of the bed and hence its expansion characteristics and phase holdups.

Michelsen and Ostergaard (1970) have observed that in beds of 1 mm, 3 mm, and 6 mm particles, the liquid holdup increased with increases in liquid velocity and decreases in gas velocity (Fig. 3.11). Similar observations were made by Ostergaard (1978) and Kato, Uchida, Kago and Morooka (1981) who have also reported that liquid holdup increased with increases in liquid velocity and decreases in gas velocity and particle diameter.

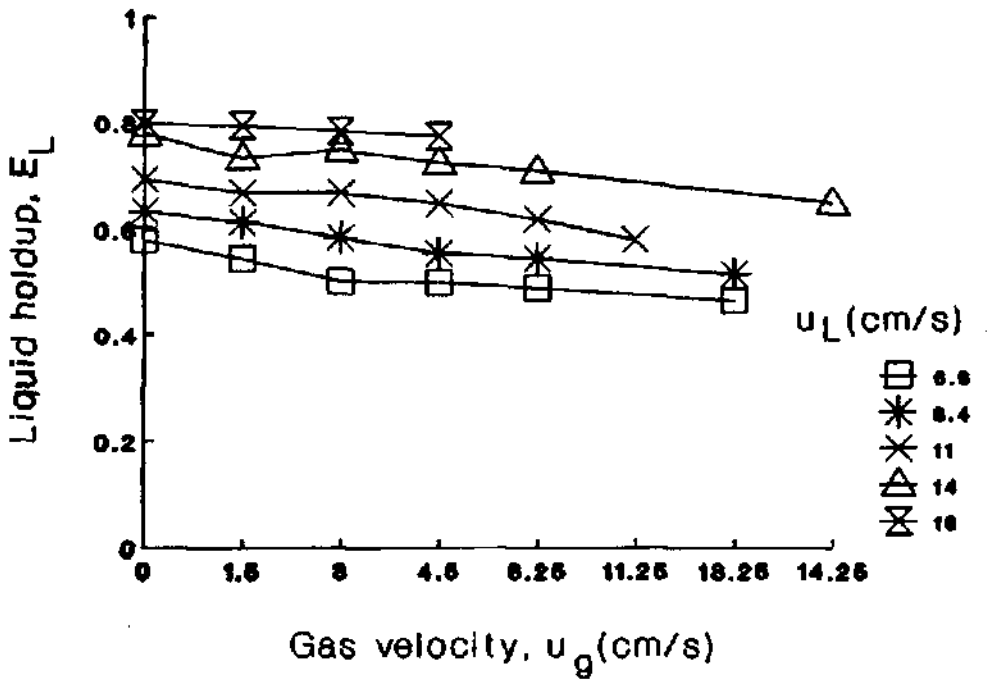


Fig. 3.11: Effect of gas and liquid velocities on liquid holdup

(Michelsen and Ostergaard, 1970)

But, Kim *et al.* (1972) noted increases in ε_L with increases in liquid and gas velocities. It is not known why the results of Kim *et al.* (1972) differed from other observations. It may be that the two dimensional contactor used by Kim *et al.* (1972) could be responsible.

In contrast, it was unanimously agreed that bed voidage (ε) increased with increases in liquid and gas velocities (Kim, Baker and Bergougnou, 1975; Dakshinamurty, Subrahmanyam and Rao, 1971; Saberian-Broudjenni *et al.*, 1987).

Few studies on the effects of liquid viscosity and surface tension on bed voidage and phase holdups have been conducted. Kim *et al.* (1975) have reported that both liquid holdup and bed voidage increased with increased viscosity in the range 1 to 70 cP, in both two phase and three phase systems, but the increase was more marked in beds of smaller particles and in the presence of flowing gas. Similarly, Nikov, Grangjeen, Carreau and Paris (1990) have also reported an increase in bed voidage with increase in viscosity in the range 10 to 124 (mPa.s), but they attributed this increase to increased slip velocity caused by the increase in liquid viscosity.

Liquid surface tension will also be expected to affect bed voidage and holdups. Kim *et al.* (1975) have studied this aspect in two phase and three phase systems. Their results showed that in a bed of 1 mm particles, both bed voidage and liquid holdup increased with increase in surface tension in the range 40 to 73 dyne/cm. In 2.6 mm gravel particles, ε_L increased with increased surface tension while ε remained constant, indicating that the gas holdup was decreased, presumably, as a result of greater bubble coalescence. Finally, in a bed of 6 mm particles, the gas holdup was not affected by increase in surface tension.

Density of particles will also be expected to affect bed voidage and phase holdups. Tang and Fan (1989) have studied the hydrodynamics of three phase fluidized beds containing low density particles in the range 1.05 to 1.3 g/cm^3. They noted significant axial variation in solids concentration, the extent of which, depended on the prevailing flow regime; large bubbles, in the coalescence

flow regime, help to transport finer particles and cause more variation in axial solids concentration.

It can be deduced from the above discussion that particle size affects the bed voidage and phase holdups. Generally, the bed voidage and liquid holdup decrease with an increase in particle size (Kato *et al.*, 1981; Saberian-Broudjenni *et al.*, 1987). Of particular interest in fluidized bed hydrodynamics, is the contraction of a bed of small particles, upon injection of gas. This phenomenon was observed by many researchers (Michelsen and Ostergaard, 1970; Dakshinamurty *et al.* 1971; Kim *et al.*, 1972; Kim *et al.*, 1975; and Song, 1978). It was generally accepted to be due to the solid free liquid wake which accompanies the rising bubble and hence moves at velocity greater than the average bulk liquid velocity. This causes the entire bed to contract and a sharp decrease in bed voidage occurs (Epstein, 1981; Darton, 1985).

3.5.1.1 *Bed contraction*

Whether a bed expands or contracts, due to introduction of gas, depends on the particle size, gas flow rate and liquid properties such as surface tension and viscosity (Epstein, 1976). Kim *et al.* (1972) reported that the contraction of a bed on injection of gas diminished as the particle size was increased and that the critical size for particles having a density similar to glass is about 2.5 cm. But Song (1978) has reported that bed expansion or contraction can be predicted from the ratio of fluidized bed height in three phase and two phase systems at the same liquid velocity. A ratio greater than one implies that the bed will contract when gas is introduced into the column and a value less than one indicates that the bed will expand upon introduction of gas. Epstein (1981) has shown that particles, of sizes less than 3 mm in diameter and density the same as that of glass, will contract upon introduction of gas into the

fluidized bed. This is in agreement with the report of Kim *et al.* (1972).

3.5.1.2 *Expansion of bioactive beds*

Studies of bed expansion of biologically active particles in fluidized beds, are few. Smith *et al.* (1978) have noted that the presence of a gas phase considerably reduces the terminal velocity of microbial aggregates and this has the effect of increasing bed voidage at relatively low liquid velocity. But Davison (1988) and Setiadi (1989) have independently found that gas velocities up to 0.2 cm/sec reduced bed voidage by a maximum of less than 7.7%; therefore, for gas velocities less than 0.2 cm/sec, the bed voidage can reasonably be estimated from the corresponding two phase system.

The special characteristic of active biological systems is the growth of microorganisms, which has the effect of increasing both the size and density of bioparticles. These changes have significant effects on the behaviour of beds containing bioparticles (Timmermans and van Haute, 1984). Changes in the density of bioparticle due to biomass growth, was documented by Setiadi (1989) for the case of biofilm supported on sand particles, as shown in Table 3.7. The biofilm thickness increased from 2.05 to 15.2 μm with a corresponding decrease in bioparticle density of 2.52 to 1.98 g/cm^3. This decrease in density caused the difference ($\rho_p - \rho_L$) to decrease and this may result in increased bed voidage (Saberian-Broudjenni *et al.*, 1987).

Microbial flocs may, however, differ from supported microbial films. With the flocs, increase in size was shown to cause an increase in floc density which may cause a decrease in bed voidage (Brohan and McLoughlin, 1984c). Furthermore, in tower fermenters, segregation of flocs does occur with the largest being at the bottom of the tower. Therefore, the observations of bed behaviour, with

respect to supported biofilms, may not be applicable to microbial flocs.

Table 3.7: Density changes due to biomass growth

Biofilm thickness, r_{bf} (μm)	Bioparticle diameter, d_{bp} (μm)	Bioparticle density, ρ_{bp} (g/cm^3)
2.05	146.4	2.52
6.10	154.5	2.31
11.30	164.9	2.11
15.20	172.7	1.98

(Setiadi, 1989)

3.5.2 Correlations for bed voidage and phase holdups

There are a number of correlations, in the literature, that aim to relate various phase holdups to the particle and liquid properties and the operating conditions. In this section correlations, for two phase, three phase and biological systems, are separately presented and discussed.

3.5.2.1 *Two phase fluidized beds*

One of the earliest and most widely used relationship is the empirical correlation of Richardson and Zaki (1954), which has the form of equation 3.2a (Richardson and Meikle, 1961)

$$\frac{u_L}{u_t} = \varepsilon^n \qquad 3.22a)$$

where the index n, depends on the particle Reynolds number and the ratio of the particle to column diameters, as follows;

$$Re_{p,t} < 0.2; \qquad n = 4.65 + 19.5\frac{d_p}{D_c} \qquad 3.22b)$$

$$0.2 < Re_{p,t} < 1; \quad n = (4.36 + 17.6\frac{d_p}{D_c})Re_{p,t}^{-0.03} \qquad 3.22c)$$

$$1 < Re_{p,t} < 500; \quad n = 4.45Re_{p,t}^{-0.1} \qquad 3.22d)$$

$$500 < Re_{p,t} < 7000; \; n = 2.39 \qquad 3.22e)$$

Though, equation 3.22a is simple and widely used, its major problem is in the use of the particle terminal velocity. This parameter must have to be measured or obtained from other correlations. It is related to the physical properties of particle and liquid by the following equation (Tambo and Watanabe, 1979; Schugerl, 1989):

$$u_t = \sqrt{\frac{4g}{3C_D}\frac{(\rho_s - \rho_L)}{\rho_L}d_p} \qquad 3.22f)$$

Where $C_D = 18.5Re_{p,t}^{-0.6}$ 3.22g)

Using a theoretical approach involving equilibrium forces acting on particles in a fluidized bed, Wen and Yu (1966) have derived another correlation for bed voidage as follows;

$$\varepsilon^{4.7} = \frac{Ga}{18Re_p + 2.7Re_p^{1.687}} \qquad 3.23)$$

This equation is valid for d_p of 2.03 to 6.35 mm and ρ_p of 2.36 to 7.84 g/cm^3. This relationship is also widely used and was recommended by Muroyama and Fan (1985). The equation was used to fit experimental data and literature

data, from various sources, with an average deviation of 25%.

Kim et *al.* (1972) have obtained another empirical relationship as follows:

$$(\varepsilon_L)_{u_g=0} = 0.409\left(\frac{Fr_{p,L}\rho_s}{\rho_L}\right)^{0.193}(Re_{p,L})^{0.074} \qquad 3.24)$$

The correlation fitted experimental data with a standard error of estimate of 1.1%. The maximum deviation between this equation and that of Richardson and Zaki (1954) (Eqn. 3.22a), was 8%.

Using a similar approach to that of Wen and Yu (1966), Ramamurthy and Subbaraju (1973) obtained generalized equations for predicting ε by using equation of motion for multiparticle systems in homogeneous fluidized bed. They proposed three set of relationships for laminar, intermediate and turbulent flow regimes,

$$\frac{Ga}{18Re_p} = \Phi_s^{1.55} \qquad 3.25a)$$

$$\frac{Ga}{13.9Re_p^{1.4}} = \Phi_s^{2.21} \qquad 3.25b)$$

$$\frac{3Ga}{Re_p^2} = \Phi_s^{3.11} \qquad 3.25c)$$

Where Φ_s is the velocity correction factor and was given by

$$\Phi_s = [1-1.2(1-\varepsilon)^{\frac{2}{3}}]^{-1} \qquad 3.25d)$$

The equations are valid for:

$0.15 < d_p < 6.35$ mm

$0.05 < Re_p < 2240$

$0.42 < \varepsilon < 0.95$

$$0.004 < d_p/D_c < 0.14$$
$$12 < Ga < 4.65 \times 10^6$$

These equations were used to predict literature data, with a standard deviation of 14.7%. But, the difficulty in determining flow regimes makes these relationships difficult to use.

Garside and Al-Dibouni (1977) have used particle sizes in the range 0.167 to 3.07 mm in diameter, corresponding to Re_p of 3.84 to 1180 and showed that a correlation of the same form as that of equation 3.22a, but with a modified value of n, namely:

$$\frac{5.09-n}{n-2.73} = 0.104 Re_{p,t}^{0.877} \qquad 3.26)$$

fitted their experimental data with a standard deviation of 9.8%. However, they still proposed another empirical relationship (Eqn. 3.27), which they said fitted their data best, with a standard deviation of 8.6%, but was more difficult to use.

$$\frac{u_R-A}{B-u_R} = 0.06 Re_{p,t}^{\varepsilon+0.2} \qquad 3.27)$$

Where, $A = \varepsilon^{4.41}$ and $B = \varepsilon^{1.68}$. Equation 3.23 is valid for ε = 0.4 to 0.95.

A different approach was used by Kmiec (1982). He derived a correlation (Eqn. 3.28) from the equations describing the equilibrium forces in a fluidized bed.

$$\varepsilon = \left(\frac{F_d}{F_g}\right)^{0.209} \qquad 3.28a)$$

Where, Fd and Fg are the drag and gravitational forces, respectively, acting on a particle and their ratio was given by:

$$\frac{F_d}{F_g} = \frac{3}{4} C_D \frac{Re_P^2}{Ar} \qquad 3.28b)$$

While Archimedes number, Ar is the same as the Galileo number. This equation was valid for:

$$12 < Re_p < 877$$

$$0.006 < Ar < 3.79 \times 10^6$$

$$0.4 < \varepsilon < 0.98$$

For $Re_p < 500$, $C_D = \frac{24}{Re_p}(1+0.15Re_p^{0.687})$ 3.28c)

But for heigher Re_p, $C_D = 0.44$. They fitted experimental data with a mean deviation of 3.9%.

3.5.2.2 *Three phase systems*

All the above correlations for bed voidage related to two phase fluidized beds. There are, however, few relationships that correlate bed voidage or phase holdups to physical characteristics of liquid and solids as well as operating conditions, in three phase fluidized beds. Kim *et al.* (1972) have proposed the following empirical correlations.

$$(\varepsilon_L)_{u_g=0} - \varepsilon_L = 0.0025\left(\frac{FI_{p,L}\rho_s}{\rho_L}\right)^{0.149}\left(\frac{FI_{p,g}\rho_s}{\rho_g}\right)^{0.161}(Re_pRe_{p,g})^{0.259}$$

3.29a)

and $$\varepsilon_g = 1 - \varepsilon_L - \frac{W_s}{\rho_s H_b A}$$ 3.29b)

With a standard error of estimate of 0.018. Equation 3.29a was obtained for a two dimensional fluidized bed and did not take into consideration the effects of surface tension and liquid viscosity.

Kim *et al.* (1975) have, however, decided to consider the effects of viscosity and surface tension on the liquid holdup and accordingly, proposed another relationship of the form;

$$\varepsilon_L = 1.504\,(Fr_{p,L})^{0.234}\,(Fr_{p,g})^{-0.066}\,(Re_p)^{-0.082}\,(We)^{0.092} \qquad 3.30)$$

Where We is the Weber number given by: $We = \frac{u_g \upsilon}{\psi}$ and υ was the generalized viscosity constant. Equation 3.30 was found to fit the data with a standard error of estimation of 3.9%. A similar empirical relationship was developed by Begovich and Watson (1978) who used their experimental data and literature data, from eight different sources. They obtained the following correlation for ε,

$$(1 - \varepsilon_s) = 0.371 u_L^{0.271} u_g^{0.041} (\rho_s - \rho_L)^{-0.316} d_p^{-0.268} \eta_L^{0.055} D_c^{-0.033} \qquad 3.31a)$$

and, $$\varepsilon_g = 0.048 u_g^{0.720} d_p^{0.168} D_c^{-0.125} \qquad 3.31b)$$

Equation 3.31a fitted 2381 data points with a correlation coefficient of 0.87, but its use is rather limited, for it should only be used for conditions close to those for which it was obtained. At zero gas velocity, it shows that the liquid holdup is zero which is not true. Moreover it predicts an increase in solid holdup at increasing gas velocity and this is also contrary to experimental observation (Fan, 1989). Nonetheless, Nikov *et al.* (1990) have shown that equation 3.31a has fitted their data well, with an average deviation of about 0.26%. Equation 3.31b fitted 913 data points with a correlation coefficient of 0.93.

Kato *et al.* (1981), have reported that for a two phase (S-L) bed, the correlation of Garside and Al-Dibouni (1977) fitted their experimental data well. But, for a three phase bed, the equation was modified as follows:

$$\frac{u_L}{u_t} = \left(\frac{\varepsilon_L}{\varepsilon_L^*}\right)^n \qquad 3.32a)$$

where ε_L^* is the extrapolated value of the liquid holdup at $u_L = u_t$ and was given by;

$$\varepsilon_L^* = 1 - 9.7\,(350 + Re_{p,t}^{1.1})^{-0.5} K^{-0.092} \qquad \text{and} \qquad K = \frac{\rho_L u_g^4}{g\psi},$$

while the value of n was given by the relationship;

$$\frac{5.1(1 + 16.9K^{0.285}) - n}{n - 2.7} = 0.1(1 + 4.43K^{0.165}) Re_{p,t}^{0.9} \qquad 3.32b)$$

These equations were shown to agree well with the experimental data. Furthermore, when there is no gas flow ($u_g = 0$), ε_L^* becomes unity and equation 3.32b becomes the same as equation 3.26 for the two phase (S-L) system.

Saberian-Broudjenni *et al.* (1987) have shown that their data was well correlated, with mean deviation of 7%, by the correlation of Begovich and Watson (1978). Nonetheless, they further developed another empirical correlation of the form;

$$\varepsilon = \varepsilon_o \left(\frac{u_L}{u_{mf}'}\right)^{0.27} (1 + 0.07 Re_{p,g}^{0.34}) \qquad 3.33a)$$

$\varepsilon_o = (14\psi_p)^{-\frac{1}{3}}$; $\psi_p = \dfrac{2d_{sph}^2}{d_p^2 + 2d_p L_p}$ $\qquad Re_{p,g} = \dfrac{\rho_L u_g d_p}{\eta_L}$. The gas and liquid holdups were obtained using the relationships:

$$\varepsilon_g = \varepsilon \left(\frac{u_g - u_{gL}}{u_g + u_L}\right) \qquad 3.33b)$$

$$\varepsilon_L = \varepsilon \left(\frac{u_{gL} + u_L}{u_g + u_L} \right) \qquad 3.33c)$$

where, the slip velocity is given in S.I units by;

$$u_{gL} = 0.017 \left(\rho_L u_g^2 \right)^{0.45} \qquad 3.33d)$$

This equation is applicable to non spherical particles and predicted their data with mean deviation of less than 12%.

3.5.2.3 *Biological systems*

Correlations for bed voidage and holdups, for use in biologically active systems, have not been developed. But, Smith *et al.* (1978) have shown that the correlation of Richardson and Zaki (Eqn. 3.22a) has fitted their data well. They obtained the values of the index n, to be in the range 7.5 to 14 for yeast flocs and 8.7 to 10.3 for flocs of *Aspergillus niger*.

A similar conclusion was reached by Ngian and Martin (1980) who found that the relationship between liquid velocity and bed voidage, in biologically active fluidized beds containing bioparticles, was correlated by equation 3.22a. Hermanowicz and Ganzarczyk (1983) have also found that the equation was applicable to biological fluidized beds, but only when the drag coefficient (Eqn. 3.22g) was modified to:

$$C_D = 17.1 Re_p^{0.47} \qquad 3.34)$$

The modification was necessary because the drag force acting on a falling bioparticle was found to be larger than that acting on a particle having the same density, due perhaps to the roughness of the bioparticle, which tends to affect the liquid boundary layer around it.

In contrast, Brohan and McLoughlin (1984b) have shown that the correlation of Richarson and Zaki (Eqn. 3.22a)

was not suitable for active yeast flocs, because the logarithmic plot of liquid velocity and bed voidage produced a curve instead of a straight line as shown in figure 3.12. But, non active yeast flocs behaved in accordance with that correlation. They further showed that the behaviour of fluidised beds, containing yeast flocs, depended, to a large extent, on the nature of the yeast.

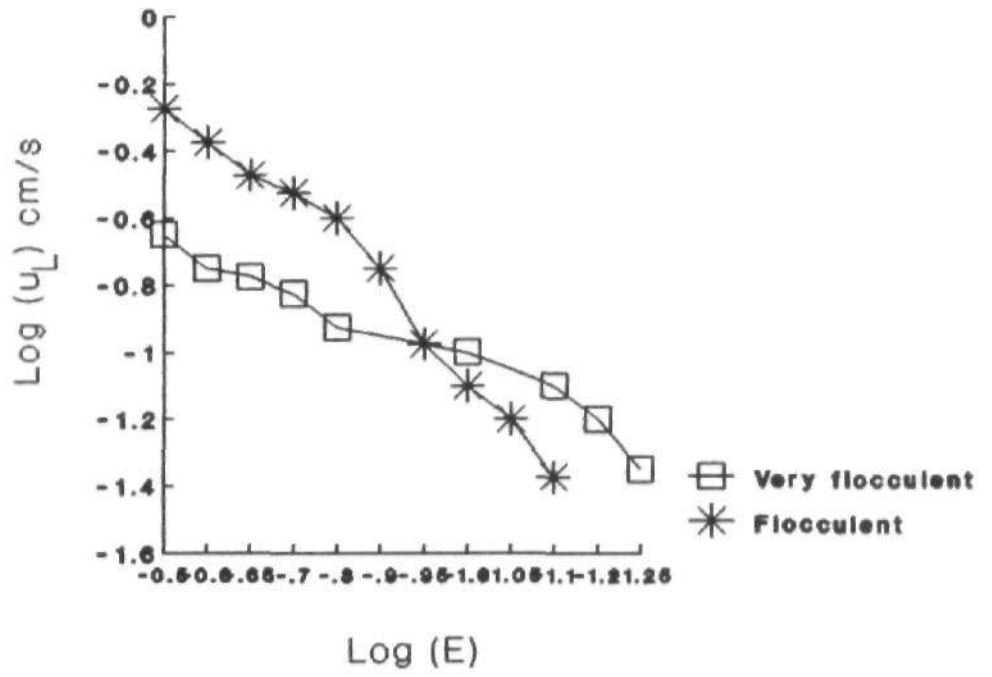


Fig. 3.12: Velocity-voidage relationship for biological system

(Brohan and McLoughlin, 1984b)

Setiadi (1989) has noted that the correlations of Richardson and Zaki (Eqn. 3.22a) and Wen and Yu (Eqn. 3.23) and the modified equation of Hermanowicz and Ganzarczyk (1983) have fitted his data with a mean deviation of 11.5%, 5% and 11.6% respectively. Though the fits seemed good, he further proposed another correlation which was found to be suitable for non spherical particles and fitted his data with mean deviation of only 1.7%. The correlation has the form:

$$\varepsilon = 1.72 Re_p^{0.203} Ga^{-0.179} \qquad 3.35)$$

Equation 3.35 was also found to fit the data of Ngian and Martin (1980) and Timmermans and van Haute (1984) with mean deviations of 6.9% and 14.1% respectively.

In conclusion, it can be said that the existing correlations are varied and contrasting. Their applicability to bioactive systems has not been well demonstrated. There is, therefore, the need to further test these correlations for their applicability to active biofluidized beds and, if found necessary, modify them or develope new correlations that can, with confidence, be used for active biosystems.

CHAPTER FOUR

MATERIALS AND METHODS

4.1 MATERIALS

Many materials were used in the course of accomplishing this work. They include chemicals, organisms, fermentation and subculture media and tracers.

4.1.1 Chemicals

The chemicals used are listed below. They are Analar grade reagents and are suplied by Merck, Pool (Formerly BDH) except where, otherwise, indicated.

Ammonium sulphate
4-Aminophenazone
Calcium chloride, fused
2,4-Dichlorophenyl (Sulphonated)
Di-sodium hydrogen ortho-phosphate
Ethanol, Absolute (University of Strathclyde, Glasgow)
Glucose Oxidase (Sigma, Pool)
Glucose
Hydrochloric acid
Magnesium sulphate hepta-hydrate
Malt extract agar (Oxoid, Basingtoke)
Methanol (HipherSolv)
Peroxidase (Sigma, Pool)
Potassium di-hydrogen ortho-phopsphate
Sodium azide
Sodium di-hydrogen ortho-phosphate-di-hydrate
Sodium chloride
Sodium hydroxide (A & J Beveridge, Edinburgh)
Yeast extract (Gibco, Paisley)

4.1.2 Organisms

Flocculating strains of the yeast *S. cerevesiae* were used. Four of these strains were obtained from the department of Bioscience and Biotechnology, University of Strathclyde, Glasgow. They are code-named ABXR 11B, ABXR LID, Y6 and EM 93. The other strain, NCYC 1026, was

obtained from the National Collection of Yeast Cultures, Norwich.

4.1.3 Media

The medium used in continuous fermentation and in the Chemap fermenter contained, per liter of distilled water,

Ammonium sulphate, 4.0 g
Calcium chloride, 0.25 g
Glucose, 100 g
Magnesium sulphate hepta-hydrate, 1.0 g
Potassium dihydrogen orthophosphate, 1.5 g
Yeast extract, 6.0 g

(Prince and Barford, 1982a).

Medium used in the LH fermenter contained, per liter of distilled water,

Glucose, 20 g
Yeast extract, 5 g

The medium used for subculture preparation contained 5.0 g malt extract agar per 100 ml of distilled water.

4.1.4 Tracer material

The five tracer materials used are listed below.

Aniline blue (Merck, Pool)
Dextran blue (Sigma, Pool)
Fluorescein, water soluble (Aldrich, Gillingham)
Methyl green (Merck, Pool)
Methyl violet (Merck, Pool)

4.2 EQUIPMENT

Two batch fermenters and a fluidized bed fermenter were used in the course of this work. These equipment are described in this section. Other laboratory equipment, used mostly for sample analysis, are listed.

4.2.1 Fluidized bed fermenter

Continuous anaerobic fermentation was carried out in a fluidized bed fermenter. This was a vertical column made of polycabonate material. It consisted of three sections; a conical bottom, the main column and a particle separator. Details of the fluidized bed fermenter are presented in figure 4.1. A schematic diagram of the experimental set-up is shown in fiqure 4.2 while figure 4.3 shows a picture of the unit.

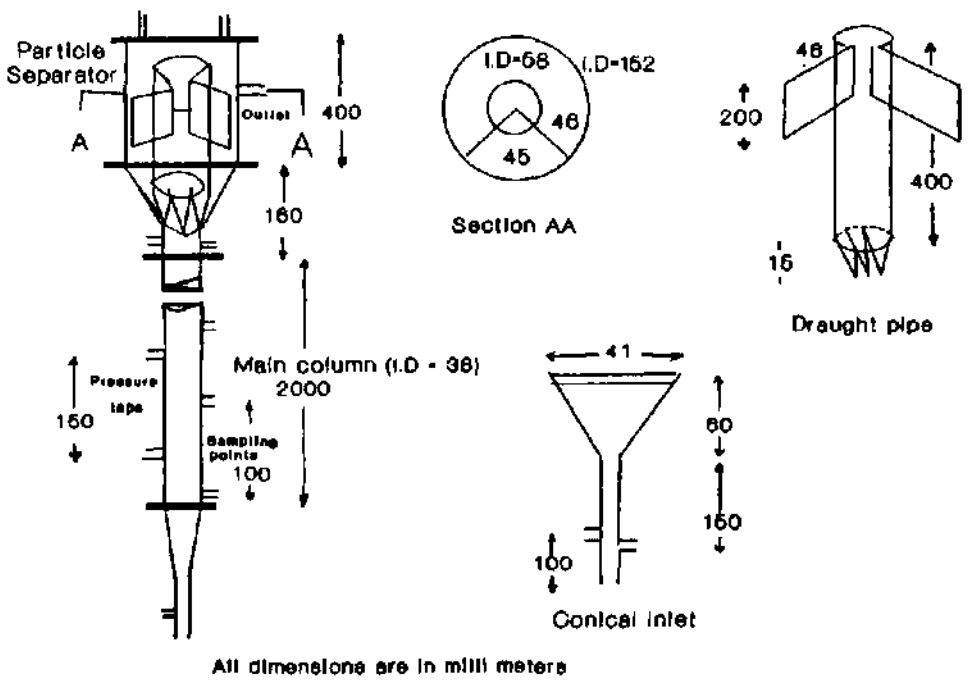


Fig. 4.1: Details of fluidized bed fermenter

The conical bottom: This provided an inlet for the media and air. It was made of a small cone 6 cm in length and 4.10 cm internal diameter (ID) at top, attached to a short pipe of 15 cm length and 0.8 cm ID. Medium was pumped into the column by a calibrated peristaltic pump (Watson-Marlow Ltd., Falmouth) through a 0.4 cm ID, 0.2 cm thick silicone tube connected to the short pipe. Air was passed into the column at a point 10 cm along this pipe. A Y-type junction, at the end of the pipe, provided the

means to drain off the column when required. The cone was randomly packed with glass spheres, 0.5 cm in diameter, that help to uniformly distribute medium at the entrance to the column. A sintered glass filter disc, pyrex, of 4.0 cm in diameter and porosity of 16 to 40 μm (P40, grade 3, Philip Harris Scientific, Glasgow) was positioned, inside the cone, at the top. This disc was used as liquid distributor.

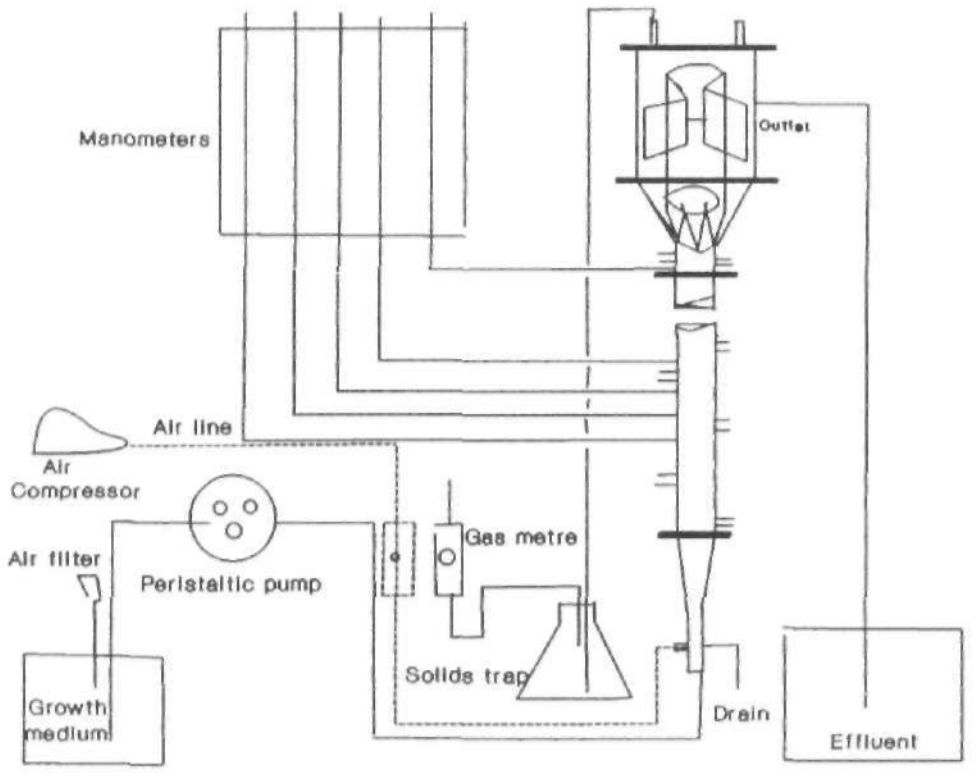
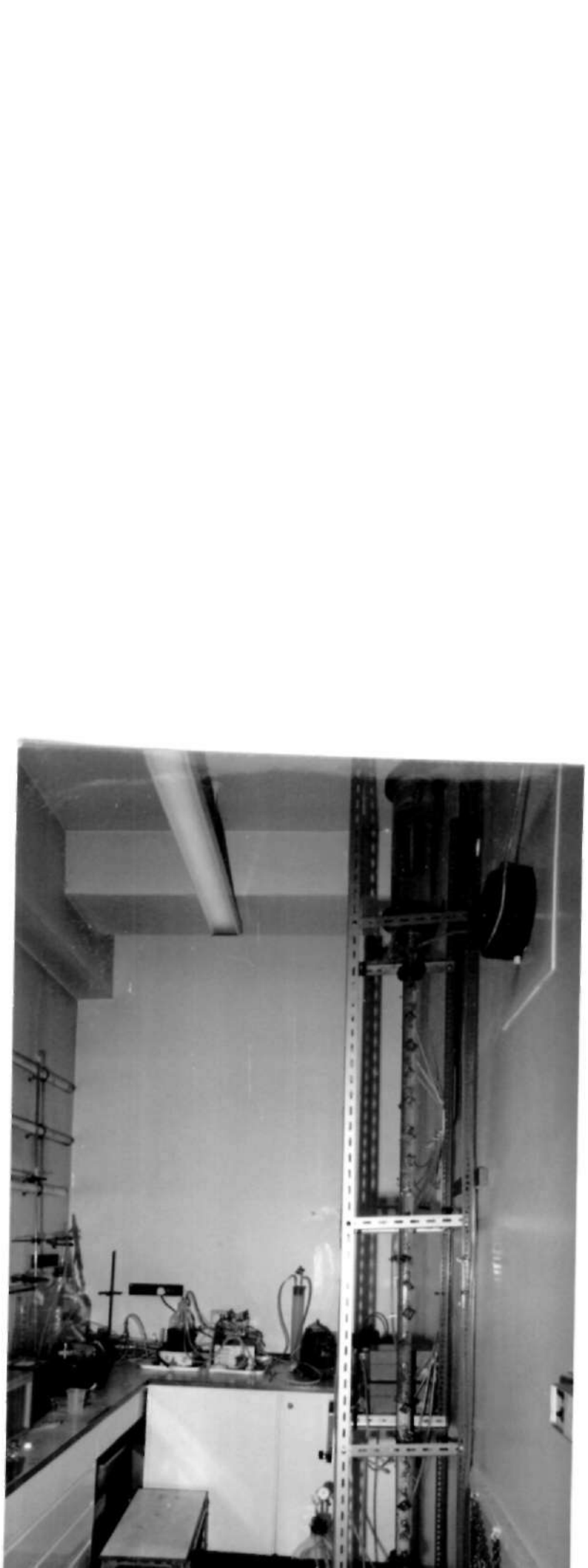


Fig. 4.2: Schematic diagram of fluidized bed fermenter

Main column: This section was of 200 cm length, 3.81 cm ID and 0.3 cm wall thickness. It had twenty sampling points, situated at a distance of 10 cm apart, on one side and thirteen pressure taps, 15 cm apart, on the other. Both the pressure taps and the sampling points were made of copper pipes of length 5 cm and 0.6 cm ID. The pressure taps were fitted with wire mesh and flushed to the inside wall of the column, so as not to interfere with liquid



flow. They were connected, by silicone tubes, to glass manometers mounted on a wall beside the column.

The sampling points were fitted with 0.4 cm ID silicon tubings that were extended to the centre of the column to ensure that samples were taken from that point. The silicone tubes were held firmly with a silicone sealant. The first sampling point was situated at 3 cm from the liquid distributor, so it could also be used for tracer injection. It was fitted with a T-type junction and a 10 cm needle (18 G) that was extended to the centre of the column, allowing tracer to be injected at the centre of the column.

Scales graduated to one millimeter were fixed to the column. This scale was calibrated (40 cm on scale ≡ 39 cm).

Particle separation section: This section consisted of a cylinder of 40 cm length and 15.2 cm ID connected to the main column by a 16 cm high cone. A draught pipe of 40 cm length and 5.8 cm ID was seated in the funnel on three legs 1.5 cm high. The draught pipe was fitted with two stainless steel flanges placed at 90^0 apart and at 0.1 cm away from the cylinder wall. A small weir was made, on the pipe, between the flanges. Liquid, with particles, from the column, was forced to pass up through the draught pipe and down into the cylinder, between and under the two flanges, before passing out through the quiescent zone to the outlet. This was at a point 7 cm from the top of the cylinder. In following this path, the particles were made to settle back into the column. Discharged liquid was collected in 40 liter plastic jars and sterilized, chemically, by the addition of 30 ml of concentrated solution of sodium hypochlorite to every five liters of the discharge liquid, before disposal.

The top of the separator was covered with a polycarbonate plate 1 cm thick and 17.2 cm in diameter. Two points, similar to the sampling points described

above, were made on this cover. One of the points was used as an exit for the carbon dioxide gas produced during fermentation. It was connected, by silicone tubing, to a carbon dioxide flow meter (Platon Flow Bits, Basingstoke) via a trap that removed any accompanying yeast paticles. The other point was closed up and used for cleaning purposes when required.

4.2.1.1 *Temperature control*

The fluidized bed fermenter was assembled in a room maintained at a constant temperature of 30 ^{0}C, using greenhouse wall heaters, and a contact thermometer.

4.2.1.2 *Aeration*

Air, when required, was passed into the column through a copper pipe 5 cm in length and 0.6 cm ID connected to the conical bottom. The air was pumped in by an air pump (Campton, Dawson & Dawson Ltd., Ashbourne) and was passed, in series, through filters of 0.2 μm (Whatman Ltd., Maidstone, WCN type, PTFE L1233) and 0.45 μm (Whatman Ltd., Maidstone, WCN type, 47 mm diameter) porosity and an air rotameter (Platon Flow Bits, Basingstoke) that was used to measure the flow.

4.2.2 LH batch fermenter

This was a one liter fermenter manufactured by LH Fermentation Ltd. (Reading). It was used for the purpose of selecting tracer material. It consisted of a glass vessel and a stainless steel head plate from which a magnetic bar was suspended. The head plate had an adequate number of ports for addition of medium and inoculum, sample withdrawal and attachment of the condenser. Mixing was achieved by using a magnetic stirrer (Stuart Scientific Co. Ltd., Redhill). The fermenter was used in a constant, 30 ^{0}C, temperature room. No pH control was applied. A picture of this fermenter is shown in fiqure 4.4.

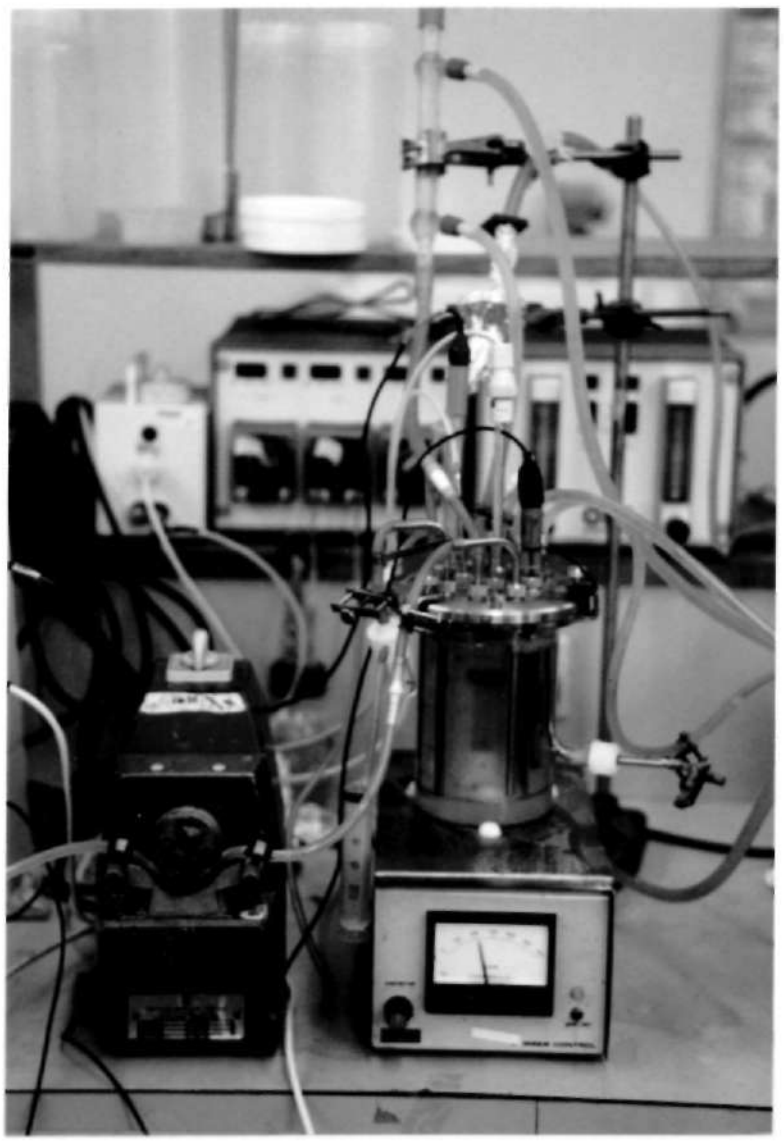


Fig. 4.4 LH batch fermenter

4.2.3 Chemap fermenter

This batch fermenter had a seven liter total volume and was used for the preparation of the inoculum needed for the column fermentation. It was manufactured by Chemap AG, 8708 Mannedorf, Switzerland. It consisted of a glass cylinder sandwiched between two stainless steel plates. Mixing was provided by impellers attached to a shaft, which was driven by a steples D.C, bottom entry motor. The fermenter had a hot water circulation system that was used to keep the broth at constant temperature. A reflux condenser was attached to the fermenter, at the top, and it was used to reflux ethanol vapour and also provided an exit for the carbon dioxide gas produced during the fermentation. No pH control was applied. A picture of this equipment is presented in figure 4.5.

4.2.3.1 *Temperature control*

The fermentation temperature was kept constant at 30 ^{0}C, by controlling the temperature of the circulating hot water, using a contact glass thermometer (Jumo D.B.P. West Germany).

4.2.3.2 *Aeration*

Air was pumped by an air pump (Campton, Dawson & Dawson Ltd., Ashbourne) through a carbon filter of 0.2 μm porosity and an air rotameter (Platon flow bits, Basingstoke). The air was pumped at a flow rate of four liters per hour.

4.2.4 Equipment used in sample analysis

The following laboratory equipment were used in the analysis of sample for the different parameters determined.

Microscope (Galen II, Bousch and Lomb, New York, U.S.A.)

Microcentrifuge (MSE Scientific Instruments, Sussex)

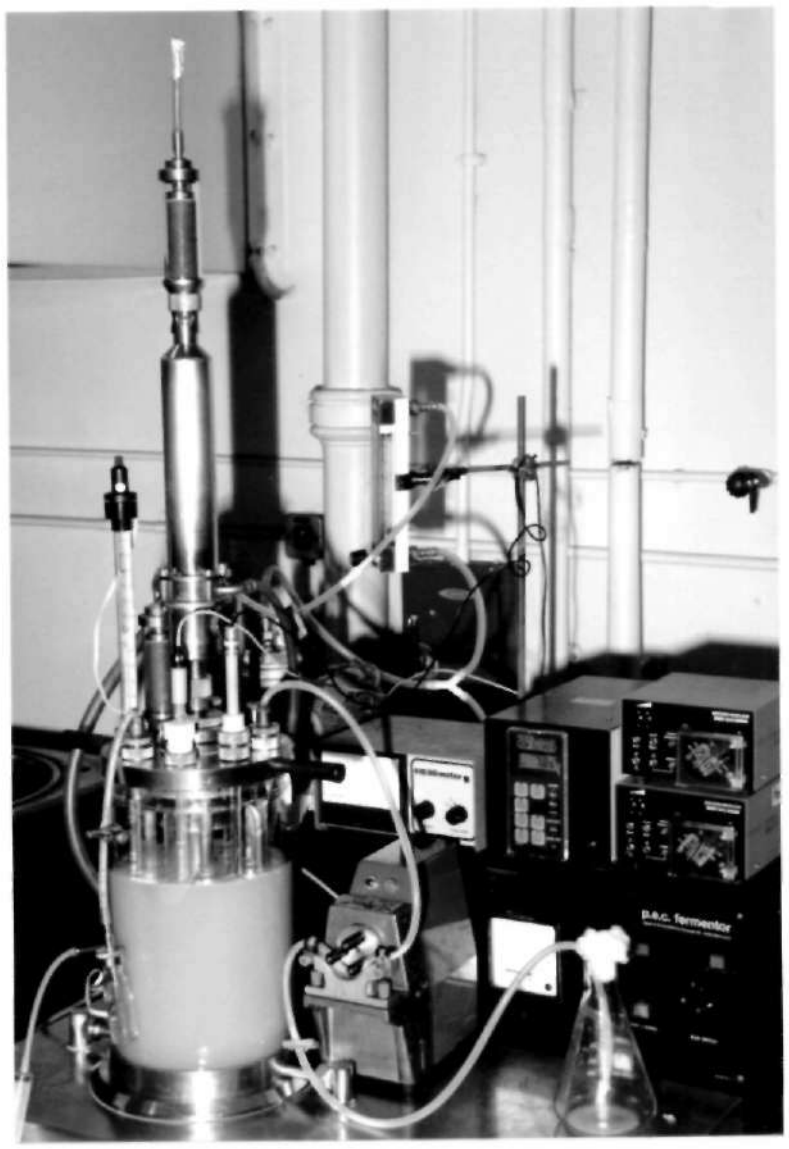


Fig. 4.5 Chemap batch fermenter

Gas chromatograph (Model 8500, Perkin-Elmer Ltd., Buckinghamshire)
Integrator (LCI 100, Perkin-Elmer Ltd., Buckinghamshire)
Oven (Macfarlane Robson Ltd., London)
Orbital shaker (LH Engineering Ltd., Reading)
Spectrophotometer (Shimadzu, Model UV 120-02, V.A.Howe & Co. Ltd., London)
Water bath (Grant Instruments Ltd., Cambridge)
pH meter (Model 8521, CP Instrument Ltd., Bishop's Stortford)
Autoclave (Model 225 EV, Laboratory Thermal Equipment, Oldham)
Weighing machines (Sartorius and Solex model SC 240)
Centrifuge (Centaur 2, MSE Scientific Instruments, Sussex)

4.3 EXPERIMENTAL METHODS

Before experiments were started, the yeast cultures received, were first subcultured on slopes. These subcultures were then used to prepare inoculum for use in fermentation experiments. Preparation of subculture and inoculum, medium preparation, sterilization of equipment and medium, selection of yeast strain, operation of column fermenter, and experiments performed for the purpose of determining liquid axial dispersion coefficient and liquid holdup, are explained in this section.

4.3.1 Preparation of media

Medium for subculturing and for use in batch fermenters and the fluidized bed fermenter, were prepared in accordance to the recipe given in section 4.1.3. Medium was sterilized before use.

4.3.2 Media and equipment sterilization

Medium and equipment, except the column fermenter,

were sterilized in an autoclave (Model 225 EV, Laboratory Thermal Equipment, Oldham) at 16 psi (121 ^{0}C), for twenty five minutes.

The column fermenter and all its connected tubing was sterilized chemically with a solution of sodium hypochlorite. This solution was prepared by adding 30 ml of concentrated sodium hypochlorite solution into five liters of distilled water. The hypochlorite solution was pumped into the column. When the column was filled up, the solution was left for five hours before it was discharged. After the solution was drained off, the column was then rinsed with 20 liters of sterilized distilled water.

4.3.3 Preparation of subculture

Yeast cultures recieved were subcultured on slopes before storage. 5 g of malt extract agar was dissolved in 100 ml of distilled water in a beaker. It was covered with an aluminium foil and heated with steam for twenty minutes to dissolve the malt extract. The resulting solution was distributed equally into ten, labelled, McCartney bottles, sterilized, and sloped. The bottles were left, over night, to solidify. Each bottle was aseptically inoculated in a laminar flow cabinet. The slopes were left for three days in a constant, 30 ^{0}C, temperature room. They were then transferred into another constant, 4 ^{0}C, temperature room for storage. Subculturing was repeated every two months.

4.3.4 Preparation of inoculum

For shake flasks and batch fermentations, inoculum was prepared with 50 ml medium put into a 250 ml conical flask. The medium was sterilized and inoculated using the slope subcultures earlier prepared. It was then placed on an orbital shaker, in a constant temperature room at 30 ^{0}C, for twenty-four hours. More flasks were simultaneously used if more than 50 ml of inoculum was required.

The inoculum for the column fermenter was prepared in

the Chemap batch fermenter. The fermenter was sterilized and five litres of sterilized medium containing 50 g/l of glucose was prepared, as explained in section 4.3.1. It was aseptically pumped into the fermenter using a peristaltic pump. The fermenter was inoculated with 100 ml of inoculum prepared as explained above. Fermentation temperature and stirrer speed were maintained at 30 ^{0}C and 100 rpm respectively. Air was pumped into the fermenter through a sterilized carbon filter of 0.2 μm porosity, at a flow rate of 4 liters per minute. After forty eight hours of fermentation, the fermenter was aseptically evacuated by pumping its contents into a clean, sterilized aspirator bottle. The procedure was repeated twice in order to get enough biomass for the start-up of the column.

With the strain NCYC 1026, additional inoculum was prepared in 10 liter aspirator bottles.

4.3.5 Selection of yeast strain

The yeast strain that will give discrete particles of measurable sizes was prefered. The four yeast strains recieved from the Department of Bioscience and Biotechnology, were tested for floc formation and distribution of floc size in shake flask fermentation experiments. Four 250 ml conical flasks, each containing 50 ml of medium (made up of 20 g/l glucose and 5 g/l yeast extract), were prepared. Each flask was inoculated with a different strain of yeast in a laminar flow cabinet. The flasks were then placed on an orbital shaker in a room maintained at 30 ^{0}C. After forty eight hours, the flasks were removed in turn and the sizes of the particles formed were measured using a microscope equipped with an eye piece graticle. About twenty particles were measured from each flask, to give a representative particle size. The strain that produced particles of moderate sizes and narrow size distribution was considered for use in the

column fermentation experiments.

4.3.6 Operation of continuous reactor

The liquid axial dispersion coefficient was determined during an anaerobic fluidized bed fermentation carried out in a 0.3 mm thick, 38.1 mm I.D. and 200 cm long column fitted, at the top, with a particle separation chamber. Start-up of the column, addition of growth medium and sampling from the column are covered in this section.

4.3.6.1 *Start-up of column*

The column was started up by aseptically pumping in ten litres of inoculum, prepared as explained in section 4.3.4. It entered the column at a point about 200 cm above the liquid distributor. The yeast was allowed to settle and the supernatant liquid drained off. Filter-sterilized air was pumped into the column at a point below the liquid distributor. Air flow rate was maintained at 2 litres per minute. Media containing 50 g/l glucose was pumped into the column, from the bottom, at a velocity of 0.0175 cm/sec. The column was operated in fed-batch form and whenever the liquid level reached the outlet, the medium and air flows were stopped and the yeast allowed to settle. The supernatant liquid was then decanted off. This procedure was repeated till the settled yeast reached a height of 50 cm to 80 cm when it was considered ready.

4.3.6.2 *Medium addition during continuous fermentation*

A combined flow of sterile air and medium was used to break-up the settled yeast. Then, the yeast was allowed to settle again against the medium flow. Sterilized medium was continously pumped into the column, from the bottom, using a pre-calibrated peristaltic pump (Watson & Marlow, WM 502-S, 50). The glucose concentration in the medium was kept at 50 g/l while the medium velocity was adjusted to 0.0084 cm/sec. The column was allowed to reach steady

state as indicated by changes of less than 10% in glucose and ethanol concentrations of samples taken at two points, 50 cm apart, within a period corresponding to one residence time, based on the empty column. When steady state was established, samples were taken along the column length for the determination of pH, ethanol, biomass and glucose concentrations. Dispersion and bed expansion experiments were then performed. Sampling and experiments were repeated at medium velocities of 0.0175, 0.0235 and 0.0351 cm/sec while the glucose concentration in the medium was kept constant.

The experiments were repeated using media containing glucose of 100 g/l for the strain Y6 and 30 and 70 g/l for the strain NCYC 1026.

4.3.6.3 *Reactor sampling*

After the steady state was established, 10 ml samples were taken, at the sampling points, along the column length. Not less than ten samples were taken during any experiment. Samples were removed with a 20 ml syringe that was kept in an ice bath. 1.5 ml of each sample was placed into microcentrifuge vials and centrifuged at 13000 rpm (MSE Microcentaur) for ten minutes. The supernatant liquid was decanted and kept in a freezer for glucose and ethanol analysis at a later time. 7 ml of the sample was placed into 10 ml sterilized plastic bottles. Its pH was measured and immediately placed in a freezer for biomass analysis at a later time.

4.3.7 Axial dispersion experiments

Residence time distribution technique was used to determine the axial liquid dispersion coefficient and the liquid holdup. Both pulse and step-change injection methods were used. In the pulse method, a known quantity of tracer material was injected into the fluidized bed and in the step-change method, the tracer concentration in the

bed was instanteneuously increased from zero to a known value. The type and nature of the tracer material used could have an effect on the residence time distribution obtained. For this reason experiments, for the selection of a suitable tracer material, were carried out before the start of dispersion experiments.

4.3.7.1 *Selection of tracer material*

Five tracer materials were selected, for experimentation, among many considered. The criteria for selection were based mainly on the material's toxicity, and availability. Those selected are presented in Table 4.1.

A three stage screening method was employed. At the first stage, shake flask fermentations were carried out and in the second stage, anaerobic batch fermentations were performed with those tracer materials that indicated suitability during the first stage tests. Finally, further tests were performed in column fermenter.

Shake flask experiments: Six 500 ml conical flasks each containing 100 ml of media (made up of 20 g/l glucose and 5 g/l yeast extract) were prepared.

Table 4.1: Tracer materials selected

Tracer	Molecular weight	Estimated cost (£/100 g)*
Fluorescein	374.86	4.9
Methyl green	472.51	139.6
Methyl violet	393.96	8.9
Aniline blue	799.80	30.0
Dextran blue	2,000,000	480.0

* (Aldrich, 1991)

Tracer materials were added into the flasks such that each flask contained a different tracer. The sixth flask was left as a control. The concentration of each tracer in the resulting solutions was determined as explained in section 4.4.7. All the six flasks were sterilized and 4 ml of an earlier prepared yeast culture was aseptically added into each flask. They were placed on a rotary shaker for twenty four hours in a constant, 30 ^{0}C, temperature room. Finally, the concentrations of biomass and ethanol formed as well as the residual glucose and tracer, in each flask, were determined and compared with that of the control. The experiment was repeated with different concentrations of tracer materials.

Anaerobic batch fermentation: Three tracer materials, fluorescein, aniline blue and dextran blue, were further tested in an anaerobic batch fermentation performed in a one litre LH fermenter. A 900 ml tracer-added-medium containing 20 g/l glucose, 5 g/l yeast extract and a known concentration of tracer material was prepared. The fermenter was prepared and sterilized along with the medium. The medium was aseptically pumped into the fermenter using a peristaltic pump (Watson-Marlow 502 S). An earlier prepared 50 ml inoculum was used to inoculate the fermenter. The fermentation was allowed to proceed in a room controlled at a temperature of 30 ^{0}C.

Initial and hourly 10 ml samples were aseptically removed from the fermenter. The pH of the sample was measured immediately. The tracer concentration in each sample was also measured after centrifuging at 3400 rpm for ten minutes. Biomass, ethanol and glucose concentrations, in each sample, were determined.

Each batch fermentation was carried out with a single tracer material and was repeated. Another batch fermentation, in which no tracer was added, was used as a control.

4.3.7.2 *Tracer injection into column*

After taking samples along the column length, the tracer was injected into the column. Both the pulse injection and the step-change methods were used.

Two tracer materials were used; fluorescein and dextran blue. They were used in a slightly different manner as explained in the preceeding paragraphs.

Pulse injection:- With this method, tracer was injected into the column at a point 3 cm above the liquid distributor. It was injected by means of a syringe attached to a 10 cm needle (18 G) that was extended to the centre of the column. In separate experiments, 0.2 ml, 1.5 ml and 10 ml of 25 g/l fluorescein solutions were injected into the column. With dextran blue, a 25 g/l solution was prepared. 2 ml of this solution was injected into the column. For Y6 strain, inlet glucose concentrations of 50 g/l and 100 g/l were used, while liquid velocity was varied. But, for the strain NCYC 1026, the inlet glucose concentration was 30, 50 and 70 g/l.

In all cases, the period of injection was less than five seconds. Considering the small medium velocity, and the short period of injection, the signal was assumed to be a perfect pulse.

Step change:- In the step change experiments, a sterilized medium containing 50 g/l glucose and a known concentration of fluorescein, was prepared. When the column was operating at steady state, medium supply was quickly swiched to the bottle containing the tracer-added-medium. The period of switching to the tracer-added-medium was less than five seconds. The signal was assumed to be a perfect step change. Step change dispersion experiments were performed with strain Y6, at the required liquid velocities and initial tracer concentrations of 0.15 g/l and 0.01 g/l respectively.

4.3.6.2 *Tracer sampling from column*

A point within the yeast bed, where dispersion of injected tracer was to be monitored, was selected. A 7 ml sample was then taken at this point about ten minutes before tracer injection. This sample was centrifuged at 4000 rpm for twenty minutes. The supernatant liquid was decanted and its optical density read, using distilled water as a blank. Optical density was read at a wavelength corresponding to the wavelength of maximum light absorption (λ_{max}) of the tracer to be used in the experiment. This reading provided the background optical density at the point of tracer monitoring. Sampling for the tracer was started one or two minutes after tracer injection and continued at an interval of one or two minutes, for a period lasting not less that three times the estimated residence time, based on liquid volume. For fluorescein samples, the pH was adjusted to the range 4.7 to 5.3 by the addition of about 50 µl of 0.1 molar sodium hydroxide. No pH adjustment was required for dextran blue samples. All samples were centrifuged at 4000 rpm for twenty minutes (Centaur 2, MSE Scientific Instruments, Sussex) and the tracer concentration, of the supernatant solution, was determined as explained in section 4.4.7.

4.4 ANALYTICAL METHODS

The analytical methods employed are grouped into three categories:

i) Analysis of fermentation samples for pH, biomass, glucose and ethanol concentrations,
ii) Measurements of physical parameters; bed height, pressure drop and particle size.
iii) Determination of tracer concentration and carbon dioxide flow rate.

4.4.1 pH

The pH of samples was measured, using a bench pH

meter, by simply dipping the pH electrode and the temperature compensating probe into the sample. pH reading was recorded after it had stabilized.

4.4.2 Biomass

Biomass was determined by the dry weight method. The sample was first thoroughly shaken and a known volume was pipetted and filtered, with the aid of suction, through a membrane filter of porosity 0.45 μm and diameter 47 mm (Whatman Ltd., Maidstone, type WCN). The filter was previously dried to constant weight at 105 °C, cooled in a desiccator and weighed. The deposited biomass on the filter was washed twice, each time with 10 ml of distilled water. It was then placed into a Petri dish and dried to constant weight in an oven at 105 °C. The dried filter was then cooled in a desiccator containing silica gel granules, for two hours. It was weighed again after cooling. The biomass concentration was calculated as:

$$C_b = \left(\frac{W_{fd} - W_f}{V_f}\right) 1000 \qquad 4.1)$$

4.4.3 Glucose analysis

The concentration of glucose, in a sample, was determined using the method of Barnham and Trinder as described by Brown (1988). The method was best used for samples with glucose concentrations in the range 0.025 g/l to 0.2 g/l. Consequently, all samples were diluted with distilled water in order to get glucose concentation in that range, before analysis proceeded.

Four groups of reagents associated with this method were prepared and used in the analysis. These reagents are:-

Phosphate buffer: 2.83 g of Na_2HPO_4 was dissolved in 100 ml of distilled water (Solution A). Also 3.12 g of

NaH_2PO_4 was dissolved in 100 ml of distilled water (Solution B). Then, 61 ml of solution A was added to 29 ml of solution B and the volume made up to 200 ml with distilled water. The pH of this solution was 7.01.

Enzyme solution: This solution was prepared by dissolving 30 mg of glucose oxidase and 5 mg of peroxidase into 100 ml of phosphate buffer. To the resulting mixture, 50 mg of sodium azide and 35 mg of 4-amino phenazone were added. The solution was stable for four weeks when stored at 4 ^{0}C.

Coupler solution: This solution was prepared by diluting 2,4-dichlorophenol (sulphonated) with phosphate buffer in the ratio 1:25.

Glucose standards: A stock solution containing 0.2 g of glucose in one litre of distilled water was prepared. Dilutions of the stock solution in the ratios 1:2, 1:4, and 1:8 were also prepared using distilled water as diluent. The stock solution and the dilutions were used to give glucose standards of 0.2, 0.1, 0.05, and 0.025 g/l respectively.

After preparation of the above reagents, glucose concentration was determined using the following procedure; 3 ml of coupler solution and 1 ml of enzyme solution were placed in a glass test tube and allowed to stand in a 37 ^{0}C water bath for two minutes. 0.2 ml of diluted sample was added and mixed with a votex mixer. The test tube was put back into the 37 ^{0}C water bath and left for fifteen minutes. It was then removed and cooled in an ice bath for one minute, after which its optical density was read at 515 nm. A blank was prepared by replacing the 0.2 ml of sample with 0.2 ml of distilled water. A calibration curve was also prepared, for each set of analysis, using the standard glucose solutions. The glucose concentration in the fermentation sample was calculated by multplying the glucose concentration obtained with the approperiate dilution factor.

4.4.4 Ethanol analysis

Ethanol was analysed using a gas chromatograph (Perkin Elmer, model 8500) connected to a Perkin Elmer LCI-100 integrator. The gas chromatograph was fitted with a flame ionization detector and a two metre long, 2 mm ID. glass column packed with Porapak-Q (80-100 mesh). Nitrogen was used as the carrier gas at a pressure of 20 psi. The gas chromatograph was operated with detector and column temperatures of 250 ^{0}C and 185 ^{0}C respectively. The run time was 2.5 minutes.

0.2 ml of sample was diluted with 0.2 ml of 0.2% v/v methanol in distilled water, which was used as an internal reference. 1 μl of the diluted sample was injected into the gas chromatograph. A solution containing 0.1% v/v ethanol in distilled water and 0.1% v/v methanol in distilled water was used as standard. 1 μl of this solution was also injected during each set of analysis.

Ethanol concentration was calculated using the areas of the projected chromatographs as follows:-

$$C_e = \left(\frac{A_{eu}}{A_{mr}}\right) \left(\frac{A_{mr}}{A_{es}}\right) C_{es} D_f \qquad 4.2)$$

4.4.5 Measurement of bed height

In all experiments the bed height was distinctly visible. Hence, bed height was measured visually using a graduated scale fixed to the column.

4.4.6 Measurement of particle size

Particle size was measured using a microscope fitted with an eye piece graticle. The graticle was calibrated using a stage micrometer (one division on graticle ≡ 0.026 mm). A small amount of the sample was placed on a glass slide by means of a dropping pipette. The slide was mounted on a microscope. The number of graticle divisions

corresponding to the diameter of a particle was read and converted to size using the calibration obtained earlier. The diameters of ten to twenty particles were determined and considered as representative of each sample. The particles were assumed to be spherical and the average particle size for each sample was calculated from the relation (Bailey and Ollis, 1977; Shieh, Sutton and Kos, 1981):

$$d_p = \frac{\sum_{i=1}^{n} d_i^3}{\sum_{i=1}^{n} d_i^2} \qquad 4.3)$$

where n is the number of measurements.

4.4.7 Measurement of tracer concentration

The concentrations of the tracers used were determined using the spectrophotometric technique. There was, however, a slight difference in sample treatment for the tracers prior to the use of the spectrophotometer.

For fluorescein, the pH of the samples was adjusted to give a pH in the range 4.7 to 5.3, by the addition of 50 μl of 0.1 molar sodium hydroxide solution to 7 ml of the sample. It was then centrifuged for twenty minutes at 4000 rpm (MSE Centaur 2). The optical density (OD) of the supernatant solution was then measured, after it was carefully decanted. Optical density measurement was made at a wavelength of 490 nm, using distilled water as a blank. The optical density of the background medium, measured at the same wavelength as the sample and using distilled water as a blank, was also measured. It was subtracted from the value of the optical density of the supernatant, to give the correct OD value for the sample. The concentration of fluorescein, in the sample solution, was calculated from the value of the corrected optical

density obtained, using a calibration curve earlier prepared.

Calibration was effected by measuring the OD of fluorescein solutions of known concentrations at various pH values. The optical density measurement was made at 490 nm using distilled water as a blank. A relationship between the optical density, pH and fluorescein concentration was obtained by multiple regression. The relationship was given as:

$$C_{fl} = 0.0130 - 0.00253\ pH + 0.0233\ OD_{490} \qquad 4.4)$$

Goodness of fit $R^2 = 98.7\%$

For the other tracers, pH adjustment was not made, but samples were centrifuged at 4000 rpm for twenty minutes. OD measurements for dextran blue, aniline blue, methyl violet and methyl green were made at wavelengths of 625 nm, 600 nm, 585 nm and 635 nm respectively. Calibration curves were also prepared for these tracers in a similar manner to that explained above. The relationships between concentrations of tracers and optical densities were expressed linearly by regression. These relationships were found to be:

$$C_{db} = 1.1846\ OD_{625} - 0.0009172 \qquad 4.5)$$

$R^2 = 99.8\%$

$$C_{ab} = 0.0436\ OD_{600} - 0.000412 \qquad 4.6)$$

$R^2 = 99.8\%$

$$C_{mv} = 0.00754\ OD_{585} + 6.549\ x\ 10^{-5} \qquad 4.7)$$

$R^2 = 99.8\%$

$$C_{mg} = 0.0239\ OD_{635} + 5.227\ x\ 10^{-4} \qquad 4.8)$$

$R^2 = 99.6\%$

The wavelength used, for each tracer material, corresponded to its wavelength of maximum light absorption. These were obtained by preparing solutions of tracers of known concentrations and then measuring the optical densities of these solutions at various wavelengths. For a particular material the wavelength at which the optical density was highest was considered to be its wavelength of maximum light absorption and was used in subsequent optical density measurements.

4.4.8 Determination of carbon dioxide flow rate

Carbon dioxide (CO_2) flow rate was estimated using a CO_2 rotameter. A trap was placed in the CO_2 line in order to remove the accompanying yeast particles. The CO_2 flow rate was also estimated from ethanol concentration profiles.

4.5 DATA ANALYSIS

Some parameters were not directly obtainable from the experiments performed, but were calculated from the data generated. For example, the data generated from the dispersion experiment was used to calculate the liquid axial dispersion coefficient. Also the carbon dioxide profile was evaluated from the ethanol concentration gradient. The techniques used to analyse the data are explained in this section.

4.5.1 Calculation of liquid axial dispersion coefficient

The technique of calculating the liquid axial dispersion coefficient (D_z) depends on the method of tracer injection used and also on the manner in which the tracer was injected and monitored. In this section, details of the calculation procedure involved for both the pulse method and the step change method are explained. In both cases, the mean and variance of the distribution obtained,

from the dispersion experiment, were equated to the mean and variance of a theoretical distribution obtained from an appropriate flow model of the system. As earlier mentioned, the dispersed plug flow model was considered appropriate to our system; the mean and variance of theoretical distributions derived from this flow model were used.

4.5.1.1 *Pulse method*

Tracer was injected within the bed and it was sampled within the bed at a selected point downstream of the injection point. There were no changes in medium flow pattern at the point of tracer injection and sampling; the system was operated with open boundries. Sampling of the tracer was done by taking samples at known time intervals; i.e. by the *mixing-cup* method. Since the system was open and the tracer sampling was by the *mixing-cup* method, the closed system boundary conditions are applicable (Levenspiel, 1972). In a particular dispersion experiment, the mean and variance of the distribution obtained, were calculated from equations 4.9 and 4.10 respectively. The mean and variance were also calculated, in dimensionless form, from the theoretical distributions obtained using the dispersed plug flow model (Eqns. 4.11 and 4.12).

$$t_{avg} = \frac{\int_0^\infty t.C.\delta(t)}{\int_0^\infty C.\delta(t)} \approx \frac{\Sigma t_i.C_i.\Delta t_i}{\Sigma C_i.\Delta t_i} \qquad 4.9)$$

$$\sigma^2 = \frac{\int_0^\infty (t - t_{avg})^2.C.\delta t}{\int_0^\infty C.\delta t} \approx \frac{\Sigma t_i^2.C_i.\Delta t_i}{\Sigma C_i.\Delta t_i} - t_{avg}^2 \qquad 4.10)$$

$$\theta_{avg} = \frac{t_{avg,th}}{t_{avg,ex}} = 1 \qquad 4.11)$$

$$\sigma_\theta^2 = \frac{\sigma^2}{t_{avg}^2} = \frac{2}{Pe} - \frac{2}{Pe^2} \; x \; (1 - e^{-Pe}) \qquad 4.12)$$

where, $Pe = \frac{u_L L}{\varepsilon_L D_z}$

The calculation of D_z was done by following the procedure:-

1) The mean was calculated from equation 4.9 using the experimental data.
2) Using the calculated mean, the variance was calculated from equation 4.10.
3) The calculated variance was then used in equation 4.12 to calculate the Peclet number (Pe), by trial and error.
4) The Peclet number was finally used to calculate the liquid axial dispersion coefficient (D_z).

The amount of tracer recovered, from a dispersion experiment, was calculated from equation 4.13 and the amount of tracer injected was calculated from the product of the volume of tracer injected and the concentration of the tracer used. Hence, the percentage recovery of tracer was obtained using equation 4.14.

$$W_{tr} = Q \, \Sigma C_i \, \Delta t_i \qquad 4.13)$$

$$\%Tracer\ recovered\ (R_T) = \left(\frac{Q \, \Sigma C_i \Delta t_i}{V_{inj} \, C_{tr}}\right) 100 \qquad 4.14)$$

4.5.1.2 *Step change method*

The time record of tracer measured, at the monitoring point, as $c_{tr,t}/c_{tr,0}$, is called the **F** curve. It is related to the **C** curve according to equation 4.15. The **C** curve is therefore a normalized response obtained from a pulse experiment and normalization was done by dividing the measured tracer concentration by the area under the concentration-time curve, i.e., $C = \frac{c}{\int_0^\infty c.\delta t}$.

$$C = \frac{dF}{dt} \approx \frac{\Delta F}{\Delta t} \rightarrow C.\Delta t = \Delta F \qquad 4.15)$$

The **C** curve was obtained by taking the slopes of the **F** curve. The mean and variance, of the **F** curve, were calculated from equations 4.16 and 4.17 respectively (Levenspiel, 1972).

$$t_{avg} = \Sigma t_i.C_i.\Delta t_i = \Sigma t_i.\Delta F_i \qquad 4.16)$$

$$\sigma^2 = \Sigma t_i^2.C_i.\Delta t_i - t_{avg}^2 = \Sigma t_i^2.\Delta F_i - t_{avg}^2 \qquad 4.17)$$

The calculated variance was then matched with the theoretical variance in equation 4.12 and the D_z was calculated in accordance with the procedure outlined before.

The tracer recovered is given by the ratio $c_{tr,\infty}/c_{tr,0}$.

4.5.2 Calculation of liquid holdup

The liquid holdup was calculated from the experimentally obtained average residence time given by equation 4.19. For closed systems, the residence time can also be expressed as the ratio of liquid volume in the bed to the liquid flow rate (Levenspiel, 1972; Admassu *et al.*, 1985). Thus,

$$t_{avg} \approx \frac{\Sigma t_i . C_i . \Delta t_i}{\Sigma C_i . \Delta t_i} = \frac{\varepsilon_L V_b}{f_L} \qquad 4.18)$$

and, $$\varepsilon_L = \frac{t_{avg}\, f_L}{V_b} \qquad 4.19)$$

4.5.3 Calculation of gas flow rate

The flow rate of CO_2 gas released, during the fermentation, was obtained by considering the stochiometric relation:-

$$C_6H_{12}O_6 \rightarrow 2C_2H_5OH + 2CO_2 \qquad 4.20)$$

From the above equation, the number of moles of ethanol produced was equal to the number of moles of carbon dioxide also produced. At a temperature of 30 ^{0}C the flow of carbon dioxide at the reactor exit, where the pressure is atmospheric, is given by equation 4.21.

$$f_g\ (ml/\text{min}) = 0.54\ C_e\ f_L \qquad 4.21)$$

The rate of gas generation, in the reactor at a given height (z), is given by equation 4.22.

$$f_{g,z}\ (ml/\text{min}) = \frac{0.54\ C_{ez}\ f_L\ P_{atm}}{P_{atm} + (263 - z)\,\rho_L g} \qquad 4.22)$$

4.5.4 Regression analysis

To get relationships between parameters, regression analysis was performed using the method of least squares. Linear regressions were performed with a desk calculator (Casio Scientific, Fx-115N), whereas multiple regression was performed with the Minitab software package, on a VAX computer.

CHAPTER FIVE

RESULTS AND DISCUSSIONS

5.1 INTRODUCTION

This section is divided into four parts, namely; tracer selection, performance of fluidized bed bioreactor, axial liquid mixing and bed expansion behaviour. In each part, the results obtained are presented and discussed.

5.2 TRACER SELECTION

Selection of a suitable tracer material for use in residence time distribution (RTD) studies is important, because physical phenomena such as adsorption or absorption of tracer could have a significant effect on the nature of the RTD curve obtained. This may have a subsequent effect on the evaluation of the axial liquid dispersion coefficient and liquid holdup. The tracer may also affect the yeast metabolism by either hindering or accelerating it and these may have a profound effect on the rate of the biochemical reaction and gas production. The loss of tracer either by physical or biochemical means, may also affect the values of D_z and ε_L.

A three-stage selection procedure was adopted. In the first stage, shake flask experiments were performed with the aim of finding the effects of the tracers on the yeast metabolism and the recoverability of tracer materials. In the second stage, anaerobic fermentations were performed at conditions similar to those at which the RTD study would be conducted. Here, the main objective was to asses the effect of the tracer on yeast metabolism. At the initial stages of the fermentation this will give an indication of what may likely happen at the entrance to the column reactor. Also, the course of the fermentation, with time, could be assesed. In the final stage, the suitability of tracers was tested in a continuous column bioreactor containing fluidized flocs of yeast, strain Y6. The focus here was to assess the effect of large amount of biomass on the suitability of a particular tracer. Tracer absorption into the biomass and subsequent desorption

could affect the RTD curve and consequently, the inferred values of D_z and ε_L.

Prio to tracer selection, the wavelength of maximum light absorption (λ_{max}) was determined for each tracer and calibration curves were obtained at the λ_{max}.

5.2.1 Determination of λ_{max}

The wavelength at which each of the tracer materials had maximum light absorption λ_{max}, and the concentration ranges considered are presented in Table 5.1. The values of λ_{max} obtained are the same as those given by Aldrich (1991) with the exception of fluorescein and methyl violet, where values of 491 nm and 584 nm were given respectively. It was noted that λ_{max} was independent of concentration of tracer, within the ranges considered.

Table 5.1 λ_{max} for the tracer materials

Tracer	Wavelength λ_{max} (nm)	Tracer concn., C_{tr} (g/l)
Fluorescein	490	0.001-0.06
Dextran blue	625	0.0125-4.0
Methyl violet	585	0.01-0.12
Methyl green	635	0.001-0.05
Aniline blue	600	0.1-0.12

5.2.2 Calibrations for tracer concentration

Changes in tracer concentration with optical density OD, showed a similar pattern for all the five tracer materials. Initially, OD increased linearly with concentration but, at a certain concentration, the OD became constant and insensitive to further increases in concentration. Similar behaviour was observed for fluorescein by Setiadi (1989). The calibration curves are

shown in appendix C.

A regression analysis on the linear portions, of the concentration versus OD curves, was performed. The slope m and intercept c, of these lines, and the correlation coefficient R, in addition to the minimum detectable concentrations and the upper limits of the OD readings used in the regression, are shown in Table 5.2.

Table 5.2 Regression analysis of calibration curves

Tracer	Slope, m (g/l)	Intercept c x10^5 (g/l)	Correlation coeff., R	Min. tracer concn., C_{st} (mg/l)	Upper limit of OD
DB	1.1846	-91.72	1.000	35	0.838
FL	0.0124	-1.114	0.992	0.36	0.619
MV	0.0075	6.549	0.999	0.29	0.798
MG	0.0239	52.27	0.998	1.2	0.807
AB	0.0436	-41.17	0.999	0.9	0.926

(DB = Dextran blue, FL = Fluorescein, MV = Methyl violet, MG = Methyl green, AB = Aniline blue)

The high correlation coefficients indicated that the relationships between the tracer concentration and OD, for all the tracers, were linear. The minimum detectable concentration was obtained from the slope and intercept of the lines, by considering the lower sensitivity limit of the instrument to be 0.03 as stated by Brown (1988). It was noted that fluorescein and methyl violet were detectable at concentrations lower than 1 mg/l, whereas dextran blue was detectable only above 35 mg/l. The resultant effect is that the minimum amount of dextran blue that may be required for RTD study will be about 97 times that of fluorescein or 39 times that required for

aniline blue. Methyl violet and methyl green have also very low minimum detectable concentrations of 0.29 and 1.2 mg/l respectively.

5.2.3 Effects of tracer materials on yeast metabolism in shake flasks

There are a number of ways in which the tracers may effect the yeast metabolism. A preliminary fermentation experiment was performed in shake flasks for the comparison of yeast metabolism in terms of glucose consumption, biomass and ethanol productions, against a control fermentation. The experiment was repeated with higher concentrations of tracer materials in order to confirm the results and also investigate the effects of increased tracer concentration.

As expected, the two experiments gave similar results, except for methyl violet where significant differences were observed; indicating that higher concentrations of methyl violet increased the effect on yeast metabolism. There was a remarkable similarity in both trend and magnitude of glucose consumption (Fig. 5.1) and ethanol and biomass productions (Figs. 5.2 & 5.3) in the control flask and in flasks containing fluorescein, dextran blue and aniline blue. This means that the presence of dextran blue, fluorescein and aniline blue, does not significantly affect the yeast metabolism, and both ethanol and biomass yields were found to be comparable to those obtained in the control experiment, as shown in figures 5.4 and 5.5.

On the other hand, contrasting results were obtained with methyl green and methyl violet. When compared to the control, glucose consumption, ethanol and biomass production, in the presence of methyl violet, were low. This indicated that methy violet has repressive effect on yeast metabolism. But, in the presence of methyl green, the amount of glucose consumed was the highest, at about

13 g/l. The corresponding amounts of ethanol and biomass produced were also the highest with an average of 5.8 and 1.24 g/l respectively. These results suggested that methyl green promoted yeast metabolism.

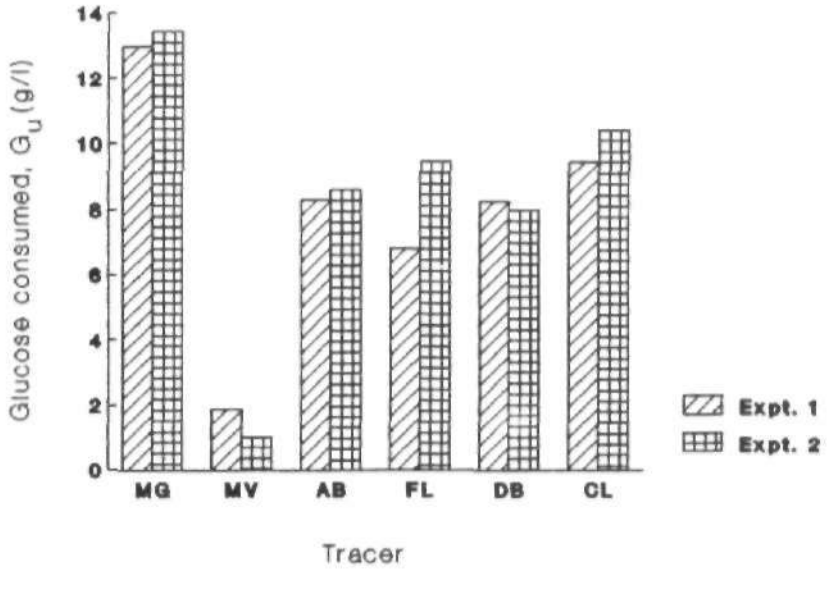


Fig. 5.1: Glucose consumption in shake flasks

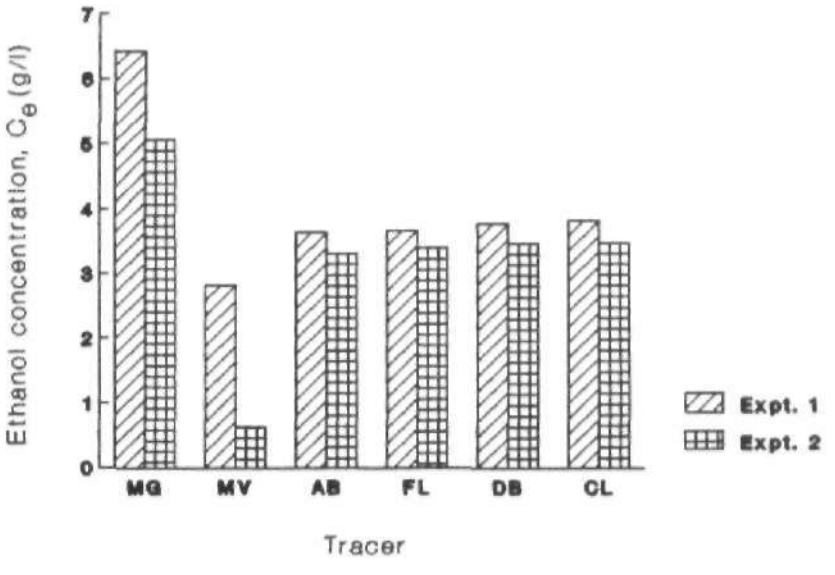


Fig. 5.2: Ethanol production in shake flasks

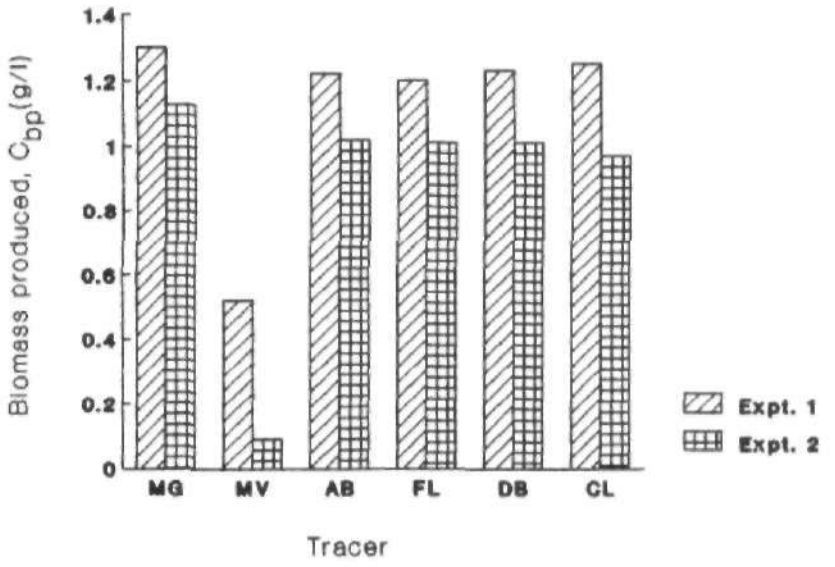


Fig. 5.3: Biomass production in shake flasks

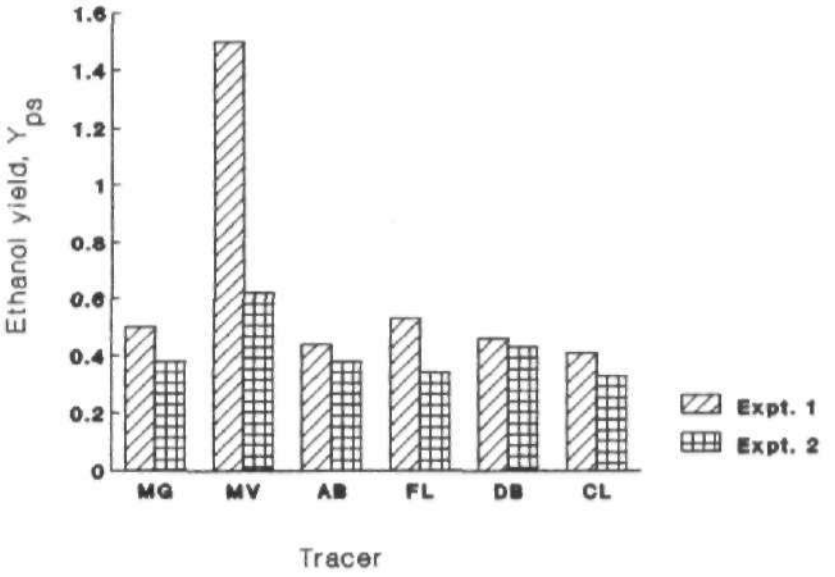


Fig. 5.4: Ethanol yield in shake flasks

(MG = Methyl green, MV = Methyl violet, AB = Aniline blue, FL = Fluorescein, DB = Dextran blue, CL = Control)

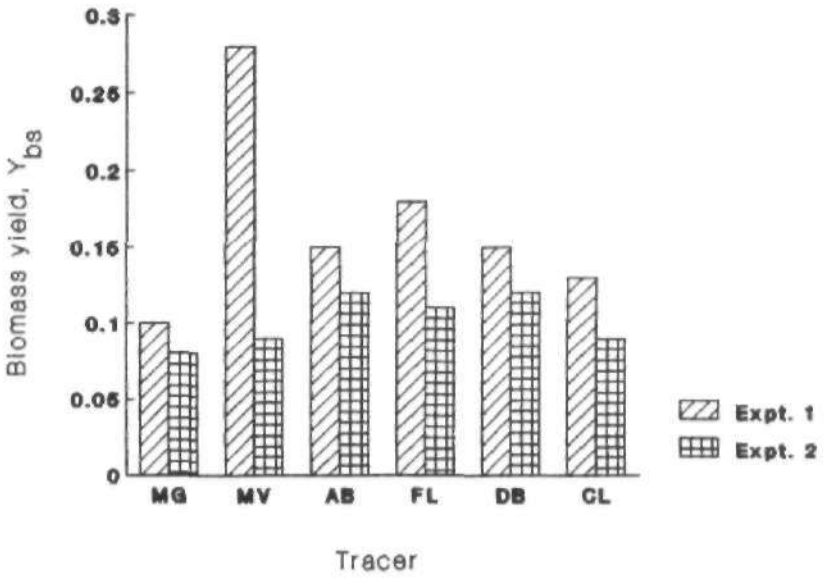


Fig. 5.5: Biomass yield in shake flasks

5.2.4 Tracer recovery in shake flasks

A tracer which has no significant effect on yeast metabolism may however prove not to be a good choice if it has poor recovery. This may be due to adsorption on cell surfaces and reactor walls or absorption into the cells. Tracers may also be affected by the biochemical changes taking place in the bioreactor.

The percentage recovery of tracers, are presented in figure 5.6. It is apparent that dextran blue has the highest percentage recovery of an average of 96%, while fluorescein was the least recovered with an average of 27%. Also only about 34% of methyl green was recovered whereas both MV and AB were fairly quantitatively recovered, with averages of 71% and 84% respectively. The loss of methyl green may be due partly to adsorption on cell surfaces and container walls or metabolization by the yeast cells. The low biomass yield in the presence of this tracer may suggest that methyl green favoured ethanol production to yeast growth. In the case of methyl violet, its loss may be due, purely, to adsorption on cell

surfaces. As this tracer was shown to repress yeast metabolism, it is not likely that it will itself be metabolizable.

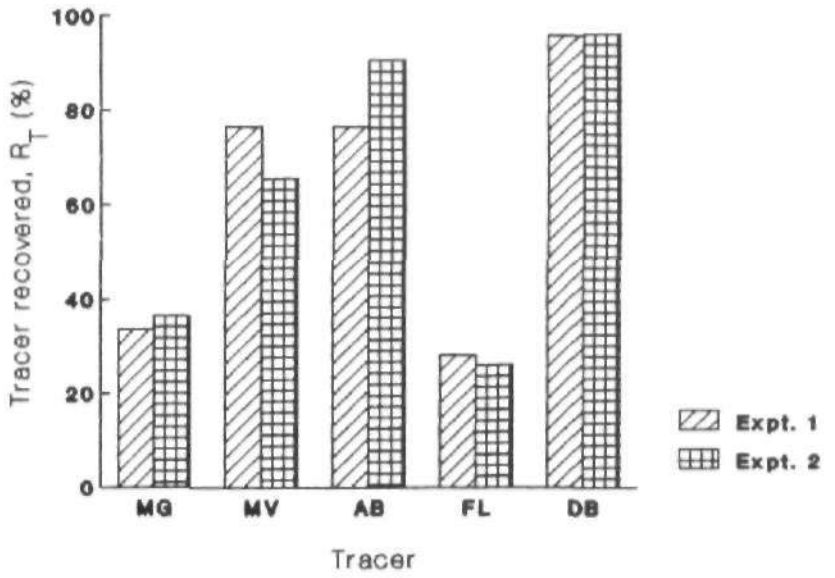


Fig. 5.6: Recovery of tracers in shake flasks

In fact on visual observation, in flasks containing methyl green and methyl violet, the yeast cells were noted to be intensely coloured, whereas only slight colouration was observed in the other flasks.

The small loss of dextran blue and aniline blue could be attributed to adsorption also, since fermentation activities in the presence of these tracers could well be compared to those of the control. Most surprising was the behaviour of the fluorescein tracer. Since fermentation activities proceeded virtually unhindered in the presence of fluorescein, the loss of about 73% of this tracer cannot be attibuted to adsorption only, though that was also noticed. This relatively large loss of fluorescein was found to be due to the drop in pH which occured during the fermentation.

5.2.4.1 *pH effects*

Optical density measurements of a fixed concentration

of fluorescein were found to fall significantly with a drop in pH as shown in Table 5.3. Thus, a pH drop from 5.32 to 3.59, decreased OD measurements by about 50%.

However, increasing the pH by the addition of sodium hydroxide solution caused an increase in the OD_{490} measurement; and bringing the pH back to its former value was noted to give reproducible OD_{490} reading for a pH of 4.29, but for a pH of 6.69, the OD_{490} reading was noted to be higher and not reproducible. These results are shown in Table 5.4 and indicated that fluorescein concentration is a function of both OD_{490} and pH. Consequently, a calibration curve was prepared by reading the OD_{490} at varying pH for fixed fluorescein concentrations.

Table 5.3 pH effect on fluoreescein OD_{490}

pH	Optical density, OD_{490}
2.7	0.253
3.05	0.264
3.59	0.292
4.19	0.359
4.7	0.427
5.32	0.520

The resulting graphs are shown in appendix C. Using multiple regression analysis, the data was found to fit equation 5.1 with a correlation coefficient of 93.6%.

$$C_{f1} = \begin{matrix} 0.0221 - 0.00549pH + 0.0435OD + 0.000217pH^2 \\ - 0.0595OD^2 + 0.0296OD^3 + 0.0016Log_{10}OD \end{matrix} \qquad 5.1)$$

Considering only the linear portions, shown in fiqure 5.7, a new correlation, for calculating fluorescein concentration, in the pH range of 5.3 to 4.7, was obtained

(Eqn. 4.7). This new relationship fitted the data with a correlation coefficient of 98.7% and was subsequently used for the calculation of fluorescein concentration.

Table 5.4 Reproducibility of optical density for fluorescein

pH	Optical density, OD_{490}
6.69	0.521
3.74	0.100
4.96	0.234
6.69	0.631
4.96	0.235

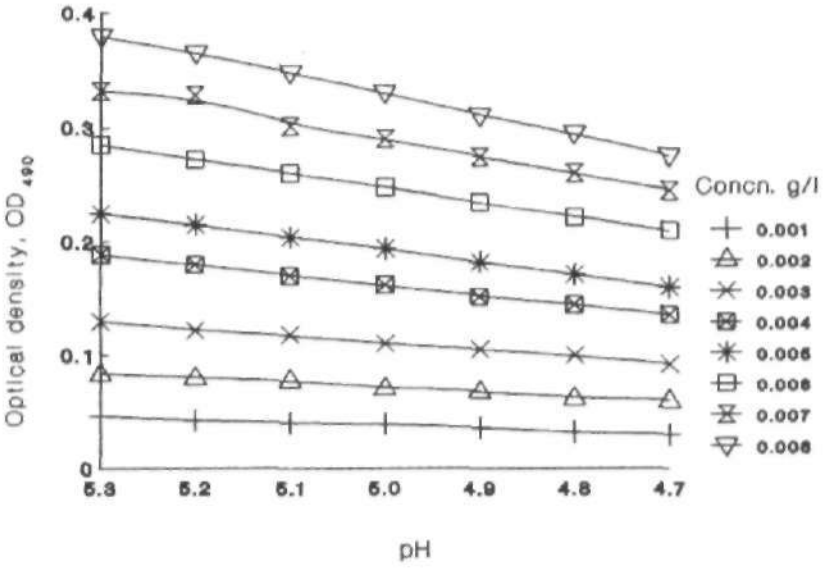


Fig. 5.7: Calibration for fluorescein concentration

The OD_{625} of a solution of dextran blue was also noted to be slightly affected by pH. A pH decrease from 6.54 to 3.82 was found to cause OD_{625} to decrease from 0.291 to

0.258 which represented an 11.3% reduction in concentration. Unlike fluorescein, increasing pH by the addition of NaOH did not increase the OD_{625} as shown in Table 5.5. This indicated that the loss of OD_{625}, due to fall in pH, was not recoverable.

The pH was found to have a slight increasing effect on the optical density of aniline blue because a drop in pH from 7.24 to 2.47 did change the OD_{600}, of a fixed concentration of aniline blue, from 0.601 to 0.792. The effect of pH on the optical density of methyl violet and methyl green solutions was not investigated, because these tracers were found to have a significant effect on the yeast metabolism and were also adsorbed on the surfaces of the yeast cells.

Table 5.5 pH effect on OD_{625} reading for dextran blue

pH	Optical density, OD_{625}
6.54	0.291
4.06	0.267
3.82	0.258
10.60	0.255
10.34	0.255
6.91	0.250
4.05	0.242
3.77	0.230
10.55	0.220
4.05	0.209

5.2.4.2 *Conclusion*

Preliminary fermentation studies have shown that methyl violet and methyl green are not suitable tracers

for RTD experiments in systems involving fermentation of glucose with *S. cerevisiae* because these materials affect the yeast metabolism; methyl violet repressed it while methyl green was found to promote it. Moreover, these tracers were poorly recovered and were adsorbed on the surfaces of cells and glass walls. But, aniline blue, dextran blue and fluorescein may be suitable, though, this depends on the pH; for constant pH, fluorescein may be most suitable, otherwise aniline blue, may be the best choice. Dextran blue has the advantage of high recovery, but its high minimum detectable concentration coupled with its high cost (Table 4.1) makes it the least viable option.

5.2.5 Effects of tracer materials on yeast metabolism during anaerobic batch fermentation

Anaerobic batch fermentations were performed in order to investigate further the effects of tracer materials at conditions similar to those at which the RTD study would be carried out. Three tracers, dextran blue, fluorescein and aniline blue were chosen because of their favourable performance during the shake flask experiments. The fermentations in the presence of these tracers were compared with a control. Changes in tracer concentrations, during the fermentation, were monitored.

Figure 5.8 showed the trend of ethanol production during the batch fermentations. There was remarkable similarity in the lag time, of about 3 hrs, for the control, dextran blue and fluorescein. But, with aniline blue, ethanol production proceeded without any lag time. However, residual glucose and biomass concentrations shown in figures 5.9 and 5.10 respectively, did not indicate this difference in lag time. There may, therefore, be no serious basis for discreminating against any of these three tracers, with respect to their effects on yeast metabolism alone.

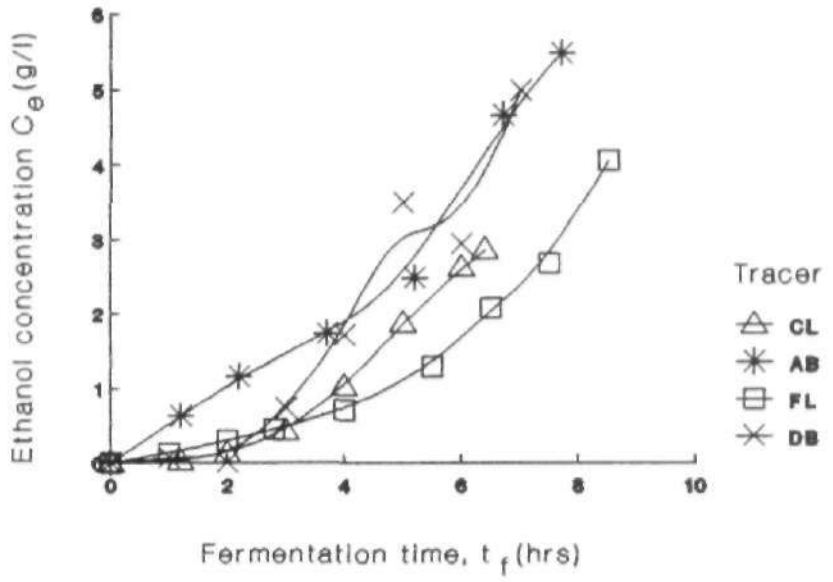


Fig. 5.8: Ethanol production in anaerobic batch fermentation

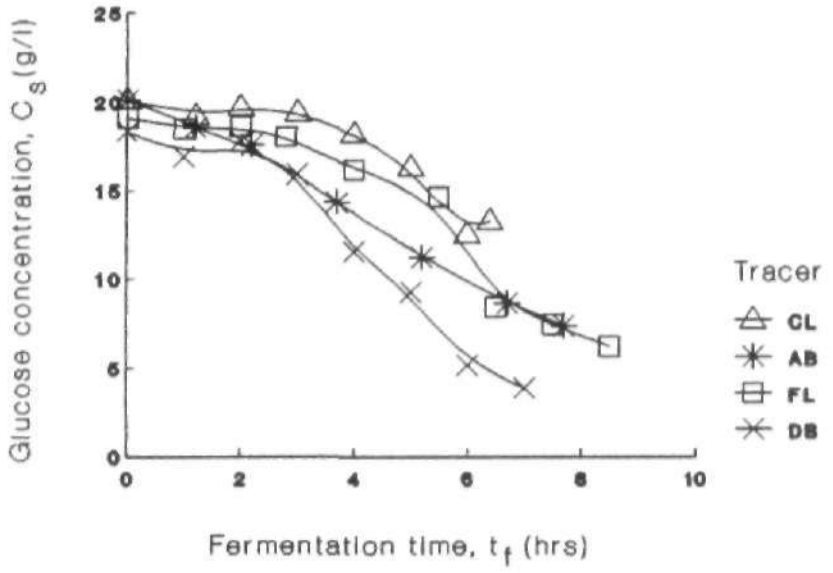


Fig. 5.9: Glucose concentration in anaerobic batch fermentation

(CL = Control, AB = Aniline blue, FL = Fluorescein, DB = Dextran blue)

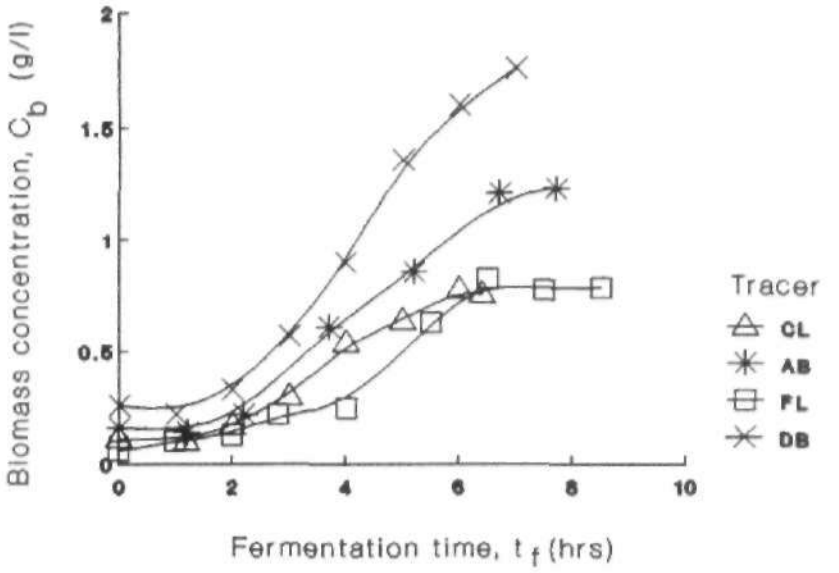


Fig. 5.10: Biomass production in anaerobic batch fermentation

Tracer concentrations, in the fermentation systems, are shown in figures 5.11, for dextran blue, and 5.12, for both aniline blue and fluorescein. The concentration of dextran blue was independent of time within the 8 hrs of fermentation. This confirmed the results obtained for dextran blue in the shake flask fermentations and also showed that adsorption of dextran blue was not significant.

Similarly, pH changes form 6.18 to 4.19, which occured during the fermentation, had no significant effect on the measured concentration of dextran blue. The apparent concentration of aniline blue remained constant for about three hours, after which, decrease was noticed. After eight hours, about 56% of the aniline blue was lost. The reason for this loss was not known, though it could be due to high ethanol concentration, because changes in pH do not have significant effect on the concentration of this tracer. The effect of ethanol concentration was, however, not investigated. When the effect of pH was taken

into consideration and equation 4.7 was used to calculate fluorescein concentration, no significant change was noticed for fluorescein during the entire period of fermentation.

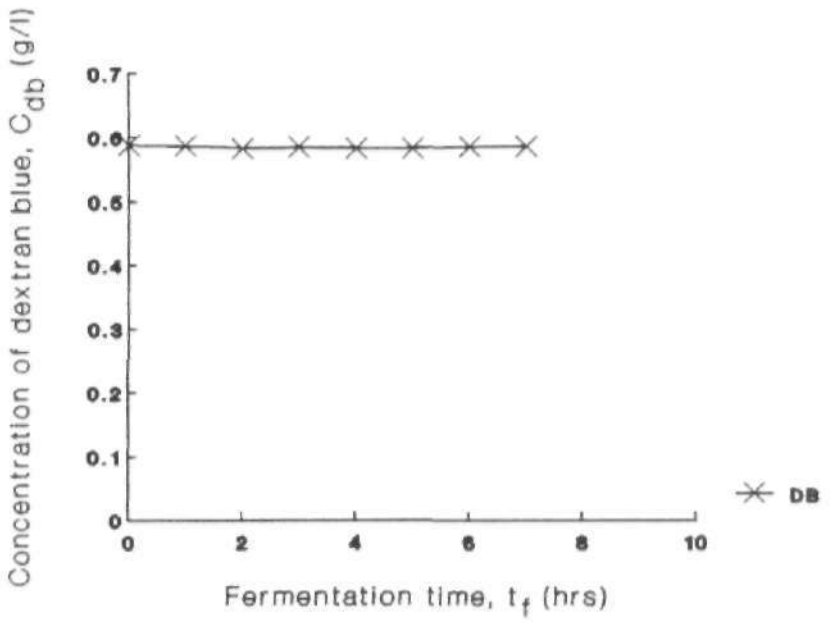


Fig. 5.11: Recovery of dextran blue during anaerobic batch fermentation

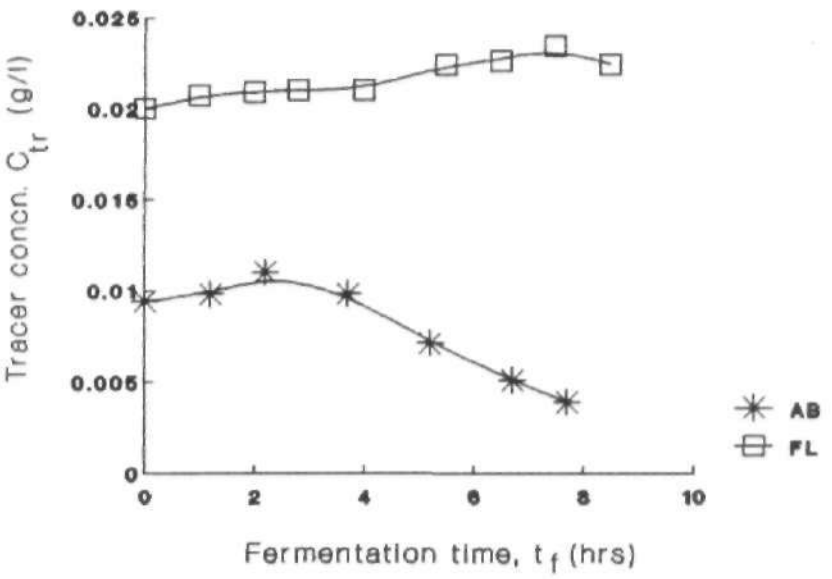


Fig. 5.12: Recovery of aniline blue and fluorescein

In conclusion, therefore, dextran blue and fluorescein are the best, but when the cost of these materials is taken into concentration, fluorescein becomes the obvious choice, because it is about 98 times less costly than dextran blue (Table 4.1). Moreover, the minimum detectable concentration of fluorescein is about 97 times lower than that of dextran blue. However, the final choice can only be possible after using these tracers in the continuous flow column bioreactor containing fluidizing flocs of yeast.

5.2.6 Tracer choice in continuous column operation

To further test the suitability of the fluorescein tracer, a known volume of a solution of fluorescein was injected into an operating column bioreactor containing flocs of yeast strain Y6. Several experiments were performed with different concentrations of fluorescein and volumes of injection, in order to find if the volume injected or the concentration of fluorescein used had any effect on the nature of the RTD curve. The Peclet number Pe', and liquid holdup ε_L, were also evaluated and compared with that obtained from similar experiments with dextran blue. Total tracer recovery was assessed while the residence times were calculated from the RTD curves and used for comparison.

In separate experiments, 0.2 ml and 1.5 ml of a 25 g/l fluorescein solution were injected into the column when liquid velocities were 0.0351 cm/s and 0.0084 cm/s respectively, representing the upper and lower limits of liquid velocities to be used in dispersion experiments. The RTD curves obtained are presented in form of E curves in figures 5.13 and 5.14 respectively. It is clear from these response curves that something was interfering with the flow of fluorescein solution in the column, because the points in the curve are dispersed and there was no peak which is a characteristic of pulse injections in

tubular flow systems.

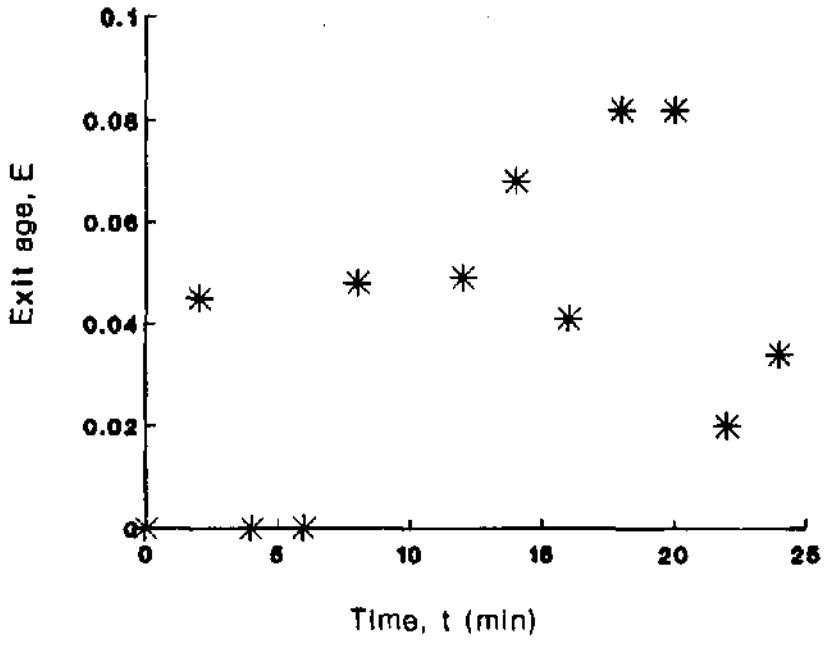


Fig. 5.13: E curve for 0.2 ml of 25 g/l fluorescein at liquid superficial velocity of 0.0351 cm/s

With higher concentration of fluorescein, a greater spread was observed. This observation may be due to tracer diffusion into the biomass and its subsequent desorption. Fluorescein with its small molecular weight may have been absorbed by the yeast cells when its concentration in the liquid was high. But as the concentration in the liquid becomes low, desorption takes place and fluorescein appeared at the monitoring point, resulting in a long tail.

On the other hand, with dextran blue, the behaviour was different even at the same liquid velocities. As shown in figures 5.15 and 5.16, there was a sharp peak in the RTD curves and this was characteristics of pulse inputs in tubular flow systems. Moreover, the tailing was absent, suggesting that the high molecular weight of dextran blue could have prevented absorption of this tracer into the yeast cells.

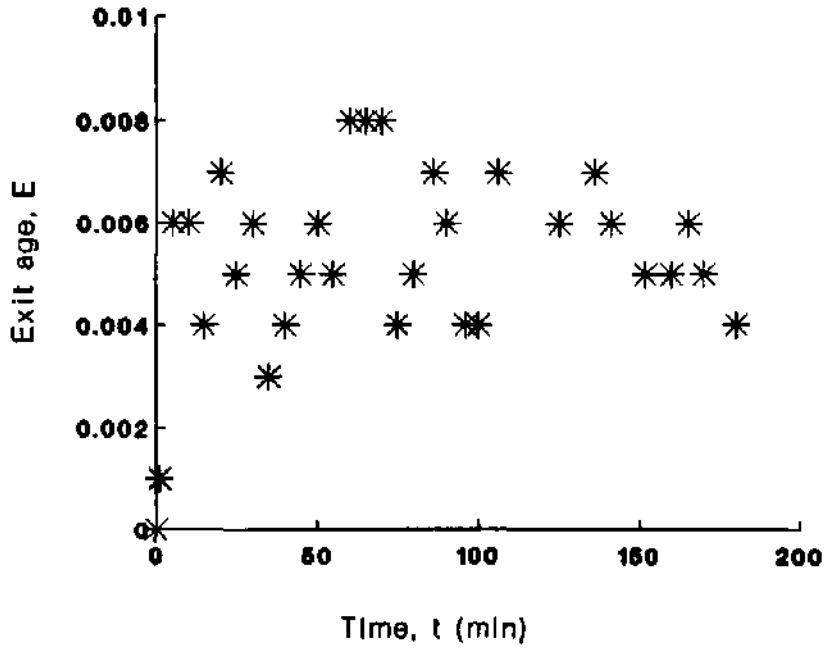


Fig. 5.14: E curve for 1.5 ml of 25 g/l fluorescein at liquid superficial velocity of 0.0084 cm/s

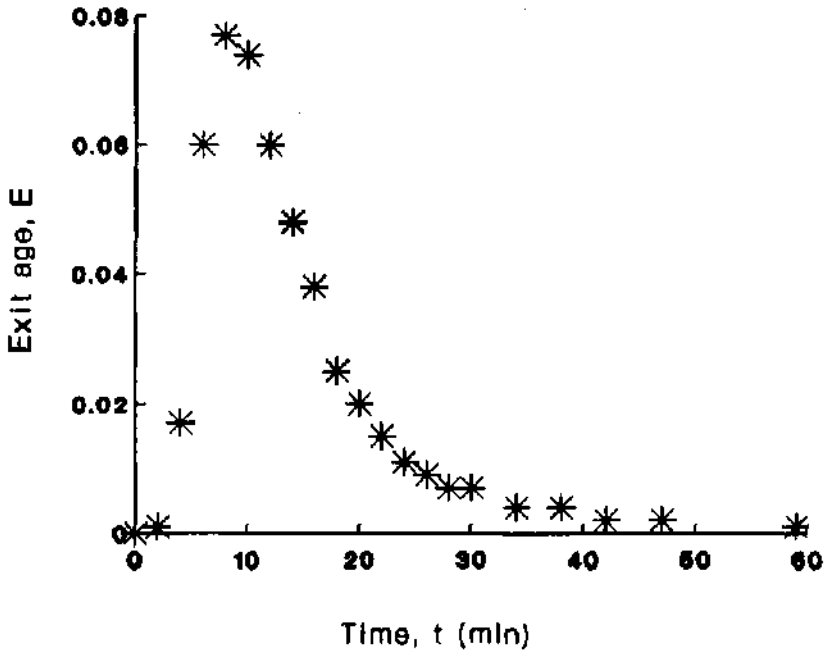


Fig. 5.15: E curve for 4 ml of 10 g/l dextran blue at liquid superficial velocity of 0.0351 cm/s

It was, therefore, not surprising that the residence times obtained using dextran blue appeared more reasonable compared to those obtained using fluorescein as shown in Table 5.6.

Table 5.6 Tracer performance in column bioreactor

Tracer	Liquid vel., u_L (cm/s)	Tracer recovd. R_T (%)	Res. time, τ_c(min)	Peclet No. $Pe' = u_L H/\varepsilon_L D_z$	$\varepsilon_L = \tau_c/\tau_\theta$
FL	0.0084	2.7	95.30	0.102	0.586
	0.0351	9.7	15.37	0.055	0.395
DB	0.0084	64.6	25.88	0.132	0.159
	0.0351	69.6	16.62	0.286	0.427
	0.0263	81.8	14.51	0.312	0.280
	0.0175	85.5	15.72	0.360	0.202

(FL = Fluorescein, DB = Dextran blue)

Comparison of the values of liquid hold up (ε_L), calculated as the ratio of residence time obtained from the RTD curve to the residence time of the empty column, at the same height, showed that with fluorescein ε_L was higher at lower liquid velocity, which was not expected. But with dextran blue, there appeared to be an increase in the liquid holdup due to increase in liquid velocity, which was expected. These differences in liquid holdup may have been responsible for the observed differences in Peclet numbers obtained with these tracers, at the same liquid velocities of 0.0351 and 0.0084 cm/s. The residence times were the times taken for the tracer to travel from the point of injection to the monitoring point, 82 cm apart.

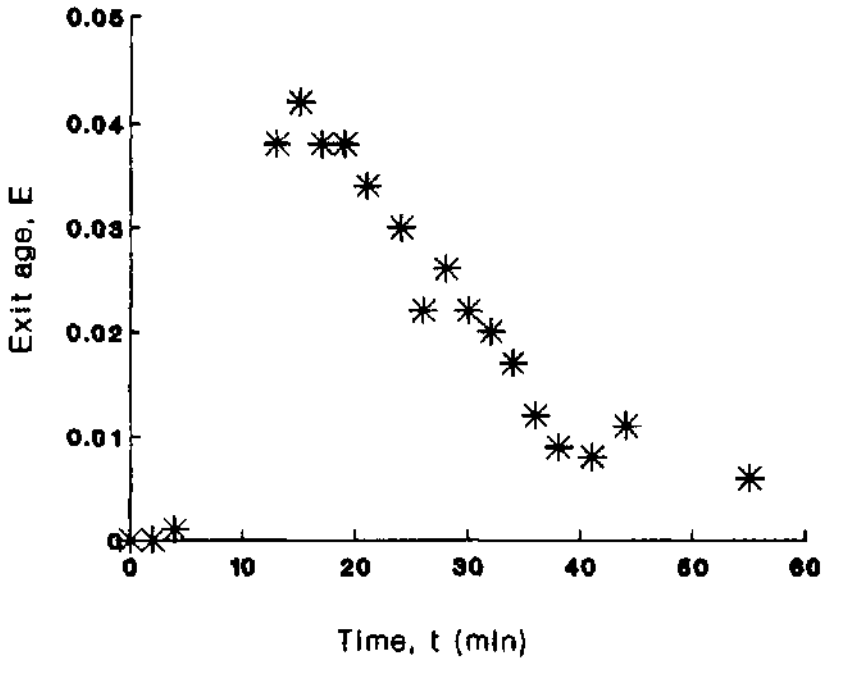


Fig. 5.16: E curve for 2 ml of 22.2 g/l dextran blue at liq. superficial velocity of 0.0351 cm/s

The holding back of fluorescein which occured due to absorption also results in poor tracer recovery. Only a fraction of what was injected, was recovered; 9.7% and 2.7% for liquid velocities of 0.0351 and 0.0084 cm/s, respectively. But about 70% of dextran blue, injected, was recovered (Table 5.6). This indicated that very little absorption of this tracer took place, owing perhaps to its high molecular weight of 2,000,000.

To further confirm the results obtained with dextran blue, more experiments were performed at two other liquid velocities of 0.0263 and 0.0175 cm/s. The RTD curves obtained are presented in figures 5.17 and 5.18 for liquid velocities of 0.0263 and 0.0175 cm/s respectively. Again, it bacame clear that with dextran blue, very good response curves were obtained. Furthermore, the recovery of this tracer was higher than 70% in most of the cases.

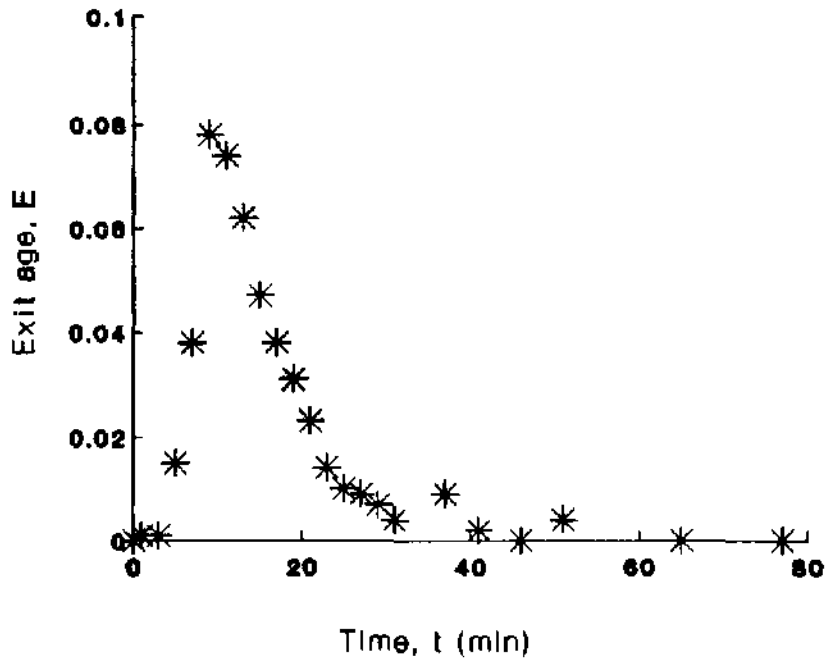


Fig. 5.17: E curve for 2 ml of 22.2 g/l dextran blue at liq. superficial velocity of 0.0263 cm/s

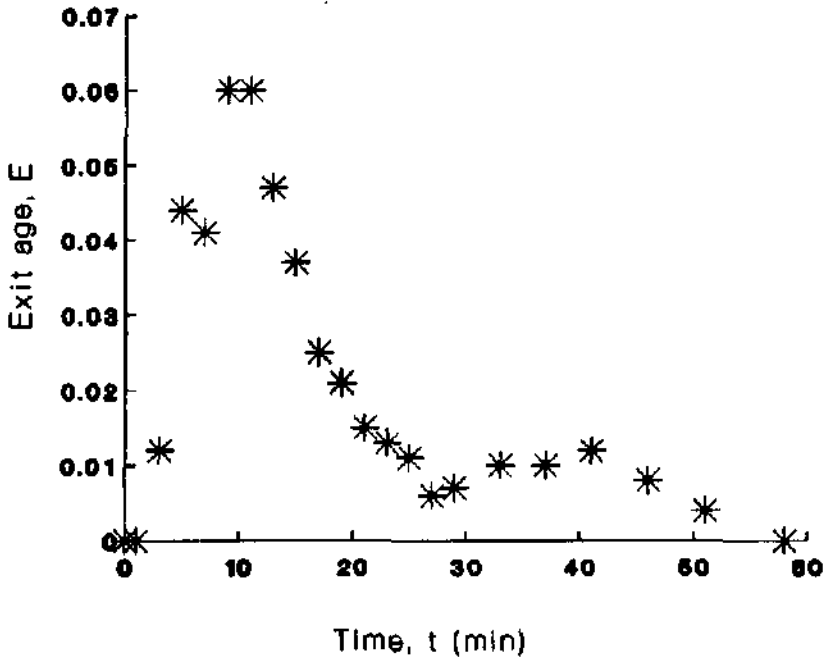


Fig. 5.18: E curve for 2 ml of 22.2 g/l dextran blue at liq. superficial velocity of 0.0175 cm/s

An attempt was made to use fluorescein as a step input. Two experiments were conducted with 0.25 and 0.005 g/l fluorescein solutions. As shown in fiqures 5.19 and 5.20, data points in the F curves obtained were scattered and only a small fraction of the tracer was recovered; 12.7% and 38.3% respectively. In fact, it was noted that traces of fluorescein did remain in the column even after flushing with fresh liquid medium for two days. But, with dextran blue, none was left few hours after injection.

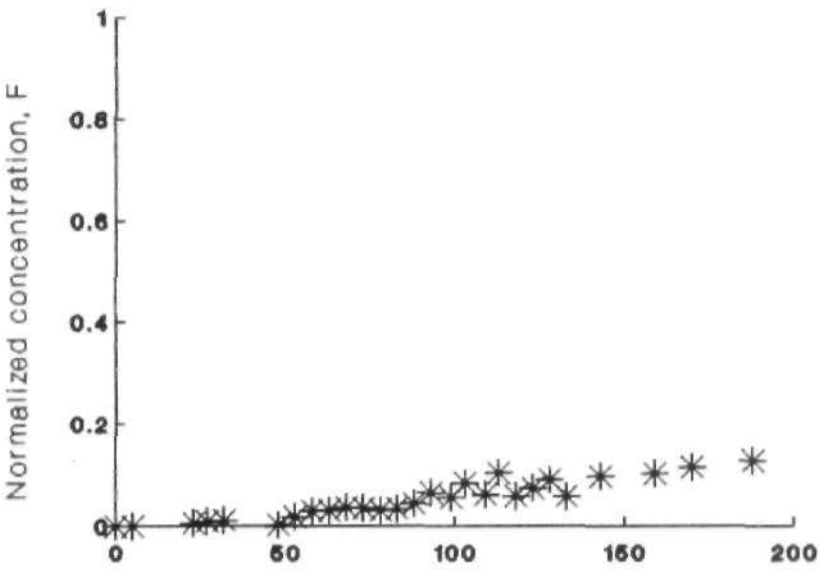


Fig. 5.19: F curve for 0.25 g/l fluorescein at liq. *superficial velocity of 0.0084 cm/s*

In conclusion, therefore, fluorescein can be said to be a poor tracer for use, either as pulse or step input, in column bioreactors containing flocculant yeast strains because it is absorbed by the biomass and is poorly recovered. Hence the RTD curves obtained have scattered points and long tails. Therefore, the use of dispersed flow model may not be appropriate for this tracer. Incorporation of the diffusion term in the dispersed flow model will complicate the mathematics.

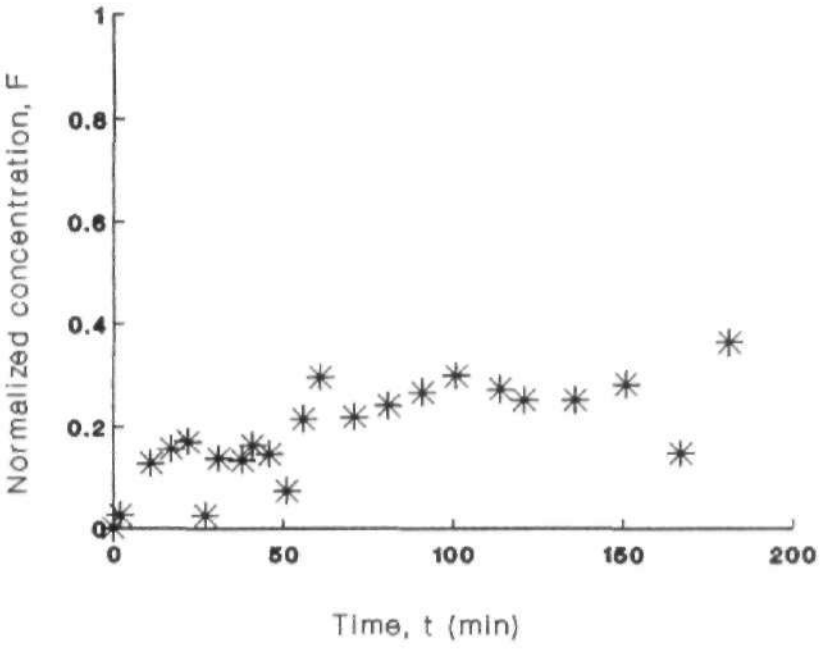


Fig. 5.20: F curve for 0.005 g/l fluorescein at liq. superficial velocity of 0.0351 cm/s

Dextran blue, on the other hand, gave good RTD curves, showed no tailing and was very well recovered. This indicated that the tracer was not absorbed by biomass and dextran blue was, therefore, the best choice for use as tracer in column bioreactors containing flocculant yeast strains. A similar conclusion was reached by Jimenez *et al.* (1988) with respect to dextran blue. They observed that dextran blue was a suitable tracer for submerged biofilter systems, for it was neither adsorbed nor absorbed and its recovery was over 90%. Dextran blue was, therefore, choosen as a tracer for all RTD determinations in this work.

5.3 PERFORMANCE OF FLUIDIZED BED ANAEROBIC FERMENTER

The performance of the fermenter was studied in order to ascertain that it was properly active and comparable with literature fermenters of the same type. In addition, the rates of gas production and superficial gas velocities were obtained from the performance study. Two strains of yeast, Y6 and NCYC 1026, were used. The choice of strain Y6 was made against four others, because preliminary investigation in shake flasks indicated that it produced smaller flocs having Sauter mean diameter of 0.487 mm with a standard deviation of 0.121. The sizes of the other strains are given in appendix A. NCYC 1026 was chosen based on literature information that it produced flocs, in tower fermenter, of average diameter of about 0.1 cm (Smith and Greenshields, 1973).

Four liquid flow rates of 5.75, 12, 18 and 24 ml/min were employed. With strain Y6, inlet glucose concentration was 50 g/l, though a run was performed with 100 g/l at liquid flow of 18 ml/min. But, with the strain NCYC 1026, three inlet glucose concentrations of 30, 50 and 70 g/l were used.

The performance of the fermenter was evaluated with respect to the effects of inlet glucose concentration and liquid flow rate on other fermentation parameters including ethanol concentration, productivity and gas production. The results obtained are presented and discussed in this section. However, the trends of the fermentation runs conducted and the general observations made, are presented first.

For the purpose of calculating fermentation parameters, the column exit referred to the end of the uniform diameter column, which was at a point 197 cm from the inlet, whereas effluent or outlet referred to the liquid stream going out of the reactor, after passing through the separator. Ethanol concentration values at points immediately above the fluidized bed level together

with the measured fluidized bed heights and the liquid holdups, obtained from the RTD study, were used to calculate ethanol productivities, based on liquid volume (P). The same concentration values were also used to calculate reactor productivity, based on empty column (P'). The fluidized bed heights and values of the liquid holdups are given in Tables 5.7 and 5.8 respectively, for all the fermentation runs performed.

Table 5.7 Fluidized bed height (cm)

Inlet glucose, C_{si} (g/l)	Liquid flow rate, f_L			
	5.75 (ml/min)	12 (ml/min)	18 (ml/min)	24 (ml/min)
30	70	69	71	74
50	50	49	55	59
70	87	88	81	84
50 (Y6)	109	124	127	129

Table 5.8 Liquid holdup (ε_L)

Inlet glucose, C_{si} (g/l)	Liquid flow rate, f_L			
	5.75 (ml/min)	12 (ml/min)	18 (ml/min)	24 (ml/min)
30	0.1708	0.1541	0.2343	0.2425
50	0.1575	0.1964	0.2232	0.2113
70	0.1112	0.1738	0.2102	0.2443
50 (Y6)	0.1591	0.2013	0.2792	0.4268

5.3.1 Trends and general observations

In all the fermentation runs, it was noted that there were gradual changes in glucose and ethanol concentrations

and pH along the column height. The occurance of gradients in these parameters was an indication that liquid phase mixing, within the yeast bed, was not complete otherwise such gradients would not occur. The fermentation with NCYC 1026 performed at 50 g/l inlet glucose concentration and a liquid flow rate of 24 ml/min, is used as an example for the purpose of discussing the observed variations of performance parameters along the column height. The fluidized bed height, at these conditions, was 59 cm.

5.3.1.1 *Trends in pH*

Figure 5.21 showed the trend in pH. It can be seen that the pH dropped from a value of 5.99, at the column inlet, to 3.93 at the top of the yeast bed and further to 3.84, at the outlet.

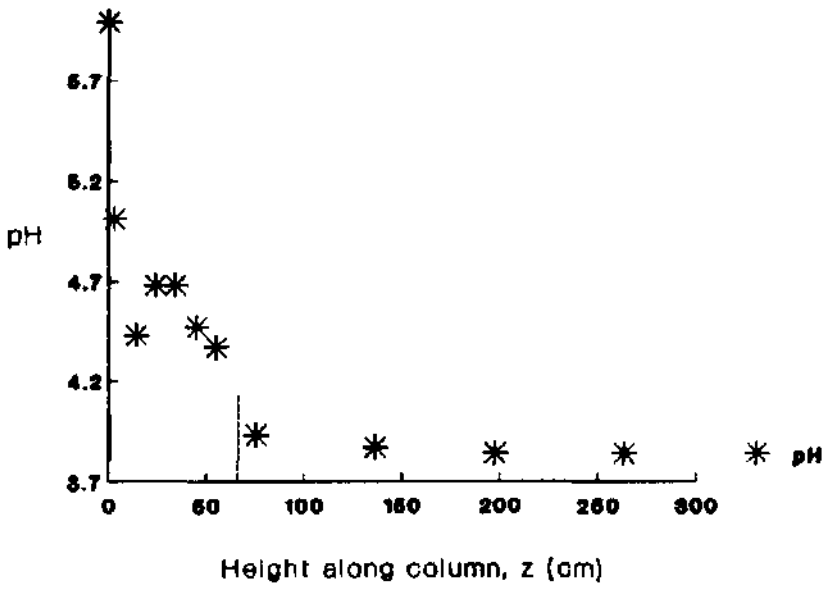


Fig. 5.21: pH profile along column height

This represented a 34.4% drop in pH within the yeast bed and is not unexpected in the anaerobic fermentation of glucose. A similar trend was reported by Jones *et al* (1984). The drop in pH may be because the microorganisms took up PO_4^{-2} ions in the process of their growth, leaving behind H^+ ions that caused the observed drop in pH.

5.3.1.2 *Glucose concentration*

Glucose concentration also dropped in a similar manner, as the pH, as shown in figure 5.22.

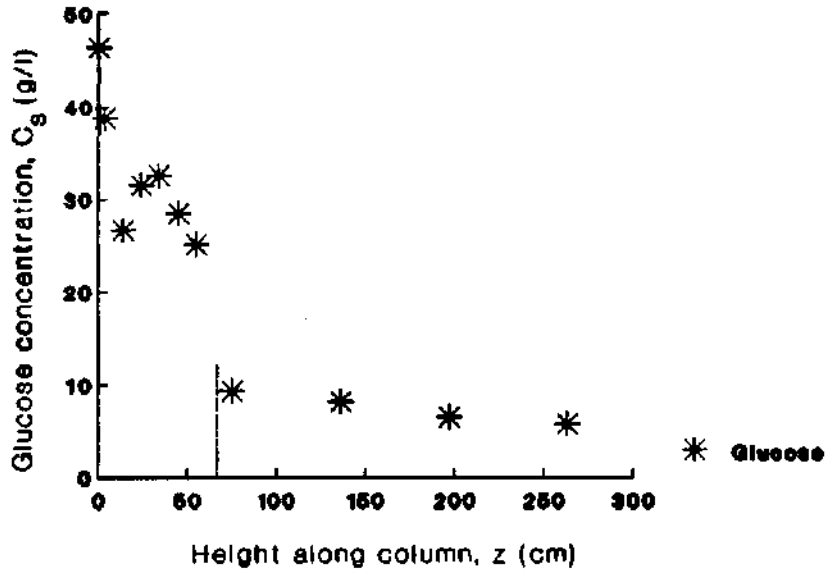


Fig. 5.22 Profile of glucose concentration along column height

The drop was from an inlet concentration of 46.4 g/l to 9.33 g/l at top of the bed and further to an outlet concentration of 5.8 g/l. This corresponds to glucose consumption of about 37.1 g/l within the bed. Such a drop in glucose concentration was expected and indicated a good level of microbial activity. Further, it confirmed that the drop in pH was as a result of the metabolic activity of the yeast.

Glucose concentrations, at points immediately above the bed, were noted to be low as shown in Table 5.9, though the actual values depended on the liquid flow rate and inlet glucose concentration used. In all the fermentation runs, glucose consumption was over 80%, except at the liquid flow rate of 24 ml/min and inlet glucose concentration of 70 g/l, where glucose consumption was about 76%.

Table 5.9 Glucose concentration at top of bed

Inlet glucose, C_{si} (g/l)	Liquid flow rate, f_L			
	5.75 (ml/min)	12 (ml/min)	18 (ml/min)	24 (ml/min)
30	0.14	1.37	5.06	2.88
50	1.11	2.42	5.69	9.33
70	1.04	2.34	7.44	17.61
50 (Y6)	0.22	2.59	2.47	8.06

5.3.1.3 *Ethanol concentration*

Ethanol concentration increased along the column height, as expected. The increase was from 2.2 g/l at a point 3 cm above the column inlet, to a value of 13.6 g/l above the yeast bed and further to 17.7 g/l, at the outlet. Based on the glucose consumption, an ethanol yield of 0.368, representing 72.2% of the theoretical yield, was obtained above the bed. Similar trends in ethanol concentration and yield value were reported by Prince and Barford (1982a) and Jones *et al.* (1984).

It was noted that the increase in ethanol concentration was much more pronounced at the liquid-solid interface. This was indicated by a sharp increase in ethanol concentration immediately above the 59 cm yeast bed, as shown in figure 5.23. Similar observations were made in all the fermentation runs conducted. It is interesting to note that the sharp increase in ethanol concentration at the top of the bed was accompanied by sharp drop in glucose concentration at the same point. The high surface area available for liquid-solid contact and the relatively smaller flocs at the top of the yeast bed were probably responsible for the observed sharp increase in ethanol concentration at this point. This pointed to an increased metabolic activity at the top of the yeast bed.

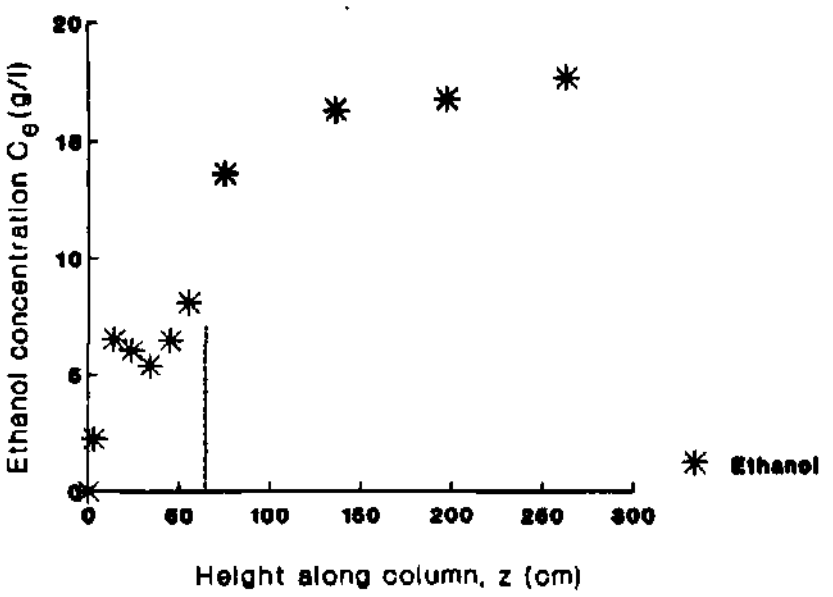


Fig. 5.23 Profile of ethanol concentration along column height

Also very little ethanol was produced above the yeast bed, suggesting that there was, virtually, no metabolic activity above the bed, as was expected, since biomass concentration above the bed was very small.

Ethanol concentrations, above the bed, were all of the same order of magnitude, as shown in Table 5.10.

Table 5.10 Ethanol concentration at top of bed

Inlet glucose, C_{si} (g/l)	Liquid flow rate, f_l			
	5.75 (ml/min)	12 (ml/min)	18 (ml/min)	24 (ml/min)
30	11.36	11.28	9.18	14.06
50	18.82	17.65	17.93	13.63
70	30.27	31.58	23.90	13.39
50 (Y6)	25.38	24.82	24.54	20.04

But, there were some variations depending on the inlet glucose concentration and the liquid flow rate employed.

5.3.1.4 *Ethanol yield*

The ethanol yield also varied with column height, as shown in figure 5.24.

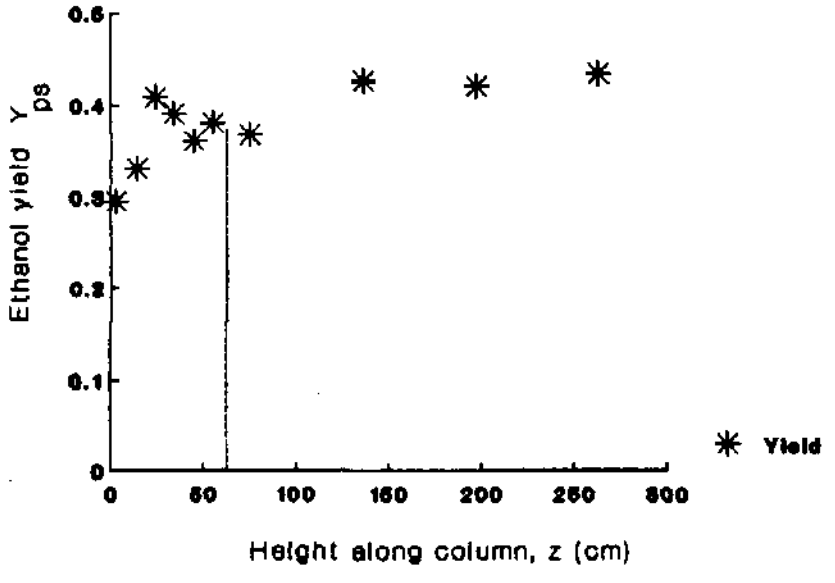


Fig. 5.24 Profile of ethanol yield along column height

Ethanol yield was 0.295 at 3 cm above column inlet, 0.368 above the bed and 0.435 at the outlet. The trend indicated that yield increased with increase in column height. Similar observation was reported by Jones *et al.* (1984). The yield values obtained, at the top of the bed, are presented in Table 5.11 and it can be agreed that there was generally high yield, except at high liquid flow rate and high inlet glucose concentration. The low yield at these conditions was probably the effect of low hydraulic retention time.

Table 5.11 Ethanol yield at top of bed

Inlet glucose, C_{si} (g/l)	Liquid flow rate, f_L			
	5.75 (ml/min)	12 (ml/min)	18 (ml/min)	24 (ml/min)
30	0.348	0.452	0.431	0.470
50	0.354	0.340	0.441	0.368
70	0.441	0.457	0.373	0.246
50 (Y6)	0.489	0.498	0.491	0.490

5.3.1.5 *Gas production*

Carbon dioxide gas production was calculated from the ethanol concentrations. Only few measurements of gas production were made with a carbon dioxide flow meter, because the meter arrived late. Some of these measurements were noted to be lower than the calculated gas flow rates, due perhaps to the dissolution of carbon dioxide by the incoming liquid. The measured values of gas flow rate are given in appendix A.

As shown in figure 5.25, gas production increased along the reactor height due to increased metabolic activity. The increase was from 23.2 ml/min, at a point 3 cm above the column inlet, to 149.5 ml/min immediately above the bed and 229.1 ml/min, at the outlet.

It was noted that gas production took place, almost entirely, within the yeast bed, though a steady increase to the reactor outlet, due to static pressure, could be noticed. There was a remarkable difference in gas production at the bottom and top of the yeast bed; it was about zero at the bottom and about 149.5 ml/min at the bed top. These gas flows corresponded to superficial gas velocities of zero at the bottom and 0.219 cm/s at the top. These imposed variations in superficial gas velocity, along the column height, could consequently cause axial variations in the liquid mixing coefficient (D_z).

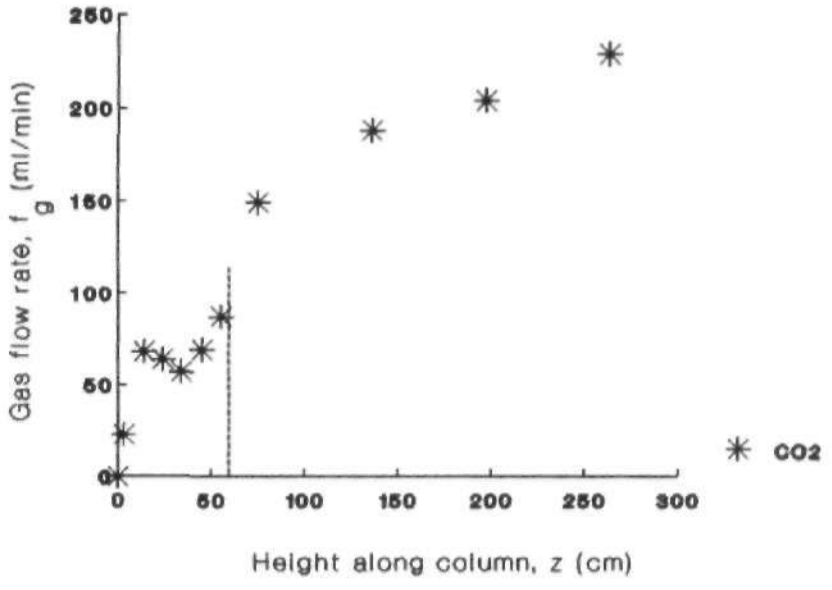


fig. 5.25 Gas production along column height

Significant differences in gas production, between the bottom and the top of the yeast bed, were manifested in all the fermentation runs performed; these are shown in Table 5.12.

Table 5.12 The difference in gas flow rates between the bottom and top of yeast bed (ml/min)

Inlet glucose, C_{si} (g/l)	Liquid flow rate, f_l			
	5.75 (ml/min)	12 (ml/min)	18 (ml/min)	24 (ml/min)
30	29.85	61.82	75.47	154.18
50	48.65	95.22	145.06	149.49
70	82.49	174.58	198.15	148.07
50 (Y6)	68.34	142.01	210.57	251.97

It can be seen that the differences are significant and of the same order of magnitude as the above, even at the lowest inlet glucose concentration of 30 g/l, where it

translated to a difference of about 0.20 cm/s in superficial gas velocity, at liquid flow rate of 24 ml/min. Both Gommers *et al.* (1986) and Setiadi (1989) have noted that such a value of gas flow rate could have significant influence on the liquid axial mixing coefficient. This case will be further discussed in section 5.4.4.

5.3.1.6 *Ethanol productivity*

Ethanol productivity, based on an empty column, P' showed a sharp drop along the reactor height (Fig. 5.26).

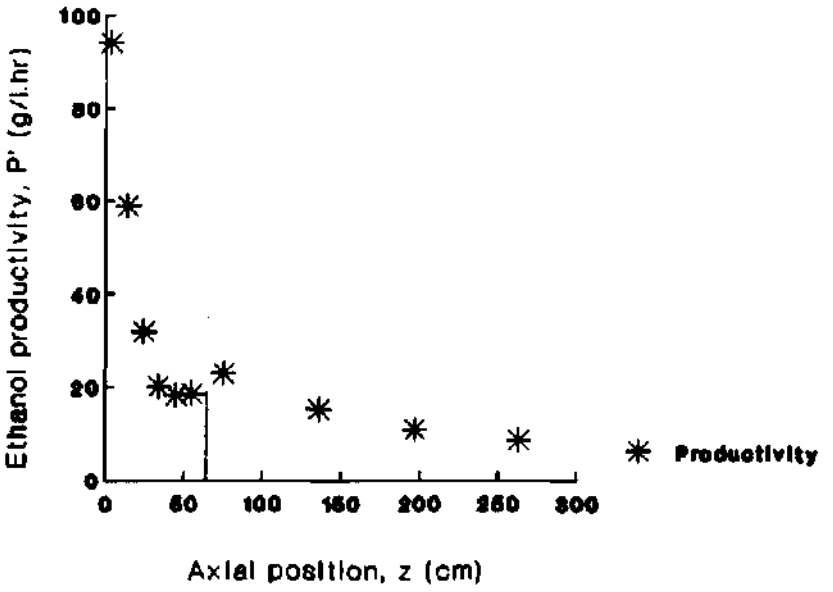


Fig. 5.26 Ethanol productivity along column height

A value of 94.15 g/(l.hr) was obtained at a point 3 cm above the column inlet and 22.96 g/(l.hr) above the bed, while at the outlet, the productivity dropped to a value of 8.49 g/(l.hr). A similar trend was observed by Admassu *et al.* (1985) in their tower fermenter where the productivity, based on liquid volume, was reported to have dropped gradually from a value of 80 g/l.hr at 10 cm, above the column inlet, to about 23 g/l.hr at a height of 70 cm.

The ethanol productivities, based on the empty column, obtained, at points immediately above the bed, are shown in Table 5.13 for all the fermentation runs. Like other fermentation parameters, this one was also influenced by the inlet glucose concentration and liquid flow rate. It is interesting to note that these productivity values compare very well to literature values as shown in Table 5.14. The relatively higher values obtained in this work were due to the higher liquid throughput used.

Table 5.13 Ethanol productivity (empty column)

Inlet glucose, C_{si} (g/l)	Liquid flow rate, f_l			
	5.75 (ml/min)	12 (ml/min)	18 (ml/min)	24 (ml/min)
30	4.58	9.50	11.59	23.68
50	10.36	20.27	30.88	22.96
70	10.78	23.47	26.64	19.90
50 (Y6)	7.32	12.44	18.45	18.62

Ethanol productivity, based on liquid volume, shows similar dependence on liquid flow rate and inlet glucose concentration, as shown in Table 5.15. The highest productivity obtained was 138.37 g/l.hr while the lowest productivity was 28.76 g/l.hr. These high productivity values were as a result of the high biomass concentration in the bioreactor. High ethanol productivities in fluidized bed bioreactors are common. Values of 80 and 23 g/l.hr were reported by Admassu *et al.* (1985). Other bioreactor types, utilizing immobilized microorganisms, were also reported to give high ethanol productivities as well. For example, productivity values of 53.8, and 49.6 g/l.hr were reported by Williams and Munnecke (1981) and

Lee *et al.* (1983), respectively, for yeast packed beds.

Table 5.14 Comparison of the productivity of bioreactors

Inlet glucose, C_{si} (g/l)	Residence time, τ (hr)	Ethanol yield Y_{ps}	Productivity, P' (g/l.hr)	Reference
30	1.58	0.47	23.7	This work
50	1.58	0.37	23.0	This work
70	1.58	0.27	19.9	This work
180	9.6	0.5	8.6	Jones *et al.* (1984)
130	5.1	0.5	11.7	Jones *et al.* (1984)
120	3.2	0.49	17.8	Prince and Barford (1982a)
152	3.8	0.49	14.3	Prince and Barford (1982a)
180	5.5	0.49	12.2	Prince and Barford (1982a)

Table 5.15 Ethanol productivity (Liquid volume)

Inlet glucose, C_{si} (g/l)	Liquid flow rate, f_l			
	5.75 (ml/min)	12 (ml/min)	18 (ml/min)	24 (ml/min)
30	28.76	76.20	52.23	98.97
50	72.32	115.83	138.37	138.10
70	96.63	113.52	132.98	85.94
50 (Y6)	45.98	62.80	66.08	51.72

Similarly, values of 26 and 40 g/l.hr were also reported by Inloes *et al.* (1983) and Mehaia and Cheryan (1984),

respectively, for hollow fibre fermenters containing immobilized yeast.

5.3.1.7 *Biomass concentration*

Variations in the concentration of biomass along the column height could not be quantified. This was due to the difficulty in sampling the tightly packed and sticky biomass, which had failed to form discrete floc particles.

With strain Y6, attempts were made to break up the seemingly packed yeast bed, by using 100 g/l of inlet glucose concentration, at a liquid flow rate of 18 ml/min, in the hope that increased metabolism might result and cause increased gas production that would eventually break up the bed, as noted by Jones *et al.* (1984). But, it was found that the bed did not break up and that glucose inhibition was manifested in form of decreased yield, ethanol concentration, gas production and ethanol productivity, when compared to the results obtained with a 50 g/l inlet glucose concentration, at the same liquid flow rate (Table 5.16).

Table 5.16 Comparison of fermentation parameters for strain Y6

Inlet glucose, C_{si} (g/l)	Exit EtOH, C_{ee} (g/l)	CO_2 flow rate, f_g (ml/min)	EtOH productivity P' (g/l.hr)	EtOH yield, Y_{ps} (-)
50	25.59	233.77	12.3	0.558
100	20.11	183.71	9.67	0.241
50+3M NaCl	1.05	9.60	0.51	0.055

When this failed, 1M, 2M and 3M NaCl solutions were added to the growth medium in separate runs. With 1M and 2M solutions, the yeast bed remained compacted. However, 3M solution succeeded in decompacting the bed, but severe

loss of activity resulted due to yeast inactivation by the salt solution. When compared with runs made without NaCl solution, severe decrease in productivity, ethanol and gas productions and yield were noticed, as presented in Table 5.16. The inability to break up the bed of strain Y6 and yet maintain its viability, necessitated the change of the strain to NCYC 1026, though that also failed to give discrete floc particles and the problem of measuring biomass concentration remained. Figures 5.27 and 5.28 are presented in order to show how compacted the Y6 and NCYC 1026 beds were. Nonetheless, estimates of biomass concentrations were made when the column was being dismantled. For the Y6 strain, the estimated biomass concentration, on a dry basis, was 63 g/l while it was 48 g/l for strain NCYC 1026. These values of biomass concentration are comparable to the values of 70 and 55 g/l reported by Prince and Barford (1982a) and Jones *et al.* (1984) respectively.

It was interesting to note that little biomass wastage occured in the effluent; at a liquid flow rate of 24 ml/min and inlet glucose concentration of 50 g/l only 0.05 and 1.04 g/l biomass was lost for the Y6 and NCYC 1026 respectively. Biomass concentrations above the bed were, similarly, low as shown in Table 5.17 for the entire set of fermentation runs, even at high liquid flow rates and high inlet glucose concentration. Furthermore, the fluidized bed surface was, distinctly, visible during all the fermentation experiments. This low biomass wastage indicated that in this system, fermentation was not limited by washout of organisms, but by liquid throughput. Thus, both the two strains used were of the flocculant-fermentation limited group which, according to Greenshields and Smith (1971), attain high concentrations and have heavy 'sticky' flocs of up to 1.3 cm in diameter. This probably caused the difficulty in sampling the biomass.



Fig. 5.27 Bed of strain Y6

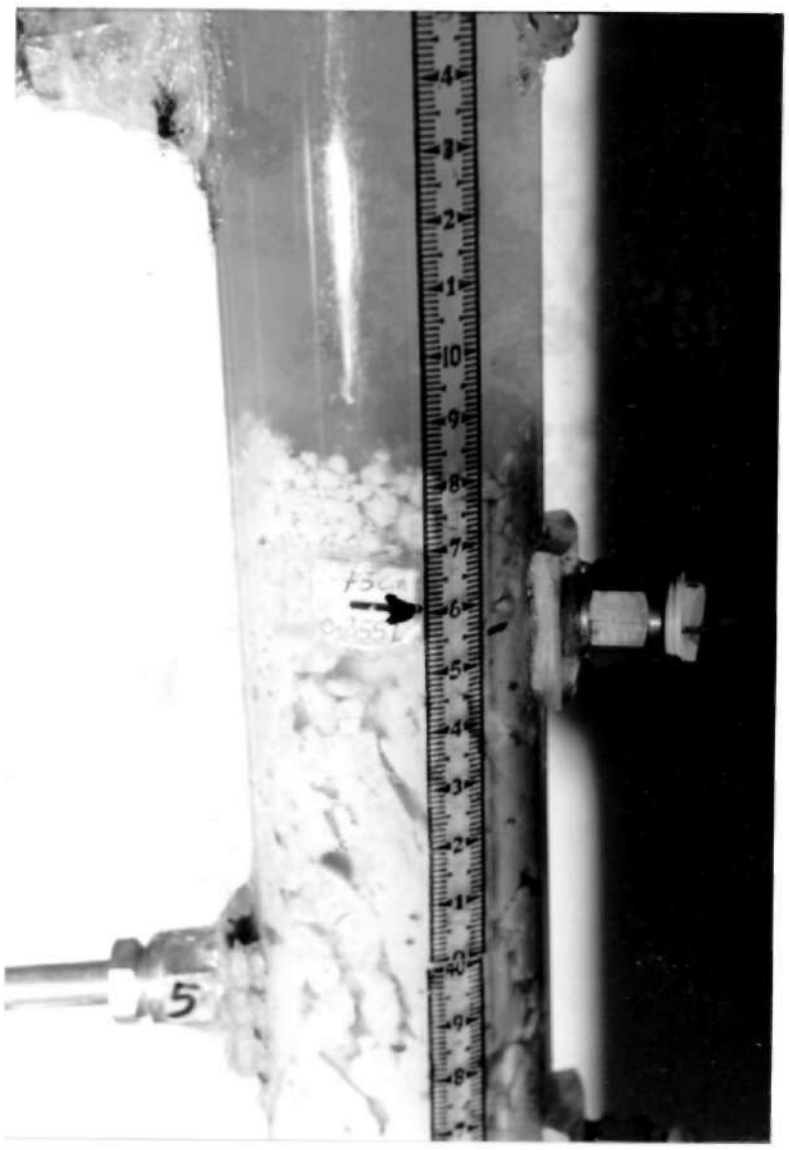


Fig. 5.28 Bed of strain NCYC 1026

Table 5.17 Biomass concentration above bed

Inlet glucose, C_{si} (g/l)	Liquid flow rate, f_L			
	5.75 (ml/min)	12 (ml/min)	18 (ml/min)	24 (ml/min)
30	1.14	1.08	1.40	1.96
50	1.78	1.55	1.37	1.64
70	1.52	2.04	3.63	2.45
50 (Y6)	0.24	0.04	0.28	0.98

5.3.1.8 *Conclusion*

It can safely be concluded that trends in fermentation parameters observed in this study were very similar to observations made by other authors, using tower bioreactors. Thus, the observed trends are normal in fluidized bed bioreactors containing flocculant strains of yeast. Furthermore, comparison of reactor productivities with reported literature values indicated very good agreement, suggesting that the reactor used in this work was very similar to those used by others.

Though, measurements of biomass concentrations, within the bed, were not reliable due to the highly flocculant nature of the organisms, results of measurements above the bed have shown that very little biomass wastage took place. This means that the yeast bed remained active and in place even at relatively high liquid flow rate of 24 ml/min, suggesting that the strains used were of the fermentation limited type.

5.3.2 ***Effects of inlet glucose concentration***

The effects of inlet glucose concentration on fermentation parameters could be seen from runs made with strain NCYC 1026, because inlet glucose concentration was varied from 30 to 70 g/l.

Figure 5.29 shows the influence of inlet glucose concentration on the glucose concentration.

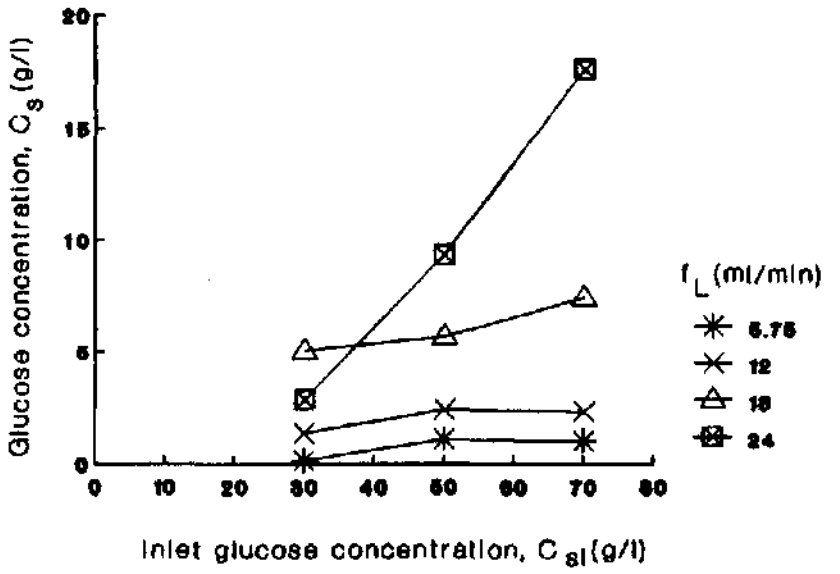


Fig. 5.29 Effect of inlet glucose concn. on glucose conc. above bed

At liquid flow rates of 5.75 and 12 ml/min, glucose concentration above the bed seemed to be independent of inlet glucose concentration and it was very low, indicating that all the glucose was utilized by the yeast, resulting in over 99% glucose consumption. But, at a flow rate of 18 ml/min, glucose concentration, above the bed, increased linearly with inlet glucose concentration.

However the influence of inlet glucose concentration on the glucose concentration above the bed, was more pronounced at a high liquid flow rate of 24 ml/min, where a sharp increase in glucose concentration was observed. Therefore, up to a liquid flow rate of 18 ml/min, the inlet glucose concentration does not seem to have strong influence on the glucose concentration. The observed trend was expected because at the highest liquid flow rate the residence time of liquid in the bed was low, about 1.58 hr and there was insufficient time for the organisms to act on the glucose substrate, meaning that the rate of glucose

assimilation was lower than its rate of supply.

Ethanol concentration increased, as was expected, with increases in inlet glucose concentration. The increase was linear at liquid flow rates of 5.75, 12 and 18 ml/min, as shown in figure 5.30.

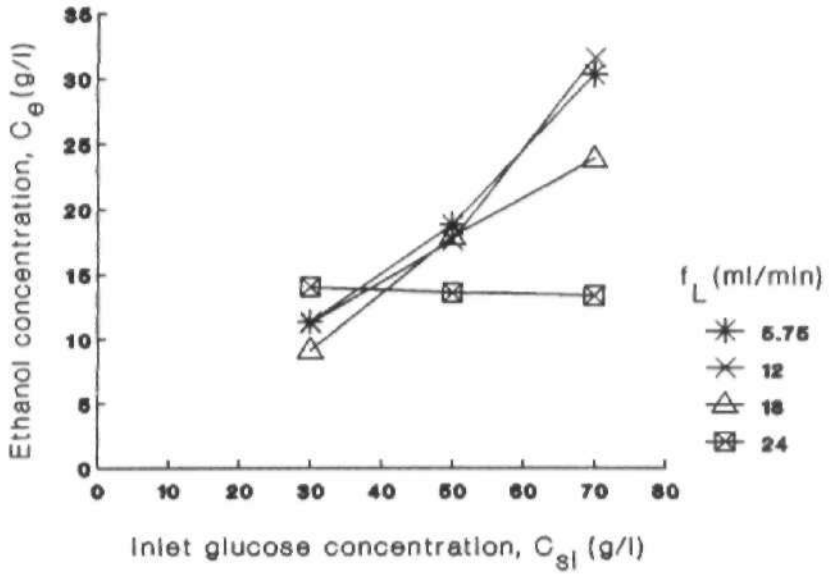


Fig. 5.30 Effect of inlet glucose concn. on ethanol concentration

At a liquid flow rate of 24 ml/min, however, ethanol concentration seemed to be independent of inlet glucose concentration. This means that the fermentation capacity of the bed was exceeded as a result of the short hydraulic residence time.

In contrast to ethanol concentration, the effect of inlet glucose concentration on ethanol yield was rather conflicting (Fig. 5.31). At a liquid flow rate of 24 ml/min, yield decreased linearly with increases in inlet glucose concentration. But, at liquid flow rate of 5.75 ml/min, there was initial insensitivity up to about 50 g/l and further increases in inlet glucose concentration caused increase in yield.

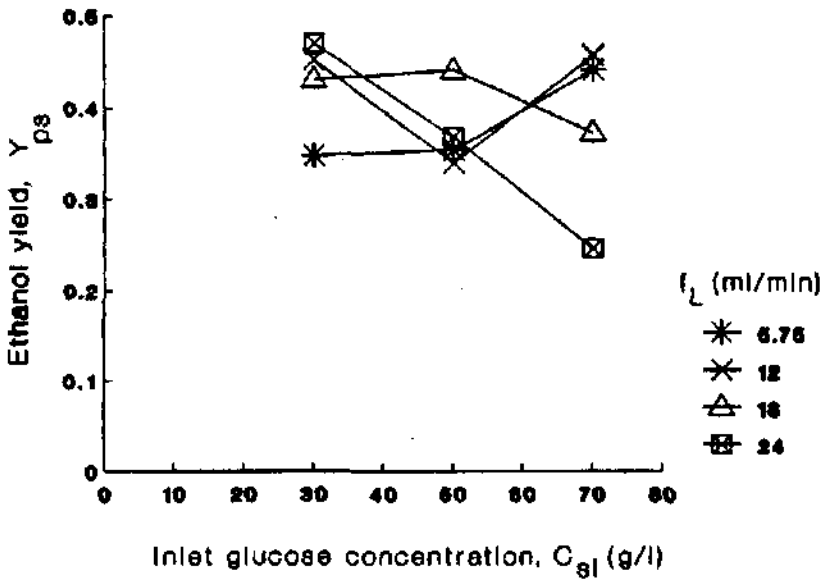


Fig. 5.31 Effect of inlet glucose concn. on ethanol yield

At an intermediate liquid flow rate of 12 ml/min, increase in inlet glucose concentration to 50 g/l, caused a decrease in yield while a further increase, increased the yield. At a liquid flow rate of 18 ml/min, there was a gentle increase of yield up to about 50 g/l and a further increase in inlet glucose concentration caused a decrease in yield. The observation of lower yield at the highest flow rate was not surprising because ethanol concentration was also low at this liquid flow rate.

The effect of inlet glucose concentration on ethanol productivity, based on the empty column, was similar to that on ethanol concentration. Productivity increased linearly with increased inlet glucose concentration at the liquid flow rates of 5.75 and 12 ml/min. At a liquid flow rate of 18 ml/hr there was an initial linear increase to 50 g/l and, thereafter, the productivity becomes independent of inlet glucose concentration. But, at a liquid flow rate of 24 ml/min, ethanol productivity seemed to decrease gently with increases in inlet glucose

concentration (Fig. 5.32).

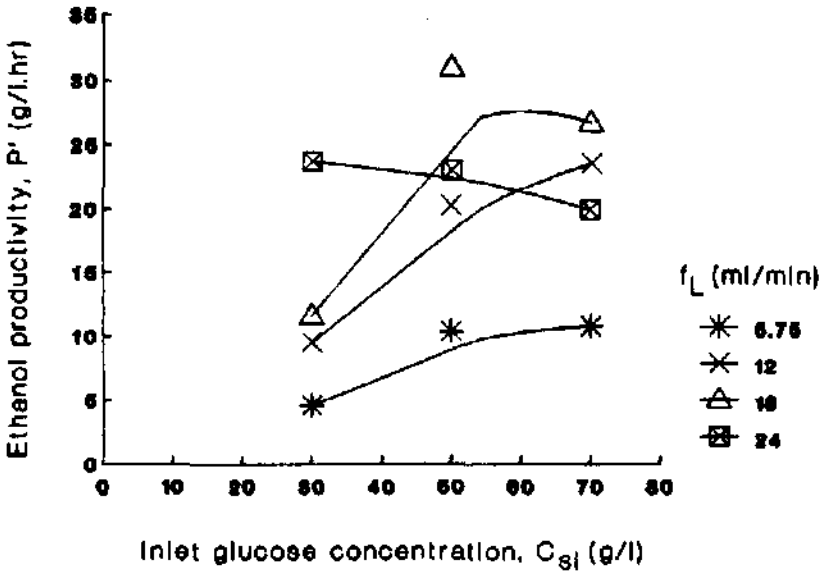


Fig. 5.32 Influence of inlet glucose concn. on ethanol productivity

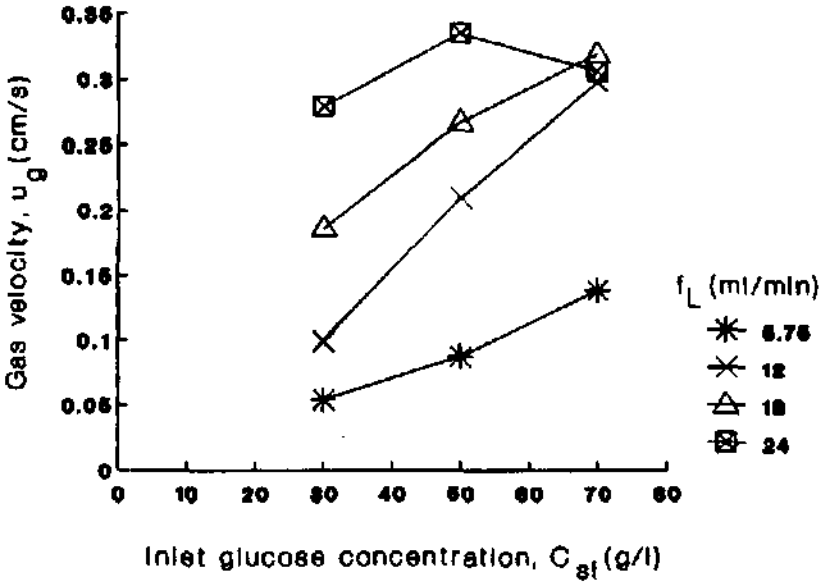


Fig. 5.33 Influence of inlet glucose concn. on gas velocity

In figure 5.33, the effect of inlet glucose concentration on calculated superficial gas velocity was shown. Like ethanol productivity, gas velocity increased

linearly with increases in inlet glucose concentration, at all liquid flow rates except 24 ml/min where a maximum was noted at an inlet glucose concentration of 50 g/l. The subsequent decrease in gas velocity at higher inlet glucose concentrations was an indication of lower metabolic activity due, perhaps, due to low hydraulic residence time.

5.3.3 Effects of liquid flow rate

Liquid flow rate was also noted to have an effect on the fermentation parameters. Increases in liquid flow rate were found to increase superficial gas velocity at all inlet glucose concentrations except 70 g/l. In the case of this high inlet glucose concentration, gas velocity increased linearly with increases in liquid flow rate, only to a liquid flow rate of 12 ml/min and it remained about constant with further increases in liquid flow, as shown in figure 5.34.

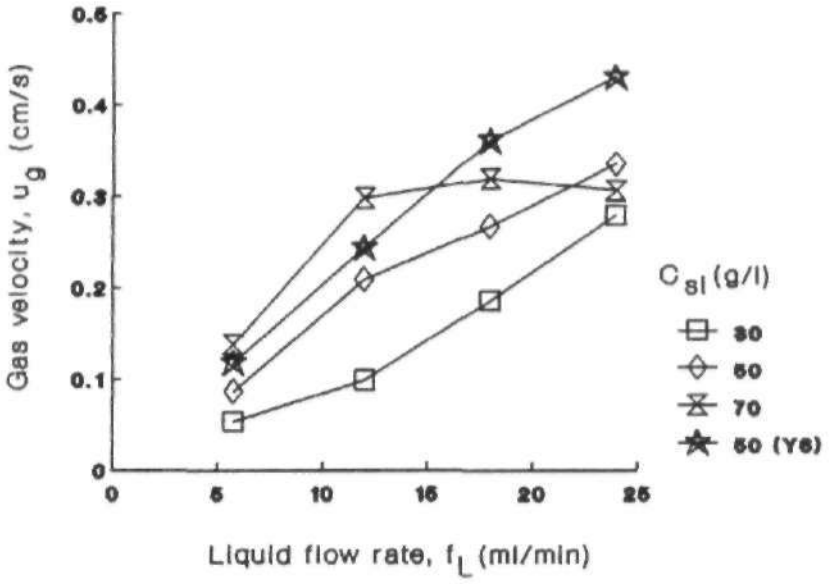


Fig. 5.34 Effect of liquid flow rate on gas velocity

At the lowest inlet glucose concentration of 30 g/l, the

effect of liquid velocity was almost parabolic, whereas it seemed linear at an inlet glucose concentration of 50 g/l.

Liquid flow rate showed little effect on ethanol concentrations for inlet glucose concentrations of 30 and 50 g/l (Fig. 5.35).

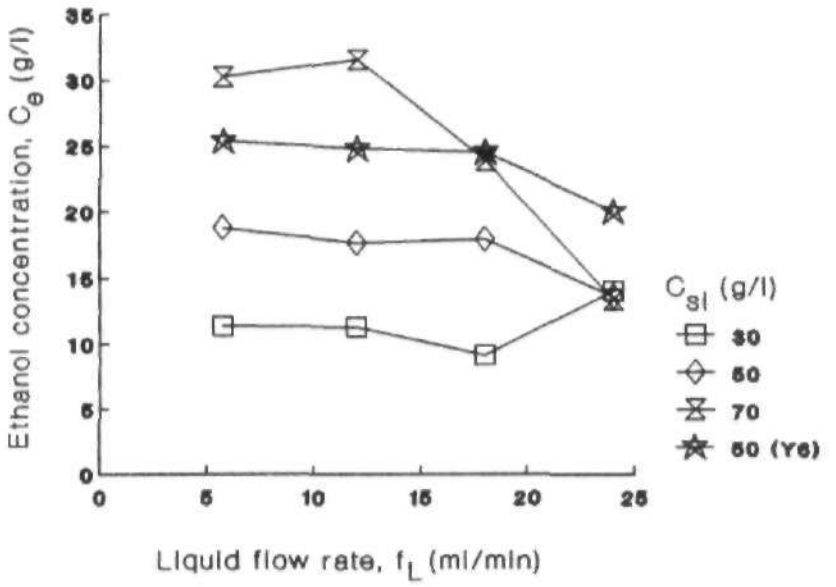


Fig. 5.35 Effect of liquid flow rate on ethanol concentration

For the former a slight minimum in ethanol concentration, at 18 ml/min, was observed, whereas for the latter, a maximum at the same liquid flow rate occured. With 70 g/l inlet glucose concentration, ethanol concentration decreased rapidly with increases in liquid flow rate. It was noted that strain Y6 had higher ethanol concentrations compared to strain NCYC 1026, at the same inlet glucose concentration and at all liquid flow rates. This may be caused by genetic differences of the strains.

Ethanol yield was also affected by liquid flow rate (Fig. 5.36). At low inlet glucose concentrations of 30 and 50 g/l, the trends indicated a gentle increase in yield due to increases in liquid flow rate. However, at an inlet glucose concentration of 70 g/l, there was a sharp

decrease in yield at liquid flow rates above 12 ml/min.

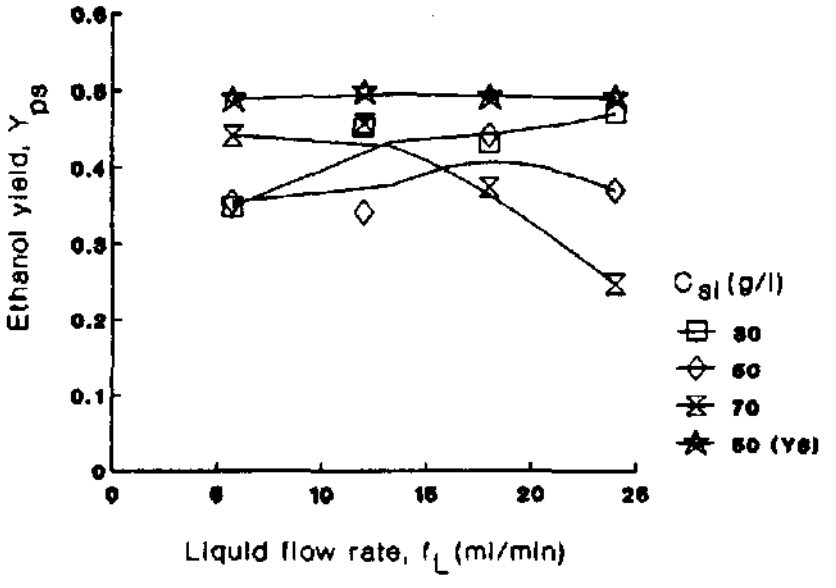


Fig. 5.36 Effect of liquid flow rate on ethanol yield

With strain Y6, the liquid flow rate did not seem to affect yield.

The liquid flow rate was found to affect ethanol productivity, as shown in figure 5.37. At a low inlet glucose concentration of 30 g/l, productivity increased linearly with liquid flow rate, but at 50 and 70 g/l inlet glucose concentrations, a maximum was noted at a liquid flow rate of 18 ml/min. A similar trend was reported by Prince and Barford (1982a). It was noted that the productivity values obtained with strain Y6 were lower than those obtained with strain NCYC 1026, at the same inlet glucose concentrations and at all liquid flow rates. This suggested that strain Y6 may be more flucculant than strain NCYC 1026. The latter strain may have formed a less compact bed and this might have facilitated the transfer of substrate into the biomass.

At all inlet glucose concentrations, there was an increase in glucose concentration above the bed, at high liquid flow rate. The increase was however more pronounced at flows higher than 15 ml/min. There was also a sharp increase in glucose concentration, above the bed, at a liquid flow rate of 24 ml/min, for 70 g/l inlet glucose concentration. This could be due to the short liquid residence time.

5.3.4 Reliability of concentration measurements

To find out the reliability of the measurements of glucose and ethanol concentrations, five measurements were made for each of the parameters, using one sample. For glucose, the results obtained from these five measurements were: 5.32, 5.40, 5.40, 5.45 and 5.32 g/l, giving a mean of 5.378 g/l and a sample standard deviation of 0.0567. This gives a 95% confidence interval of $\pm$ 2.9% of the value of a single observation.

Similarly, results of ethanol concentration measurements were: 7.964, 8.464, 8.261, 8.404 and 8.294 g/l. These give a mean of 8.277 g/l, a sample standard deviation of 0.193 and a 95% confidence interval of $\pm$6.49% of the value of a single observation.

5.3.5 Conclusion

The above results have indicated that the fermenter used in this work was comparable to other fermenters, of the same kind used by other researchers, both in terms of observed trends of fermentation parameters and the effect of inlet glucose concentration and liquid flow rate on these parameters. When values of individual parameters were considered, there was also close similarity between the value obtained here and those reported in the literature.

Though, variation in biomass concentration along the column height could not be established due to the

difficulty of sampling biomass from the fermenter, an estimate of biomass concentration in the system was nevertheless made and values obtained agreed very well with those reported in the literature. Low biomass wastage in the effluent even at high liquid thoroughput and high inlet glucose concentrations, was observed with both strains of yeast, leading to the believe that the two strains were of the fermentation limited type that have, characteristically, large and sticky flocs.

5.4 AXIAL LIQUID DISPERSION COEFFICIENT

Axial liquid dispersion coefficient (D_z) is an important parameter in the design and prediction of performance of fluidized bed bioreactors. Not only does it affect the residence time of liquid flowing into the bioreactor, it also has considerable influence on physical processes such as heat and mass transfer rates between particles and phases. But, this parameter is also significantly influenced by particle and liquid properties and process conditions.

In this work, the extent and nature of the influence of liquid and gas superficial velocities, on D_z, have been studied in a fluidized bed anaerobic bioreactor containing flocculant yeast, strain NCYC 1026. Owing to the packed nature of the yeast bed used and the failure of the yeast strains to form discrete floc particles, the influence of the particle size on D_z could not be studied.

The peculiar characteristics of this anaerobic system did not allow for the direct control of gas velocity, because the gas was generated *in situ*. Therefore, variation in gas velocity was effected by varying the glucose feed rate. This led to a linear relationship between glucose consumption rate and the superficial gas velocity, as shown in figure 5.39. Hence, the lowest superficial gas velocity employed was about 0.054 cm/s, corresponding to a superficial liquid velocity of 0.0084 cm/s and an inlet glucose concentration of 30 g/l, whereas the highest was 0.335 cm/s, which occured with inlet glucose concentration of 50 g/l and a liquid velocity of 0.0351 cm/s. On the other hand, four superficial liquid velocities of 0.0084, 0.0175, 0.0263 and 0.0351 cm/s were used.

The axial liquid dispersion coefficient was calculated from the residence time distribution (RTD) data, as explained in section 4.5.1.

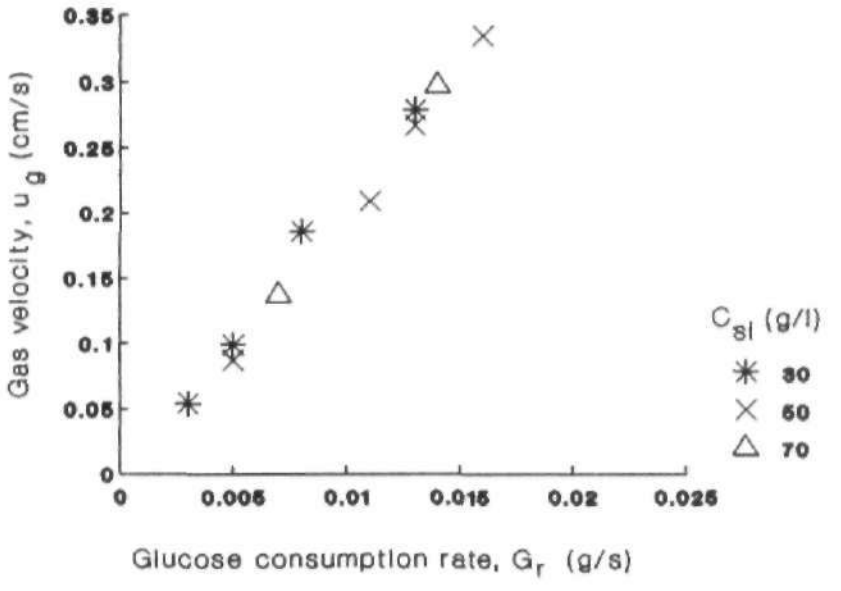


Fig. 5.39 Influence of glucose consumption rate on gas velocity

The results obtained and the influence of superficial liquid and gasvelocities, on D_z, are presented and discussed in this section. In addition, an attempt was made to correlate the D_z data with liquid and gas superficial velocities. Unfortunately, literature correlations could not be tested against the data because all the correlations were derived for fluidized beds, but proper fluidization was not obtained in this study. Moreover most of these correlations do require the particle diameter which could not be measured in this study.

5.4.1 *Magnitude of D_z values obtained*

Values of D_z obtained, in all experimental runs, are summarized in Table 5.18. The minimum value obtained was 4.67×10^{-5} m^2/s, while the highest value was 8.2×10^{-4} m^2/s. Therefore, even the lowest value of D_z, is about 4.7 times higher than the limit of 1×10^{-5} m^2/s, below which, D_z may not have significant influence on the concentration profile in a tower fermenter (Setiadi and Larsen, 1991).

Table 5.18 Axial liquid dispersion coefficient ($D_z x10^5$ m^2/s)

Inlet glucose, C_{si} (g/l)	Superficial liquid velocity, u_l			
	0.0084 (cm/s)	0.0175 (cm/s)	0.0263 (cm/s)	0.0351 (cm/s)
30	4.67	17.14	12.46	16.34
50	10.42	16.65	82.92	24.54
70	9.62	11.09	14.25	12.48
50 (Y6)	5.70	31.97	29.93	23.96

Going by the report of Setiadi and Larsen (1991) a D_z value of $1x10^{-4}$ m^2/s, would increase the height of tower, required to achieve 95% utilization of fermentable carbohydrate, by a factor of 2.4. Therefore, all the D_z values obtained in this work, could have significant influence on the concentration profile in a tower fermenter.

A comparison was made between some reported values of D_z and the values obtained in this study, as shown in Table 5.19.

Table 5.19 Comparison of D_z values

Column internal diameter, D_c (cm)	Gas velocity, u_g (cm/s)	Disp. coefft. D_z $x10^4$ (m^2/s)	Reference
5.7	0.047	0.0153	Admassu *et al.* (1985)
4	0.083	2.9-10.1	Gommers *et al.* (1986)
11.2	0.0085	20.6	Setiadi (1989)
3.81	0.087	1.042	This work

It is obvious that the simulated study of Setiadi (1989),

with alginate beads at liquid velocity of 0.142 cm/s, gave a higher value of D_z even though the gas velocity was one tenth of what was used in this work. The relatively larger column diameter used by Setiadi (9189) may have caused D_z to be high, but column diameter alone may not explain the observed difference.

Similarly, the result of Gommers *et al.* (1986) conducted in column of similar diameter to this study and at comparatively similar gas velocities have, nonetheless, D_z values that are 2.9 to 10 times higher than that obtained in this work. The reasons for these differences may be that the reported results were for fluidized beds, whereas fluidization of the yeast bed was not achieved in this work. Moreover a lower liquid velocity of 0.0084 cm/s was used in this work whereas Gommers *et al.* (1986) used a liquid velocity of 1.2 cm/s and Setiadi (1989) used 0.142 cm/s.

On the other hand the results of Admassu *et al.* (1985), for a tower fermenter, have shown a D_z value that is about 68 times lower than what was obtained in this study. The difference in gas velocities in the two studies may not account for this large difference in D_z. However, it was noted that the liquid velocity used by Admassu *et al.* (1985) was 0.0012 cm/s, which was about seven times lower than the value of 0.0084 cm/s used in this work. This large difference in superficial liquid velocities may have been responsible for the observed difference in D_z between the two studies.

5.4.2 Effect of gas superficial velocity on D_z

The effect of gas velocity on D_z was studied at four different liquid velocities. At the lowest liquid velocity of 0.0084 cm/s (Fig. 5.40), there was an initial increase in D_z from 4.67×10^{-5} to 10.42×10^{-5} m^2/s due to an increase in superficial gas velocity from 0.054 to 0.087 cm/s.

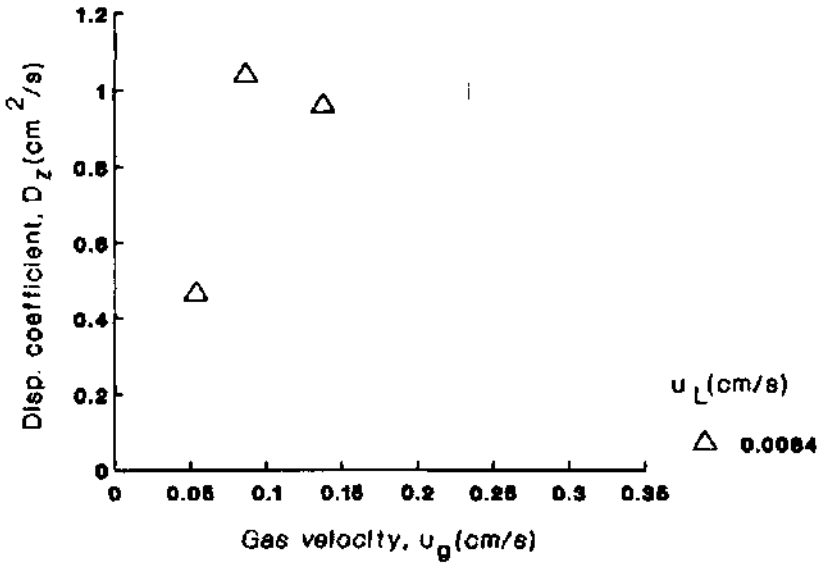


Fig. 5.40 Effect of gas velocity on axial liquid dispersion coefficient at liquid velocity of 0.0084 cm/s

But, a further increase in superficial gas velocity to 0.138 cm/s left D_z virtually unchanged, at 9.62×10^{-5} m^2/s.

Similarly at a liquid velocity of 0.0175 cm/s, an increase in gas velocity from 0.099 cm/s to 0.209 cm/s, did not significantly change D_z, which remained at 17.19×10^{-5} and 16.65×10^{-5} m^2/s respectively. But, further increase in gas velocity to 0.298 cm/s, caused D_z to decrease to 11.09×10^{-5} m^2/s, as shown in figure 5.41.

However, at a liquid velocity of 0.0263 cm/s, an increase in gas velocity from 0.186 cm/s to 0.267 cm/s increased D_z from 12.46×10^{-5} to 82.92×10^{-5} m^2/s and a further increase of gas velocity to 0.319 cm/s, caused the decrease of D_z to 14.25×10^{-5} m^2/s as shown in figure 5.42.

But at the highest liquid velocity of 0.0351 cm/s, slight decreasing and increasing trends in D_z, due to increases in gas velocity, were noticed. An increase in gas velocity from 0.279 to 0.306 cm/s decreased D_z from 16.34 to 12.48×10^{-5} m^2/s (Fig. 5.43). A subsequent increase of gas velocity to 0.335 cm/s, increased D_z to 24.54×10^{-5} m^2/s.

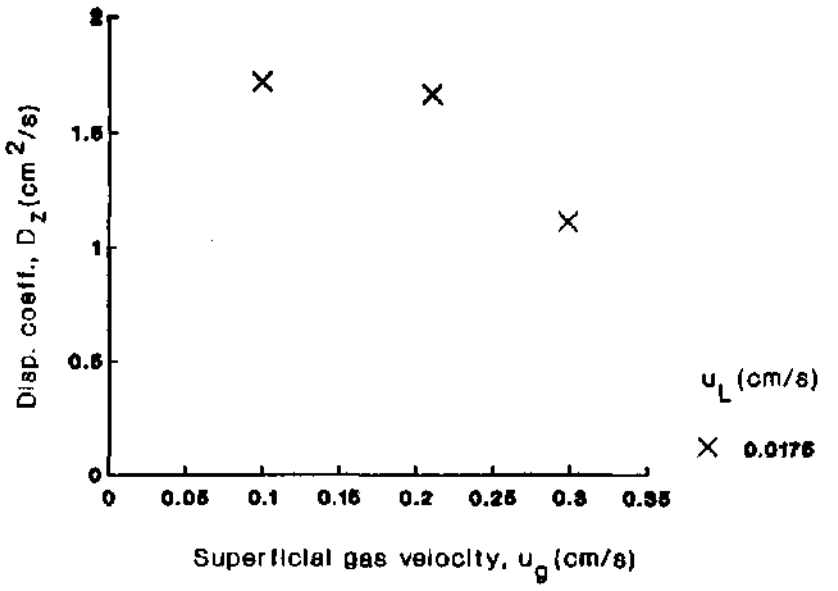


Fig. 5.41 Effect of gas velocity on D_z at liquid velocity of 0.0175 cm/s

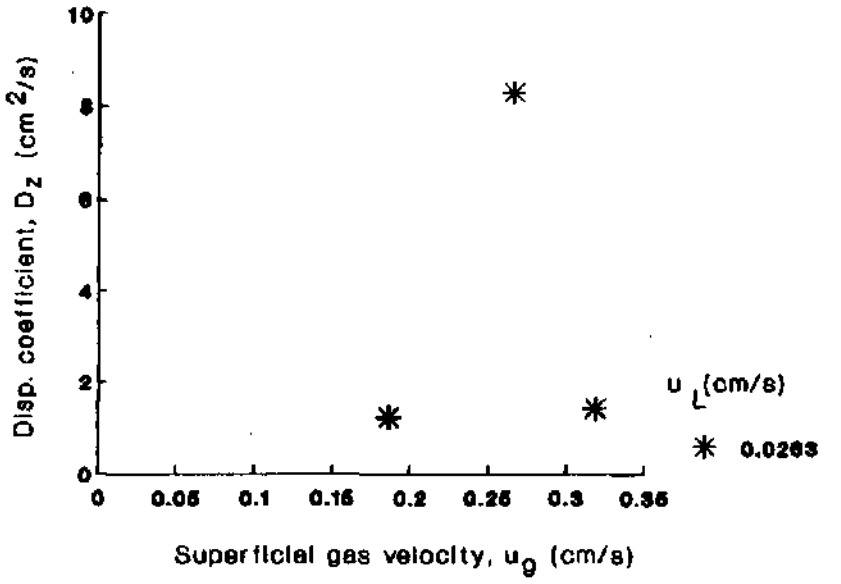


Fig. 5.42 Effect of gas velocity on D_z at liquid velocity of 0.0263 cm/s

Therefore, putting all the four sets of D_z data into perspective (Table 5.20), a trend seemed to imerge.

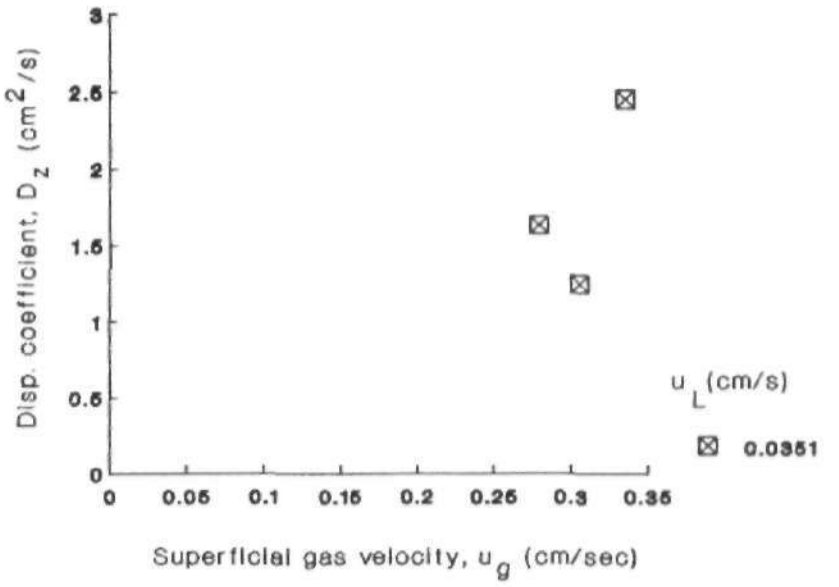


Fig. 5.43 Effect of gas velocity on D_z at liquid velocity of 0.0351 cm/s

Table 5.20 Changes in D_z with gas velocity

Gas velocity, u_g (cm/s)	Disp. coefficient, D_z x10^5 (m^2/s)
0.054	4.67
0.087	10.42
0.099	17.19
0.138	9.62
0.186	12.46
0.209	16.65
0.267	82.92
0.279	16.34
0.298	11.09
0.306	12.48
0.319	16.34
0.335	24.54

There was, generally, an increase in D_z with increases in

superficial gas velocity. However three distinct regimes, depending on the gas velocity, could easily be identified as summarized in Table 5.21.

Table 5.21 Gas flow regimes

Range of gas velocity (cm/s)	Range of D_z x10^5 (m^2/s)
0.054 - 0.099	4.67 - 17.19
0.138 - 0.267	9.62 - 82.92
0.279 - 0.335	11.09 - 24.54

In the first regime, increasing gas velocity from 0.054 cm/s to 0.099 cm/s caused a steady increase in D_z from 4.67 to 17.19x10^{-5} m^2/s. But in the second regime, an increase in gas velocity from 0.138 to 0.267 cm/s, caused D_z to increase from 9.62 to 82.92x10^{-5} m^2/s. Simliarly, in the third regime, increasing gas velocity from 0.279 to 0.335 cm/s, initially caused D_z to drop to 11.09x10^{-5} m^2/s and then it subsequently increased steadily to 24.54x10^{-5} m^2/s.

Figure 5.44 shows these gas flow regimes. It was also noted that a sharp drop in D_z occured when gas velocity was increased from 0.099 to 0.138 cm/s and 0.267 to 0.279 cm/s. The exact reason for these sharp drops in D_z is not known.

In three phase fluidized beds liquid axial mixing is partly caused by the movements of gas bubbles and their wakes. Increases in superficial gas velocity increase both the relative velocity of the bubbles (Slip velocity) and the bubble size, all of which, cause an increase in liquid axial mixing (Kim, Baker and Bergougnou, 1977; El-Temtamy *et al.* 1979a). Hence, increasing superficial gas velocity is expected to increase the axial liquid dispersion coefficient.

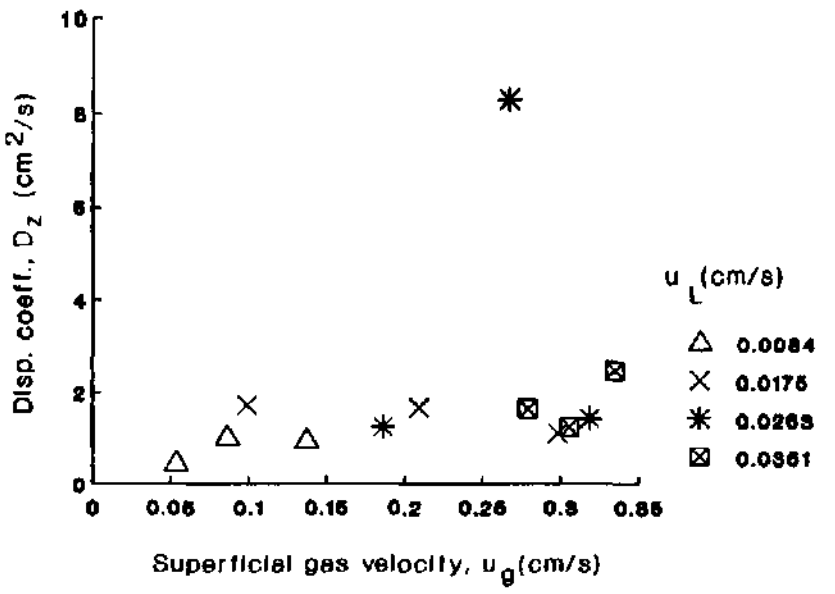


Fig. 5.44 Overall effects of gas velocity on D_z at all liquid velocities

Therefore the general increases in D_z due to increase in gas velocity, observed in this study, was expected and was in agreement with the reports of Vail *et al.* (1968); Michelsen and Ostergaard (1970); Kim *et al.* (1972); El-Temtamy *et al.* (1979a); Kim and Kim (1983); Gommers *et al.* (1986); Davison (1988) and Setiadi (1989).

However, the bubble size is also affected by the particle size and liquid velocity (Kim *et al.*, 1977; Fan, 1989). An increase in either of these parameters would cause a decrease in bubble size and might, consequently, diminish the influence of gas velocity on D_z. In this study, variations in gas velocity were achieved by increasing both the liquid velocity and the inlet glucose concentration. Perhaps, the observed decrease in the value of D_z, with increasing gas velocity, was caused by a decrease in bubble size as a result of increased liquid velocity.

5.4.3 Effect of superficial liquid velocity

The effect of liquid velocity on D_z was studied at

inlet glucose concentrations of 30, 50 and 70 g/l. At 30 g/l inlet glucose concentration, increases in liquid velocity caused D_z to change in a rather complex manner as shown in figure 5.45.

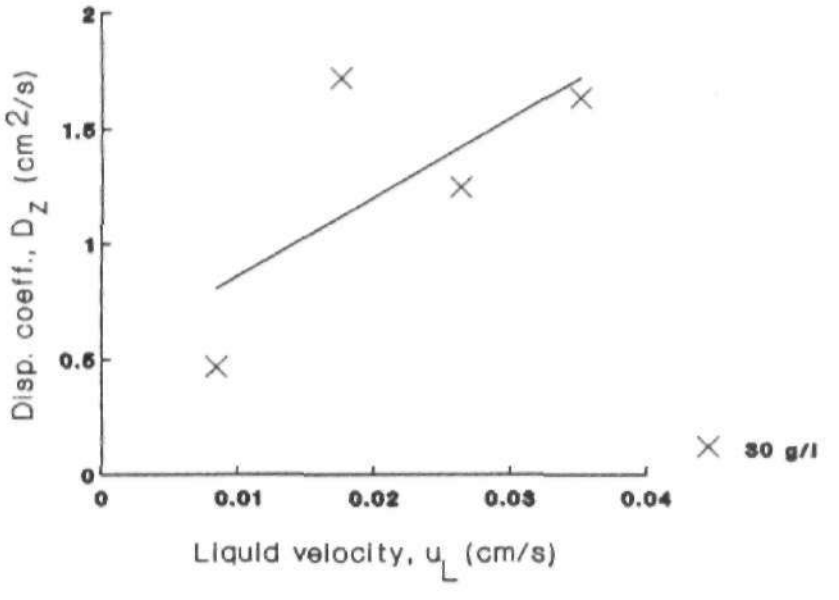


Fig. 5.45 Influence of liquid velocity on D_z at inlet glucose concn. of 30 g/l

Initially, an increase in liquid velocity from 0.0084 to 0.0175 cm/s caused D_z to increase from a low value of 4.67×10^{-5} m^2/s to 17.19×10^{-5} m^2/s, corresponding to an increase of about 73%. Further increases of liquid velocity to 0.0263 and 0.0351 cm/s, caused D_z to decrease to 12.46×10^{-5} m^2/s and then increase to 16.34×10^{-5} m^2/s respectively.

A contrasting trend was observed with an inlet glucose concentration of 50 g/l (Fig. 5.46). Here, an increase in liquid velocity from 0.0084 to 0.0175 cm/s and further to 0.0263 cm/s, caused D_z to increase steadily from 10.42×10^{-5} to 16.65×10^{-5} and 82.29×10^{-5} m^2/s respectively. But, a further increase in liquid velocity to 0.0351 cm/s, resulted in D_z decreasing to 24.54×10^{-5} m^2/s.

A similar trend was observed at the highest inlet glucose concentration. As shown in figure 5.47, an

increase in liquid velocity from 0.0084 to 0.0175 cm/s and then to 0.0263 cm/s, increased D_z from 9.62×10^{-5} m^2/s to 10.51×10^{-5} m^2/s and further to 13.81×10^{-5} m^2/s respectively.

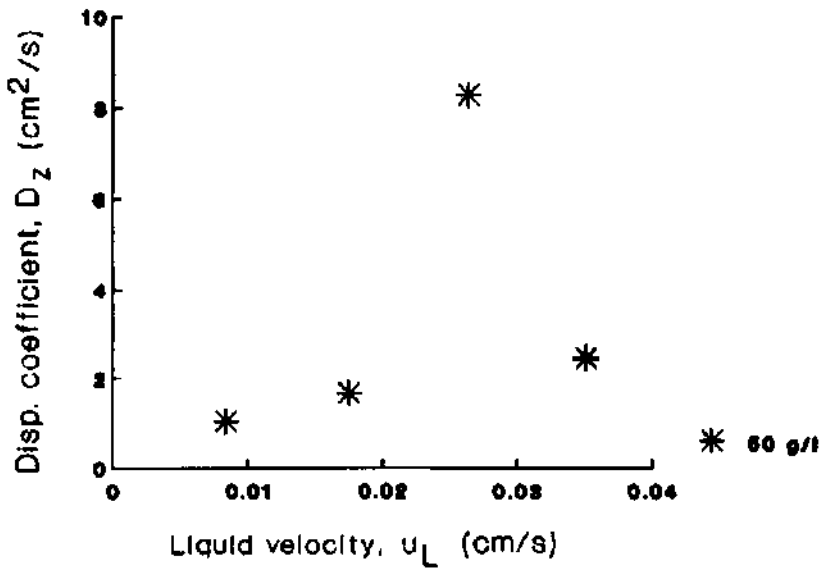


Fig. 5.46 Influence of liquid velocity on D_z at inlet glucose concn. of 50 g/l

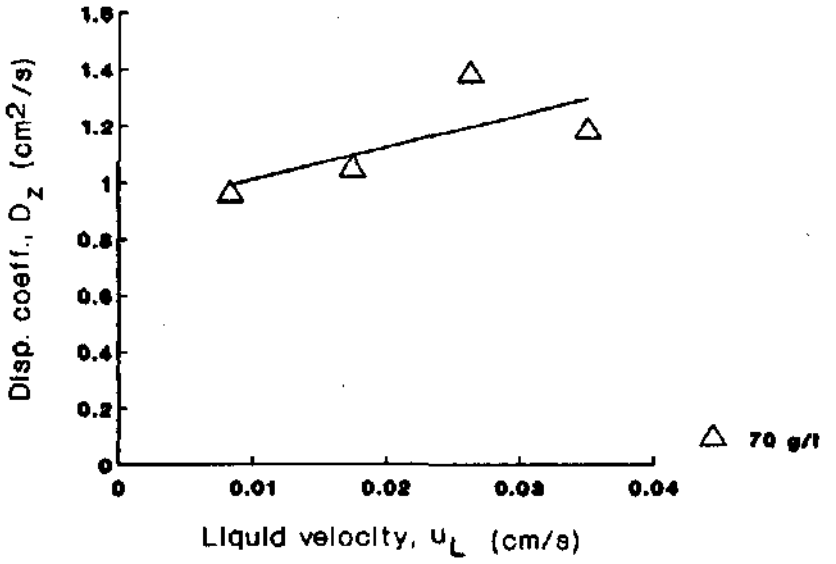


Fig. 5.47 Effect of liquid velocity on D_z at inlet glucose concn. of 70 g/l

Increasing the liquid velocity, again, to 0.0351 cm/s, decreased D_z to a value of 11.85×10^{-5} m^2/s. It was, however, noted that the changes in D_z were marginal at this inlet

glucose concentration due to a possible effect of gas velocity.

In order to assess the overall effect of liquid velocity on D_z, the three set of data were put in a single plot shown in figure 5.48.

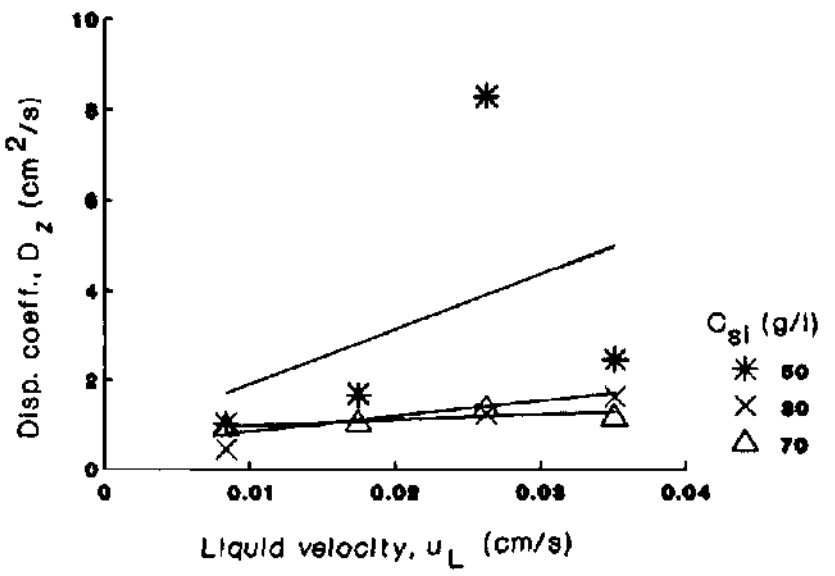


Fig. 5.48 Overall effect of liquid velocity on D_z at all inlet glucose concns.

It can be seen that the D_z data can be approximated by straight lines, with positive slopes, representing best fits and corresponding to each of the three inlet glucose concentrations.

It was noted that the D_z values, at an inlet glucose concentration of 50 g/l were consistently higher than the values obtained at the other two inlet glucose concentrations. Also, the D_z values at an inlet glucose concentration of 30 g/l were, for most of the liquid velocities, higher than the values for an inlet glucose concentration of 70 g/l. These observations are rather unusual, because an increase in inlet glucose concentration coupled with an increase in liquid velocity, resulted in higher gas production rates, which were, therefore, expected to cause an increase in D_z. Instead, the results indicated that at an inlet glucose

concentration of 70 g/l, liquid velocity had little influence on D_z and lower values of D_z were obtained.

It is believed that, in addition to bubble movements and their wakes, axial liquid mixing may also be caused by the continuous splitting up and recombination of flowing liquid elements or turbulence, due to the presence of solids that obstruct the liquid flow, and by the oscillatory movements of the particles, in the vertical direction (El-Temtamy *et al.*, 1979a). Increases in turbulence and oscillation of the particles, will cause an increase in liquid phase mixing.

Increasing superficial liquid velocity would cause an increase in the turbulence and oscillatory movements of particles, with a consequent increase in D_z. In addition, it would also cause an increase in bed voidage, which has a decreasing effect on axial liquid mixing. Therefore, an increase in superficial liquid velocity would either increase or decrease the axial liquid dispersion coefficient, depending upon which of the above three factors was most significant.

The increases in D_z, due to increase in superficial liquid velocity, which was observed in this study at inlet glucose concentrations of 30 and 50 g/l was an expected trend and in agreement with the reports of El-Temtamy *et al.*, (1979a); Kim and Kim (1983) and Setiadi (1989). Furthermore, the lower values of D_z, noted at an inlet glucose concentration of 70 g/l may have been caused by increased bed voidage, which was brought about by increased gas production at this inlet glucose concentration. The decrease in D_z, due to increases in superficial liquid velocity at high bed voidage, was reported by Kim and Kim (1983) and Setiadi (1989), for fluidized bed systems.

It should be kept in mind that, in this study, an increase in liquid velocity also increases the rate of glucose supply and consequently the rate of glucose

consumption, which was earlier (Section 5.3.2) shown to be directly proportional to the superficial gas velocity generated in the bioreactor. Therefore, the effects of liquid velocity observed, may include some influence of the gas velocity as well.

5.4.4 Axial variation in D_z

It was noted, in section 5.3.1.5, that gas production in the bioreactor varied along the column height, consequently, causing axial variations in superficial gas velocity. The effect of this axial variation in gas velocity, on D_z, was assessed by determining the coefficient at two points, 20 cm apart, at the same superficial liquid velocity and inlet glucose concentration. Three liquid velocities of 0.0175, 0.0263 and 0.0351 cm/s and inlet glucose concentration of 70 g/l were used, while D_z was determined at 45 cm and 65 cm above the column inlet. The values of D_z obtained are presented in Table 5.22 together with the calculated gas velocities at the two points.

Table 5.22 The effect of axial variation in gas velocity on D_z

Liquid vel., u_l (cm/s)	Disp. coefficient, $D_z \times 10^5$ (m^2/s)			Gas velocity, u_g (cm/s)		
	45 cm	65 cm	Increase %	45 cm	65 cm	Increase %
0.0175	10.51	11.09	5	0.115	0.145	20
0.0263	13.81	14.25	3	0.112	0.159	30
0.0351	11.85	12.48	5	0.156	0.193	19

It is interesting to note that the D_z values at the

height of 65 cm were, consistently, higher than those obtained at the height of 45 cm, though the difference was, in all the three cases, between 3% and 5%. On the other hand, there was a difference of between 19% and 30%, in superficial gas velocities, at these points. These results indicated that D_z is not seriously affected by axial variation in superficial gas velocity in this system.

5.4.5 Correlations for axial liquid dispersion coefficient

The D_z values obtained in this work have not been fitted into any of the existing correlations because fluidization of the yeast bed was not achieved, while the existing correlations were all derived for fluidized beds. Furthermore, most of the correlations require the use of the particle diameter which was not measured in this work, due to the failure of the yeast bed to form discrete floc particles.

Nonetheless, an attempt was made to relate the observed D_z values to the liquid and gas superficial velocities. Linear and exponential relationships were considered. In evaluating these relationships, only eleven out of the twelve data points were used. In both the two models, the data point with D_z value of 82.92×10^{-5} m^2/s, had very large residuals. Significance tests, using the method described by Himmelblau (1970), have shown that, with 95% confidence, the point was an outlier and was, therefore, not included in the multiple regressions. Detailed calculations are shown in appendix B.

In the linear model the D_z was given by equation 5.2

$$D_z = a_1 + a_2 u_g + a_3 u_L \qquad 5.2)$$

where a_1, a_2 and a_3 are constants and their values were obtained by multiple regression, as:

$a_1 = 0.672$; $a_2 = 0.48$; $a_3 = 27.4$

Therefore, equation 5.2 becomes:

$$D_z = 0.672 + 0.48u_g + 27.4u_L \qquad 5.3)$$

With D_z, u_g and u_L given in cm^2/s, cm/s and cm/s respectively. Equation 5.3 has a goodess of fit (R^2) of 48.1%, which was low, considering the number of data points (11). The negligible effect of gas velocity on D_z was easily apparent from the equation. t-ratio values of 1.26, 0.21 and 2.12 were obtained for the liquid velocity, gas velocity and the constant respectively. This further confirmed the negligible effect of gas velocity on D_z.

For the exponential model, D_z was related to the liquid and gas superficial velocities, by the following relationship;

$$D_z = f(u_g, u_L) \rightarrow D_z = b_1 u_g^{b_2} u_L^{b_3} \qquad 5.4)$$

Where b_1, b_2 and b_3 are constants. Linearizing equation 5.4 gives:

$$Log(D_z) = Log(b_1) + b_2 Log(u_g) + b_3 Log(u_L) \qquad 5.5)$$

Values of the constants were obtained by multilinear regression as:

$b_1 = 7.047$, $b_2 = 0.197$, $b_3 = 0.347$

Hence, equation 5.4 becomes;

$$D_z = 7.047 u_g^{0.197} u_L^{0.347} \qquad 5.6)$$

Where D_z, u_g and u_L are given in cm^2/s, cm/s and cm/s respectively. Equation 5.6 has R^2 of 52.9%, which was an improvement over the linear model (Eqn. 5.3) but, nonetheless, low when the number of data points are considered. The t-ratio values were 2.20, 0.68 and 1.11 for the constant, gas velocity and liquid velocity, respectively, indicating that the gas velocity has little effect on D_z.

The lack of proper fit of the experimental data, as indicated by the low value of R^2, into the exponential model which was the type used, for fluidized beds, by some researchers (El-Temtamy *et al.*, 1979a; Kim and Kim, 1983; Setiadi, 1989), indicated that, the system is not a fluidized bed. However, other parameters such as particle size and density and liquid density and viscosity, which have not been considered in the correlation, may have effect on the dispersion coefficient.

It was noted, from the correlation, that the exponent for the liquid velocity is about 1.8 times higher than that for the gas velocity, suggesting that, in this system, the liquid velocity had greater influence on the D_z than the gas velocity. This is, however, not surprising because proper fluidization of the yeast bed was not achieved and the bed formed a plug which might have hindered the formation of large gas bubbles, in response to increases in superficial gas velocity. Large diameter particles have been reported to cause decreases in bubble size, and a resultant decrease of the axial liquid dispersion coefficient (Michelsen and Ostergaard, 1970).

5.4.6 Conclusion

It can be concluded that the D_z values in this study are high enough to cause a considerable effect on the concentration profile in tower bioreactors. Furthermore, both the liquid and gas superficial velocities were found to affect the axial dispersion coefficient, though, the former had greater influence. The observed trends, of the effects of liquid and gas velocities, on D_z, are similar to the trends reported by other researchers and were in agreement with the established theory. However, both the linear and the exponential correlations of D_z with the gas and liquid velocities, have low values of R^2 due perhaps to the influence of other parameters such as column diameter and particle size which have not been considered here.

5.5 BED EXPANSION CHARACTERISTICS

In three phase fluidization, the volume fraction, or holdup, of each of the phases can be evaluated by simultaneously solving equations 3.19a and 3.19b, provided the pressure drop across the bed and any one of the holdups, are known. Unfortunately, attempts to measure the pressure drop across the yeast bed did not succeed, because yeast escaped into the manometer tubes and production of gas in these tubes made pressure readings impossible. Similarly, determination of the liquid holdup by draining the liquid within the bed, was attempted without success. This was because gas production continued even when the liquid flow was stopped. Draining the liquid at this stage resulted in the loss of substantial amount of biomass. When the gas production was allowed to stop, the bed was blocked-up by large agglomerates of yeast flocs.

Determination of the solid holdup, from the weight of the solids using equation 3.19, did not work either, due to the difficulty of sampling the biomass accurately. But, using the residence time distribution (RTD) data, a numerical value of the liquid holdup could be determined. Furthermore, the bed voidage was estimated from the height difference between the fluidized bed and the bed under a no-flow situation. However, the method was not very accurate owing to the compressible nature of the bed; the height of the dry bed was not constant but depended on the time the bed was left dry. Therefore, 15 hours was arbitrarily used as the time basis, after which, the dry bed height was measured. The bed voidage was then calculated as the fractional increase in bed height. Using the calculated values of the bed voidage and the values of the liquid holdup obtained, from the RTD data, the gas holdup was determined by difference and the solid hold up was consequently evaluated using equation 3.19a.

The RTD method, used to determine the liquid holdup,

was not without problems either. The main problem experienced was the lifting up of the entire bed or part of the bed, due to gas pressure (Fig. 5.49). When this occurred the residence time of the injected tracer becomes high, resulting in a higher value of the liquid holdup and this may also lead to an underestimation of the degree of liquid mixing. A few measurements of liquid holdup were made under these conditions, at a liquid velocity of 0.0351 cm/s and inlet glucose concentrations of 30 and 50 g/l, as shown in Table 5.23.

Table 5.23 Effect of bed breakage on measured liquid holdup and D_z

Parameter	Inlet glucose, C_{si} (g/l)	Bed condition	
		With breakage	Without breakage
Liquid holdup, ε_L (-)	30	0.354	0.243
	50	0.343	0.211
Disp. coefficient, $D_z \times 10^4$ (m^2/s)	30	0.541	1.634
	50	0.785	2.454

It is evident that this phenomenon of bed breakage caused an overestimation of the liquid hold up and a significant reduction in the value of the axial liquid dispersion coefficiccient. This was expected, because a lower particle concentration, as is the case when bed breakage occurs, has been reported to cause a decrease in axial liquid dispersion coefficient (Michelsen and Ostergaard, 1970; El-Temtamy *et al.* 1979a).

However, liquid holdup was determined at four liquid velocities of 0.0084, 0.0175, 0.0263 and 0.0351 cm/s and inlet glucose concentrations of 30, 50 and 70 g/l. Bed

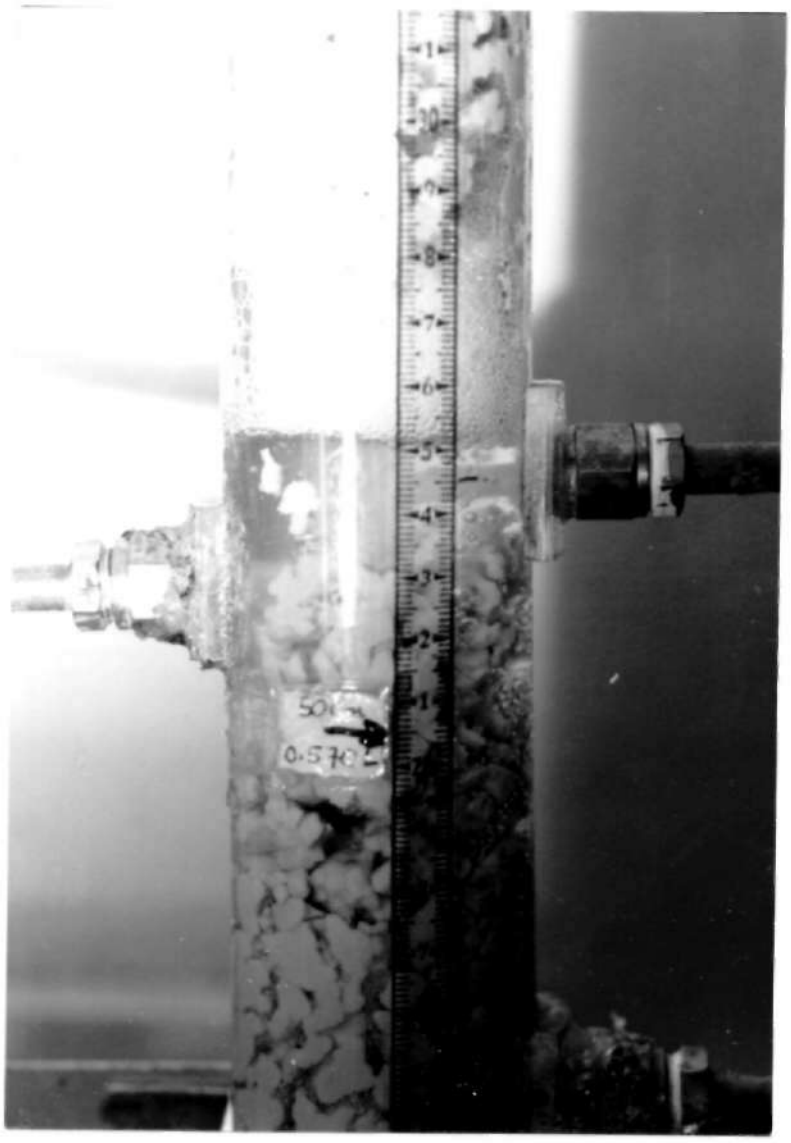


Fig. 5.49 Bed breakage during fermentation

voidage, gas holdup and solid holdup were also estimated at the same conditions.

In this section, the effects of gas and liquid superficial velocities, on the liquid holdup, are presented and discussed. In addition, a correlation relating these parameters is also presented. Furthermore, estimates of the bed voidage, gas and solid holdups are similarly presented and discussed.

5.5.1 Liquid holdup

Values of the liquid holdup obtained, are summarized in Table 5.24.

Table 5.24 Values of liquid holdup obtained

Liquid velocity, u_L (cm/s)	Inlet glucose, C_{si} (g/l	Gas velocity, u_g (cm/s)	Liquid holdup, ε_L (-)
0.0084	30	0.054	0.171
	50	0.087	0.158
	70	0.138	0.111
0.0175	30	0.099	0.154
	50	0.209	0.196
	70	0.298	0.174
0.0263	30	0.186	0.234
	50	0.267	0.223
	70	0.319	0.210
0.0351	30	0.279	0.243
	50	0.335	0.211
	70	0.306	0.234

It can be seen that the highest value of the liquid holdup, obtained, was 0.243 which occurred with an inlet glucose concentration of 30 g/l, at a liquid velocity of 0.0351 cm/s and a corresponding gas velocity of 0.279 cm/s. The lowest liquid holdup was 0.111 and occured at the lowest liquid velocity of 0.0081 cm/s, with an inlet glucose concentration of 70 g/l and a corresponding gas velocity of 0.138 cm/s. These values of liquid holdup are not far from the value of 0.25 reported by Admassu *et al.* (1985), for a tower fermenter at superficial liquid and gas velocities of 0.0012 cm/s and 0.047 cm/s respectively. But, compared to non biological beds, these values of liquid holdup are low; values in the range 0.6 to 0.8 were reported by Michelsen and Ostergaard (1970).

However, the low values of liquid holdup, obtained in this study, indicated that the yeast bed was not fluidized, but merely expanded due to increased liquid velocity.

5.5.1.1 *Effect of gas velocity on liquid holdup*

The effect of gas velocity on liquid holdup, at the lowest liquid velocity of 0.0084 cm/s, is shown in figure 5.50. It can be seen that, at this liquid velocity, an increase in gas velocity from 0.054 to 0.138 cm/s caused liquid holdup to decrease from 0.171 to 0.111. Thus, a 61% increase in gas velocity has caused liquid holdup to decrease by 35%.

At a liquid velocity of 0.0175 cm/s, a complex behaviour, involving increase and decrease in liquid holdup due to increase in gas velocity, was observed as shown in figure 5.51. Initially, an increase in gas velocity from 0.099 to 0.209 cm/s, increased liquid holdup from 0.154 to 0.196. A further increase in gas velocity to 0.298 cm/s, caused liquid holdup to decrease to 0.174.

At a liquid velocity of 0.0263 cm/s, similar trend was observed as with the lowest liquid velocity.

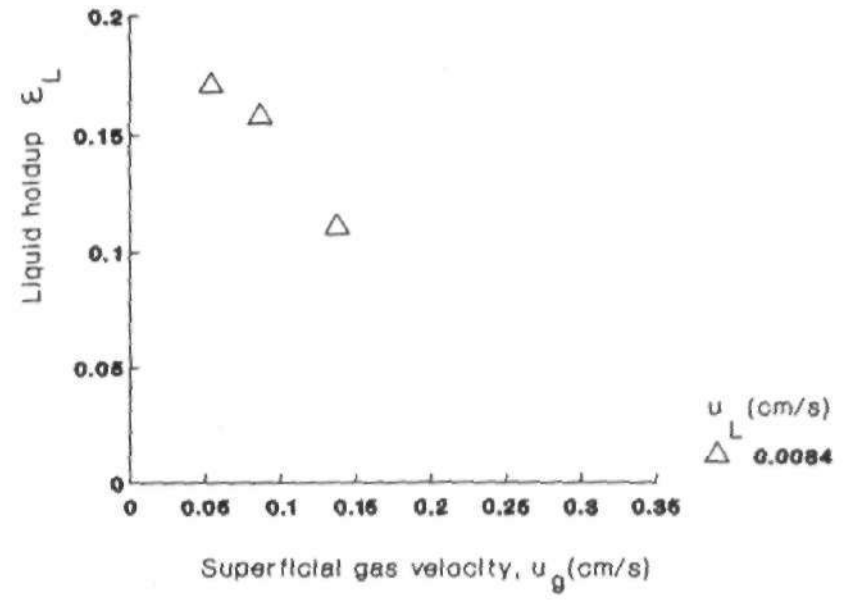


Fig. 5.50 Effect of gas velocity on liquid holdup at liquid vel. of 0.0084 cm/s

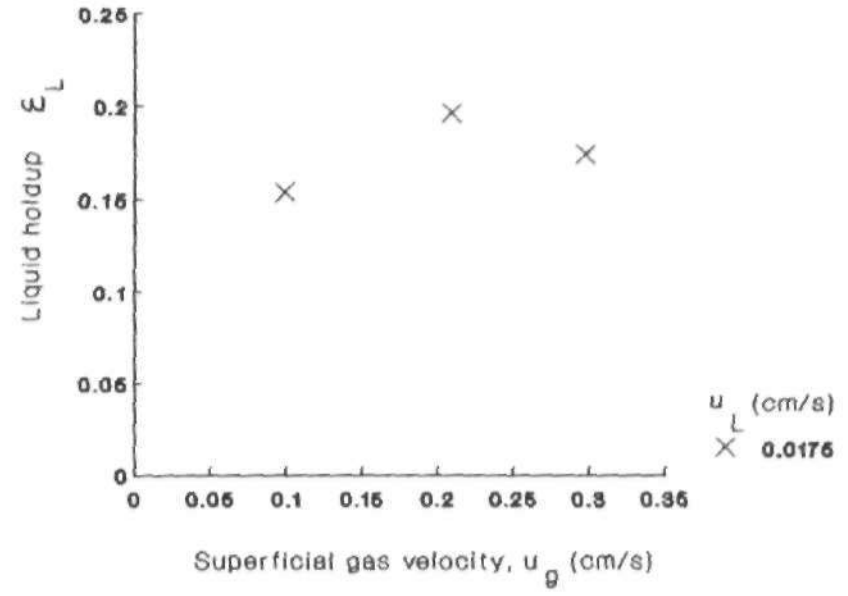


Fig. 5.51 Effect of gas velocity on liquid holdup at liquid vel. of 0.0175 cm/s

Increases in gas velocity from 0.186 to 0.267 cm/s and further to 0.319 cm/s, caused liquid holdup to decrease from 0.234 to 0.223 and further to 0.21 respectively (Fig. 5.52).

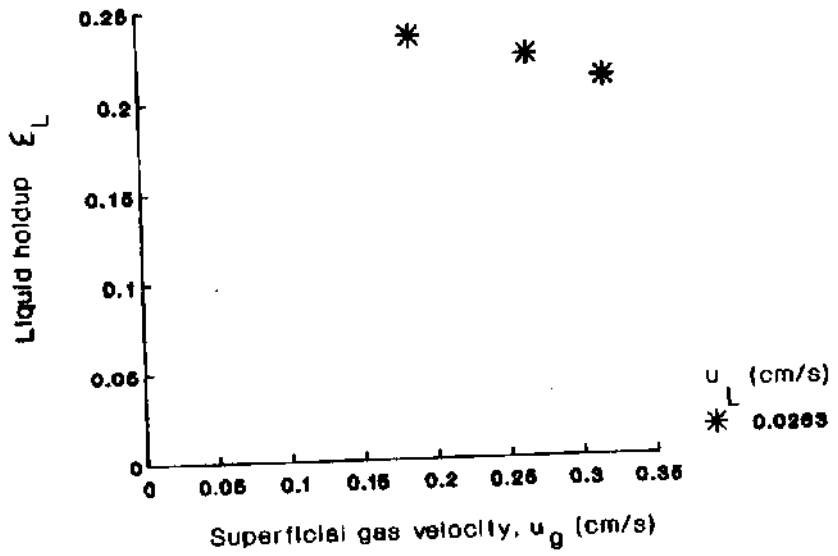


Fig. 5.52 Effect of gas velocity on liquid holdup at liquid vel. of 0.0263 cm/s

Similarly, at a liquid velocity of 0.0315 cm/s, the liquid holdup was noted to decrease from 0.211 to 0.234 and 0.243, due to increases in gas velocity from 0.279 to 0.306 and to 0.335 cm/s respectively as shown in figure 5.53.

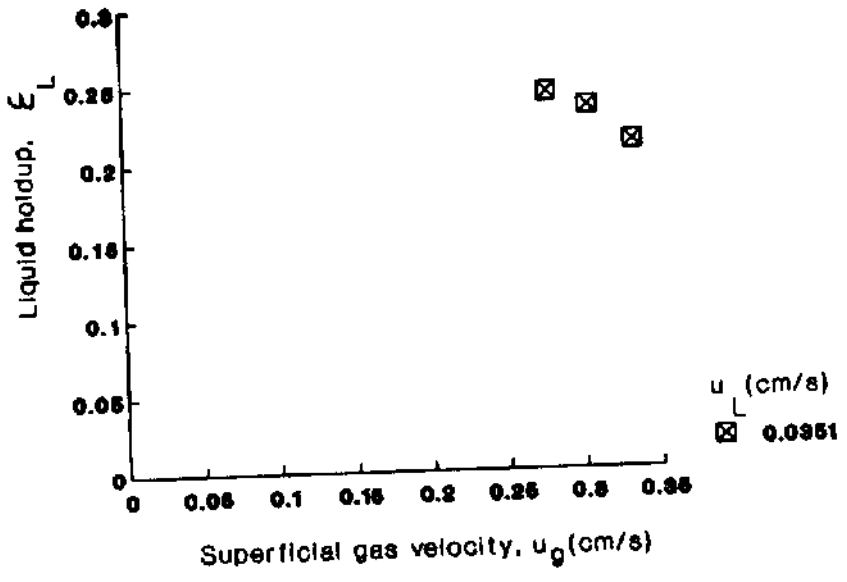


Fig. 5.53 Effect of gas velocity on liquid holdup at liquid vel. of 0.0351 cm/s

The overall effect of gas velocity on liquid holdup, for all the low liquid velocities used, is shown in figure 5.54.

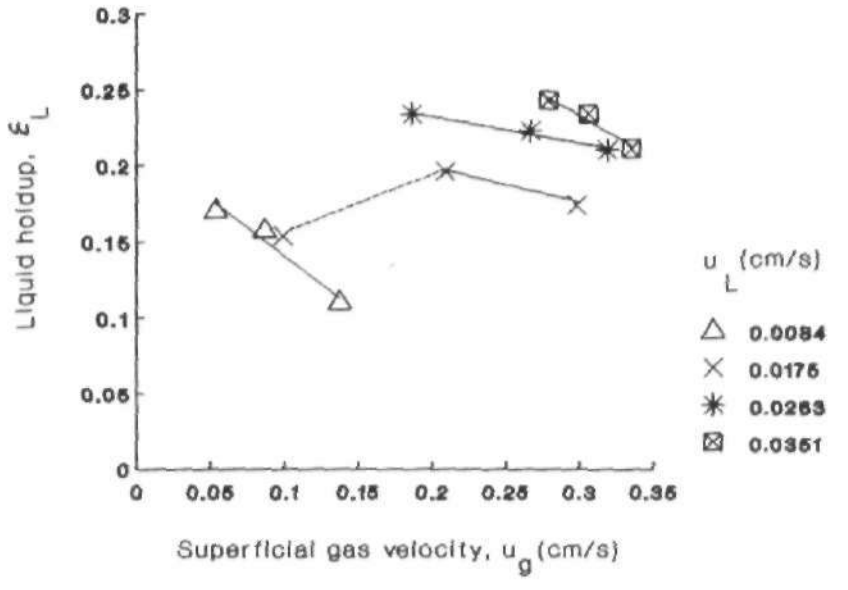


Fig. 5.54 Overall effect of gas velocity on liquid holdup at all liq. velocities

It is clear that, at each liquid velocity, all the data points, except one at a liquid holdup of 0.111, could be represented by a straight line of best fit, with negative slope. This indicated that increases in gas velocity caused decreases in liquid holdup at all liquid flow rates. The same observation was reported by Michelsen and Ostergaard (1970) for three phase fluidized beds containing air, water and glass beads of 1 mm, 3 mm and 6 mm diameter. Similar observations were also reported by Ostergaard (1978), Kato *et al*. (1981) and Setiadi (1989). This observation is, therefore, expected because increases in gas velocity will increase the bed height and since the liquid velocity remains unchanged, a decrease in the volume fraction of liquid or liquid holdup, results. But, the reason for the low liquid holdup of 0.111, is not known.

5.5.1.2 *Effect of liquid velocity on liquid holdup*

The effect of superficial liquid velocity on liquid holdup, was studied at inlet glucose concentrations of, 30, 50 and 70 g/l. At 30 g/l inlet glucose concentration, an increase in liquid velocity from 0.0084 to 0.0175 cm/s caused liquid holdup to decrease slightly from 0.171 to 0.158 possibly due to the increase in gas velocity. But, subsequent increases in liquid velocity to 0.0263 cm/s and then to 0.0351 cm/s, caused increase in liquid holdup to 0.234 and 0.243 respectively (Fig. 5.55).

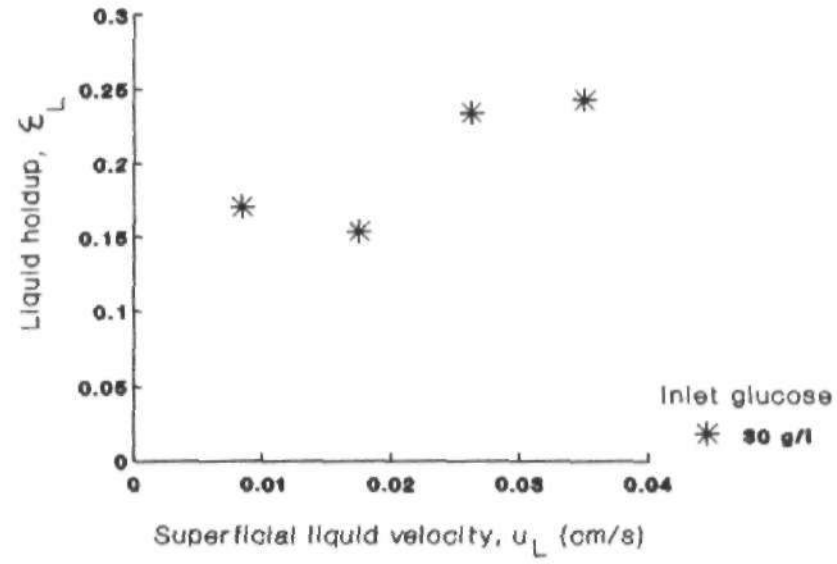


Fig. 5.55 Influence of liquid velocity on liquid holdup at inlet glucose concn. of 30 g/l

This marginal increase in liquid holdup may be because of the effect of gas velocity which also increased from 0.186 to 0.279 cm/s, due to the increased feed rate of limiting substrate, and has earlier been shown to have a decreasing effect on liquid holdup.

At an inlet glucose concentration of 50 g/l a steady increase in liquid holdup, due to the increase in liquid velocity, was noted as shown in figure 5.56. The holdup increased from 0.158 to 0.196 and further to 0.223, as a result of an increase in liquid velocity from 0.0084 to

0.0175 and further to 0.0263 cm/s respectively.

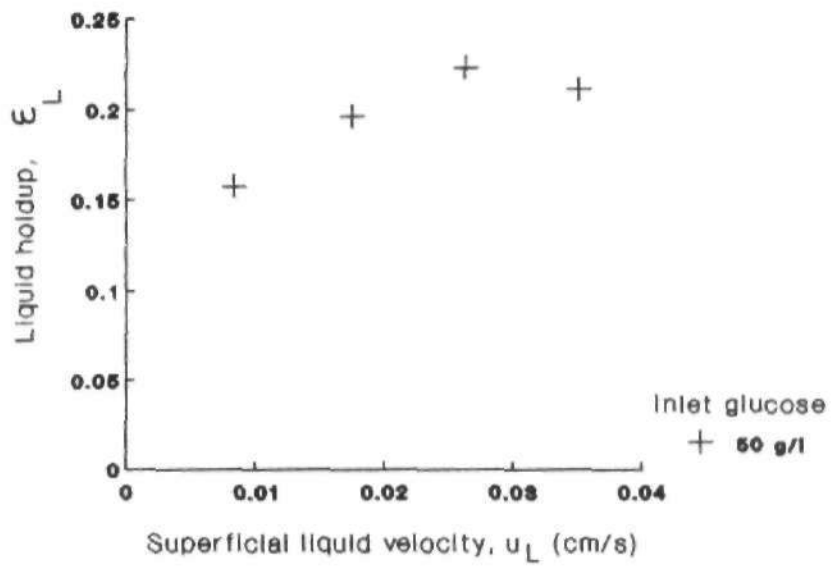


Fig. 5.56 Influence of liquid velocity on liquid holdup at inlet glucose concn. of 50 g/l

But, a further increase in liquid velocity to 0.0351 cm/s caused a decrease in liquid holdup to 0.211, probably due to the increase in gas velocity from 0.267 to 0.335 cm/s.

A similar trend was observed with an inlet glucose concentration of 70 g/l. A steady increase in liquid holdup, from 0.111 to 0.174 and then to 0.21, occured when the liquid velocity was increased from 0.0084 to 0.0175 and further to 0.0263 cm/s respectively. A further increase of liquid velocity to 0.0351 cm/s caused only a marginal increase in liquid holdup, to 0.234 (Fig. 5.57).

An overall effect of liquid velocity on liquid holdup is shown in figure 5.58 for all the inlet glucose concentrations studied. It is interesting to note that the data could be represented by straight lines of best fit, with positive slopes. This indicated that, for all the inlet glucose concentrations, increases in the liquid velocity caused linear increases in liquid holdup; an observation earlier reported by Michelsen and Ostergaard (1970), Ostergaard (1978), Kato *et al.* (1981) and Setiadi

(1989).

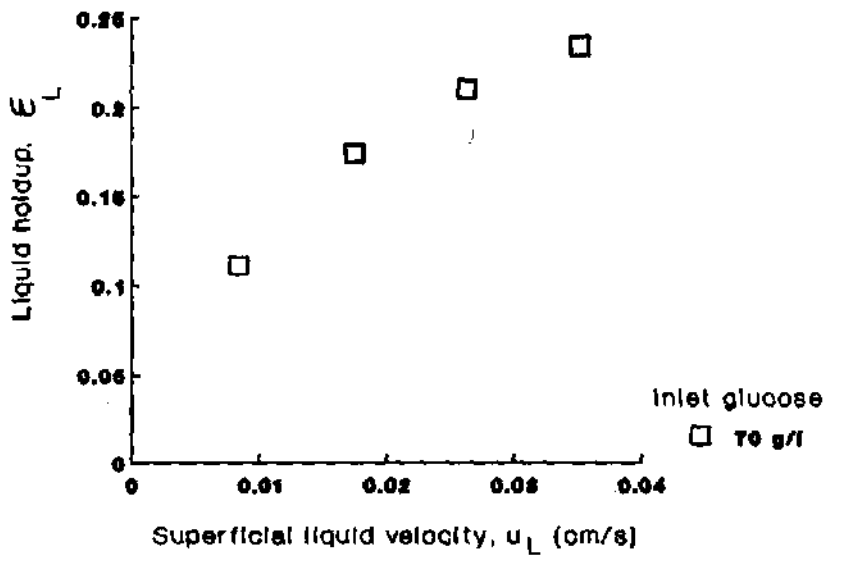


Fig. 5.57 Influence of liquid velocity on liquid holdup at inlet glucose concn. of 70 g/l

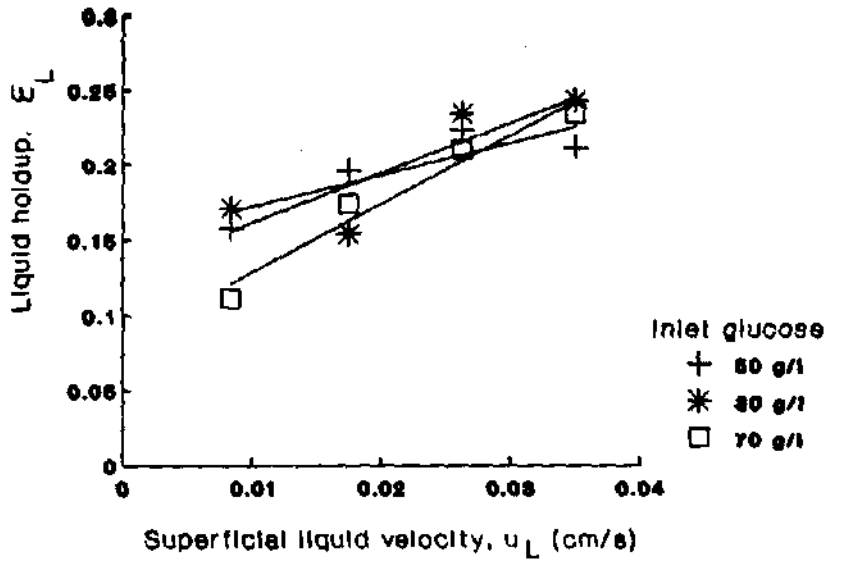


Fig. 5.58 Overall influence of liquid velocity on liquid holdup at all inlet glucose concentrations

This therefore mean that the increase in gas production, observed for an increase in liquid velocity, had less effect on liquid holdup than the liquid velocity itself.

Certainly, increases in liquid velocity are expected to increase the volume fraction of liquid within the yeast bed and, as such, the observations made in this study are expected.

5.5.1.3 *Axial variation in liquid holdup*

In order to assess the axial variation in liquid holdup, the holdup was determined at bed heights of 45 cm and 65 cm, using an inlet glucose concentration of 70 g/l and liquid velocities of 0.0175, 0.0263 and 0.0351 cm/s. The results obtained are presented in Table 5.25.

Table 5.25 Axial variation in liquid holdup

Liquid velocity, u_L (cm/s)	Liquid holdup, ε_L (-)		Gas velocity, u_g (cm/s)	
	45 cm	65 cm	45 cm	65 cm
0.0175	0.116	0.174	0.115	0.145
0.0263	0.179	0.210	0.112	0.159
0.0351	0.231	0.234	0.156	0.193

It is obvious that there was consistently higher liquid hold up for a bed height of 65 cm compared to 45 cm, at all the liquid velocities used, in spite of the increase in gas velocity which was noted to have a negative influence on liquid holdup.

It is not known why the expected decrease in liquid holdup, due to increasing gas velocity, did not occur. Perhaps, segregation of the bed might have taken place. Tower fermenter beds have been reported to segregate in accordance with the particle size distribution; with larger particles, having higher density, at the bottom of the tower and smaller ones at the upper parts (Andrews, 1986). If this happens, a higher solids concentration will

be expected at the bottom of the bed and this could cause lower liquid holdup in this lower section. These results, though not conclusive, indicate that there is an axial variation in liquid holdup, in fluidized bed anaerobic bioreactors, and that the nature of this variation is an increasing trend in the liquid holdup with increases in bed height.

5.5.1.4 *Correlations for liquid holdup*

A large number of correlations, relating liquid holdup to process parameters and particle properties have been developed, as discussed in section 3.5.2. But, the correlation of Richardson and Zaki (Eqn. 3.22a), has been the most widely used and was found to be applicable to fluidized bed bioreactors (Greenshields and Smith, 1971; Smith *et al.*, 1978; Hermanowicz and Ganzarczyk, 1983), even though it was derived for the two phase (S-L) systems. Therefore, in this section, the relationship between the liquid velocity and liquid holdup was investigated, by means of equation 3.22a. Furthermore, the effects of both liquid and gas superficial velocities were also simultaneously investigated, using multilinear regression technique.

A linearized form of equation 3.22a is given by:

$$Log(u_L) = Log(u_t) + nLog(\varepsilon_L) \qquad 5.7$$

Therefore, a plot of Log (u_L) against Log (ε_L) will give a straight line with slope of n and, a Y-axis, intercept of Log (u_t). These plots are shown in figures 5.59, 5.60 and 5.61, for inlet glucose concentrations of 30, 50 and 70 g/l, respectively and in figure 5.62, for strain Y6 at an inlet glucose concentration of 50 g/l. It can be seen that in all these fiqures, the data points could be represented by a straight line of best fit.

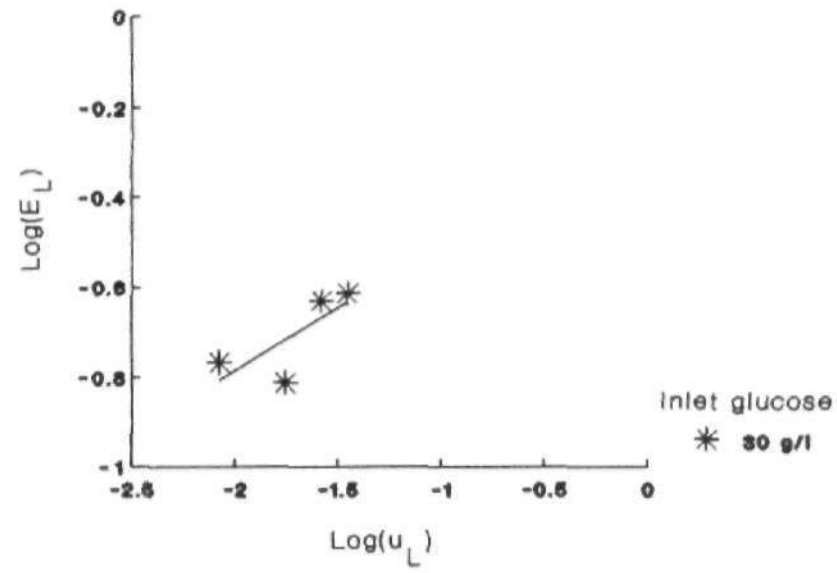


Fig. 5.59 Liquid velocity and holdup relationship at inlet glucose concn. of 30 g/l

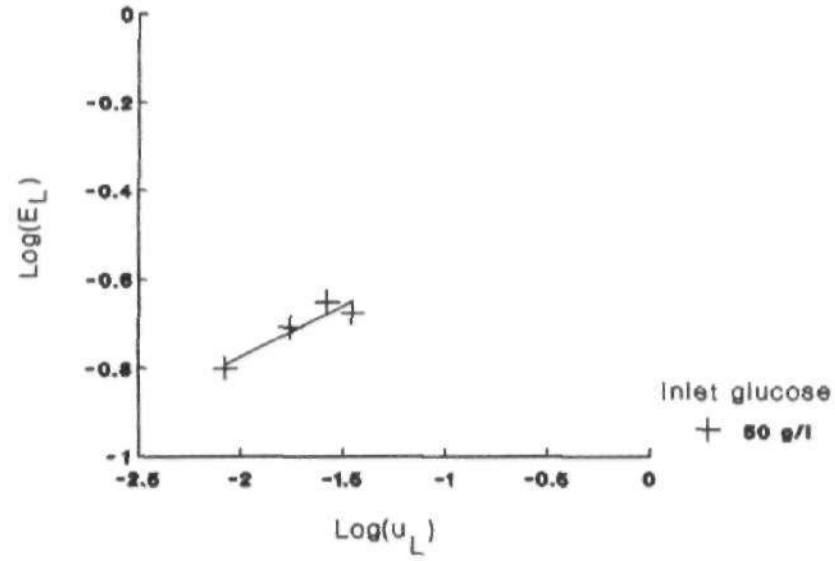


Fig. 5.60 Liquid velocity and holdup relationship at inlet glucose concn. of 50 g/l

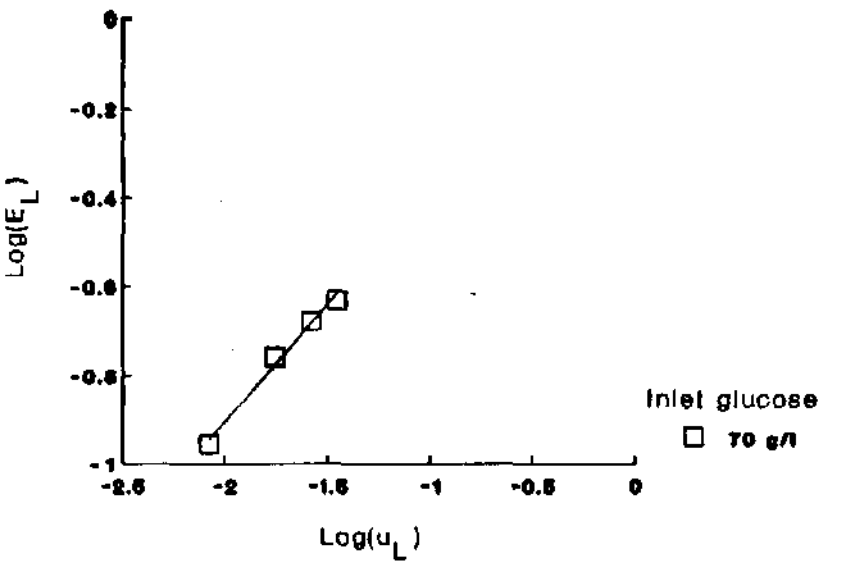


Fig. 5.61 Liquid velocity and holdup relationship at inlet glucose concn. of 70 g/l

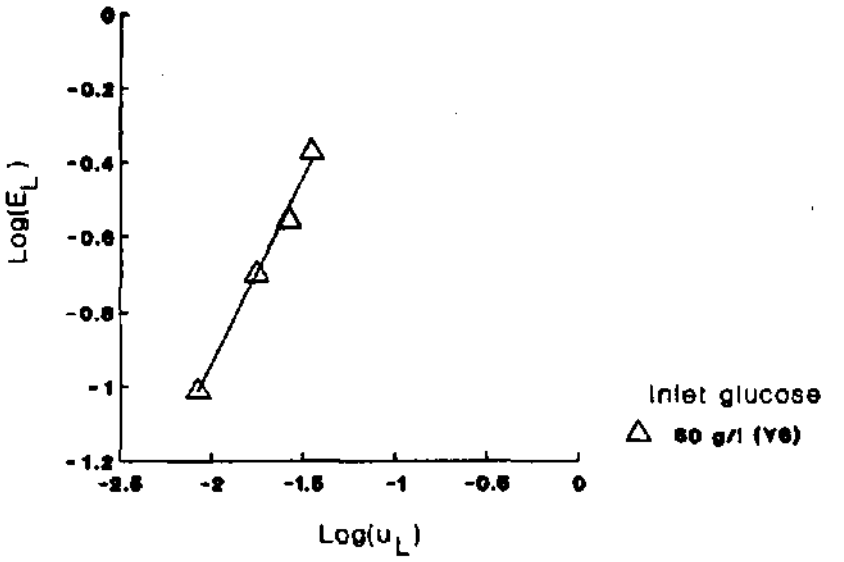


Fig. 5.62 Liquid velocity and holdup relationship at inlet glucose concn.of 50 g/l for strain Y6

A linear regression was performed and the results obtained are presented in Table 5.26.

Table 5.26 Values of n and settling velocity

Inlet glucose, C_{si} (g/l)	Exponent in eqn. 322a, n	Particle terminal vel., u_t (cm/s)	Correlation coefficient, R
30	0.278	0.590	0.761
50	0.227	0.479	0.936
	0.997'	11.34'	0.997'
70	0.528	1.414	0.995

' Values for yeast strain Y6.

It is clear that, except at the lowest inlet glucose concentration, the relationship between superficial liquid velocity and liquid holdup, can be well represented by equation 3.22a as indicated by the high correlation coefficients. Nonetheless, a further look at the values of n and the floc settling velocity u_t, suggests that these parameters are not constant but varied with strain type and with the inlet glucose concentration. The variation in the values of n and u_t with strain type is not suprising, because it was reported earlier by Brohan and McLoughlin (1984b). However, the variation of these parameters with inlet glucose concentration does indicate the possible effect of gas velocity. Therefore, the use of equation 3.22a, for predicting liquid holdup in tower fermenters, should be with great caution.

Furthermore, the values of n reported here are significantly different from the values of 4.4 and 11 reported, for yeast flocs, by Greenshields and Smith (1971) and Smith *et al.* (1978) respectively. It is important to note that both Greenshields and Smith (1971) and Smith *et al.* (1978) have used the bed voidage rather than liquid holdup, whereas it is the liquid holdup that

is required in order to evaluate liquid residence time in the bioreactor. Moreover, the results of Smith *et al.* (1978) were obtained from sedimentation studies whereas Greenshields and Smith (1971) arrived at their result by extrapolating the velocity-voidage curve. But, sedimentation tests are of limited use in predicting the expansion characteristics of fluidized beds, containing flocculent microorganisms, as noted by Brohan and McLoughlin (1984b). This is because retardation due to partial support within the yeast bed plays an important role in causing deviations from ideal behaviour. These differences in procedure, coupled with differences in the yeast strains used, could be responsible for the significant differences in the values of n obtained in this and the other two studies.

In order to take the effect of gas velocity, on the liquid hold up, into consideration, equation 5.8 was used.

$$\varepsilon_L = f(u_g, u_L) \rightarrow \varepsilon_L = c_1 u_g^{c_2} u_L^{c_3} \qquad 5.8)$$

Where c_1, c_2 and c_3 are constants. When linearized, equation 5.8 becomes:

$$Log(\varepsilon_L) = Log(c_1) + c_2 Log(u_g) + c_3 Log(u_L) \qquad 5.9)$$

Using multiple regression analysis, the values of c_1, c_2 and c_3 where found to be 0.847, -0.126 and 0.457 respectively. Hence, equation 5.9 can be written as:

$$\varepsilon_L = 0.847 u_g^{-0.126} u_L^{0.457} \qquad 5.10)$$

Both u_g and u_L are given in cm/s. Equation 5.10 has goodness of fit (R^2) of 74.3%, which may be considered fair. The t-ratio values of -0.21, -1.10 and 3.71 were obtained for the constant term, gas velocity an liquid velocity, respectively. This shows that the gas velocity has negligible influence on the liquid holdup.

However, a linear model was found to relate liquid

holdup to gas and liquid superficial velocities, better than the power relationship (Eqn. 5.10). This linear model is given in equation 5.11, with both u_g and u_L in cm/s.

$$\varepsilon_L = 0.124 - 0.067u_g + 3.85u_L \qquad 5.11)$$

Equation 5.11 has R^2 of 75.1%, which was an improvement over the exponential model. The t-ratios were 7.62, -0.58 and 3.47, for the constant, gas velocity and liquid velocity respectively. Again, the gas velocity has a weak effect on liquid holdup.

It is important to note that both the two models, used to correlate the liquid holdup to the gas and liquid superficial velocities, have low values of R^2. Perhaps other parameters such as particle size and liquid density, which have not been considered here, may have significant influence on the liquid holdup, causing R^2 to be low. Furthermore it has been noticed that, in both equations 5.10 and 5.11, the gas velocity causes a decrease in liquid holdup but its effect could be considered marginal. Using the linear model, neglecting the influence of gas velocity in calculating the liquid holdup, will cause an error of 8.5%, at the highest gas and liquid velocities of 0.335 and 0.0351 cm/s respectively. Similarly, the error will be 2.3%, at the lowest gas and liquid velocities of 0.054 and 0.0084 cm/s respectively. These levels of error could be tolerated and therefore, for gas velocities in the range 0.054 to 0.335 cm/s and liquid velocities in the range 0.0084 to 0.0351 cm/s, the influence of the gas velocity on the liquid holdup, can be neglected.

5.5.2 Estimation of bed voidage

Bed voidage was estimated from the difference in height between the dry and fluidized beds. There were two main problems with the measurements of the dry bed height. The compressible nature of the yeast flocs meant that, if left dry, the bed compressed and the resulting height

depended on the period the bed remained dry. The other problem was that as the dry bed settled, pockets of air were trapped and this caused a higher reading of the dry bed height. In view of these two problems, it was not possible to rely too much on the data for bed voidage, even though, effort was made to look out for trapped air and elimate its contribution to the dry bed height. Moreover, the bed was left dry for a constant period of 15 hours, before reading the dry bed height.

The bed voidage obtained at different gas and liquid superficial velocities is presented in Table 5.27.

Table 5.27 Estimate of bed voidage

Liquid velocity, u_l (cm/s)	Gas velocity, u_g (cm/s)	Dry bed height, H_{db} (cm)	Fluidized bed height, H_b (cm)	Bed voidage, ε (-)
0.0084	0.054	58	70	0.171
	0.087	42	50	0.160
	0.138	63	87	0.276
0.0175	0.099	55	69	0.203
	0.209	38	49	0.224
	0.298	66	88	0.250
0.0263	0.186	56	71	0.211
	0.267	42	55	0.236
	0.319	63	81	0.222
0.0351	0.279	54	74	0.270
	0.335	42	59	0.288
	0.306	55	84	0.345

The lowest value of the bed voidage was 0.16 and occured

at the lowest liquid velocity, while the highest was 0.345 which happened at the highest liquid velocity, as expected. It is important to note that the highest bed voidage was lower than 0.4, which was reported to be the voidage at the incipient or minimum fluidization condition (Greenshields and Smith, 1971). This confirmed that proper fluidization of the yeast bed was not achieved.

A further look at the bed voidage values indicates that there was an increase in bed voidage, at the same liquid velocity and this points to a possible influence of gas velocity on the bed voidage. This was, however, expected since an increase in gas velocity will be expected to cause an increase in fluidized bed height unless bed contraction occurs.

5.5.3 Estimation of gas and solid holdups

Gas holdup was estimated from the difference between bed voidage and liquid holdup, while the solid holdup was obtained by using equation 3.19a. The results are presented in Table 5.28 It is evident, from the results, that the contribution of the gas holdup to the bed voidage was very low at low gas velocities, but this increased markedly at high gas velocities and low liquid velocities as was the case at a gas velocity of 0.138 cm/s where the contribution was about 60%.

A further look at the results indicated that the gas contribution to bed voidage depended on the inlet glucose concentration; at a high inlet concentration, the contribution was high, even when the liquid velocity was high. Therefore, neglecting the contribution of the gas phase in determining the bed voidage, in this kind of bioreactor, as concluded by Davison (1988) and Setiadi (1989), could result in underestimating the bed voidage; although it should be remembered that the bed, in this work, was not fully fluidized.

Solid holdup remained high, in the range 0.84 to

0.72, for all the experiments, except at high liquid velocity and high inlet glucose concentration when it dropped to 0.66. This high solid holdup was probably responsible for the high ethanol productivity obtained in this bioreactor.

Table 5.28 Estimates of gas and solid holdups

Liquid velocity, u_L (cm/s)	Gas velocity, u_g (cm/s)	Gas holdup, ε_g (")	Solid holdup, c_s (-)	Contribution of c_q to bed voidage (*)
0.0084	0.054	0.001	0.83	0.58
	0.087	0.002	0.84	1.88
	0.138	0.165	0.72	59.78
0.0175	0.099	0.049	0.80	24.14
	0.209	0.029	0.78	11.48
	0.298	0.076	0.75	30.40
0.0263	0.186	-0.023	0.79	0.00
	0.267	0.013	0.76	5.51
	0.319	0.012	0.78	5.41
0.0351	0.279	0.027	0.73	10.37
	0.335	0.077	0.71	26.74
	0.306	0.111	0.66	32.17

5.5.4 Conclusion

It can be concluded that the liquid holdup, in this bioreactor, was affected by changes in both liquid and gas velocities. While increases in gas velocity decreased the liquid holdup, linearly, increases in liquid velocity increased the liquid holdup also in a linear manner. But, the error in neglecting the influence of gas velocity on

liquid hold up could be very little.

The relationship between liquid velocity and liquid holdup could be represented by a power correlation similar to that of Richardson and Zaki, but caution should be exercised in using this relationship, because the values of the exponent n and the settling velocity depended on the yeast strain used and on the inlet concentration of glucose employed.

The liquid holdup may not be constant, but may increase with increases in bed height due possibly to the effect of segregation of particles within the bed.

The bed voidage was also noted to depend on the inlet glucose concentration and the liquid velocity used. Furthermore, the contribution of gas velocity to the bed voidage was found to be high especially at low liquid velocity and high inlet glucose concentration. Therefore, estimating the bed voidage from the liquid holdup, alone, could result in significant error.

CHAPTER SIX

OVERALL DISCUSSION

6 OVERALL DISCUSSION

Immobilization of microorganisms provides a means for achieving high biomass concentration and high solids retention time in bioreactors. These are necessary requirements for high reactor productivity. Therefore, the successe in the development of immobilization techniques have brought about increasing interest in the use of novel bioreactors, which were found to have advantages, over the conventional batch and continuously stirred tank reactors. One of these novel reactors, is the fluidized bed bioreactor. The main advantage of this bioreactor is that the bioparticles are small with high surface areas, which are colonized by microorganisms, enabling the hydraulic retention time to be markedly reduced, resulting in high performance.

Fluidized bed bioreactors have been used for the manufacture of beer and vinegar (Greenshields and Smith, 1971) and for the treatment of domestic and industrial wastewaters (Sahm, 1984). However, despite their potential, they still remain in the laboratory and pilot scale stages. To date, only a few fluidized bed bioreactors are commercially in operation for the production of beer, vinegar and for the treatment of wastewaters (Heijnen *et al.*, 1989). One of the problems hindering the realization of their full potential, in the biochemical industry, is difficulty in modelling and, therefore, difficulty in predicting their performance (Venkatasubramanian *et al.*, 1983). This difficulty is due to the complex interaction of the various phases involved in the bioreactor. Furthermore, a number of biochemical processes produce gas in situ which adds to the complexity of the system.

However, some researchers (Ching *et al.*, 1984; Hamdane *et al.*, 1988; Setiadi and Larsen, 1991) have directed effort at the modelling of fluidized bed bioreactors. The model they all used was the dispersed

plug flow model. The axial liquid dispersion coefficient and liquid holdup are two of the important parameters in this model and are required for the evaluation and prediction of reactor performance. Though, there exists a large amount of information on the prediction of axial liquid dispersion coefficients and liquid holdup in fluidized beds, from process parameters and liquid and particle properties, the information relates to non-biological systems whereas different operating conditions and particles are used in biological systems. For example: In non-biological beds, particle Reynolds numbers are higher than 100, whereas they are lower than 100 in biological beds (Kikuchi *et al.*, 1984).

A few researchers have, however, studied liquid mixing and bed expansion by simulating gas producing anaerobic fluidized beds (Gommers *et al.*, 1986; Setiadi, 1989). They used conditions similar to those obtained in biological systems; typically low gas and liquid velocities and low density particles. But, such studies need to be verified against active biological beds in order to ascertain their applicabily to anaerobic fluidized bed system with *in situ* gas production.

In this work, the magnitude of liquid mixing and holdup, in a gas-producing anaerobic fluidized bed bioreactor and the effects of superficial liquid and gas velocities, on these parameters, were studied, using the residence time distribution technique with dextran blue as the tracer. Furthermore, tracer experiments were performed in order to find a suitable tracer material compatible with the flocculant yeast strains used. In addition, the performance of the bioreactor was evaluated.

The suitability of a tracer was assessed with respect to its effect on yeast metabolism, its metabolization by yeast, its adsorption on yeast cells and equipment, its absorption into yeast flocs and the effect of fermentation conditions on the tracer. These are all important

characteristics of a suitable tracer (Swaine and Daugulis, 1989).

Of the five tracers tested, only dextran blue was found to pass almost all the requirements, on account of its high molecular weight. Jimnez *et al.*, 1988 have also found dextran blue to be suitable for submerged biofilters. Fluorescein was absorbed by the flocs and a long tail in the RTD curve resulted. Using this tracer may require the inclusion of a diffusion term in the dispersed plug flow equation (Stevens *et al.*, 1986). In addition, its optical density was affected by pH. Decreases in pH, which ocurred during the fermentation, caused significant reduction in the optical density of fluorescein. Therefore, pH adjustments were necessary with this tracer. Aniline blue did not affect yeast metabolism but it disappeared, during anaerobic batch fermentation, possibly due to increased ethanol concentration. On the other hand, methyl green and methyl violet were found to promote and inhibit yeast growth respectively and are, therefore, not suitable as tracers in this system.

The performance of the bioreactor was comparable to others of the same type, though, higher productivity values were noted in this system on account of the high liquid thoughput used. The highest ethanol productivity, based on liquid volume, was about 138.37 g/(l.hr). The high biomass concentration of 48 to 63 g/l achieved in the reactor, coupled with the low hydraulic residence time, are thought to be responsible for the observed high ethanol productivities.

The liquid flow rate and the generated gas did not fluidize the bed properly. The yeast was noted to form very large agglomerates which might have caused high mass transfer resistance. Even then, a high glucose utilization, above 80% was obtained, in all cases, except one; at a liquid flow rate of 24 ml/min and an inlet glucose concentration of 70 g/l where glucose utilization

was found to be 76%. The biomass loss was noted to be low even at the highest liquid flow rate. This suggested that the yeast strains were of the fermentation limited type as defined by Greenshields and Smith, 1971.

The bubble size has an effect on the axial liquid dispersion coefficient, but the nature of the effect is dependent on the particle size. The inability to properly fluidize the bed and the subsequent formation of lumps of yeast could have had a significant effect on the bubble sizes and consequently on the values of D_z and the trends observed. An increase in gas velocity was noted to cause little increase in D_z, whereas increasing liquid velocity was found to increase D_z linearly at low gas velocities. But, at high gas velocities, an increase in liquid velocity caused a decrease in D_z possibly due to increased bed voidage. A similar trend was observed by Kim and Kim 1983, and Setiadi, 1989, for fluidized beds.

Axial variation of D_z was not pronounced due to the weak effect of gas velocity on the dispersion coefficient. A correlation of D_z with gas and liquid velocity, has indicated this weak effect, and further, a significance test has also confirmed that the effect of gas velocity could be neglected.

Results for the liquid holdup have shown trends similar to what was reported for fluidized beds. There was a decrease in liquid holdup due to increasing gas velocity. But, an increase in liquid velocity caused an increase in liquid holdup. The gas velocity was, however, noted to have little effect on liquid holdup. Therefore, for this sytem, the liquid holdup can be estimated from the liquid velocity alone.

The relationship between liquid velocity and liquid holdup could be represented by the equation of Richardson and Zaki (1954), but the exponent, n was found to have values that were significantly different from the values obtained by Greenshields and Smith, 1971 and Smith *et al.*,

1978. Furthermore, it is influenced by the strain type and the inlet glucose concentration. Therefore, the use of such correlations should be with extreme caution. A linear correlation was found to fit the liquid holdup data, with a goodness of fit of 75.1%.

Estimates of gas holdup have shown that the contribution of the gas phase to the bed voidage could be signigicant especially at low liquid velocity and high inlet glucose concentrations.

CHAPTER SEVEN

CONCLUSIONS

7 CONCLUSIONS

Based on the results obtained in this study, the following conclusions can be made.

1) Dextran blue is a suitable tracer for use in the determination of liquid residence time in gas producing anaerobic biorector containing flocculant *Saccharomyces cerevisiae*.

2) Fluorescein, aniline blue, methyl violet and methyl green are not suitable for residence time distribution study in bioreactor system containing yeast flocs.

3) The bioreactor used for this study is similar, in terms of ethanol productivity and glucose utilization, to other tower bioreactors containing flocs of yeast.

4) The magnitude of the axial liquid dispersion coefficient was high enough to affect the substrate concentration profile in the bioreactor.

5) The axial dispersion coefficient increased with increases in liquid velocity at low bed voidage, but decreased at high bed voidage.

6) Increases in gas velocity increased the axial liquid dispersion coefficient marginally.

7) Axial variation in axial liquid dispersion coefficient was not well pronounced in this system.

8) An increase in gas velocity decreases the liquid holdup linearly, but the effect is marginal.

9) Increases in liquid velocity increased the liquid holdup linearly.

10) The correlation of Richardson and Zaki (1954) was applicable to the liquid holdup data, but the exponent n, was noted to depend not only on the strain type but also on inlet glucose concentration.

11) Any axial variation in liquid holdup was not pronounced.

12) The contribution of gas holdup to the bed voidage could be high at low liquid velocity and high inlet glucose concentrations.

CHAPTER EIGHT

RECOMMENDATIONS FOR FUTURE WORK

5) Large columns need to be used in liquid phase mixing and bed expansion studies, in order to understand the effect of liquid circulation on these parameters. This may also make the results more readily acceptable for industrial scale applications.

6) The method for floc sampling need to be improved. Their fragile nature and bed contamination should, however, be taken into consideration.

7) Another method for measuring the pressure drop across the fluidized bed needs to be devised, because the conventional manometric method does not work with this system.

8) There is need to integrate results from mixing and hydrodynamic studies with the kinetic and mass transfer aspects, in order to have a complete model of the system.

REFERENCES

Atkinson, B. and Daoud, I.S. (1976) 'Microbial flocs and flocculation process engineering', Advances in Biochemical Engineering and Biotechnology, Vol. 4, edt. T.K.Ghose, A.Fiechter and N. Blakebrough, 41-124

Ault, R.G., Hampton, A.N., Newton, R. and Roberts, R.H.,

REFERENCES

Admassu, W., Korus, R.A. and Heimsch, R.C., (1985), 'Ethanol fermentation with a flocculating yeast', The Chemical Engineering Journal, Vol. 31, B1-B8

Aiba, S. and Nagatani, M. (1971) 'Separation of cells from culture media', Advances in Biochemical Engineering and Biotechnology, Vol. 1, edt. T.K.Ghose and A.Fiechter, 31-54

Aiba, S., Shoda, M. and Nagatani, M., (1968), 'Kinetics of product inhibition in alcohol fermentation', Biotechnology and Bioengineering, Vol. 10, 845-864

Andrews, G.F., (1986), 'Selecting particles for fluidized bed bioreactors with flocculent biomass', Biotechnology Progress, Vol 2, No. 1, March, 16-22

Andrews, G.F. and Przezdziecki, J., (1986), 'Design of fluidized bed fermenters', Biotechnology and Bioengineering, Vol. 28, 802-810

Anselme, M.J. and Tedder, D.W., (1987), 'Characteristics of immobilized yeast producing ethanol from glucose', Biotechnology and Bioengineering, Vol. 30, 736-745

Ationu, A. (1986) 'Comparison of fixed *Acetobacter* film fermenter systems', Ph.D. Thesis, University of Strathclyde, Glasgow

Atkinson, B. and Fowler, H.W., (1974), 'The significance of microbial film in fermenters', Advances in Biochemical Engineering and Biotechnology, Vol. 3, edt. T.K.Ghose, A.Fiechter and N. Blakebrough, 221-277

Boening, P.H. and Larsen, V,F., (1982), 'Anaerobic fluidized bed whey treatment', Biotechnology and Bioengineering, Vol. 24, 2539-2556

Boontanjai, C., (1983), 'Tower fermentation of whey permeate and sucrose enriched whey permeate to ethanol', Ph.D. Thesis, Massey University, New Zealand

Brohan, B. and McLoughlin, A.J. (1984a) 'The influence of yeast metabolism on dispersion in fluidized yeast bed', Appl. Microbiol. Biotechnol., 20: 146 - 149

Brohan, B. and McLoughlin, A.J. (1984b) 'The behaviour of yeast flocs in hindered settling and fluidized bed regimes', Appl. Microbiol. Biotechnol., 20: 10 - 15

Brohan, B. and McLoughlin, A.J. (1984c) 'Characterization of the physical properties of yeast flocs', Appl. Microbiol. Biotechnol., 20: 16 - 22

Brown, C.D. (1988) 'A study of the physiology and kinetics of recombinant yeast fermentations', Ph.D. Thesis, University of Strathclyde, Glasgow

Bull, M.A., Sterritt, R.M. and Lester, J.N. (1982) 'The effect of organic loading on the performance of anaerobic fluidized beds treating high strength wastewaters', Trans. Instn. Chem. Engr., Vol. 60, 373-376

Bull, M.A., Sterritt, R.M. and Lester, J.N., (1984), 'An evaluation of single and separated phase anaerobic industrial wastewater treatment in fluidized bed reactors', Biotechnology and Bioengineering, Vol. 26, 1054-1065

Cairns, E.J. and Prausnitz, J.M., (1960), 'Longitudinal mixing in fluidization', AIChE Journal, September, 400-405

Chang, M.M., Chou, T.Y.C. and Tsao, G.T., (1981), 'Structure, pretreatment and hydrolysis of cellulose', Advances in Biochemical Engineering and Biotechnology, Vol. 20, edt. A. Fiechter, 15-42

Chen, S.J., Li, C.T. and Shieh, W.K., (1985a), 'Performance evaluation of the anaerobic fluidized bed system: I. Substrate utilization and gas production', J. Chem. Tech. Biotechnol., Vol. 35B, 101-109

Chen, S.J., Li, C.T. and Shieh, W.K., (1985b), 'Performance evaluation of the anaerobic fluidized bed system: II. Biomass holdup and characteristics', J. Chem. Tech. Biotechnol., Vol. 35B, 183-190

Ching, C.B., Ho, Y.Y. and Rathor, M.N., (1984), 'Isomerization of glucose to fructose in a fluidized bed reactor', Biotechnology and Bioengineering, Vol. 26, 820-823

Chung, S.F. and Wen, C.Y., (1968), 'Longitudinal dispersion of liquid flowing through fixed and fluidized beds', AIChE Journal, Vol. 14, No. 6, 857-866

Coppella, S.J. and Durjati, P., (1989), 'A detailed analysis of Saccharomyces cerevisiae growth kinetics in batch, fed-batch and hollow fibre biorectors', The Chemical Engineering Journal, Vol. 41, B27-B35

Couderc, J.-P., (1985), 'Incipient fluidization and particulate systems', in Fluidization, Second edition, edt. by J.F. Davidson, R. Clift and D. Harrison, Academic Press, 1-46

Coulson, J.M. and Richardson, J.F. (1979) 'Chemical Engineering', Vol. 3, 2ed., Pergamon press

Dakshinamurty, P., Subrahmanyam, V. and Rao, J.N., (1971), 'Bed porosities in gas-liquid fluidization', Ind. Eng. Chem., Process Des. Develop., Vol. 10, No. 3, 322-328

Danckwerts, P.V., (1981), 'Insights into Chemical Engineering', Pergamon Press

Darton, R.C., (1985), 'The physical behaviour of three phase fluidized beds', in Fluidization, Second edition, edt. by J.F. Davidson, R. Clift and D. Harrison, Academic Press, 495-528

Darton, R.C. and Harrison, D., (1975), 'Gas and Liquid holdup in three phase fluidization', Chemical Engineering Science, Vol. 30, 581 - 586

Davison, B.H., (1988), 'Dispersion and holdup in three phase fluidized bed bioreactor', Presented at the tenth symposium on biotechnology for fuels and chemicals, Gatlinburg, Tennessee, May 16-20

Deeslie, W.D. and Cheryan, M. (1981) 'A CSTR - hollow fibre system for continuous hydrolysis of proteins: Performance and kinetics', Biotechnol. Bioeng., Vol. 23, 2257

El-Temtamy, S.A. and Epstein, N., (1979), 'Contraction or expansion of three phase fluidized beds containing fine/light solids', The Canadian Journal of Chemical Engineering, Vol. 57, August, 520-522

El-Temtamy, S.E., El-Sharnoubi, Y.O. and El-Halwagi, M.M., (1979a), 'Liquid dispersion in gas-liquid fluidized beds: Part I. Axial dispersion. The axially dispersed plug-flow model', The Chemical Engineering Journal, Vol. 18, 151-159

El-Temtamy, S.E., El-Sharnoubi, Y.O. and El-Halwagi, M.M., (1979b), 'Liquid dispersion in gas-liquid fluidized beds: Part II. Axial and Radial dispersion. The plug flow model', The Chemical Engineering Journal, Vol. 18, 161-168

Epstein, N., (1976), 'Criterion for initial contraction or expansion of three phase fluidized beds', The Canadian Journal of Chemical Engineering, Vol. 54, August, 259-263

Epstein, N. (1981) 'Three phase fluidization: Some knowledge gaps', The Canadian Journal of Chemical Engineering, Vol. 59, December, 649-657

Falch, E.A. and Gaden, Jr., E.L., (1970), 'A continuous, multistage tower fermenter: II. Analysis of reactor performance', Biotechnology and Bioengineering, Vol. 12, 465-482

Fan, L.-S., (1989), 'Gas-liquid-solid Fluidization Engineering', Butterworths

Garcia, I.G., Martin, A.M., Ruiz, O.J.M. and Parez, A.C. (1989) 'Kinetic study of the production of ethanol with *Saccharomyces cerevisiae* immobilized on berl saddles', The Chem. Eng. J. Vol. 42, B1-B7

Garside, J. and Al-Dibouni, M.R., (1977), 'Velocity-Voidage relatioships for fluidization and sedimentation in solid-liquid systems', Ind. Eng. Chem., Process Des. Develop., Vol. 16, No. 2, 206-214

Ghose, T.K. and Tyagi, R.D., (1979a), 'Rapid ethanol fermentation of cellulose hydrolysate. I. Batch versus continuous systems', Biotechnology and Bioengineering, Vol. 21, 1387-1400

Ghose, T.K. and Tyagi, R.D., (1979b), 'Rapid ethanol fermentation of cellulose hydrolysate. II. Product and substrate inhibition and optimization of fermenter design', Biotechnology and Bioengineering, Vol. 21, 1401-1420

Godia, F., Casas, C. and Sola, C., (1987a), 'Mathematical modelization of a packed bed reactor performance with immobilized yeast for ethanol fermentation', Biotechnology and Bioengineering, Vol. 30, 836-843

Godia, F., Casas, C. and Sola, C., (1987b), 'A survey of continuous ethanol fermentation systems using immobilized cells', Process Biochemistry, April, 43-48

Gommers, P.J.F., Christoffels, L.P., Kuenen, J.G. and Luyben, K.Ch.A.M., (1986), 'Gas phase influence on the mixing in a fluidized bed bioreactor', Appl. Microbiol. Biotechnol., Vol. 25, 1-7

Gommers, P.J.F., Bijleveld, W. and Kuenen, J.G., (1988a), 'Simultaneous sulphide and acetate oxidation in a denitrifying fluidized bed reactor: I. Start-up and reactor performance', Water Research, Vol. 22, No. 9, 1075-1083

Gommers, P.J.F., Bijleveld, W., Zuijderwijk, F.J.M. and Kuenen, J.G., (1988b), 'Simultaneous sulphide and acetate oxidation in a denitrifying fluidized bed reactor: II. Measurements of activities and conversion', Water Research, Vol. 22, No. 9, 1085-1092

Gong, Ch.-S., Chen, L.F., Flickinger, M.C. and Tsao, G.T., (1981), 'Conversion of hemicellulose carbohydrates', Advances in Biochemical Engineering and Biotechnology, Vol. 20, edt. A. Fiechter, 93-118

Gorowara, R.L. and Fan, L.-S., (1990), 'Effects of surfactants on three phase fluidized bed hydrodynamics', Ind. Eng. Chem. Res., Vol. 29, 882-891

Gorris, L.G.M., van Deursen, J.M.A., van der Drift, C. and Vogels, G.D., (1989), 'Biofilm development in laboratory methanogenic fluidized bed reactors, Biotechnology and Bioengineering, Vol. 33, No. 1, 687-693

Greenshields, R.N., and Smith, E.L., (1971), 'Tower fermentation systems and their applications', The Chemical Engineer, May, 182 - 190

Hamdane, M., Wilhelm, A.M. and Riba, J.P., (1988), 'Modelling of a fluidized bed immobilized enzyme reactor: Application to the hydrolysis of maltodextrines', The Chemical Engineering Journal, Vol. 39, B25-B30

Heijnen, J.J., Mulder, A., Enger, W. and Hoeks, F., (1989), 'A review on the application of anaerobic fluidized bed reactors in wastewater treatment', The Chemical Engineering Journal, Vol. 41, B37-B50

Hermanowicz, S.W. and Ganczarczyk, J.J., (1983), 'Some fluidization characteristics of biological beds' Biotechnology and Bioengineeering, Vol. 25, 1321 - 1330

Himmelblau, D.M. (1970) 'Process analysis by statistical methods', John Wiley & Sons, Inc., 135

Hoppe, G.K. and Hansford, G.S., (1982), 'Ethanol inhibition of continuous anaerobic yeast growth', Biotechnology Letters, Vol. 4, No. 1, 39-44

Hoppe, G.K. and Hansford, G.S., (1984), 'The effect of micro-aerobic conditions on continuous ethanol production by *Saccharomyces cerevisiae*', Biotechnology Letters, Vol. 6, No. 10, 681-686

Inloes, D.S., Tylor, D.P., Cohen, S.N., Michaels, A.S. and Robertson, C.R. (1983) 'Ethanol production by *Saccharomyces cerevisiae* immobilized in hollow fibre membrane bioreactors', Applied Environmental Microbiology, Vol. 46, 264-278

Jewell, W.J. (1985) 'The development of anaerobic wastewater treatment', Proceedings of the Seminar/Workshop Anaerobic Treatment of Sewage, edt. M.S. Switzenbaum, June 27-28, University of Massachusetts at Amherst, U.S.A., 17-54

Jimenez, B., Noyola, A., Capdeville, B., Roustan, M. and Faup, G. (1988) 'Dextran blue colorant as a reliable tracer in submerged filters', Water Research, Vol. 22, No. 10, 1253-1257

Jones, R.P. and Greenfield, P.F, (1984), 'Kinetics of apparent cell death in yeasts induced by ethanol', Biotechnology Letters, Vol. 6, No. 7, 471-476

Jones, R.P., Pamment, N. and Greenfield, P.F., (1981), 'Alcohol fermentation by yeast: The effect of environmental and other variables', Process Biochemistry, Vol. 16, No. 3, April/May, 42-49

Jones. S.T., Korus, R.A., Admassu, W. and Heimsch, R.C., (1984), 'Ethanol fermentation in a continuous tower fermenter', Biotechnology and Bioengineering, Vol. 26, 742-747

Joshi, J.B., (1980), 'Axial mixing in multiphase contactors; A unified correlation', Trans. IChemE, Vol. 58, 155-165

Karkare, S.B., Dean Jr., R.C. and Venkatasubramanian, K., (1985), 'Continuous fermentation with fluidized slurries of immobilized microorganisms', Bio/Technology, Vol. 3, March, 247-251

Kato, Y., Uchida, K., Kago, T. and Morooka, S., (1981), 'Liquid holdup and heat transfer coefficient between bed and wall in liquid-solid and gas-liquid-solid fluidized beds', Powder Technology, Vol. 28, 173-179

Kato, Y., Morooka, S., Koyama, M., Kago, T. and Yang, S.-Z., (1985), 'Longitudinal dispersion coefficient of liquid in three phase fluidized bed for gas-liquid-solid systems', Journal of Chemical Engineering of Japan, Vol. 18, No. 4, 313-318

Keim, C.R. and Venkatasubramanian, K. (1989) 'Economics of current biotechnological methods of producing ethanol', TIBTECH, Vol. 7, February, 22-29

Kennedy, J.F. and Cabral, J.M.S., (1983), 'Immobilized living cells and their applications', Applied Biochemistry and Bioengineering; Immobilized Microbial Cells, Vol. 4, edt. by I. Chibata and L.B. Wingard, Jr., Academic Press, 189-280

Kikuchi, K.-I., Konno, H., Kakutani, S., Sugawara, T. and Ohashi, H., (1984), 'Axial dispersion of liquid in liquid fluidized beds in the low Reynolds number region', Journal of Chemical Engineering of Japan, Vol. 17, No. 4, 362-367

Kim, S.D. and Kim, C.H., (1983), 'Axial dispersion characteristics of three phase fluidized beds', Journal of Chemical Engineering of Japan, Vol. 16, No. 3, 172-178

Kim, S.D., Baker, C.G.J. and Bergougnou, M.A., (1972) 'Holdup and axial mixing characteristics of two and three phase fluidized beds', The Canadian Journal of Chemical Engineering, Vol. 50, December, 695-701

Kim, S.D., Baker, G.J. and Bergougnou, M.A., (1975) 'Phase holdup characteristics of three phase fluidized beds', The Canadian Journal of Chemical Engineering, Vol. 53, April, 134 - 139

Kim, S.D., Baker, C.G.J. and Bergougnou, M.A., (1977), 'Bubble characteristics in three phase fluidized beds', Chemical Engineering Science, Vol. 32, 1299-1306

Klein, J. and Wagner, F., (1983), 'Methods for the immobilization of microbial cells', Applied Biochemistry and Bioengineering; Immobilized Microbial Cells, Vol. 4, edt. by I. Chibata and L.B. Wingard, Jr., Academic Press, 11-51

Klein, J., vorlop, K.D., Eng, H., Kluge, M. and Washausen, P. (1979) 'Procedures for polymer entrapment of whole cells', in characterization of immobilized biocatalysts, DECHEMA Manographs, Vol. 84, Verlag Chemie, 274-276

Kmiec, A. (1982) 'Equilibrium of forces in a fluidized bed -Experimental verification', The Chemical Engineering Journal, Vol. 23, 133-136

Kosaric, N. and Blaszczyk, R., (1990), 'Microbial aggregates in anaerobic wastewater treatment', Advances in Biochemical Engineering and Biotechnology, Vol. 42, edt. A. Fiechter, 27-62

Kosaric, N., Duvnjak, Z. and Stewart, G.G., (1981), 'Fuel ethanol from biomass: Production, Economics and Energy', Advances in Biochemical Engineering and Biotechnology, Vol. 20, edt. A. Fiechter, 119-151

Krishnaswamy, P.R. and Shemilt, L.W., (1972), 'Correlations for axial mixing in liquid fluidized beds', The Canadian Journal of Chemical Engineering, Vol. 50, June, 419-420

Krishnaswamy, P.R. and Shemilt, L.W., (1973), 'Frequency response in liquid fluidized systems: Part I. Effect of particle density and size', The Canadian Journal of Chemical Engineering, Vol. 51, December, 680-687

Krishnaswamy, P.R., Ganapathy, R. and Shemilt, L.W., (1978), 'Correlating parameters for axial dispersion in liquid fluidized systems', The Canadian Journal of Chemical Engineering, Vol. 56, October, 550-553

Lee, T.H., Ahn, J.C. and Ryu, D.D.Y., (1983), 'Performance of an immobilized yeast reactor system for ethanol production', Enzyme Microb. Technol., Vol. 5, January, 41-45

Levenspiel, O. (1972) 'Chemical Reaction Engineering', John Willey & Sons

Lievense, J.C. and Lim, H.C. (1982) 'The growth and dynamics of *Saccharomyces cerevisiae*', Annual Report on Fermentation Processes, Vol. 5, 211-262

Lin, S.H. (1991) 'A mathematical model for biological fluidized bed reactor', J. Chem. Tech. Biotechnol., Vol. 51, 473-482

Linko, P. and Linko, Y.-Y., (1983), 'Applications of immobilized microbial cells', Applied Biochemistry and Bioengineering; Immobilized Microbial Cells, Vol. 4, edt. by I. Chibata and L.B. Wingard, Jr., Academic Press, 53-151

MacDonald, W.J., (1991), 'Bioreactor development for ethanol production by *Pachysolen tannophilus*; Application of a novel soft packing material', Ph.D. Thesis, University of Strathclyde, Glasgow.

Maiorella, B., Wilke, Ch.R. and Blanch, H.W., (1981), 'Alcohol production and recovery', Advances in Biochemical Engineering and Biotechnology, Vol. 20, edt. A. Fiechter, 41-92

Maiorella, B.L., Blanch, H.W. and Wilke, C.R., (1984), 'Feed component inhibition in ethanolic fermentation by *Saccharomyces cerevisiae*', Biotechnology and Bioengineering, Vol. 26, 1155-1166

Margaritis, A. and Merchant, F.J.A., (1987), 'The technology of anaerobic yeast growth', Yeast biotechnology, edt. by D.R. Berry, I. Russell and G.G. Stewart, Allen and Unwin Inc., 231-276

Mecklenburgh, J.C. and Hartland, S., (1975), 'The theory of backmixing', John Wiley & Sons, 41

Mehaia, M.A. and Cheryan, M., (1984), 'Ethanol production in a hollow fiber bioreactor using S. cerevisiae', Appl. Microbiol. Biotechnol., Vol. 20, 100-104

Mehta, S.C. and Shemilt, L.W., (1976), 'Frequency response of liquid fluidized systems: Part II. Effect of liquid viscosity', The Canadian Journal of Chemical Engineering, Vol. 54, February/April, 43-51

Michelsen, M.L. and Ostergaard, K. (1970) 'Holdup and fluid mixing in gas-liquid fluidized beds', The Chemical Engineering Journal, Vol. 1, 37-45

Morikawa, Y., Karube, I. and Suzuki, S., (1980), 'Continuous production of Bacitracin by immobilized living whole cells of *Bacillus sp.*, Biotechnology and Bioengineering, Vol. 22, 1015-1023

Muroyama, K. and Fan, L.-S., (1985), 'Fundamentals of gas-liquid-solid fluidization', AIChE Journal, Vol. 31, No. 1, 1-34

Muroyama, K., Hashimoto, K., Kawabata, T. and Shiota, M. (1978) 'Axial liquid mixing in three phase fluidized bed', Kagaku Kogaku Ronbunshu, Vol. 4, 622-628, as reported in Muroyama and Fan (1985)

Nagashima, M., Azuma, M., Noguchi, S., Inuzuka, K. and Samejima, H., (1984), 'Continuous ethanol fermentation using immobilized yeast cells', Biotechnology and Bioengineering, Vol. 26, 992-997

Narjari, N.K., Khilar, K.C. and Mahajan, S.P., (1984), 'Biological denitrification in a fluidized bed', Biotechnology and Bioengineering, Vol. 26, 1445-1448

Nauman, E.B., (1981), 'Residence time distributions and micromixing', Chem. Eng. Commun., Vol. 8, 53-131

Netto, C.B., Destruhaut, A. and Goma, G. (1985) 'Ethanol fermentation by flocculent yeast: Performance and stability dependence on critical fermentation rate', Biotechnology Letters, Vol. 7, No. 5, 355-360

Ngian, K.-F. and Martin, W.R.B., (1980), 'Bed expansion characteristics of liquid fluidized particles with attached microbial growth', Biotechnology and Bioengineering, Vol. 22, 1843-1856

Nguyen-Tien, K., Patwari, A.N., Schumpe, A. and Deckwer, W.-D. (1984) 'Liquid dispersion in three phase fluidized beds', Journal of Chemical Engineering of Japan, Vol. 17, No. 6, 652-653

Nikov, I., Grandjean, B.P.A., Carreau, P.J. and Paris, J., (1990), 'Viscosity effects in cocurrent three phase fluidization', AIChE Journal, Vol. 36, No. 10, 1613 - 1616

Ostergaard, K. (1978) 'Holdup, Mass transfer and Mixing in three phase fluidization', AIChE Symposium Series, Vol. 74, No. 176, 82 - 86

Parsons, R.V., McDuffie, N.G. and Din, G.A., (1984), 'pH inhibition of yeast ethanol fermentation in continuous culture', Biotechnology Letters, Vol. 6, No. 10, 677-680

Pfeffer, J.T. and Suidan, M.T., (1989), 'Continuous processing of toxic organics in a fluidized bed granular activated carbon (GAC) reactor', Biotechnology and Bioengineering, Vol. 33, No. 1, 139-148

Prince, I.G. and Barford, J.P., (1982a), 'Continuous tower fermentation for power ethanol production', Biotecnology Letters, Vol. 4, No. 4, 263-268

Prince, I.G. and Barford, J.P., (1982b), 'Tower fermentation of sugar cane juice', Biotecnology Letters, Vol. 4, No. 7, 469-474

Prince, I.G. and Barford, J.P., (1982c), 'Tower fermentation using *Zymomonas mobilis* for ethanol production', Biotecnology Letters, Vol. 4, No. 8, 525-530

Ramamurthy, K. and Subbaraju, K., (1973), 'Bed expansion characteristics of annular liquid fluidized bed', Ind. Eng. Chem. Process Des. Develop., Vol. 12, No. 2, 184-189

Richardson, J.F. and Zaki, W.N. (1954) 'Sedimentation and fluidization: Part I, Trans, Instn. Chem. Engr., Vol. 32, 35-53

Richardson, J.F. and Meikle, R.A. (1961) 'Sedimentation and fluidization part III: The sedimentation of uniform fine particles and of two component mixtures of solids', Trans. Instn. Chem. Engrs., Vol. 39, 348 - 356

Rodrigues, A.E., Zuping, L. and Loureiro, J.M., (1991), 'Residence time distribution of inert and linearly adsorbed species in a fixed bed containing ''large-pore'' supports: Applications in separation engineering', Chemical Engineering Science, Vol. 46, No. 11, 2765-2773

Ruggeri, B., Specchia, V., Sassi, G. and Gianetto, A. (1988) 'Numerical estimation of biokinetic parameters', The Chemical Engineering Journal, Vol. 39, B17-B24

Saberian-Broudjenni, M., Wild, G. and Kim, S.D. (1989) 'Liquid axial dispersion in gas-liquid-solid fluidized beds', The Chemical Engineering Journal, Vol. 40, 83-92

Saberian-Broudjenni, M., Wild, G., Charpentier, J.-C., Fortin, Y., Euzen, J.-P. and Patoux, R. (1987) 'Contribution to the hydrodynamic study of gas-liquid-solid fluidized bed reactors,' International Chemical Engineering, Vol. 27, No. 3, 423 -440

Sahm, H., (1984), 'Anaerobic wastewater treatment', Advances in Biochemical Engineering and Biotechnology, Vol. 29, edt. A. Fiechter, 83-115

Schoutens, G.H., Guilt, R.D., Zieleman, G.J., Luyben, K.C.A.M. and Kossen, N.W.F. (1986) 'A comparative study of a fluidized bed reactor and gas lift loop reactorfor IBE process: Part I. Reactor design and scale down approach', J. Chem. Technol. Biotechnol., Vol. 36, 335-343

Schugerl, K. (1989) 'Biofluidization: Application of the fluidization technique in biotechnology', The Canadian Journal of Chemical Engineering, Vol. 67, 178-184

Scott, C.D. (1983) 'Ethanol production in fluidized bed bioreactor utilizing flocculating *Zymomonas mobilis* with biomass recycle', Biotechnology and Bioengineering Symposium, No. 13 287-298

Scott, C.D., (1987), 'Immobilized cells: A review of recent literature', Enzyme Microb. Technol., Vol. 9, February, 66-73

Setiadi, T. (1989) 'Liquid mixing and bed expansion in a fluidized bed reactor with particular reference to gas producing anaerobic systems', Ph.D. Thesis, University of Strathclyde, Glasgow

Setiadi, T. and Larsen, V.F. (1991) 'Modelling of concentration profiles in tower fermenter: The influence of the axial dispersion coefficient', Biotecnology Letters, Vol. 13, No. 9, 647-652

Shieh, W.K. and Keenan, J.D., (1986), 'Fluidized bed biofilm reactor for wastewater treatment', Advances in Biochemical Engineering and Biotechnology, Vol. 33, edt. A. Fiechter, 131-169

Shieh, W.K., Sutton, P.M. and Kos, P., (1981), 'Predicting biomass concentration in fluidized bed system', Journal of WPCF, Vol. 53, 11, 1574-1584

Smith, E.L., and Greenshields, R.N., (1973), 'Tower fermentation systems: Their application in continuous brewing', Biotechnol. and Bioeng. Symp., No. 4, 519 - 533

Smith, E.L., James, A. and Fidgett, M., (1978), 'Fluidization of microbial aggregates in tower fermenters', in Fluidization: Proceedings of the second engineering conference, edt. J.F.Davison and D.L.Keairns, Cambridge University press, 196 - 201

Song, W.Y., (1978), 'Bed expansion in three phase fluidization' Ind. Eng. Chem. Process Des. Dev., vol. 17, No. 1, 33 -36

Stevens, D.K., Berthouex, P.M. and Chapman, T.W., (1986), 'The effect of tracer diffusion in biofilm on the residence time distributions', Water Research, Vol. 20, No. 3, 369-375

Stronach, S.M., Rudd, T. and Lester, J.N. (1986a) 'The influence of variable organic loading on the start-up of an anaerobic fluidized bed reactor, Biotechnology Letters, Vol. 8, No. 7, 521-524

Stronach, S.M., Rudd, T. and Lester, J.N. (1986b) 'Anaerobic digestion processes in industrial wastewater treatment', Biotechnology Monographs, Vol. 2, edt. by L.T. Fan, A. Fiechter and K. Schugerl, Springer-Verlag Inc, New York.

Stronach, S.M., Diaz-Baez, M.C., Rudd, T. and Lester, J.N. (1987) 'Factors affecting biomass attachment during startup and operation of anaerobic fluidized beds', Biotechnology and Bioengineering, Vol. 30, 611-620

Swaine, D.E. and Daugulis, A., (1988), 'Review of liquid mixing in packed bed biological reactors', Biotechnology Progress, Vol. 4, No. 3, 134-148

Swaine, D.E. and Daugulis, A.J., (1989), 'Liquid residence time distributions in immobilized cell bioreactors', Biotechnology and Bioengineering, Vol. 33, 604-612

Switzenbaum, M.S., (1985), 'Fluidized bed anaerobic reactors', in Comprehensive Biotechnology, Vol. 4, ed. M. Moo-Young, Pergamon Press, 1017-1026

Tambo, N. and Watanabe, Y., (1979), 'Physical characteristics of flocs -I. The floc density function and aluminium floc', Water Research, Vol. 13, 409 - 419

Tang, W.-T. and Fan, L.-S., (1989), 'Hydrodynamics of a three phase fluidized bed containing low density particles', AIChE Journal, Vol. 35, No. 3, 355-364

Timmermans, P. and Van Haute, A., (1984), 'Influence of the type of organisms on the biomass holdup in a fluidized bed reactor', Appl. Microbiol. Biotechnol., Vol. 19, 36-43

Vail, Y.K., Manakov, N.Kh. and Manshilin, V.V., (1968), 'Turbulent mixing in a three phase fluidized bed', Intanational Chemical Engineering, Vol. 8, No. 2, 293-296

van Deemter, J.J., (1985), 'Mixing in fluidization', in Fluidization, Second edition, edt. by J.F. Davidson, R. Clift and D. Harrison, Academic Press, 331-355

Venkatasubramanian, K., Karkare, S.B. and Vieth, W.R., (1983), 'Chemical Engineering analysis of Immobilized cell systems', Applied Biochemistry and Bioengineering; Immobilized Microbial Cells, Vol. 4, edt. by I. Chibata and L.B. Wingard, Jr., Academic Press, 311-349

Vijaikishore, P. and Karanth, N.G., (1986), 'Glycerol production by immobilized cells of *Pichia farinosa*', Biotechnology Letters, Vol. 8, No. 4, 257-260

Wall, J.B. and Hill, G.A., (1992), 'Optimum CFST bioreactor design: Experimental study usingbatch growth parameters for *Saccharomyces cerevisiae* producing ethanol', The Canadian Journal of Chemical Engineering, Vol. 70, February, 148-152

Wen, C.Y. and Yu, Y.H., (1966), 'Mechanics of fluidization', Chemical Eng. Symposium Series, No. 62, Vol. 62, 100 - 111

APPENDICES

APPENDICES

APPENDIX A: Experimental data

Table a.1 Data for shake flask experiment one

Tracer	Glucose consmd. (g/l)	Ethanol concn. (g/l)	Biomass concn. (g/l)	Ethanol yield (-)	Biomass yield (-)	Tracer Recd. (%)
MG	12.98	6.45	1.3	0.5	0.1	33.56
MV	1.88	2.82	0.52	1.5	0.28	76.67
AB	8.28	3.63	1.22	0.44	0.15	76.6
FL	6.8	3.66	1.2	0.53	0.18	28.0
DB	8.24	3.76	1.23	0.46	0.15	95.89
CL	9.43	3.81	1.25	0.41	0.13	-

(MG = Methyl green; MV = Methyl violet; AB = Aniline blue; FL = Fluorescein; DB = Dextran blue; CL = Control)

Table a.2 Data for shake flask experiment two

Tracer	Glucose consmd. (g/l)	Ethanol concn. (g/l)	Biomass concn. (g/l)	Ethanol yield (-)	Biomass yield (-)	Tracer Recd. (%)
MG	13.44	5.06	1.13	0.38	0.08	36.51
MV	1.02	0.63	0.09	0.62	0.09	65.54
AB	8.6	3.3	1.02	0.38	0.12	90.61
FL	9.44	3.38	1.01	0.34	0.11	26.0
DB	7.98	3.45	1.01	0.43	0.12	96.54
CL	10.41	3.47	0.97	0.33	0.09	-

Table a.3 Glucose concentration during anaerobic batch fermentation

Time (hr)	CL (g/l)	AB (g/l)	Fl (g/l)	DB (g/l)
0	20.12	20.12	19.1	18.3
1			18.48	16.86
1.2	19.2	18.55		
2	19.7		18.59	17.76
2.2		17.52		
2.8			18.03	
3	19.4			15.88
3.7		14.32		
4	18.2		16.12	11.53
5	16.28			9.26
5.2		11.19		
5.5			14.62	
6	12.51			5.16
6.4	13.27			
6.5			8.41	
6.7		8.63		
7				3.88
7.5			7.43	
7.7		7.34		
8.5			6.21	

Table a.4 Ethanol concentration during anaerobic batch fermentation

Time (hr)	CL (g/l)	AB (g/l)	Fl (g/l)	DB (g/l)
0	0	0	0	0
1			0.13	0.08
1.2	0.02	0.64		
2	0.13		0.31	0.01
2.2		1.16		
2.8			0.46	
3	0.43			0.74
3.7		1.73		
4	1.02		0.71	1.71
5	1.87			3.5
5.2		2.49		
5.5			1.29	
6	2.63			2.95
6.4	2.86			
6.5			2.08	
6.7		4.67		
7				4.99
7.5			2.68	
7.7		5.49		
8.5			4.06	

Table a.5 Biomass concentration during anaerobic batch fermentation

Time (hr)	CL (g/l)	AB (g/l)	Fl (g/l)	DB (g/l)
0	0.114	0.16	0.06	0.26
1			0.1	0.22
1.2	0.1	0.14		
2	0.171		0.13	0.33
2.2		0.22		
2.8			0.22	
3	0.3			0.57
3.7		0.61		
4	0.54		0.25	0.9
5	0.64			1.36
5.2		0.86		
5.5			0.63	
6	0.78			1.6
6.4	0.76			
6.5			0.83	
6.7		1.21		
7				1.76
7.5			0.78	
7.7		1.23		
8.5			0.79	

Table a.6 Tracer recovery during anaerobic batch fermentation

Time (hr)	CL (g/l)	AB (g/l)	Fl (g/l)	DB (g/l)
0		0.009	0.02	0.588
1			0.021	0.587
1.2		0.01		
2			0.021	0.582
2.2		0.011		
2.8			0.021	
3				0.584
3.7		0.01		
4			0.021	0.582
5				0.582
5.2		0.007		
5.5			0.022	
6				0.586
6.4				
6.5			0.023	
6.7		0.005		
7				0.586
7.5			0.023	
7.7		0.004		
8.5			0.022	

Table a.7 Recalibration of fluorescein tracer

pH	Concentration, (g/l)							
	0.001	0.002	0.003	0.004	0.005	0.006	0.007	0.008
5.3	.046	.084	.13	.189	.225	.285	.332	.38
5.2	.042	.08	.122	.18	.215	.272	.328	.365
5.1	.04	.078	.118	.17	.204	.26	.301	.348
5.0	.039	.071	.11	.162	.194	.248	.29	.33
4.9	.036	.068	.105	.152	.182	.235	.274	.31
4.8	.032	.062	.1	.145	.171	.222	.26	.295
4.7	.03	.06	.092	.136	.16	.21	.245	.275

Table a.8 Data for measured gas flow rate

Calculated gas flow rate (ml/min)	Measured gas flow rate (ml/min)	Liq. flow rate (ml/min)	Inlet glucose concn. (g/l)
36.8	100	5.75	30
67.9	100	12	30
127.5	130	18	30
190.9	130	24	30
80.7	40	5.75	50
143.2	100	12	50
229.1	175	18	50
94.2	300	5.75	70
204	300	12	70
218	350	18	70
209.2	350	24	70
185.4	200	18	100

Table a.9 Data for tracer experiments with fluorescein

Data for fig. 5.13		Data for fig. 5.14		Data for fig. 5.19		Data for fig. 5.20	
Time (min)	Exit age, E	Time	Exit age, E	Time (min)	F= C/Co	Time (min)	F= C/Co
0	0	0	0	0	0	0	0
2	.045	1	.001	5	0	2	.026
4	0	5	.006	23	.006	11	.128
6	0	10	.006	27	.009	17	.156
8	0.048	15	.004	32	.011	22	.171
12	0.049	20	.007	48	.003	27	.026
14	0.068	25	.005	53	.018	31	.138
16	0.041	30	.006	58	.029	38	.134
18	0.082	35	.003	63	.03	41	.164
20	0.082	40	.004	68	.036	46	.146
22	0.02	45	.005	73	.035	51	.074
24	0.034	50	.006	78	.03	56	.215
		55	.005	83	.033	61	.296
		60	.008	88	.043	71	.219
		65	.008	93	.065	81	.241
		70	.008	99	.055	91	.267
		75	.004	103	.083	101	.299
		80	.005	109	.061	114	.273
		86	.007	113	.103	121	.252
		90	.006	118	.058	136	.252
		96	.004	123	.073	151	.283
		100	.004	128	.089	167	.148
		106	.007	133	.057	181	.363
		125	.006	143	.097		
		136	.007	159	.102		
		141	.006	170	.114		
		152	.005	188	.127		

Table a.10 Data for tracer experiments with dextran blue

Data for fig. 5.15		Data for fig. 5.16		Data for fig. 5.17		Data for fig. 5.18	
Time (min)	Exit age, E	Time (min)	Exit age, E	Time (min)	Exit age, E	Time (mn)	Exit age, E
0	0	0	0	0	0	0	0
2	.001	2	0	1	.001	1	0
4	.017	4	0.001	3	.001	3	.012
6	.06	13	.038	5	.015	5	.044
8	.077	15	.042	7	.038	7	.041
10	.074	17	.038	9	.078	9	.06
12	.06	19	.038	11	.074	11	.06
14	.048	21	.034	13	.062	13	.047
16	.038	24	.03	15	.047	15	.037
18	.025	26	.022	17	.038	17	.025
20	.02	28	.026	19	.031	19	.021
22	.015	30	.022	21	.023	21	.015
24	.011	32	.02	23	.014	23	.013
26	.009	34	.017	25	.01	25	.011
28	.007	36	.012	27	.009	27	.006
30	.007	38	.009	29	.007	29	.007
34	.004	41	.008	31	.004	33	.01
38	.004	44	.011	37	.009	37	.01
42	.002	55	.006	41	.002	41	.012
47	.002			46	0	46	.008
59	.001			51	.004	51	.004
				65	0	58	0
				77	0		

Table a.11 Data on the profile of fermentation parameters

Column height (cm)	pH	Glucose (g/l)	Ethanol (g/l)	Ethanol yield (-)	Gas flow (ml/min)	Productivty P' (g/l.hr)
0	5.99	46.37	0	0	0	0
3	5.01	38.79	2.24	.295	23.15	94.15
14	4.43	26.67	6.52	.331	68.12	58.85
24	4.68	31.52	6.07	.409	63.92	31.96
34	4.68	32.57	5.4	.391	57.26	20.05
45	4.47	28.44	6.48	.361	69.29	18.18
55	4.37	25.13	8.09	.381	87.32	18.59
75	3.93	9.33	13.63	.368	149.49	22.96
136	3.87	8.16	16.33	.427	188.45	15.17
197	3.84	6.51	16.78	.421	204.38	10.76
263	3.84	5.76	17.68	.435	229.08	8.49

Table a.12 Data for fig. 5.39

Glucose consumption rate (g/s)	Gas velocity (cm/s)
.003	.054
.005	.099
.008	.186
.013	.279
.005	.087
.011	.209
.013	.267
.016	.335
.007	.138
.014	.298

Table a.13 Data for figures 5.29 to 5.38

Inlet glucose (g/l)	Liquid flow (ml/min)	Glucose (g/l)	EtOH (g/l)	EtOH yield	Gas vel. (cm/s)	Productvty P'(g/l.hr)
30	5.75	.14	11.36	.348	.054	4.58
30	12	1.37	11.28	.452	.099	9.5
30	18	5.06	9.18	.431	.186	11.59
30	24	2.88	14.06	.47	.279	23.68
50	5.75	1.11	18.82	.354	.087	10.36
50	12	2.42	17.65	.34	.209	20.27
50	18	5.69	17.93	.441	.267	30.88
50	24	9.33	13.63	.368	.335	22.96
70	5.75	1.04	30.27	.441	.138	10.78
70	12	2.34	31.58	.457	.298	23.47
70	18	7.44	23.9	.373	.319	26.64
70	24	17.61	13.39	.246	.306	19.9
50(Y6)	5.75	.22	25.38	.489	.118	7.32
50(Y6)	12	2.59	24.82	.498	.244	12.44
50(Y6)	18	2.47	24.54	.491	.361	18.45
50(Y6)	24	8.06	20.04	.49	.430	18.62

Table a.14 Sizes of flocs formed by different yeast strains

Yeast strain	Sauter mean diameter of flocs (mm)	Standard deviation
Y6	0.487	0.121
ABX-LID	0.732	0.136
EM-93*	0.325	0.063
ABXR-11B	1.448	0.359

* Flocs formed by this strain dissentegrate easily with slight shaking.

Table a.15 Data for axial liquid dispersion coefficient and liquid holdup

Inlet glucose (g/l)	Liquid flow rate (ml/min)	Axial disp. coefficient, $D_L \times 10^5$ (m^2/s)	Liquid holdup, ε_L
30	5.75	4.67	0.171
30	12	17.14	0.154
30	18	12.46	0.234
30	24	16.34	0.243
50	5.75	10.42	0.158
50	12	16.65	0.196
50	18	82.92	0.223
50	24	24.54	0.211
70	5.75	9.62	0.111
70	12	11.09	0.174
70	18	14.25	0.223
70	24	12.48	0.234

APPENDIX B: Specimen calculations

1. Rejection of outlier

The method described by Himmelblau (1970) was used to reject a suspected outlier. For an assumed model, the ratio

$$\frac{|R^* - R'|}{S_{yi}} = V$$ is calculate. Where, R' is the residual of

the suspected outlier, R' is the average residual of the other observations and S_{yi} is the standard deviation of the observations excluding the suspected outlier. If the value of V exceeds the t-ratio at 95% confidence, then the hypothesis H_0 : the observation does not correspond to an outlier, is rejected.

The analysis was performed with respect to the

observation with D_z of 8.29×10^{-4} m^2/s.

For the linear model, $R^* = 3.09659$, $R' = -0.001837$ and $S_{\bar{y}i} = 0.3011$. Therefore, the value of V was found to be 5.646 which exceeded the t-ratio value of 3.54 and the observation was concidered as an outlier.

For the exponential model, $R^* = 2.68746$, $R' = -0.02693$ and $S_{\bar{y}i} = 0.19751$, resulting in V value of 13.743. Here again, the observation was rejected.

2. Calculation of gas flow rate

Gas flow rate was calculated from the equation:

$$f_g\ (ml/\text{min}) = \frac{0.54 C_e f_L P_{atm}}{P_{atm} + (263 - z)\,\rho_L g}$$

$P_{atm} = 1.0133 \times 10^5$ $Kg/m.s^2 \equiv 3.648 \times 10^9$ $g/cm.min^2$, $\rho_L = 1$ g/ml and $g = 9.81$ $m/s^2 \equiv 3.532 \times 10^6$ cm/min^2. Therefore, for liquid flow of 24 ml/min and ethanol concentration of 13.63 g/l and column height of 75 cm, the gas flow rate was calculated as 149.489 ml/min which corresponds to a gas velocity of 0.219 cm/s.

APPENDIX C: Calibration curves for concentration of tracers

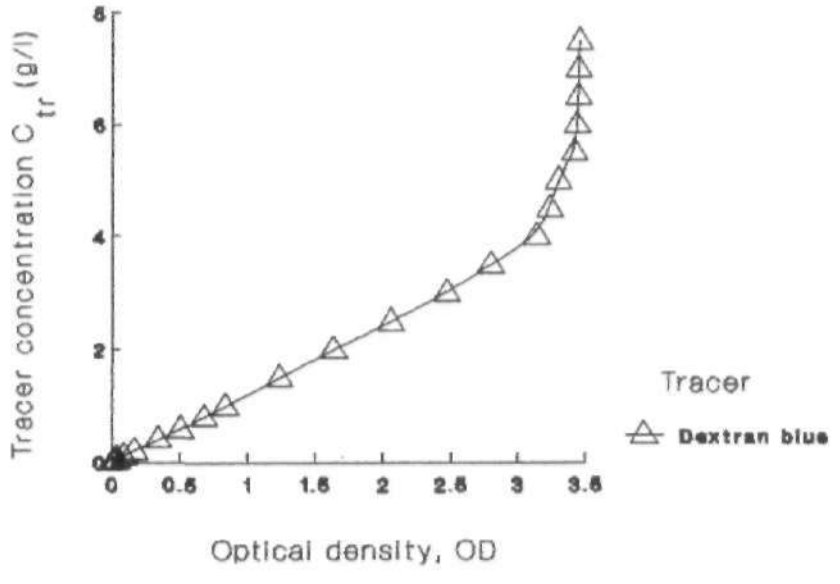


Fig. c.1 Change in optical density with concentration for dextran blue

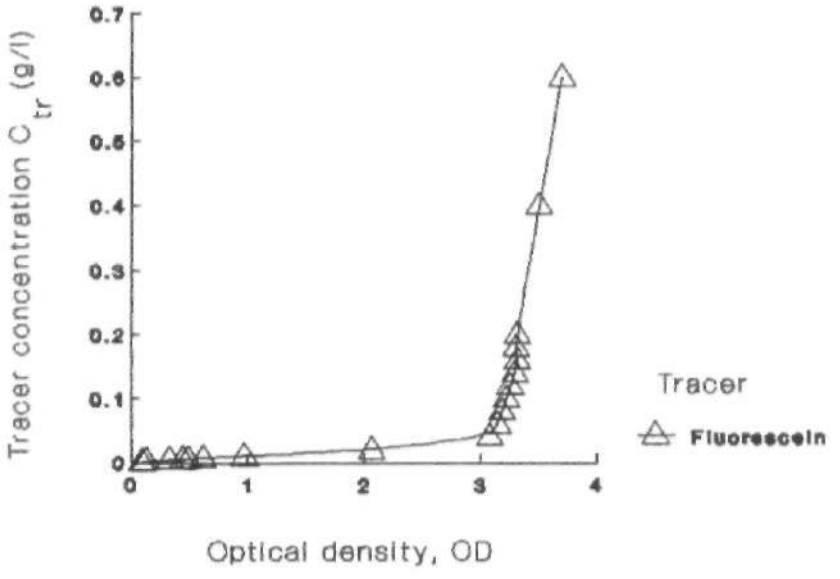


Fig. c.2 Calibration of fluorescein without pH adjustment

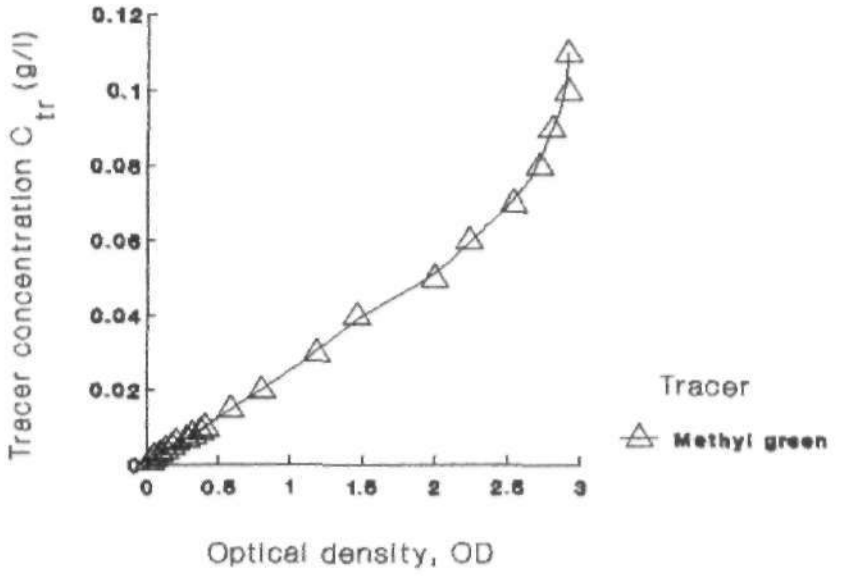


Fig. c.3 Calibration for methyl green tracer

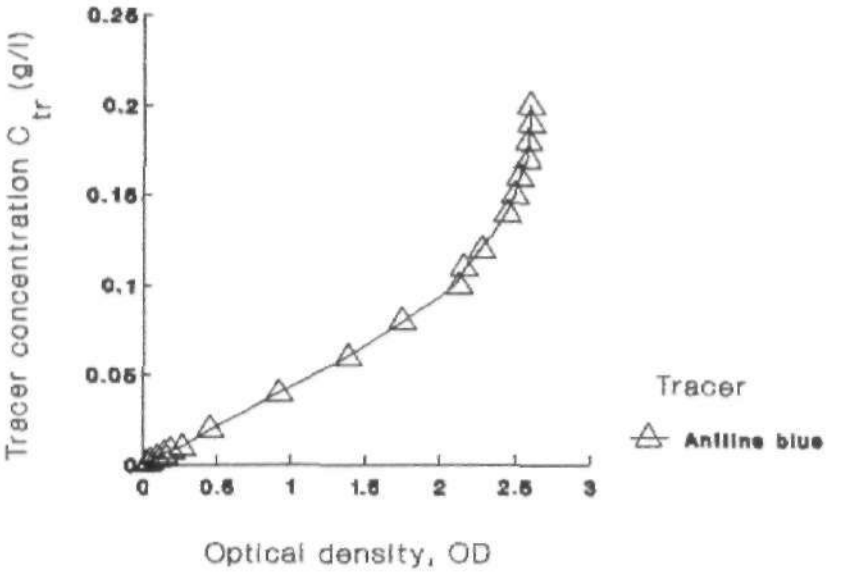


Fig. c.4 Calibration for aniline blue tracer

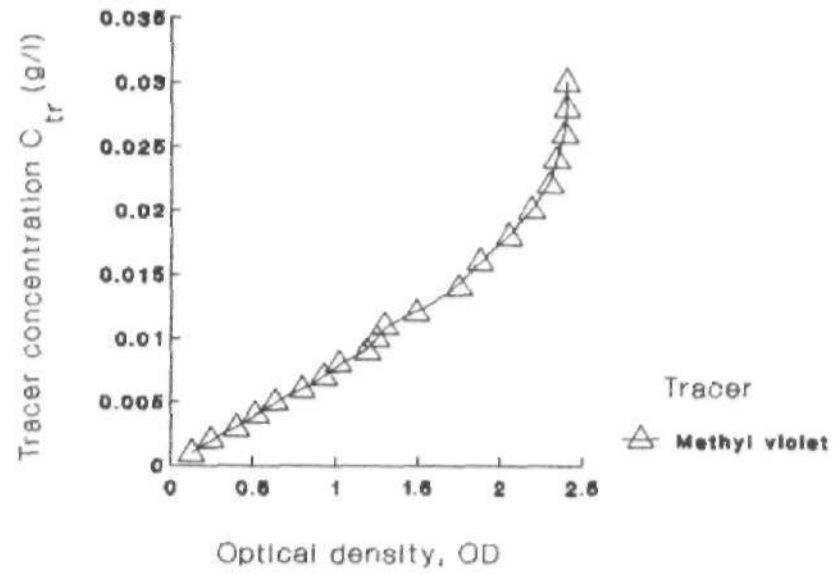


Fig. c.5 Changes in optical density with concentrations of methyl violet